Assessing Coastal Change in Support of the 2023 Texas Coastal Resiliency Master Plan

Mukesh Subedee, Marissa Swift, Lihong Su,

Pu Huang, Jessica Magolan, James Gibeaut

December 31, 2023

Table of Contents

Introduction

The Harte Research Institute (HRI) conducted sea level rise (SLR), storm surge, and wave modeling to provide quantitative information about the potential environmental impacts due to rising sea level and concomitant enhanced storm surge caused by higher sea level and changes in land cover in the Texas coast. This work follows on progress made during the development of the 2019 Plan, where analysis of recent coastal change, model projections of future change, and map visualizations, provided a preliminary understanding of the dynamics of the coastal zone affecting the ecosystem and community resiliency. The prior modeling was an important component of the Plan, however, the results were limited because only 6 storm scenarios and 1 SLR scenario were modeled.

This study used the same successful modeling approach implemented in the 2019 Plan but used ensembles of storms and SLR scenarios to better gauge the human and natural vulnerabilities of the coastal zone. By compiling new and improving existing geospatial data layers of topography, geoenvironments, socio-economic setting, and model projections of change caused by sea level rise and hurricanes, this study provided a fuller range of vulnerability, and therefore, better defined the requirements for projects and programs to address resiliency now and in the future.

The intent of the modeling effort was to further understand and quantify the future impacts of sea level rise and storm surge events, and to compare a no-action scenario without any additional resiliency projects vs. a future with-project scenario by incorporating both Tier 1 and conceptual resiliency projects. Additionally, geohazard and vulnerability maps were also developed showing the changes or vulnerabilities relative to time due to these gradual (sea level rise) and immediate (storm surge) coastal changes.

Living with a Changing Coast

The Texas coast is a system of barrier islands, lagoons, estuaries, plains, and rivers on a low-lying coastal plain. Embedded in this natural and dynamic system are a variety of human developments and activities including oil and gas production, heavy industry, shipping, commercial fishing, recreational fishing, agriculture, tourism, and small and large communities dotted throughout the landscape. The natural systems of the coastal plain, however, are dynamic and subject to sudden hazards such as floods, storm winds, storm surge, and erosion superimposed on longer term processes of ongoing erosion caused by sediment supply changes, shifting habitats, sea level rise, and climate change.

Dynamics of the natural system can have profound effects on the human system altering the course of development and economic activity. An example of this is when the growing port of Indianola in Matagorda Bay was severely impacted by the 1886 hurricane resulting in the abandonment of a growing community of 5,000 people and an important economic asset. On the other hand, human activities can alter natural dynamics. One example is the restoration of habitats such as beaches and marshes. Some attempts at mitigating natural processes effect on human activities set up feedback loops that can have detrimental secondary impacts, such as seawalls enhancing beach or mash erosion in front of or along the shoreline.

The Texas coast, before large-scale development began in the late 1800's to early 1900's, was mostly a natural system that could significantly regulate human activities, but human activities only made small-scale alterations to natural processes. It was a simpler, one-way system and hostile to the type of

socioeconomic activity that would develop in the following decades. An activity that caused significant impacts to socioeconomics and natural processes was the development of deep-water ports. The naturally shallow bays with less than 10 feet water depth and dangerous shifting inlets for ships to pass through between the Gulf and the bays were not conducive to port expansion. The dredging of ship channels and stabilization of inlets with long jetties in the early 1900's allowed the expansion of ports and port industries, particularly the petrochemical industry. This industrial development, along with continued expansion of agriculture and tourism, caused coastal population to reach 6.5 million in 2000 and is expected to increase to 9 million by 2050. This socioeconomic activity constructed a physical infrastructure that now alters the dynamics of the natural system. It is important, therefore, to consider the Texas coastal plain as a Coupled Human and Natural System (CHANS) with reciprocal effects and feedback loops (Liu et al., 2007)

The Texas Coastal Resiliency Master Plan (TCRMP) Planning Framework (Figure 1) lays out the approach to improving coastal resiliency. On the left are Drivers of the coastal system which are fundamental "forces" occurring not just in the coastal plain but beyond it as well. The drivers, classified as economic, social, or natural, create Pressures that are sources of environmental stress such as sea level rise, increasing storm intensity, development, and population increase to name a few broad types. How the system responds to Drivers and Pressures may result in Vulnerabilities that can decrease coastal resilience.
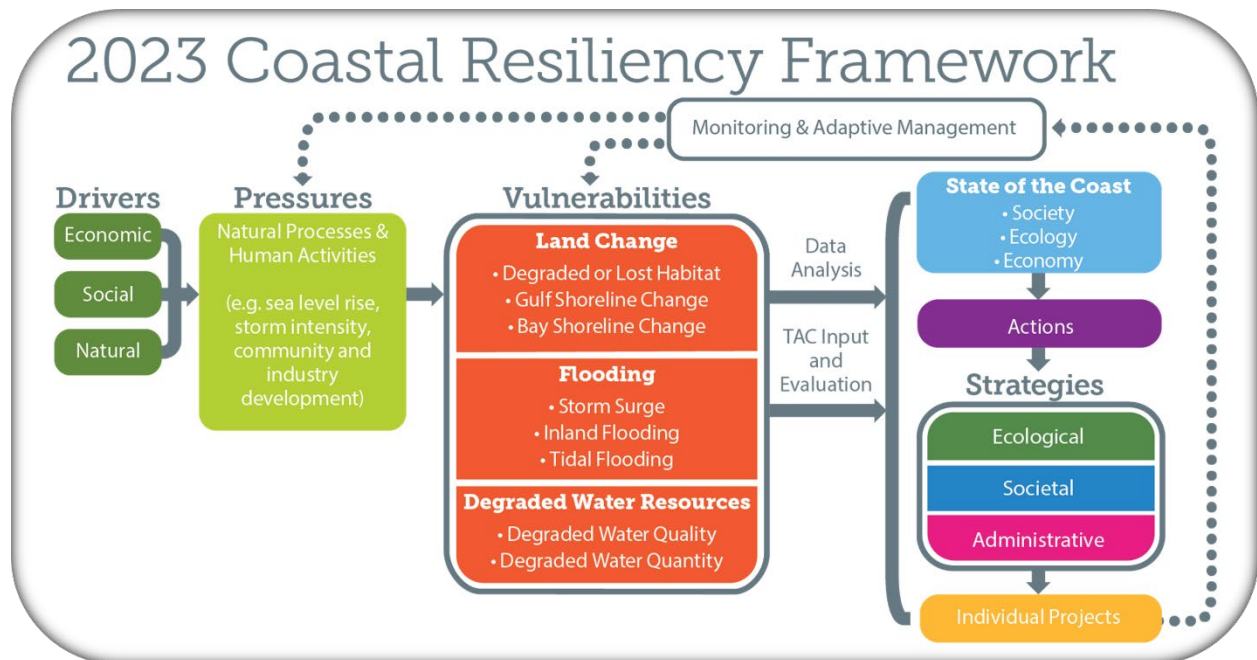
Figure 1. Framework for placing Drivers, Pressures, and Vulnerabilities in context with TCRMP activities to improve resiliency.

Determining how and to what extent vulnerabilities may decrease resiliency requires a spatial view of the coastal CHANS as it exists today, in the past, and with projections of the future given predictions of changes in Drivers and Pressures. Because of feedback loops and the legacy effects of pressures created

by decades-old infrastructure as well as the effects of sea level rise and subsidence, it is useful to study past changes to understand how the CHANS may evolve in the future.

Figure 2 shows where the coastal landscape is currently changing the most as measured by mapping the extent of conversion of land to water from 1984 to 2020 using thousands of Landsat satellite images (Pekel et al., 2016). Also shown on the map is an indication of where the land will convert to water by 2100. The 2100 projection is from modeling landscape impacts of a 1-m rise in sea level and local land subsidence. This modeling was conducted for the 2019 Plan using the methods described later in this report. Each square is approximately 1.5 km east to west and 1.7 km north to south and classified as being either above or below average for present and future amounts of land converting to water. Land includes wetlands and uplands in this analysis.
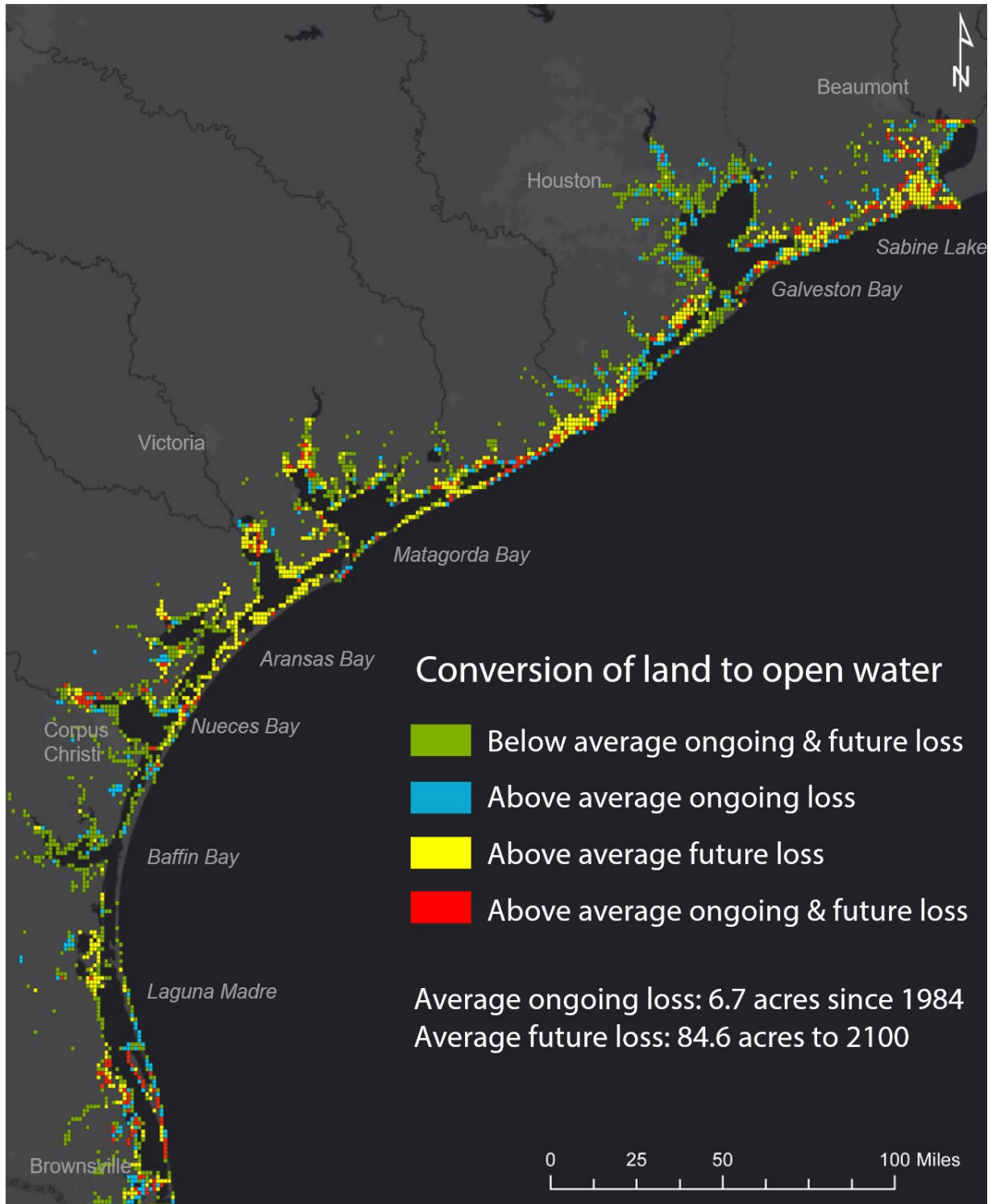
Figure 2. Relative amounts of conversion to open water both currently and in the future caused by 1-m of global mean sea level rise by 2100.

Overall, the Texas coast is losing land to open water and is projected to continue to lose land as global mean sea level rises 1 meter and local land subsidence continues to 2100. Every colored square in Figure 2 is a location that is either losing land or will lose land between now and 2100. Since 1984,

approximately 18,000 acres turned to open water and by 2100 approximately 230,000 more acers are projected to convert to open water. As expected, land loss is occurring around most bay and gulf shorelines with notable exception of Padre Island seaward of Baffin Bay where an alongshore convergence of sediment occurs. Areas in green are experiencing below average loss and are expected to continue losing at a below average rate. These areas are likely to need and respond well to restoration and nature-based solutions. Blue areas are losing at an above average rate, but future loss is relatively low. Blue areas are scattered throughout and indicate hotspots of recent loss, and they may need to be addressed depending on infrastructure impact. Yellow areas are not experiencing high loss but are expected to start to lose at an above average rate in the future. These areas should not be overlooked and are places where land acquisition could provide future space for habitat transitions and a buffer to development. Red areas are problematic in that they are currently losing at a relatively high rate and are expected to continue to lose at a high rate. The Gulf shoreline just east of Matagorda Bay is retreating at the highest rate on the Texas coast. Bay head deltas and the chenier plain of east Texas have red areas along with yellow and blue. These areas are critical and will require multiple approaches, including acquisition, protection, and restoration, to improve resiliency.

Methods

The Modeling Framework

For the 2019 Plan modeling study, HRI developed a dynamic modeling framework to assess quantitative information regarding the impacts of SLR and associated enhanced future storm surge caused by higher sea level and changes in land cover (Subedee et al. 2019). The framework comprised of the state-of-the-art and computationally expensive models including Sea Level Affecting Marshes Model (SLAMM), Advanced CIRCulation (ADCIRC), Simulating Waves in the Nearshore (SWAN), and HAZUS-MH (Figure 3). The same successful modeling approach is used with ensembles of storms and SLR scenarios to better assess the human and natural vulnerability of the Texas coastal zone for the 2023 Plan.

Given the vulnerability of wetland habitats to SLR, this study employed the SLAMM to project future changes in the distribution of specific environments in a quantitative and spatiotemporal manner. SLAMM is a rule-based spatial model that predicts landcover changes induced by SLR in coastal areas at a local or regional scale. It uses a complex decision tree that incorporates geometric and qualitative relationships to determine transitions among habitat classes as sea level rises (Clough, Park, and Fuller 2010). SLAMM requires several map-based inputs and numerical parameters along with sea level rise condition in the year 2100 and it gives maps of updated elevations and land cover classes in the year 2100 along with other numerical outputs. Two SLR scenarios were used for this study as it is recommended to use a range of future conditions to support a diversity of users who potentially may have very different decision contexts and risk tolerances in their planning (Parris et al. 2012; Sweet et al. 2017). This approach allows for a range of potential sea level rise scenarios to be considered in the coastal resilience planning process.

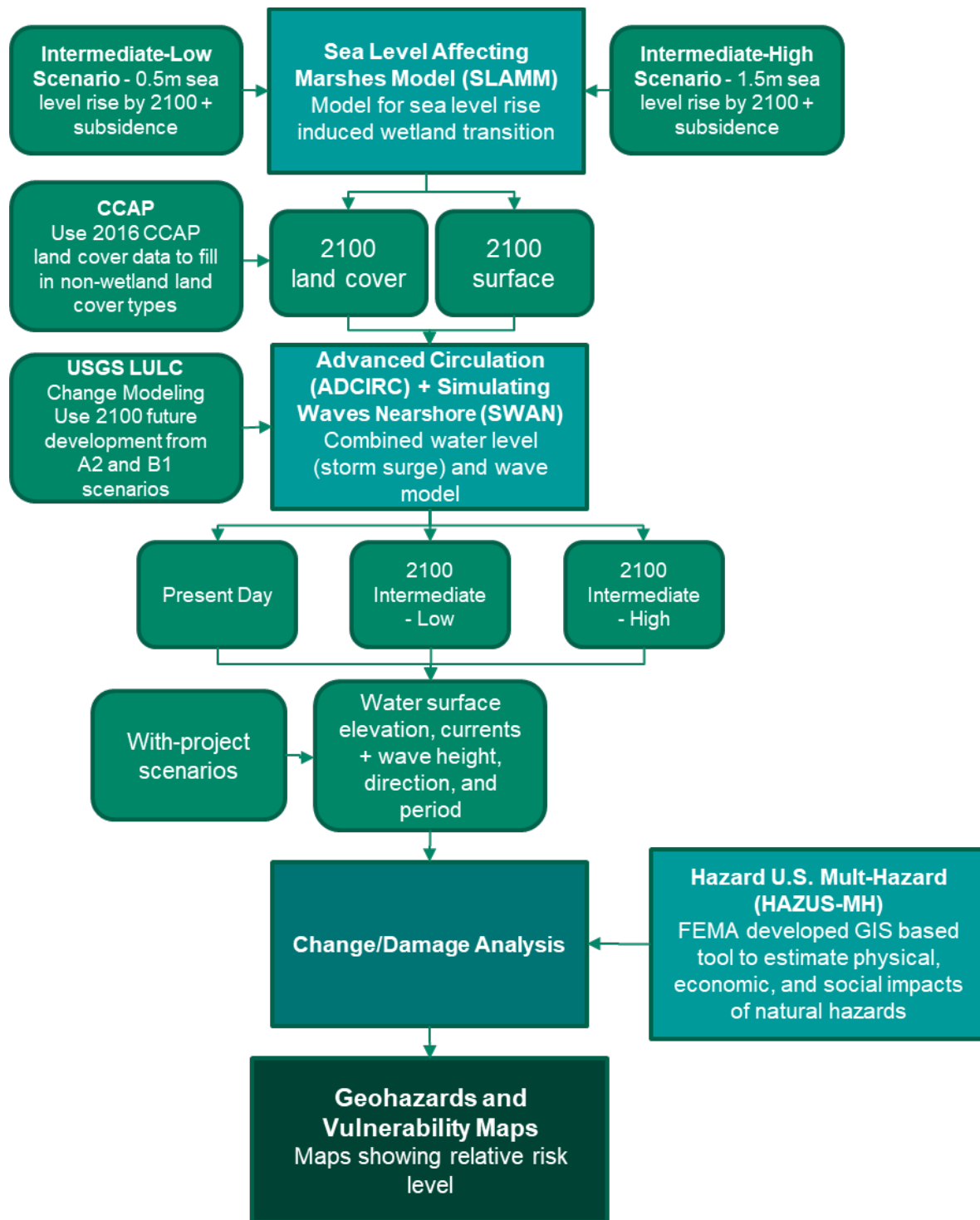*Figure 3. Modeling framework showing the input/output data, modeling tools and processes used in this study.*

The future topographic surface output by SLAMM was used to update the computational mesh for storm surge analysis. Similarly, the future landcover output by SLAMM was used to generate the Manning's *n* friction coefficients representative of future conditions for the storm surge analysis. The

future landcover dataset developed by the US Geological Survey (Sohl et al. 2014) was also used to generate the Manning's n coefficients for the inland area where the SLAMM modeling was not possible.

This study employed the coupled ADCIRC+SWAN model for the storm surge analysis. Both these models are tightly coupled as an integrated circulation and wave model that operates on the same unstructured mesh and gives the time and spatially varying water surface elevation, currents, wave height, wave direction, and wave period. The model was forced using meteorological wind and pressure fields of 19 synthetic storm events making landfall in different parts of the Texas coast. The same 19 storms were forced to the present-day surface and landcover condition as well as the two modeled future landscape conditions considering two SLR scenarios. Therefore, a total of 57 ADCIRC+SWAN simulations were performed for three scenarios.

Subedee et al. 2019 have provided details of each of these modeling tools as the same modeling framework has been used for the 2023 Plan. Similarly, Subedee et al. 2019 provide granular details of each input used in the SLAMM and ADCIRC+SWAN modeling, methods used to update and run these models for different scenarios, numerical parameters used to run each model, and model calibration and validation steps. This study used the same approach and parameters as in the 2019 Plan described in Subedee et al. 2019. This report only focuses on the enhancements made to each of the models in the framework. The major updates made for the 2023 Plan are the model inputs, SLR scenarios, storm scenarios, and improved with-project modeling, and are explained in the following sections. The major enhancements to the modeling process from the previous version of the Plan include:

- Updates to SLAMM and the ADCIRC+SWAN inputs, including land cover and topography – development of high-resolution seamless Digital Elevation Model (DEM) of the coastal plain
- Modeling of multiple global mean sea level rise scenarios from the NOAA 2017 Technical Report Global and Regional Sea Level Rise Scenarios for the United States (Sweet et al. 2017) Scenarios modeled in this Plan include the Intermediate-Low and Intermediate-High (0.5m and 1.5m by 2100 respectively). The 2019 Plan modeled one scenario from the report, Intermediate (1.0m by 2100).
- Modeling additional hypothetical storms from the U.S. Army Corp of Engineers synthetic storm suite. Nineteen total storms were modeled for this Plan – 10 Category 1, 3 Category 3, and 6 Category 2 storms. The 2019 Plan modeled only the 6 Category 2 storms.
- Analysis of SWAN model output for with-project scenarios, a new approach to assessing the efficacy of the projects on the future condition landscape

Improvements to Sea Level Rise and Landscape Change Modeling

Digital Elevation Model (DEM)

The topographic digital elevation model (DEM) is one of the key inputs to SLAMM as well as ADCIRC+SWAN, and an extensive effort was put to generate a high-resolution DEM of the Texas coast using the latest and most accurate lidar-derived datasets. For the 2019 TCRMP, topographic DEM with 3 m resolution was developed using a fusion of 35 airborne topographic lidar surveys conducted between the years 2005 – 2016. Newer lidar surveys have been available since the publication of 2019 Plan. Therefore, a new seamless high resolution, 2 m, DEM of the Texas coast was developed for this study (Figure 4). The elevations in the DEM represent the topographic bare-earth surface. The dataset is a

fusion of several airborne topographic light detection and ranging (lidar) surveys acquired by various surveyors primarily from 2018 and 2019. The landward extent of the lidar surveys selected for the creation of this DEM was determined by the boundary of the ADCIRC mesh used for the storm surge modeling in this study. Elevations in the DEM were in meters relative to the NAVD88 datum, geoid2012b. A very similar approach as used in the 2019 TCRMP was used for processing the lidar data as explained below.

The las files were first checked if they fall in the boundary of the ADCIRC mesh for further processing. A las tile is considered being inside the boundary if any one of its four corners falls within the mesh boundary. All selected las file's horizontal coordinates were converted to either UTM 14 or 15 and vertical coordinates to NAVD88. Furthermore, any files that used geoid1999, geoid2003, or other geoids were converted to geoid2012b. The las files were then gridded by inverse distance weighting (IDW) with the three nearest points to produce 2 m cell raster files. If no lidar points are within the search range of 3 m, the cell was assigned no data. Five parameters were computed for each 2 m cell: point density, average elevation, minimal elevation, maximum elevation, and elevation variance. Only ground points within a 2 m cell were included.

A lidar survey usually had 10 to 2000 files that gave 10 to 2000 raster tiles after gridding lidar points in those las files. These raster tiles were then mosaicked into larger images to fuse multiple surveys. The algorithm to mosaic these tiles first collected the geographic range of all tiles and also gathered the extent of each lidar survey. If the range of the survey was larger than 15,000 x 15,000 pixels of 2 m cell, it was divided into 2 to 10 sub-ranges, so that each sub-range was smaller than 15,000 cells. After obtaining the geographic extent of each sub-range, all tiles were mosaicked into a sub-range if the left-upper corner of a tile was in the geographic extent of a sub-range. This finally gave 2 to 10 mosaic images based on the number of sub-ranges obtained earlier.

Some mosaicked images had data holes due to the presence of water bodies or gaps between the raster tiles in a mosaic image. To fill in the no data holes that existed in new mosaicked images, a morphology closing operation was used to close all holes that are less than 41 x 41 pixels in the mosaicked images. To fill in these holes of size equal to or less than 80 m x 80 m, a buffer of 50 pixels from the boundary of any no data area (hole) was generated. The no data cells next to valid elevation data were assigned a value of 1, the no data cells next to value 1 cells were assigned a value of 2, and so on until all no data cells were filled within the 50 buffer cells. The computed elevation for a buffer cell was the average elevation of its 3x3 neighboring cells. First the elevation of cell of value 1 were computed, then cell of value 2, and so on until 30 buffer cells for all no data areas were closed using this morphology closing operation. Therefore, all holes less than 41 x 41 pixels were filled in the mosaicked images.

Table 1 lists multiple lidar surveys used to develop the seamless DEM of the entire Texas coast. The las files in each survey were gridded separately and were combined to get the final seamless DEM. To make a smooth surface along the edges of lidar surveys so that there were no sharp edges between the surveys, a similar method used to fill no data holes was used by considering a buffer of 10 pixels instead of 50 pixels used for the hole filling. However, if multiple surveys were available and there was an overlap along the edges, a weighted average method was used to compute the elevation for 10 cells along the edges. Once these smooth gaps-filled raster tiles were generated, they were mosaicked together to obtain the final seamless DEM of the Texas coast. The final 2-m DEM was clipped to the modeling study area and is also available for download from the GRIIDC. The dataset is broken down

into the upper Texas coast (https://doi.org/10.7266/2MYPTJ7Y) and the lower Texas coast (https://doi.org/10.7266/Z7WG9EGN). The same DEM was used to develop a slope raster which is one of the other inputs to the SLAMM.

Table 1 List and description of lidar surveys used to develop bare-earth topographic surface of Texas.

Name	Published Date	Originator	UTM
Texas Coastal Lidar Mapping Project (Upper Coast Lidar)	2018/04/08	Texas Water Development Board (TWDB)	15
Texas Coastal Lidar Mapping Project (Jefferson, Liberty, & Chambers Counties Lidar)	2017/04/20	TWDB	15
Texas Neches Lidar Project	2017/11/21	U. S. Geological Survey (USGS)	15
2015 Matagorda Bay Topographic Lidar	2016/11/09	Bureau of Economic Geology (BEG), University of Texas at Austin	15
South Texas Lidar	2019/04/29	USGS	14
2010-2011 ARRA Lidar: Calhoun, Nueces, Willacy, & Hidalgo Counties Lidar	2011/01/01	USGS	14
Texas Coastal Lidar: Kleberg & Kenedy Counties Lidar	2008/11/01	USGS	14
Matagorda Bay Lidar	2019/09/17	USGS	14
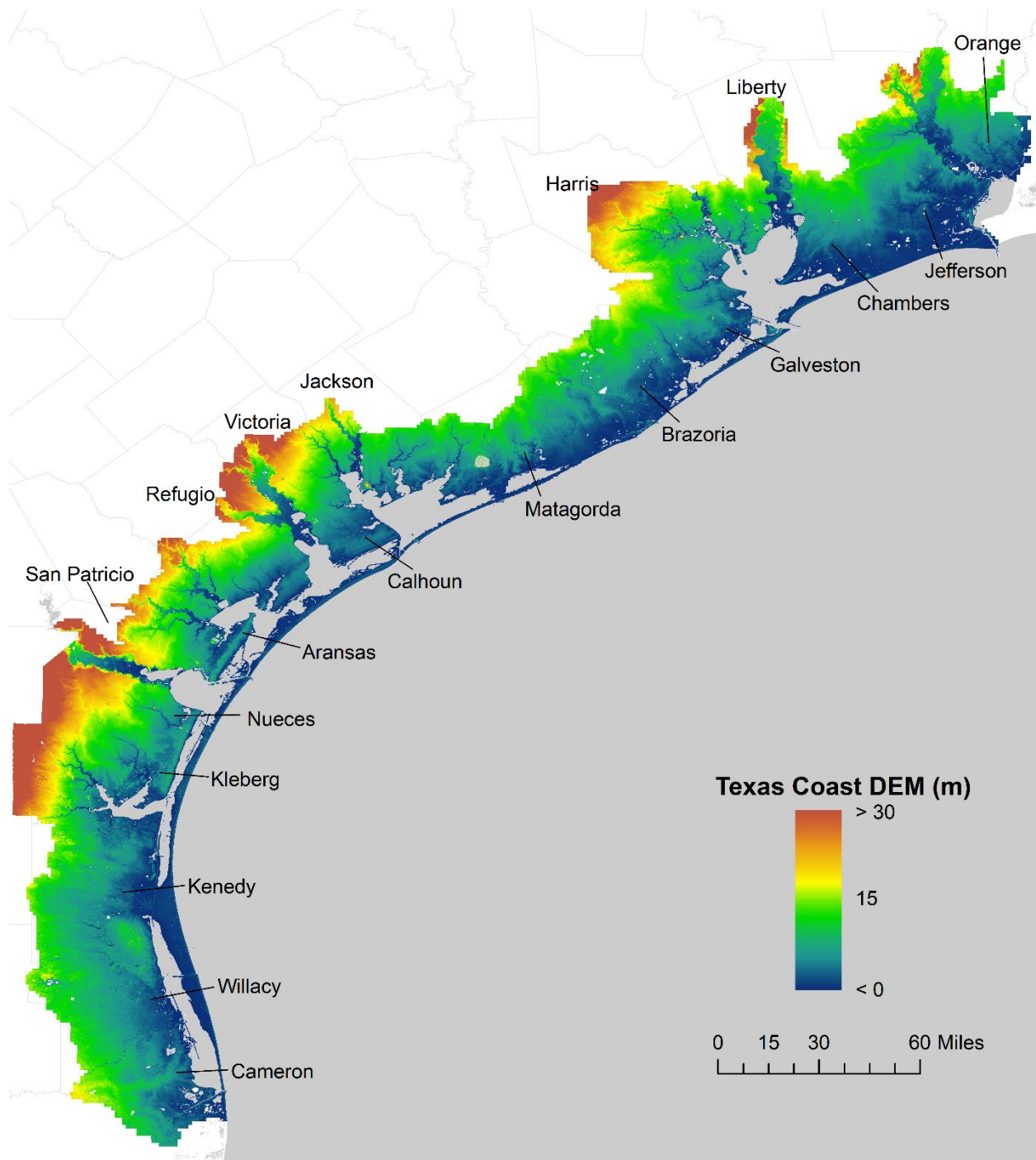
Figure 4. Topographic bare-earth DEM of the Texas coast in meter with coastal county labels

Land Cover Inputs

The latest National Wetlands Inventory (NWI) dataset for Texas at the time of modeling (U.S. Department of the Interior, Fish and Wildlife Service 2019) was downloaded from the U.S. Fish and Wildlife Service's (USFWS) website. The NWI utilizes the Cowardin classification system, where wetland classes describe generic habitat type more than specific species composition (Cowardin et al. 1979). This dataset was cross-walked from Cowardin codes to the SLAMM land cover classes using the lookup table

provided in the SLAMM's supporting documentation. All dry land within the study region that did not have NWI data were assigned the Undeveloped Dry Land classification, since the NWI only describes wetlands and not upland land cover. The NWI, which is provided by USFWS as a shapefile, was then rasterized to a 2m resolution grid to be used in the SLAMM.

To determine where upland areas are developed, the National Land Cover Database percent impervious cover raster was overlaid on top of the land cover raster derived from the NWI. Developed areas are classified where the input land-cover class is Undeveloped Dry Land and percent impervious cover is greater than or equal to 25%.

For the ADCIRC-SWAN models, the Undeveloped Dry Land class needed to be classified as a more specific land cover type to provide a more accurate roughness coefficient. The latest release of the Coastal Change Analysis Program Regional Land Cover and Change raster was downloaded from the NOAA Office for Coastal Management website. This dataset provided upland land cover classes such as forests, grasslands, agricultural lands, and other non-wetland land cover types.

Furthermore, to estimate future development in 2100 as an additional input to the ADCIRC+SWAN models, output from the United States Geological Society's FORE-SCE land cover change projection datasets (Sohl et al. 2014) were added to the 2100 SLAMM land cover outputs wherever SLAMM output predicted undeveloped dry land and the USGS predicted developed dry land in 2100. The USGS model uses IPCC Special Report on Emissions Scenarios (SRES) to predict changes in land cover, with a focus on anthropogenic land use versus natural environments. The SRES storylines modeled by USGS are the A1B, A2, B1, and B2 scenarios. Of the SRES scenarios, "A" represents more economically driven future conditions ("business as usual"), whereas "B" scenarios are representative of more environmentally conscious policies being enacted to reduce carbon emissions over time (Eggleston et al. 2006).

This study used two SLR scenarios for modeling based on Sweet et al. 2017 – Intermediate-Low (0.5 m of SLR by 2100) and Intermediate-High (1.5 m of SLR by 2100) (more details in SLR Scenario section). The Intermediate-Low scenario used in this Plan was modeled after the B1 emissions scenario (Sweet et al. 2017). The B1 scenario forecasts increasing population and economic growth but with a greater focus on environmental conservation and global cooperation resulting on limited land-use impacts on natural land covers. In the SLAMM 2100 output of Intermediate-Low scenario, the projected future development from the USGS model for B1-2100 was superimposed on top of the SLAMM land cover. The NOAA Intermediate-High scenario, however, is based on the A1F scenario, which the USGS modeling team did not include in their projections. A1F is in the same A1 family as A1B, but A1F represents a fossil fuel intensive future whereas A1B's storyline shows a balance between fossil fuels and renewable energy. Based on this storyline, the closest scenario modeled by USGS is A2 which also shows an increase in reliance on fossil fuels and increasing carbon dioxide emissions into the next century. The planning team decided to use the A2 2100 output superimposed on the 2100 Intermediate-High SLAMM land cover.

Sea Level Rise Scenarios

The average global mean SLR rate was approximately 0.06 inches per year (in/yr) over the past century. However, the rate is accelerating – it has more than doubled throughout most of the twentieth century to 0.14 in/yr from 2006-2015 (Church and White 2011). Because sea level changes unevenly, some communities are at higher risk of being impacted than others. Relative SLR (RSLR) rates are different due

to local factors like vertical land motion (subsidence), local wind, atmospheric pressure, and ocean circulation (Mimura 2013). The 367 miles of Texas Gulf coastline has varying RSLR rates ranging from 15 in/100 years in the lower coast to 26 in/100 years in the Galveston Bay region based on the tide gauge data (Figure 5).

Figure 5. Historic RSLR rates on the Texas coast measured by tide gauges.

NOAA Technical Report NOS CO-OPS 083 provides a scenario range for possible global mean sea level (GMSL) rise for the 21st century and a set of 1-degree (~70 miles) gridded relative sea level rise (RSLR) projections along the United States coastlines where no gauge data is available (Sweet et al. 2017). The methodology for determining scenarios and rates of both GMSL and RSLR are well documented and based on peer-reviewed, established methods. Additionally, the GMSL scenarios are built from the previous, extensively cited NOAA sea level report (Parris et al. 2012) and emissions pathways (RCPs, Representative Concentration Pathways) from van Vuuren et al. 2011 used in the IPCC Assessment Report 5 (Church et al. 2013) .

To address the impacts of RSLR through the year 2100, the 2019 Plan modeled only one SLR scenario which was an intermediate scenario of 1m of GMSLR by 2100. However, because of the large uncertainties involved in predictions of the contribution of land-based ice melting to the GMSLR, a scenario approach covering a broad range of existing sea level study results is recommended for robust planning decisions.

For this study, a probabilistic range approach was used by modeling intermediate-low and intermediate-high scenarios which are 0.5m and 1.5m of GMSLR by 2100 from (Sweet et al. 2017) (Table 2). The start date for these scenarios is the year 2000. According to (Kopp et al. 2014), under the RCP8.5 emissions scenario there is a 96% chance GMSLR will exceed 0.5m and a 1.3% chance it will exceed 1.5m (Table 3). These two GMSLR scenarios cover a probable range of possible SLR outcomes without going too low or too high – although there is precedent in other state plans for modeling up to 2m of GMSLR (0.3% chance of exceedance) (see Table 4 and Table 5). The 2019 TCRMP already modeled a central estimate (1 m of SLR by 2100), so this is a step forward towards identifying areas at risk over multiple scenarios within a highly likely range.

To estimate the long-term contribution of non-climatic processes such as vertical land movement (VLM), tectonics, and sediment compaction to relative sea level change, results from a spatiotemporal statistical model of tide gauge data based upon methods described in Kopp et al., 2014. In this model, the spatiotemporal field of relative sea level change over 1900–2012 is represented as the sum of three signals: 1) a globally uniform sea level change, 2) a constant-rate average, long-term, regionally varying trend, and 3) temporally and spatially varying regional sea-level contributions. This model is separately fitted to tide gauge data in several different regions. The spatial scales of variability of processes 2 and 3, and the temporal scale of variability of process 3, are learned in each region from the tide gauge data. The globally uniform signal is assumed to match the GMSL signal estimated by Church and White 2011 (~1.4mm/year); the discrepancy among different estimates of this signal likely contributes ~0.2 mm/year uncertainty to estimates of the long-term background relative sea level trend, which is considered small enough to neglect.

The non-climatic background relative sea level trend is assumed to continue at a constant rate. This assumption is accurate for isostatic rebound, but likely less so for unsteady processes such as those resulting from tectonic processes and/or anthropogenic disturbances (e.g., subsurface fluid withdrawal), which may increase or decrease over time. Both the regional degree of spatial variability in the background relative sea level trend and the density of nearby tide gauges affects the magnitude of the standard error during trend computation at the center of each 1-degree grid point.

Non-climactic background relative sea level from tide gauges and GPS vertical land movement trends were compared and found to be similar. This study assumed background RSLR rate persistence this century, but that assumption could become invalid if, for example, most of the underlying signal stems from anthropogenic-induced VLM, and the driving disturbance ceases at some point in the future. Additionally, larger discrepancies between background relative sea level and GPS VLM trends occur in regions where rates are high and likely influenced by human activities that have varied through time, such as pumping of groundwater/fossil fuels. This finding leads us into the conclusion that the subsidence rate grid developed by HRI should be used in Region 1, where subsidence is driven by subsurface fluid withdrawal.

Figure 6 shows the location of tide gauges and 1-degree grid centers with the RSLR rates along the Texas coast from Sweet et al. 2017. Figure 7 shows the selected two GMSLR scenarios used in this study. The graph shows predicted changes in the sea level from the start date (2000 AD) to the end of this century (2100 AD) based on Sweet et al. 2017. Similarly, Figure 8 - Figure 11 shows the RSLR scenarios calculated based on Sweet et al. 2017 using a set of 1-degree gridded relative sea level rise (RSLR) projections for four regions. A quick study was conducted to understand what SLR scenarios other states in the US have

used in their planning. Table 4 summarizes the SLR planning scenarios used in other Gulf States and Table 5 summarizes scenarios used in other States on the east and west coast.

Table 2. GMSLR scenarios defined by Sweet et al., 2017.

Scenario	Rise by 2100 (m) (Anchored in the year 2000)	Description
Low	0.3	Represents an amount about 5 cm above the extrapolated rate of the GMSL rise trend over the 20th century. Based on 3mm/year GMSL rise rate from altimeters and reconstruction of GMSL from tide gauge data over the last 30 years
Intermediate-Low	0.5	Discretized 0.5-m increment
Intermediate	1.0	Discretized 0.5-m increment
Intermediate-High	1.5	Discretized 0.5-m increment. Rounded from (Rahmstorf et al., 2007; Horton et al., 2008) (1.2 to 1.4m)
High	2.0	Discretized 0.5-m increment
Extreme	2.5	Potential upper limit of GMSL rise. Increased from 2m in previous report based on updated Greenland & Antarctic ice sheet models showing accelerated loss

Table 3. Probability of Exceeding GMSL Scenarios in 2100 (Kopp et al., 2014)

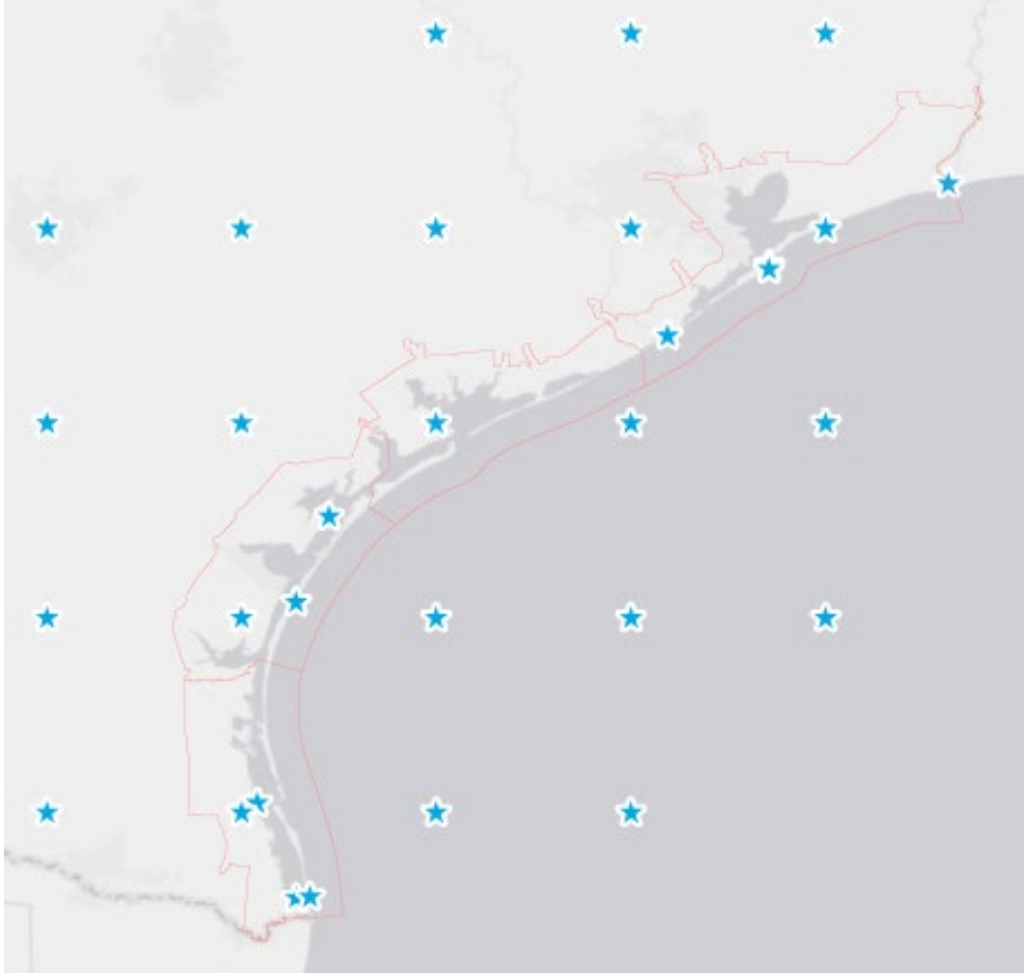| GMSL rise Scenario	RCP2.6 (Strong mitigation, net-negative emissions by 2100)	RCP4.5 (Moderate mitigation, stabilizing emissions by 2050 and declining thereafter)	RCP8.5 ("Business as usual", fossil-fuel intensive, continue increasing emissions)
Low (.3m)	94%	98%	100%
Intermediate-Low (.5m)	49%	73%	96%
Intermediate (1m)	2%	3%	17%
Intermediate-High (1.5m)	0.4%	0.5%	1.3%
High (2m)	0.1%	0.1%	0.3%
Extreme (2.5m)	0.05%	0.05%	0.1%

Figure 6. Locations of tide gauges and grid centers for NOAA RSLR rates along Texas coast.
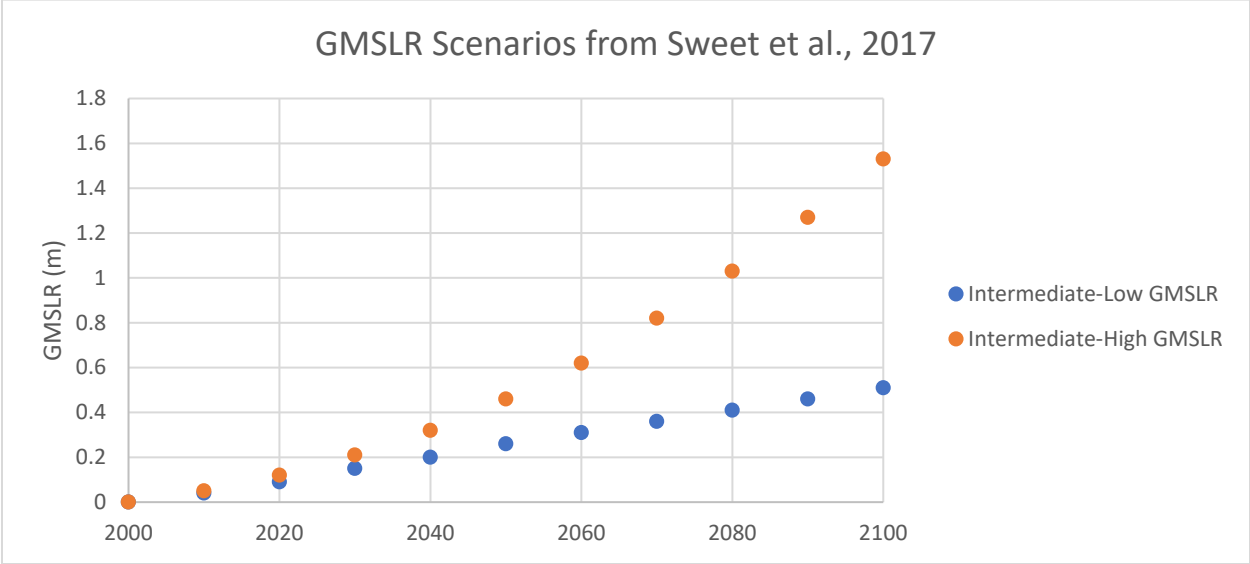

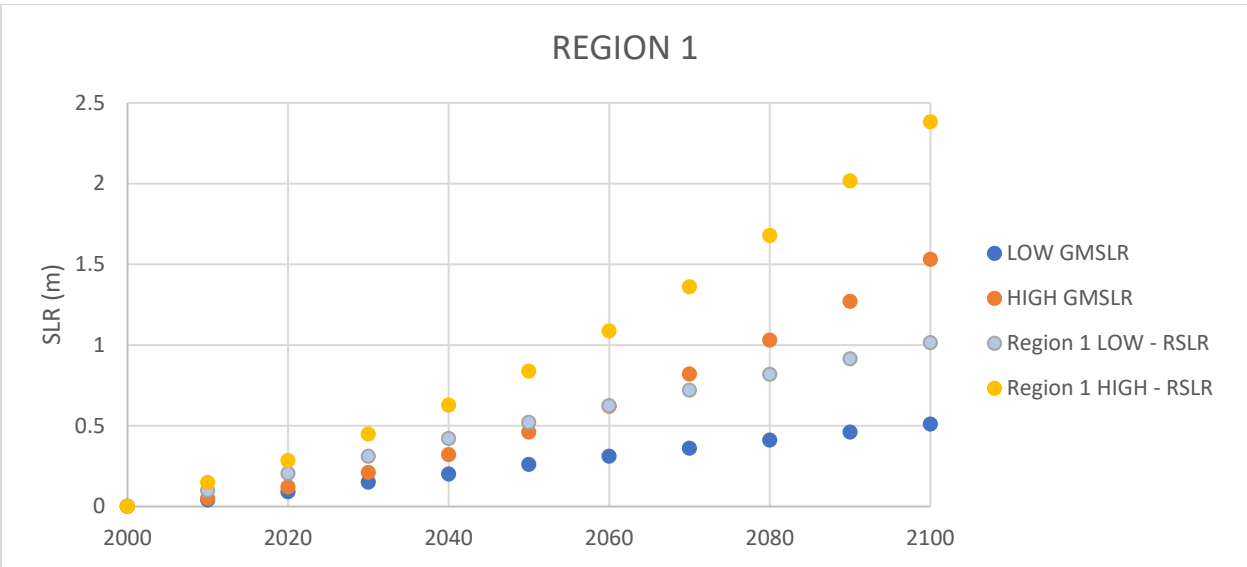*Figure 7. GMSLR scenarios used in this study from Sweet et al., 2017.*

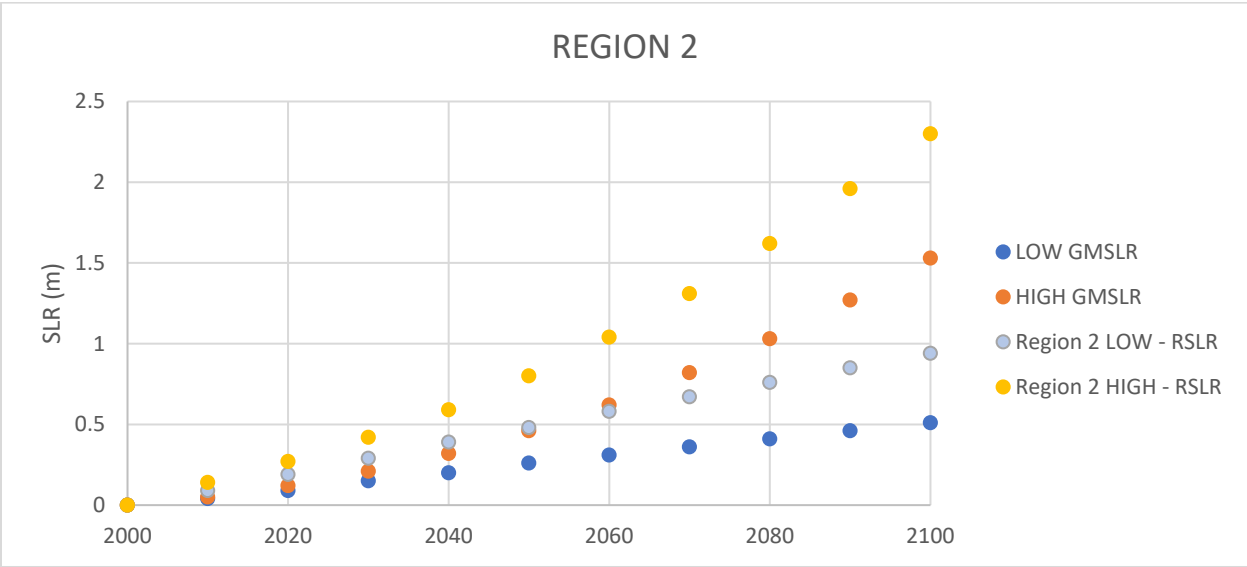*Figure 8. RSLR rate curve used in Region 1.*
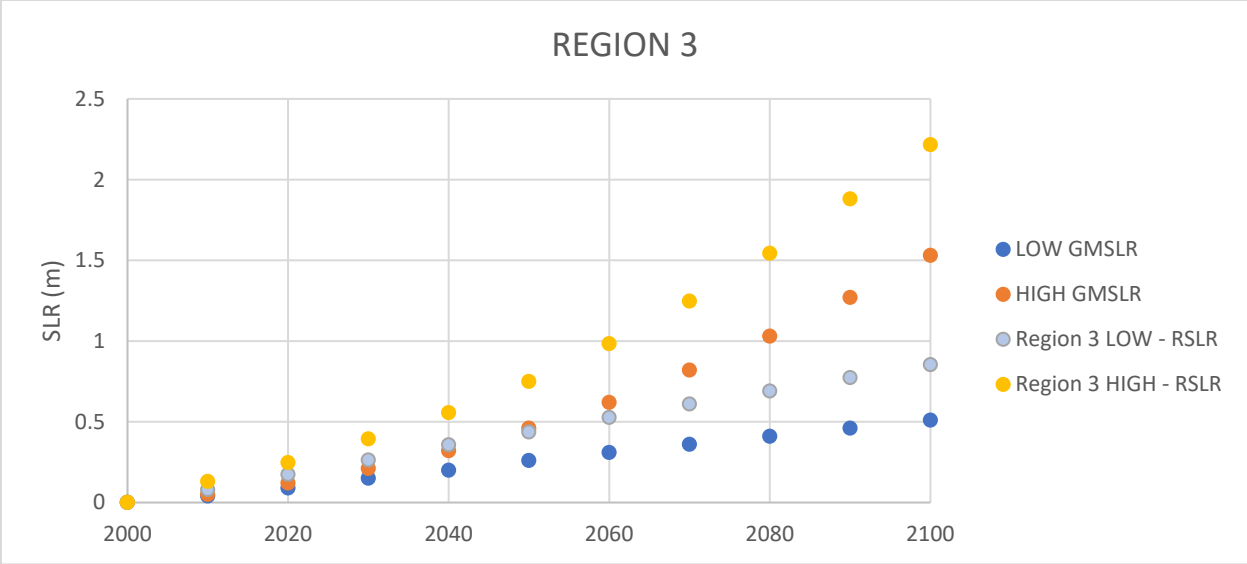

Figure 9. RSLR rate curve used in Region 2.
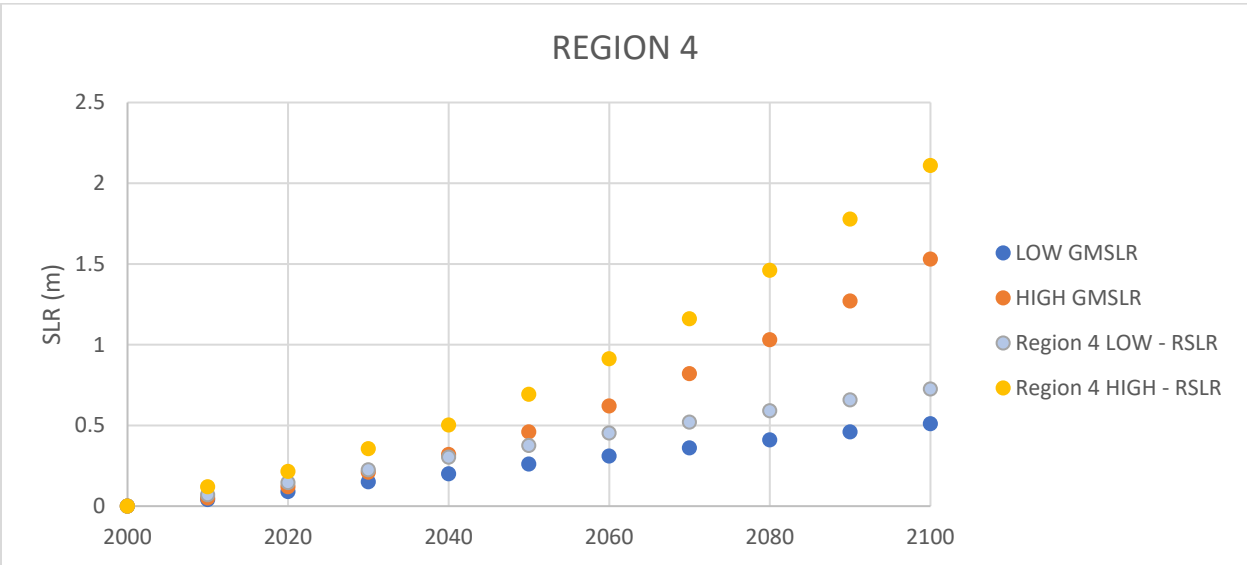
Figure 10. RSLR rate curve used in Region 3.

Figure 11. RSLR rate curve used in Region 4.

Table 4. SLR planning scenarios used in Gulf States.

State	Scenarios	Scenario sources	Link to Source
Louisiana	0.31m by 2100 1.98m by 2100	Church et al., 2013 Jevrejeva et al., 2012	Louisiana Coastal Master Plan, 2017, CPRA
Alabama	.5m by 2100 1m by 2100 2m by 2100	Sweet et al., 2017 Intermediate-Low, Intermediate and High scenarios	Alabama State Hazard Mitigation Plan, 2018, State of Alabama
Florida	0.7 - 1 ft by 2100 1.7 - 2 ft by 2100 4 - 4.3 ft by 2100 5 - 5.3 ft by 2100 6.6 - 7 ft by 2100	USACE Low (2013)/NOAA Low (2012) USACE Intermediate (2013)/NOAA Intermediate Low (2012 NOAA Intermediate High (2012) USACE High (2013) NOAA High (2012	Florida Sea Level Scenario Sketch Planning Tool, 2017, University of Florida GeoPlan Center
Mississippi	16.6 inches in twenty years, 41.5 inches in fifty years, and 74.7 inches by the year 2100.	n/a	Assessment of Sea Level Rise in Coastal Mississippi (no longer online), 2011, Mississippi Department of Marine Resources

Table 5. SLR planning scenarios used in other States.

State	Scenarios	Scenario sources	Link to Source
Rhode Island	1 ft 3 ft 5 ft 7 ft	NOAA	Vulnerability of Municipal Transportation Assets to Sea Level Rise and Storm Surge, 2016, Rhode Island Statewide Planning Program
California	1.6 ft [RCP4.5] 2.5 ft [RCP8.5] 2.4 ft [RCP4.5] 3.4 ft [RCP8.5] 5.7 ft [RCP4.5] 6.9 ft [RCP8.5] 10.2 [Sweet et al., 2017]	Kopp et al., 2014 (used in Sweet 2017) Probabilistic Central Likely 1 in 20 Extreme	State of California Sea Level Rise Guidance, 2018, California Natural Resources Agency

Maryland	3 ft 2.0 to 4.2 ft 5.2 ft 6.9 ft (Only listing RCP8.5)	Kopp et al., 2014 Probabilistic Central Likely 1 in 20 1 in 100	Sea Level Rise Projections for Maryland, 2018, University of Maryland Center for Environmental Science (In fulfillment of requirements of the Maryland Commission on Climate Change Act of 2015)

Updates to Storm Surge Modeling

Along with modeling additional SLR scenarios, the 2023 Plan included additional and more varied storm scenarios modeled using ADCIRC+SWAN models versus the 2019 Plan. These additional storms provided better understanding of relative vulnerability of the Texas coastal zone due to storm surge flooding. Nineteen total storms from the USACE synthetic storm suite that pass through different area along the coast were modeled, compared to 6 from 2019. Additionally, while the 2019 Plan only modeled Category 2 storms, the 2023 TCRMP also modeled Category 1 and 3 storms. To be able to compare outcomes with the previous plan, the 6 storms modeled from 2019 were also included in the 2023 effort.

The same computational mesh used in the 2019 Plan, referred to as *TX2008_R35H*, was used for the ADCIRC+SWAN modeling. The mesh has 3,352,598 nodes and 6,675,517 elements, and more than ninety percent of the computational nodes of the mesh reside in the Texas coast. The element size varies from multiple kilometers in the open ocean to resolutions as fine as 15 m in the channels and rivers. The existing bathymetric data in the mesh was not changed for this study, however, topographic data along the Texas coast was updated with the seamless high resolution, 2-m, lidar-based topographic DEM of the Texas coast for the present condition storm surge analysis. The Manning's *n* coefficient values that represent the frictional roughness was updated in the model as in the 2019 TCRMP. Please find more information about the model and methodology to update DEM and Manning's *n* values in Subedee et al. 2019.

Model Storm Selection

This study utilized the hypothetical storms developed by the USACE as the historical storms that have struck the Texas coast do not sufficiently cover the multiple storm conditions along the Texas coast. The USACE storm database has a set of 660 synthetic storms in 88 base tracks. Mostly Category 1 and 2 hurricanes were selected for this study from the database because they have a higher frequency of occurrence (Figure 12) and most of the coastal population have experienced them or can easily imagine themselves being impacted in their lifetime. Three Category 3 hurricanes that pass near to three major city centers in the Texas coast were also selected.
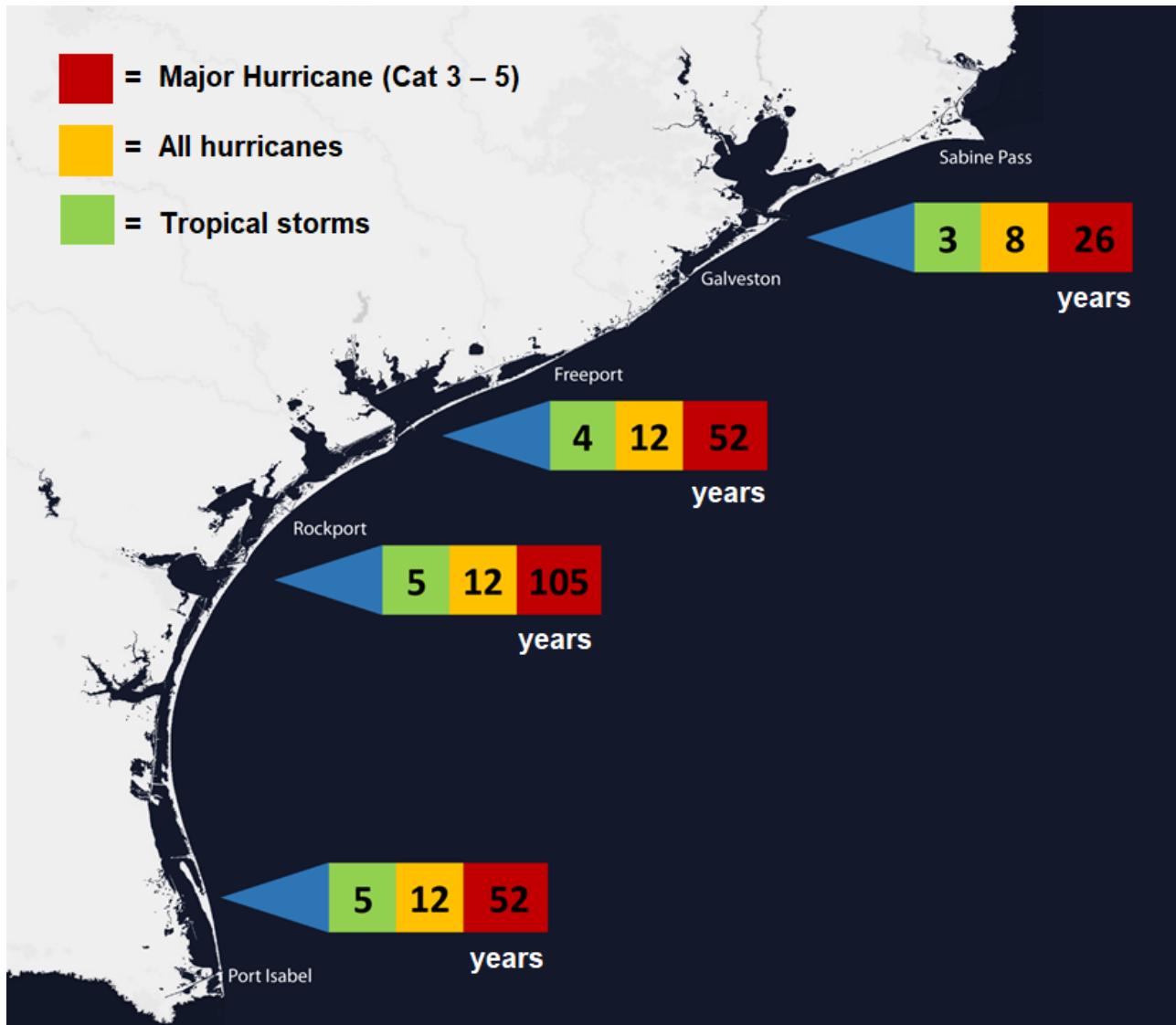
Figure 12. Frequency of tropical storms and hurricanes striking the Texas coast, 1901-2005, based on Keim et al. 2007.

The following methodology was used to select storms for this study from a set of 660 synthetic storms:

1. Identified five city centers along the coast and also included Matagorda Bay region in Region 2:
   - Beaumont/Sabine Pass
   - Houston-Galveston
   - Freeport
   - Corpus Christi
   - South Padre Island
   - Port O'Connor/Port Lavaca (Matagorda Bay region)
2. Chose reference points which are the entrance channel of the adjacent major bay system in these six locations except for South Padre Island (see Figure 13)
   - Sabine Pass
   - Houston Ship Channel

- Freeport Channel
- Corpus Christi Ship Channel
- South Padre Island
- Matagorda Ship Channel

3. Selected storms that pass through 80 miles south of the US-Mexico border and 34 miles east of Texas-Louisiana border
4. Calculated the linear distance between the reference point and the storm landfall point
5. Calculated a non-dimensional comparative value: (distance between reference point and landfall point)/storm radius of maximum wind (RMW) at landfall
6. Prioritized the storms with distance between 1 and 2.5 times the RMW away from the reference point
7. Selected only Cat 1, 2 and 3 storms at landfall that pass southeast of the reference points, and ignored all storms that made landfall twice

From the analysis considering all the above-mentioned criteria, a total of 128 storms are selected (Table 6) which are individually screened by their characteristics (wind speed, forward speed, central pressure, radius of maximum wind (RMW), track orientation, etc.) to narrow down to 19 storms. Finally, nineteen total storms including same six storms from the 2019 TCRMP were selected. Among these 19 storms, 6 are Category 1 hurricane, 10 are Category 2 hurricane and 3 are Category 3 hurricane (Figure 14, Table 7). Figure 15 shows the radius of maximum wind (RMW) buffer of each storm at landfall. The color of each radius of maximum wind buffer circle corresponds to the Saffir-Simpson hurricane wind scale. Most of the coast was impacted with the selected ten Category 2 storms as can be seen with the yellow buffer circles in the map.
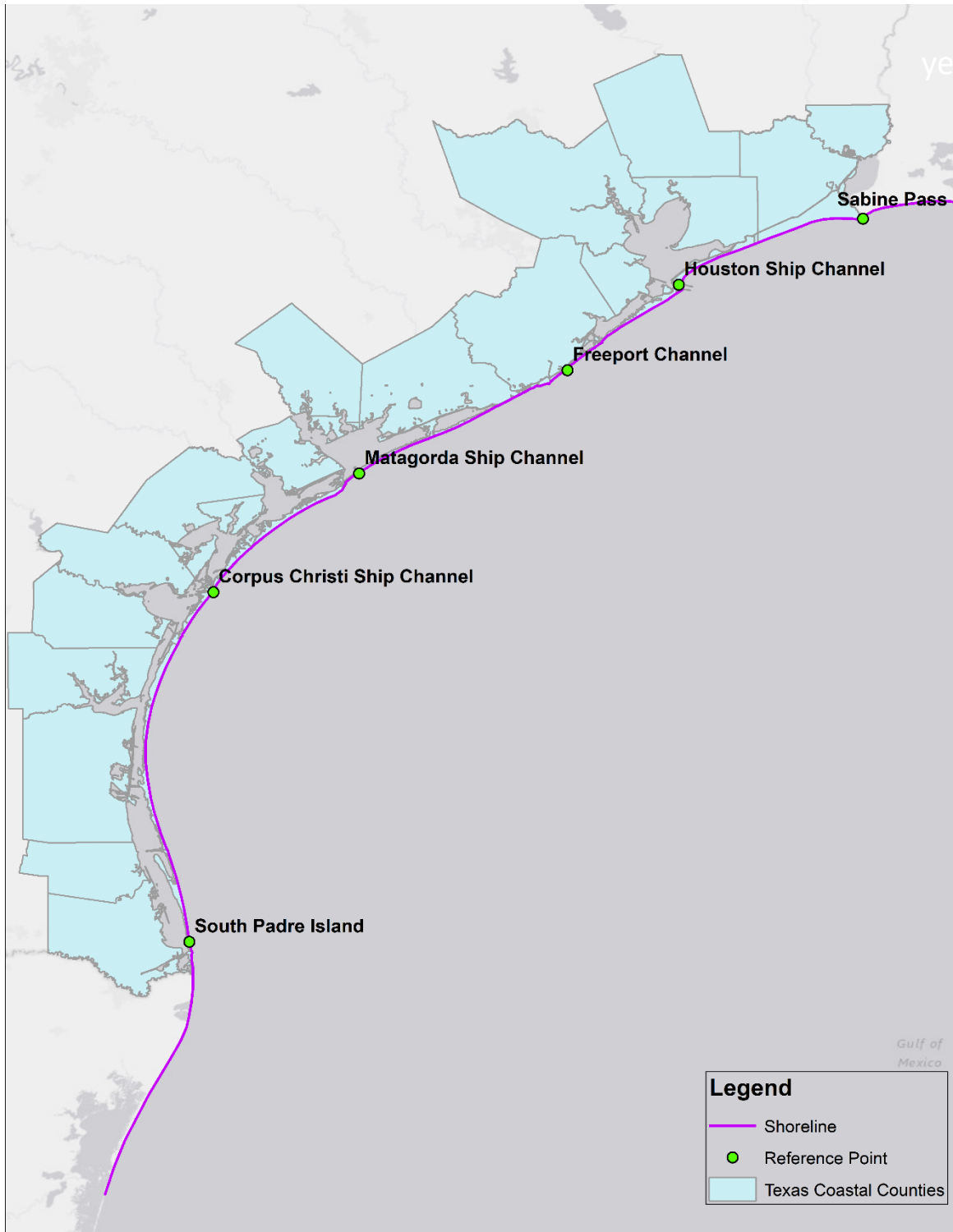
Figure 13. Selected reference points along the Texas coast and extended shoreline for the analysis south of the US-Mexico border and east of TX-LA border.

Table 6. Selected storms in each city centers considering all 7 criteria.

	Category 1	Category 2	Category 3	Total Storm
Beaumont/Sabine Pass	8	10	12	30
Houston-Galveston	6	4	11	21
Freeport	8	9	7	24
Port O'Connor/Port Lavaca	3	4	7	14
Corpus Christi	10	5	13	28
South Padre Island	4	2	5	11

Table 7. Selected storms and their characteristics (the yellow highlighted storms were used in the 2019 TCRMP)

| Candidate Storm	Region	Wind Speed (kt)	Saffir–Simpson scale	RMW (Nmi)	Forward Speed (kt)	Distance from Reference Point (mile)	Central Pressure (mb)	Heading (deg)	Total Hour	Time Step (min)
TC_JPM0305	4	101.3	3	9.89	6.8	17	905.2	-40	282	15
TC_JPM0206	4	83.4	2	31.19	13.4	5.5 (N)	921.3	-60	222	5
TC_JPM0400	4	79.44	1	32.71	13.6	75	933.7	-20	222	5
TC_JPM0222	3	96.68	3	18.98	8.4	29	921.3	-60	282	15
TC_JPM0322	3	86.77	2	30.28	4.6	21	940.4	-40	312	15
TC_JPM0214	3	76.44	1	35.06	4.6	67	921.3	-60	312	15
TC_JPM0416	3	87	2	16.86	11	26.5	933.7	-20	252	5
TC_JPM0328	2	95	2	15.12	10.4	42	927.3	-40	252	5
TC_JPM0240	2	84.61	2	23.26	17.7	14	947.7	-60	162	5
TC_JPM0587	1A	96.55	3	17.33	7.9	26	910.2	20	282	15
TC_JPM0262	1A	84.21	2	22.86	5.9	6	921.3	-60	312	15
TC_JPM0358	1A	86.91	2	10.08	9.5	13	955.4	-40	252	15
TC_JPM0524	1A	81.35	1	23.58	13.1	7	940.4	0	222	5
TC_JPM0449	1A	74.67	1	34.9	19.5	47	947.7	-20	132	5
TC_JPM0146	1A	83.83	2	34.89	18.3	42	927.3	-80	162	5
TC_JPM0154	1A	87.77	2	34.71	10.3	31	940.4	-80	252	5
TC_JPM0160	1B	86.99	2	7.29	8.6	41	927.3	-80	282	15
TC_JPM0363	1B	76.84	1	20.17	6.2	36	927.3	-40	312	15
TC_JPM0466	1B	63.14	1	37.33	6.5	33	963.7	-20	282	15
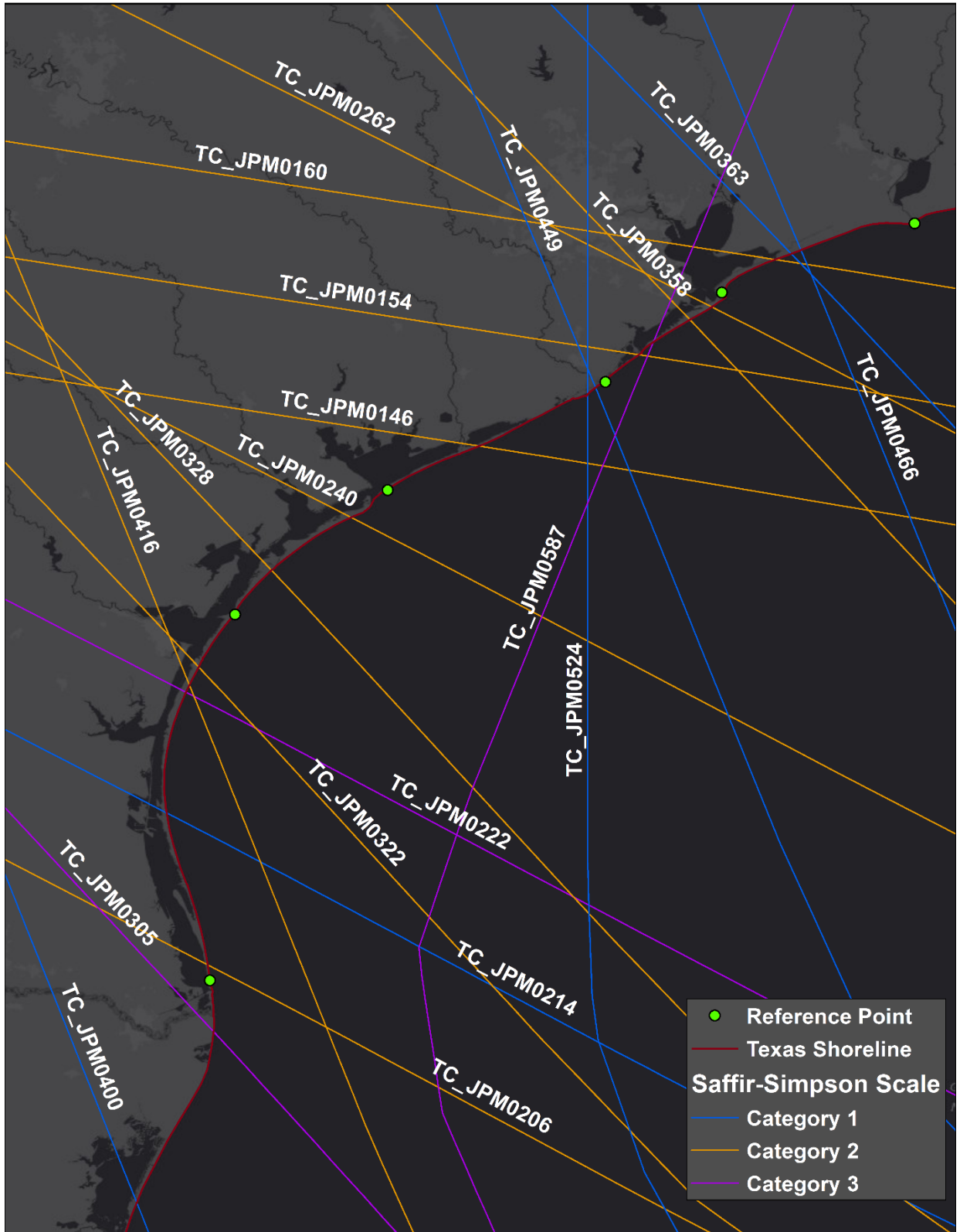
Figure 14. Storm tracks of total 19 storms selected. The reference points are the six city centers chosen for the storm selection process.
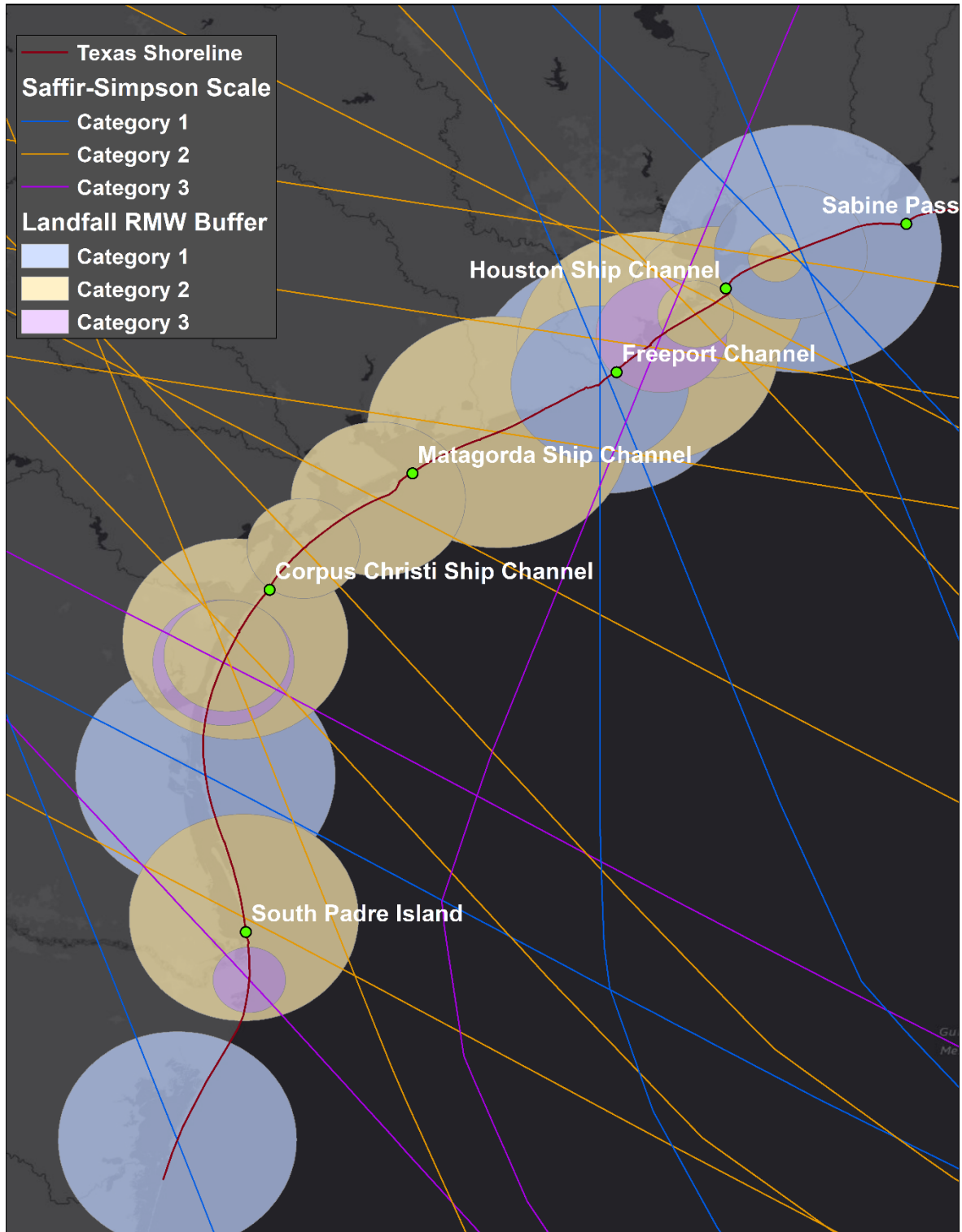
Figure 15. Storm tracks of 19 selected storms and the RMW buffer of each storm at landfall. The color of each RMW circles corresponds to the Saffir-Simpson hurricane wind scale.

Resiliency Projects Modeling

The 2023 Plan also assessed how the implementation of conceptual coastal resiliency projects could mitigate the negative impacts of RSLR and future storm surge. So, this study ran simulations of a select number of storms on future landscapes with ("with-project") and without ("no action") certain conceptual coastal resiliency projects, to determine the potential benefits of these projects on storm damage. The modeled projects include island restoration, breakwaters, and living shorelines, as well as habitat restoration and conservation projects. These project types were chosen because they could be representative of large-scale sediment planning proposed by many of the 2023 Tier 1 projects, but they are not intended to directly represent the Tier 1 projects in this 2023 Plan.

The same storms were modeled over the conceptual "with-project" scenarios that were used for predicting landscape change to determine the benefits of these projects on future storms. The conceptual projects modeled for the 2023 Plan have more focus on reducing wave energy either directly through breakwaters and living shorelines or indirectly through habitat restoration and conservation as buffers to storm impacts. Reducing wave energy in turn reduces damages from storm surge and vulnerability to shoreline and habitat erosion.

Two bay environments, Sabine Lake and Corpus Christi Bay, were selected for the storm surge modeling to determine the potential benefits of various projects on storm damage in the intermediate-low SLR scenario. These two regions were chosen because they have different risk profiles and represent different vulnerability realities.

The Technical Advisory Committee (TAC) identified Region 1 as being especially vulnerable to coastal storms and inland flooding, and so the projects modeled around Sabine Lake were primarily focused on reducing wave energy and the extent of storm surge penetration. The Sabine Lake/Port Arthur area was selected for with-project modeling due to the high vulnerability of the low-lying environments in Region 1A to inundation resulting from SLR and land surface subsidence, as well as the high social vulnerability and flood risk faced by communities within the region. Implementing projects in this area has the potential to enhance the resiliency of these vulnerable populations.

The projects modeled here consist of marsh conservation projects and restoring the islands near Old River Cove and Pleasure Island as shown in Figure 16. The focus for the SLR modeling for the Sabine Lake area was on restoring and conserving the marshes around the Lower Neches WMA, utilizing the same SLAMM parameters used in other SLAMM modeling. Only the intermediate-low SLR scenario was modeled as the higher scenario would result in the complete inundation of the landscape within the region. Two project types were simulated: Beneficial Use of Dredge Material (BUDM) and island restoration (Figure 16). Table 8 presents the details of these project types.

For the BUDM conceptual project, GIS was employed to identify all salt and brackish water marshes. During the SLAMM model simulation, the model was halted every 25 years to add 0.20m of elevation to these marsh areas, specifically in 2050 and 2075. This approach ensured that the marshes could maintain pace with the rate of rise in the intermediate-low SLR scenario. For island creation, the focus was on Old River Cove and Pleasure Island. Historical aerial imagery was examined to determine the former extent of the islands (Figure 17). In GIS, island elevations were raised to match existing islands, and the land cover type was altered to align with the surrounding islands. This approach aimed to restore these areas and provide additional protection against wave energy and storm surge. For Old

River Cove, additional islands were created to maximize the wave buffering effects in the storm surge model (Figure 18).
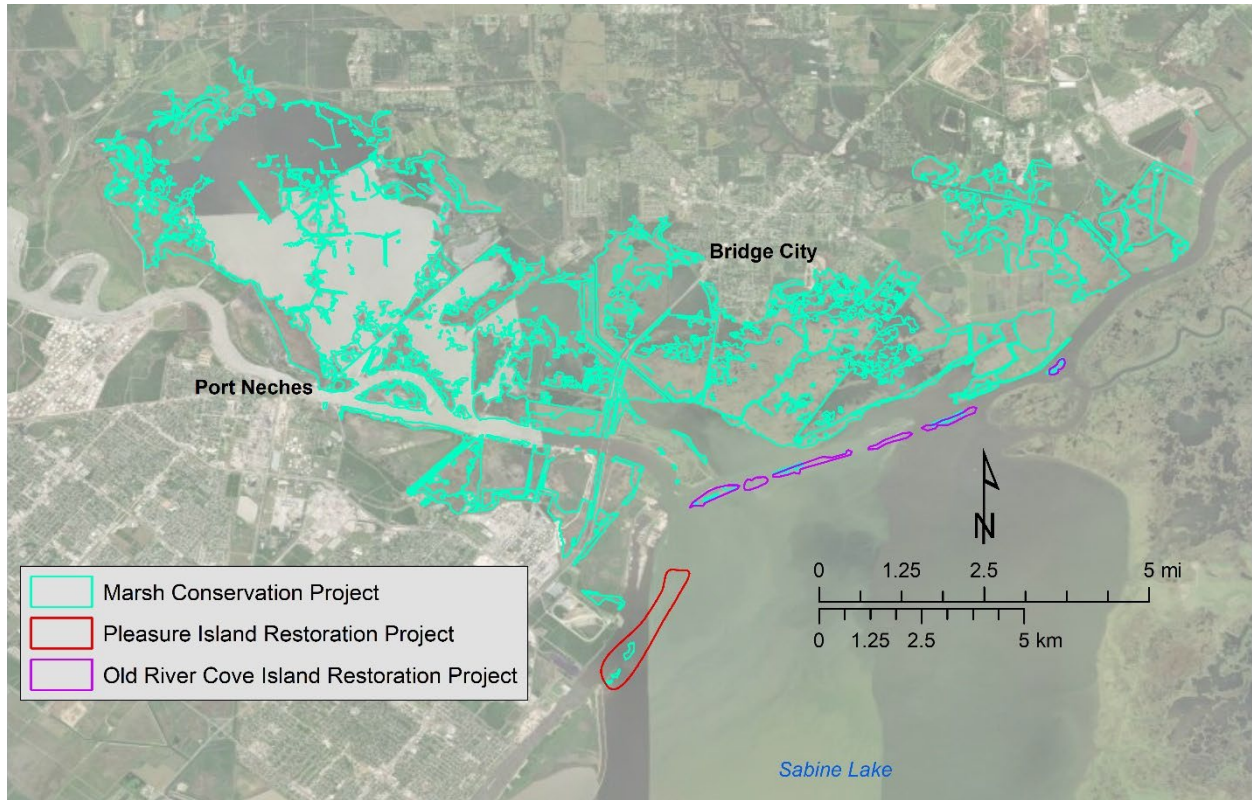

Figure 16. Location of modeled resiliency projects in Region 1 for the with-project modeling.

Table 8. Details of different resiliency project types modeled in Region 1 for the with-project modeling.

| Project Concept	Locations	Desired Outcome	Models Used	Inputs Altered/Updated	Output Analysis
Dredge Placement (BUDM)	All salt and brackish marshes, most located in Lower Neches WMA	Protect habitats from SLR by boosting elevation	SLAMM, SWAN	Elevation, slope, Manning's N, vertical accretion rates	Analysis of land cover changes, wave height and water surface elevation reduction
Island Creation	Pleasure Island, Old River Cove	Reduce flood risk	SLAMM, SWAN	Elevation, Manning's N, add structure in Surface-water Modeling System (SMS)	Analysis of wave height and water surface elevation reduction
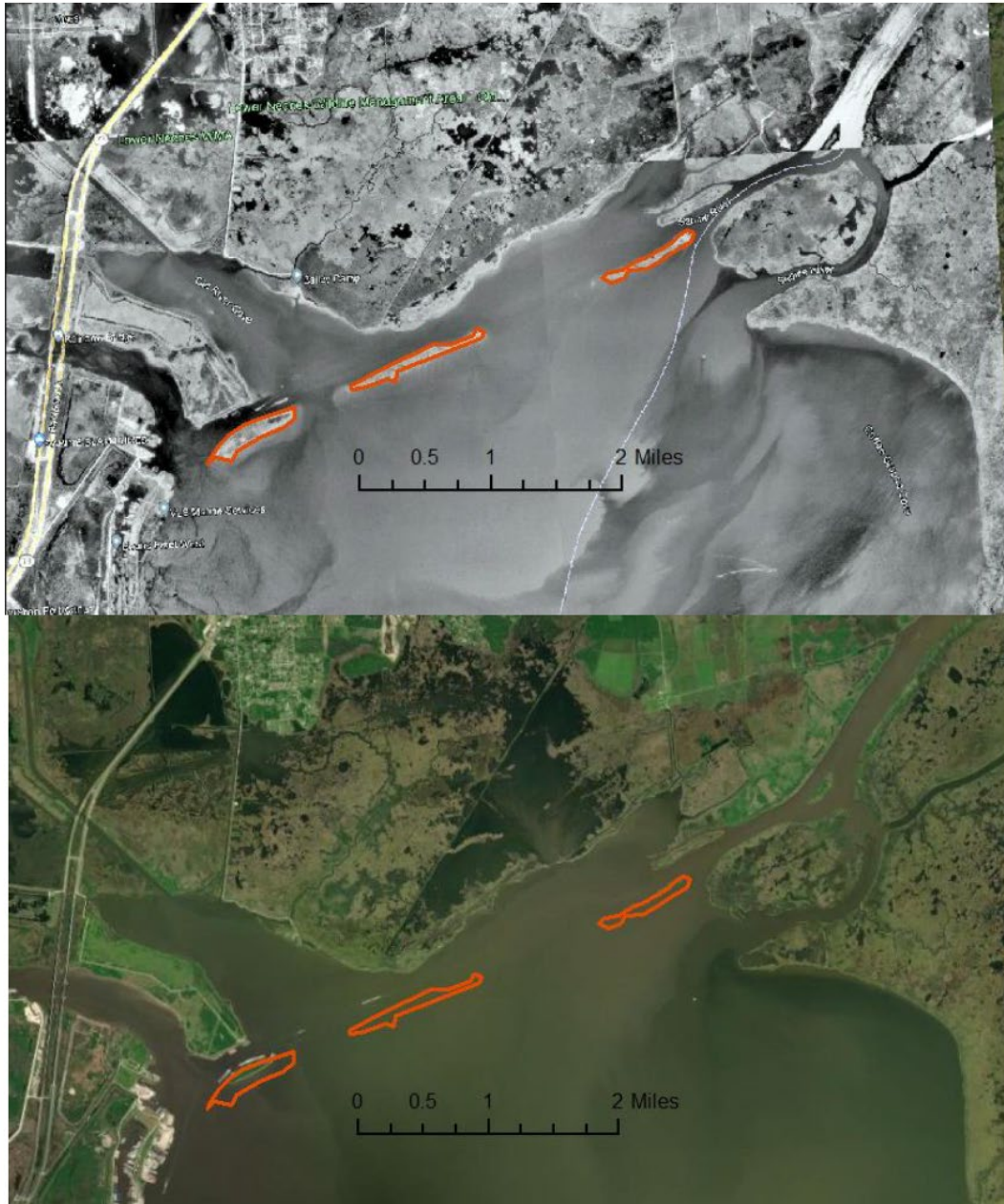
Figure 17. The outline of the historic islands around Old River Cove in 1989 (top) and present-day (below).

Figure 18. The full configuration of modeled islands.

Similarly, the TAC identified the top vulnerabilities in Region 3 as habitat loss and bay shoreline erosion, so the projects modeled around Corpus Christi Bay were mainly focused on conserving habitat and stabilizing shorelines. Corpus Christi Bay area was selected for with-project modeling in Region 3 as the area presents a highly populated area encompassing diverse natural environments, such as barrier island brackish-salt marshes and fresh marshes along the Nueces River Delta. SLR modeling results indicate that these environments are at risk of conversion to open water by 2100. With-project modeling in this region concentrated on multiple projects dispersed across vulnerable locations with varying natural and built environment conditions, such as North Beach, Flour Bluff, and the backside of Mustang Island. The SLAMM model was executed solely for the intermediate-low SLR scenario, as higher scenarios would result in the complete inundation of the landscape within the region. The kinds of projects modeled include: BUDM, living shorelines, and shoreline armoring (Figure 19 and Table 9).

Figure 19. Location of modeled resiliency projects in Region 3 for the with-project modeling.

Table 9. Details of different resiliency project types modeled in Region 3 for the with-project modeling.

Project Concept	Locations	Desired Outcome	Models Used	Inputs Altered/Updated	Output Analysis
Dredge Placement (BUDM)	Nueces River Delta, Port Aransas Nature Preserve, Mustang Island, North Padre Island	Protect habitats from SLR by boosting elevation	SLAMM, SWAN	Elevation, slope, Manning's N, vertical accretion rates	Analysis of land cover changes, wave height and water surface elevation reduction
Living Shoreline	Nueces River Delta, North Beach	Build a marsh and breakwaters to reduce	SLAMM, SWAN	Land cover, elevation, slope, Manning's N	Analysis of wave height and water surface elevation reduction

		wave energy and protect exposed and eroding habitats			
Shoreline Armoring	Portland, Flour Bluff (Laguna Shores)	Protect communities and industry from flood risk	SLAMM, SWAN	Elevation, Manning's N, add structure in SMS	Analysis of wave height and water surface elevation reduction

In Region 3, various methods were applied for each project type, as described below:

1. Shoreline Armoring:
   - The digital elevation model (DEM) was altered to incorporate elevation changes resulting from the installation of breakwaters, sills, and other structures. The input dike file was also modified to represent the barrier.
2. Living Shorelines:
   - Potential project areas were identified using living shoreline site suitability approaches and analyzing land cover data. The DEM was altered to account for elevation changes due to breakwaters, sills, and other living shoreline components, similar to the shoreline armoring process. Additionally, low marsh land cover was added behind the barrier to the existing shoreline.
3. Dredge Placement and Wetland Restoration:
   - This method was applied similarly to the approach used in Region 1A, adding 0.2m of elevation every 25 years to wetland areas to allow them to keep pace with the rate of the intermediate-low SLR scenario.

The results from the landscape change modeling done in these marsh conservation, island restoration, and BUDM-type resiliency projects were integrated into the storm surge and wave model. The updated future land cover obtained from the landscape change modeling in these project sites was inputted into the ADCIRC+SWAN model for the "with-project" modeling. Similarly, the shoreline armoring project in Region 3 was implemented by updating the 2100 DEM, which was incorporated into ADCIRC+SWAN modeling by updating the mesh file.

The same post-processing steps used for the future condition storm surge modeling were performed to obtain inputs for the "with-project" modeling. The Manning's n values of the land cover within the project area where the SLAMM modeling was done were updated in the future condition Manning's n file. This updated Manning's n file was interpolated to the ADCIRC nodal attribute file (fort.13) to model storm surge under 2100 conditions with the resiliency projects. Similarly, the topographic surfaces predicted by the SLAMM model within the project sites were updated in the future condition ADCIRC mesh file prepared for the future condition storm surge modeling. Two Category 2 storms that made landfall in the vicinity of these selected project locations were selected for the storm surge and wave modeling. Storm 160 was selected for Region 1, and Storm 416 was selected for Region 3. Figure 20 shows the 2100 land cover after combining the C-CAP data and 2100 USGS land cover data around the selected resiliency projects in Region 1A, and Manning's n value based on the combined land covers.

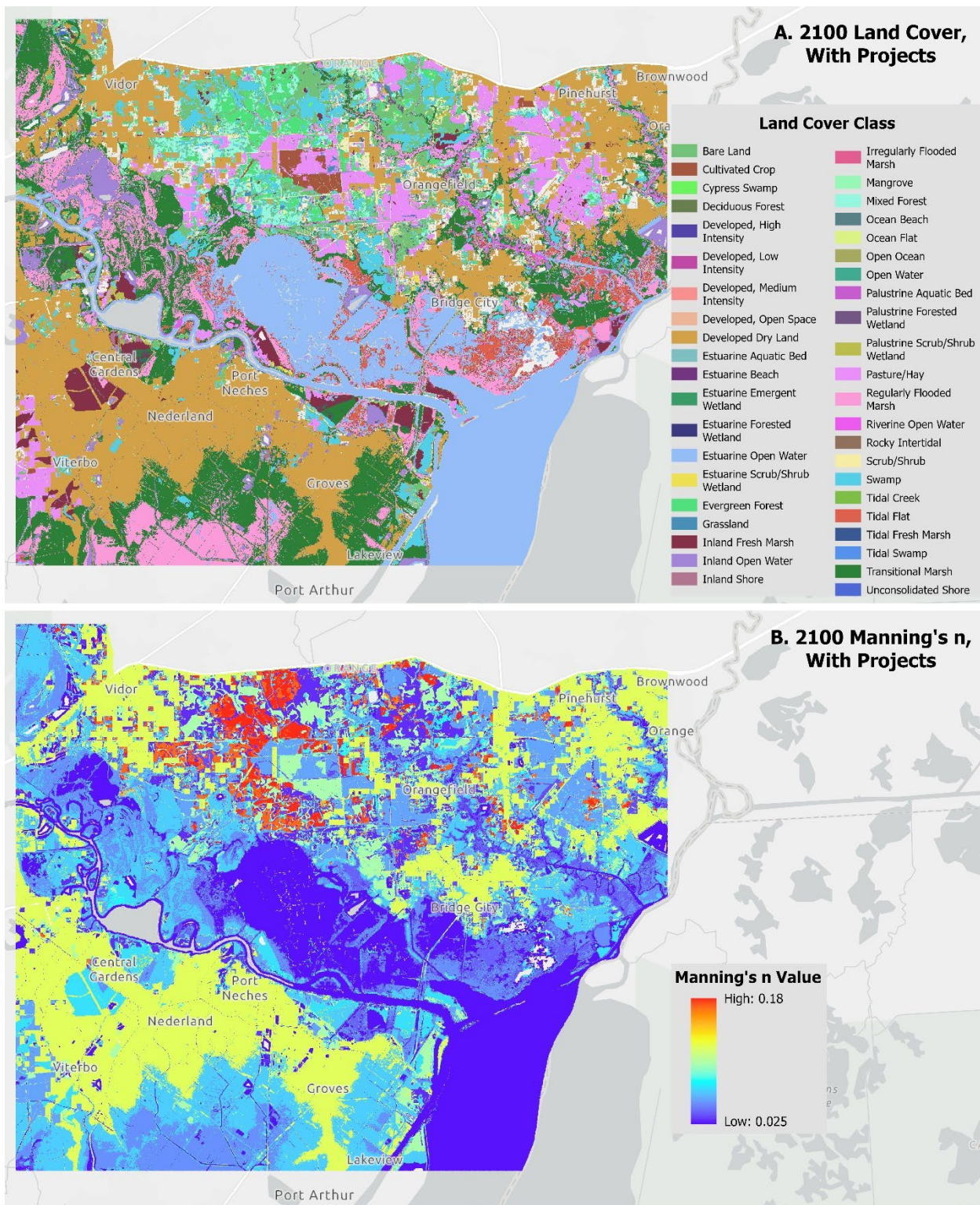**A. 2100 Land Cover, With Projects**

Land Cover Class

Bare Land	Irregularly Flooded Marsh
Cultivated Crop	Mangrove
Cypress Swamp	Mixed Forest
Deciduous Forest	Ocean Beach
Developed, High Intensity	Ocean Flat
Developed, Low Intensity	Open Ocean
Developed, Medium Intensity	Open Water
Developed, Open Space	Palustrine Aquatic Bed
Developed Dry Land	Palustrine Forested Wetland
Estuarine Aquatic Bed	Palustrine Scrub/Shrub Wetland
Estuarine Beach	Pasture/Hay
Estuarine Emergent Wetland	Regularly Flooded Marsh
Estuarine Forested Wetland	Riverine Open Water
Estuarine Open Water	Rocky Intertidal
Estuarine Scrub/Shrub Wetland	Scrub/Shrub
Evergreen Forest	Swamp
Grassland	Tidal Creek
Inland Fresh Marsh	Tidal Flat
Inland Open Water	Tidal Fresh Marsh
Inland Shore	Tidal Swamp
	Transitional Marsh
	Unconsolidated Shore

B. 2100 Manning's n, With Projects

Manning's n Value
High: 0.18
Low: 0.025

Figure 20. Map showing (A) The 2100 land cover "with-project" scenario around the selected resiliency projects in Region 1A with added C-CAP data and 2100 USGS model output, and (B) The 2100 Manning's

n values for the 2100 "with-project" land cover classes used for input into the future condition storm surge and wave modeling.

Geohazards Mapping

The geohazards map is a synthesis of all the modeling work done for the TCRMP in one product as a map. It describes the effect of ongoing geological processes including relative sea-level rise (RSLR), erosion, historic washover locations, storm surge inundation, and future evolution of critical environments including wetlands, dunes, and beaches in response to RSLR and storm surge in the next 80 years. The map helps inform planners, decision-makers, and the public about the challenges and limitations of living on the coastal plain. The geohazards map also provides a picture of how the Texas coastal plain may look in the next 80 years in response to the effects of coastal hazards.

The geohazards maps show both the present hazardous areas and information about the future spatial location of critical coastal environments. They are different than coastal flood maps as they not only delineate hazardous areas but also provide a holistic understanding of how the coastal plain may look in the future, thus allowing the identification of critical areas to avoid or preserve. They also provide important information for developing resiliency and adaptation strategies for RSLR and storm surge inundation on the Texas coastal plain.

The geohazards map was developed with a detailed mapping of the different geo-environments currently present on the Texas coastal plain as well as modeling the future evolution of critical coastal environments along the Texas coast. It also incorporates the impacts of both present storm surge and enhanced storm surge caused by higher sea levels and changes in land cover in the future along the coastal plain. Several map-based inputs resulting in a comprehensive geo-environment spatial inventory were used to create the geohazards map that shows the relative susceptibility to negative impacts on the natural and built environments along the coast.

Development of the Geohazards Map

In response to the need for guiding development toward safer areas from the most populated barrier islands on the Texas coast, HRI developed a series of geohazards maps for three barrier islands: Galveston, Mustang and North Padre, and South Padre Islands in the past. A similar but an improved approach was taken to develop the geohazards map of the whole Texas coastal plain. These maps show hazardous areas coupled with information about the future spatial distribution of critical environments. These maps aid the assessment of an area's resilience by displaying where assets are subject to geohazards. The geohazards map was developed by combining multiple data layers through data development and modeling. Two sets of geohazards maps were developed for two sea-level rise scenarios modeled – Intermediate Low (0.5 m of GSLR by 2100) and Intermediate High (1.5m of GSLR by 2100).

An SLR transition model (SLAMM) and an integrated wave and circulation model (SWAN+ADCIRC) were used to assess the vulnerabilities to RSLR and associated enhanced storm surge caused by higher sea levels and changes in land cover in the year 2100. Details of these modeling are presented earlier in this report and Subedee et al. 2019. By incorporating detailed lidar DEMs, the latest land-cover dataset, and geomorphic analyses in these models, a series of maps of the current and future distribution of critical geo-environments were developed and their hazardous potential related to RSLR, storm surge, and

erosion are ranked. The six geohazard potentials in the map are based on this ranking which are described in the following section.

Storm Surge Vulnerability Mapping

The low-lying and gently sloping Texas coastal plain is highly vulnerable to storm surge and waves caused by hurricanes. Storm surge is also one of the top vulnerabilities listed by the Technical Advisory Committee (TAC) members who provide critical input throughout the entire planning process. Furthermore, the storm surge risk assessment provides the basis for risk mitigation and related decision-making for adaptation and resilience. Therefore, it is both sensible and imperative to incorporate exposure to the risks of storm surge and waves in the geohazards mapping.

A storm surge vulnerability map was developed by considering simulated storm surge inundation due to nineteen storms modeled. These selected storms of varied characteristics pass throughout the Texas coast and provide good coverage along the coast as shown by their radius of maximum wind in Figure 15. Table 7 summarizes the storm characteristics for each of the selected storms and Figure 14 shows the storm tracks. A total of 57 ADCIRC+SWAN model simulations were forced using meteorological wind and pressure fields for each of the nineteen hurricane events. The nineteen hurricane events were simulated on the present landscape, and again on the two future 2100 landscapes - Intermediate Low (0.5 m of GSLR by 2100) and Intermediate High (1.5m of GSLR by 2100). The maximum water surface elevation (MAXELE) was derived for each storm simulation and analyzed along the whole Texas coast which resulted in 57 MAXELE scenarios.

In order to calculate the storm surge vulnerability score along the Texas coast using these 57 scenarios, each node in the computational mesh is examined to find out how many times it is inundated in the 57 scenarios. It is then divided by the total 57 scenarios considered to obtain the storm surge vulnerability normalized index of the range 0 - 1, where a value of 1 means an area is inundated in all 57 scenarios, and 0 means it is not inundated in any scenarios. Once the index value in the range of 0 – 1 is assigned to each node in the computational mesh, a storm surge normalized vulnerability index raster was generated using Kernel Smoothing interpolation. The interpolation was done by breaking down the Texas coast into multiple regions to get better interpolation results. For Kernel Smoothing, the fifth-order polynomial function was used as a kernel function.

The Geohazards Maps

The geohazards map presents a synthesis of datasets developed through various modeling and the latest datasets obtained from multiple sources. It incorporates the topographic DEMs developed using the latest lidar surveys, future land cover data modeled by applying SLAMM, a storm surge vulnerability map developed by modeling multiple storms under three sea-level scenarios, and various publicly available datasets. It not only shows areas that are presently exposed to hazardous conditions that might be generally protected by regulations but also shows areas that are not protected and should receive special management consideration. It also shows the vulnerable infrastructure that will be exposed to hazardous conditions in the future and requires special attention if progress is to be made in how we live with RSLR. The geohazards map shows six geohazard potential categories: Extreme, Imminent, Future Flooding, High, Moderate, and Low.

The presently vulnerable habitats that will be open water in the future and historic storm washover channels were designated as **Extreme** geohazard potential areas. The future open water layer used in

the Extreme category is based on the SLAMM modeling results. **Imminent** geohazard potential areas include the presently critical environments such as freshwater wetlands, transitional wetlands, regularly flooded estuarine wetlands, tidal flats, and beach/foredune systems. These areas are designated based on the latest NWI dataset. Areas of present development and road that are expected to flood due to sea level rise in the future are designated as a **Future Flooding** geohazard potential. The present development for this category was based on the 2019 National Land Cover Database (NLCD) dataset where classes 21 - 24 represent the different types of development, and the present road network was based on the latest road layer by the Texas Department of Transportation (TxDOT).

The presently upland areas projected to become critical environments in the future due to sea level rise are designated as **High** geohazard potential areas and are based on the SLAMM modeling results. Areas designated as having **Moderate** geohazard potential are uplands that are neither currently nor expected to become critical environments in the future. Furthermore, these areas are prone to storm surge flooding causing them to be inundated during a storm event with a storm surge normalized vulnerability index value greater than 0.5. Finally, the remaining upland areas that are less susceptible to geohazards are designated as having a **Low** geohazard potential as they are inland at higher elevation or interior location to the island. These areas have a storm surge normalized vulnerability index value of less than 0.5. Therefore, the Moderate and Low geohazard potential areas were differentiated based on the storm surge normalized vulnerability index value considering 0.5 as a cutoff value. A value of 0.5 means an area is inundated by at least half of the total 57 storm scenarios considered.

Results

Sea Level Rise Modeling

This section presents the results from the sea level rise modeling part of the study. Firstly, the study examines the entire Texas coast, comparing the 2100 land cover outputs in both intermediate-low and intermediate-high sea level rise (SLR) scenarios to the initial conditions in the form of maps, graphs, and tables. The Texas coast is also compared to separate regions.

Subsequently, a more detailed approach is taken for each of the four regions, providing information on the vulnerability that each region faces as the sea level rises, altering the landscape into the future. The analysis offers insights on how the projected changes are likely to affect the region's environment, and community, highlighting the potential risks that may arise from sea level rise.

SLAMM includes 21 different land cover classes which are condensed into 6 classes for this analysis.

Table 10 shows what classes are aggregated for this study.

Table 10. Aggregation of SLAMM output land cover classes to new classes for change analysis

SLAMM Codes	SLAMM Description	New Code	New Description
1	Developed Dry Land	1	Developed Dry Land
2	Undeveloped Dry Land	2	Undeveloped Dry Land
3, 4, 5	Non-tidal Swamp, Cypress Swamp, Inland-Fresh Marsh	3	Freshwater, non-tidal
6, 7, 8, 9, 20, 23	Tidal-Fresh Marsh, Trans. Salt Marsh, Regularly-Flooded Marsh, Mangrove, Irreg.-Flooded Marsh, Tidal Swamp	4	Saltwater and Brackish tidal marshes
12, 22, 10, 11, 13, 14	Ocean Beach, Inland Shore, Estuarine Beach, Tidal Flat, Rocky Intertidal, Ocean flat	5	Beaches and flats
15, 16, 17, 19	Inland Open Water, Riverine Tidal, Estuarine Open Water, Tidal Creek, Open Ocean	6	Open water

Coastwide

The Texas coast is predicted to experience significant effects from sea level rise, which will vastly alter the landscape by 2100. Figure 21 shows the current and future landscapes in 2100 under intermediate-low and intermediate-high sea level rise scenarios, while Figure 22 shows the areal changes in square miles by land cover type. Figure 23 and Figure 25 depict individual losses and gains of freshwater and saltwater marsh, and open water in the intermediate-low scenario, and Figure 24 and Figure 26 do the same in the intermediate-high scenario. With both 0.5 meters and 1.5 meters of sea level rise, combined with varying subsidence/uplift rates along the coast by 2100, a significant decrease in the amount of inland-fresh marshes and swamps is observed. Slightly more than 60% of their initial area is predicted to remain by the year 2100 in the intermediate-low scenario, and less than 27% of their initial area is predicted to remain by the year 2100 in the intermediate-high scenario (Table 11). The model suggests that these habitats will transition to transitional scrub-shrub wetlands, regularly flooded marsh, or tidal flats. Almost all saltwater and brackish marshes seen along the Texas coast are expected to be affected by sea level rise, with both loss through inundation and gain by upward migration. The lost low marsh area is likely to be converted to tidal flat or open water, while salt and brackish marshes will migrate

landwards if migration space is available, contributing to a net gain of 86% by 2100 in the intermediate-low scenario and 82% in the intermediate-high scenario.

In addition to impacts on the natural environment, a substantial amount of developed land is also projected to be inundated by 2100 in both scenarios. A total of 108 square miles of developed land along the coast is expected to be impacted by 0.5 meters of sea level rise, and the number is predicted to increase to 145 square miles with 1.5 meters of sea level rise. Most of these areas at risk are low-lying coastal communities and critical infrastructure, including water treatment and power plants. These vulnerable areas will be discussed in subsequent sections.
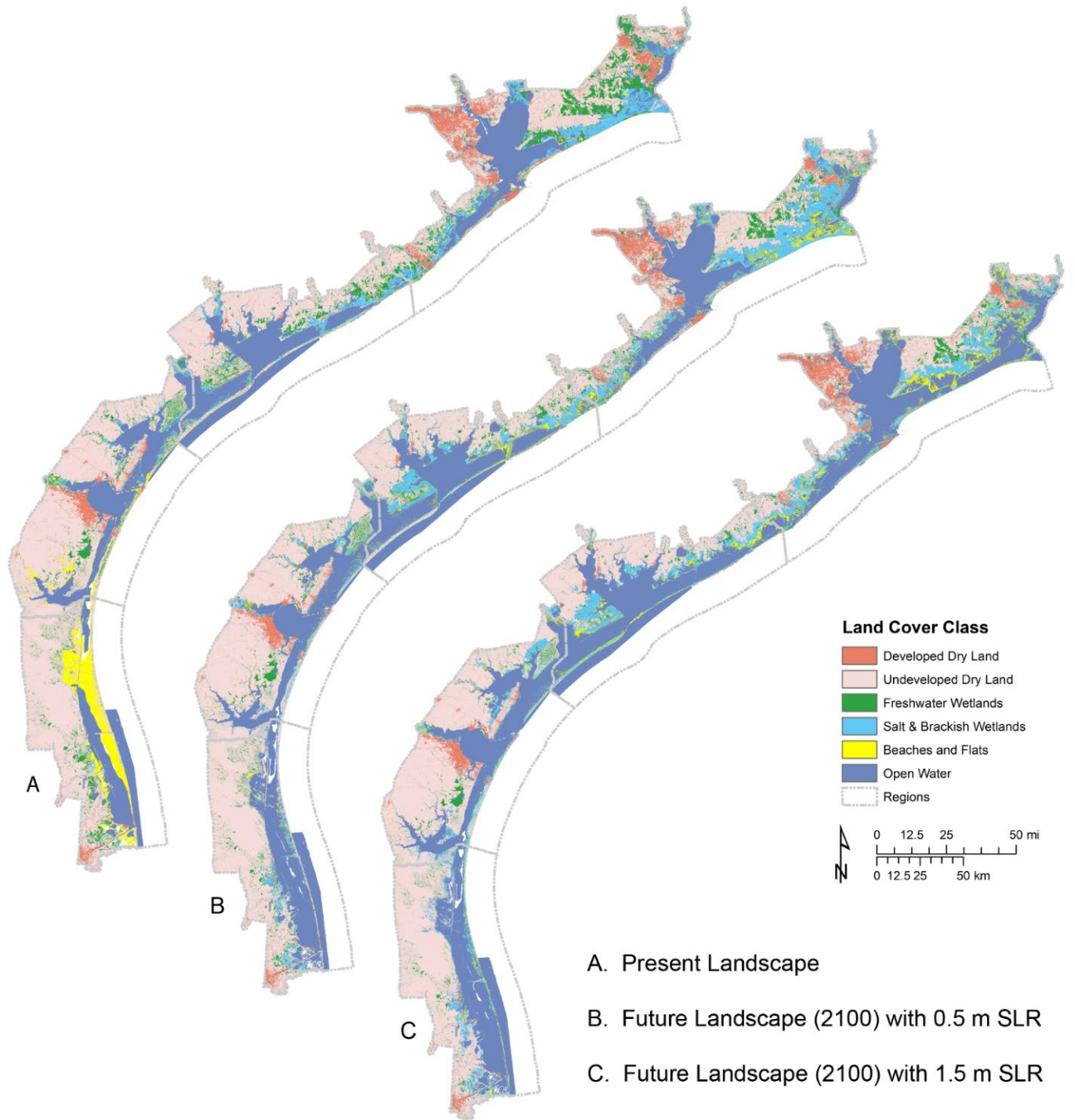
Figure 21. Comparison of Present Landscape and future landscapes along the Texas coast. (A) Present Condition (2019) land cover data used by SLAMM. (B) Future Condition with 0.5 m SLR in 2100 land cover output from SLAMM. (C) Future Condition with 1.5 m SLR in 2100 land cover output from SLAMM.

Texas Coast Landscape Change
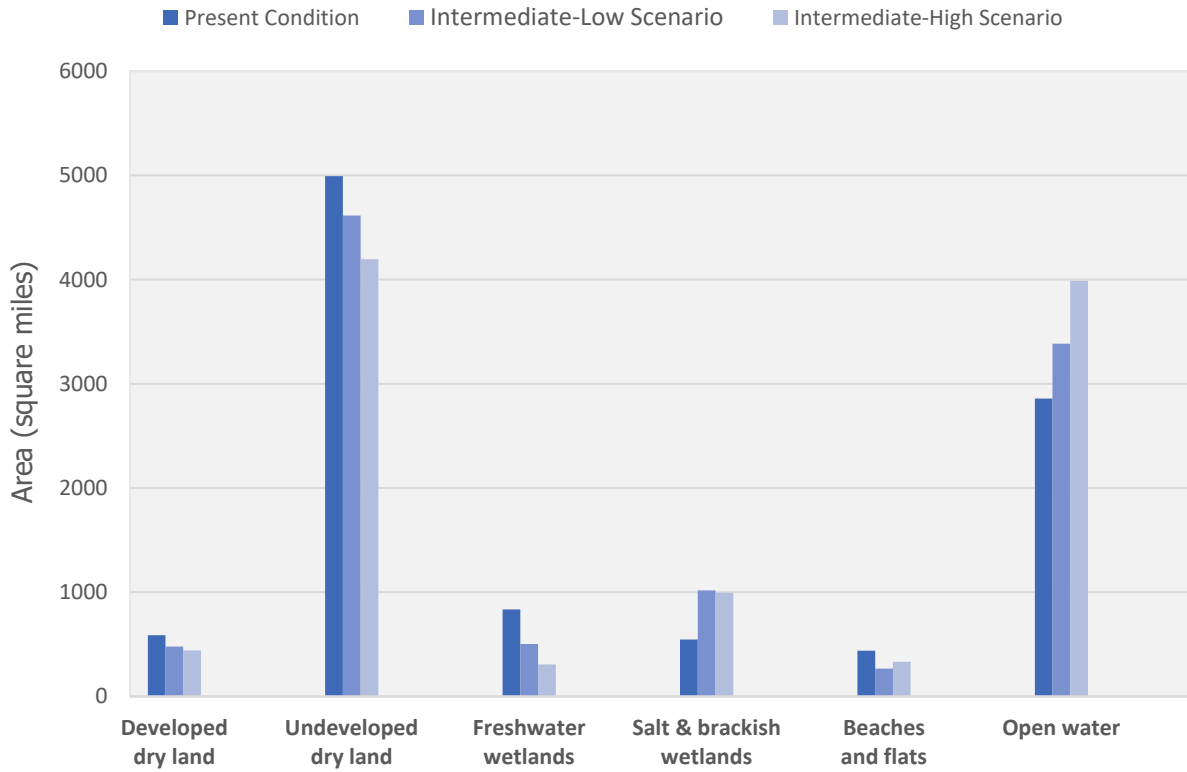
Figure 22. Areal changes (in square miles) of individual land cover types between Present Condition and Future Conditions along the Texas coast.

Table 11. Areal and percent difference of each land cover type between Present Condition (2019) and two Future Conditions (2100) along the Texas coast.

Land cover class	2019 (sq. miles)	Intermediate-Low (sq. miles)	% Difference	Intermediate-High (sq. miles)	% Difference
Developed dry land	586.99	479.17	-18.37	442.44	-24.63
Undeveloped dry land	4991.9	4613.78	-7.57	4196.02	-15.94
Freshwater wetlands, non-tidal	834.91	503.36	-39.71	305.95	-63.36
Salt & brackish emergent wetlands, tidal	546.11	1016.76	86.18	994.99	82.20
Beaches and flats	438.01	266.88	-39.07	332.26	-24.14
Open water	2858.2	3385.34	18.44	3987.59	39.51
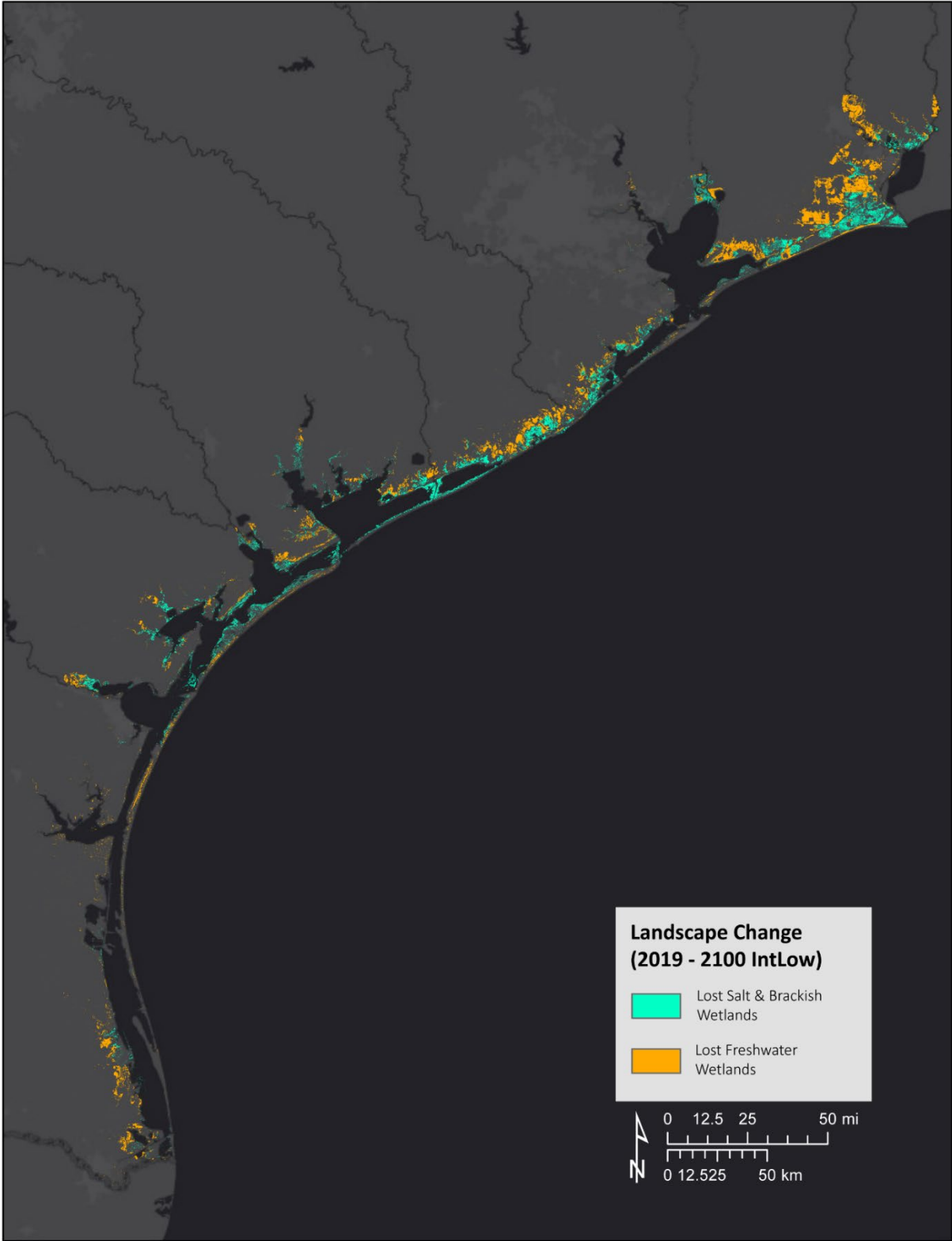
Figure 23. Map showing the extent of lost salt and brackish water wetlands and freshwater wetlands by the year 2100 in the intermediate-low SLR scenario.
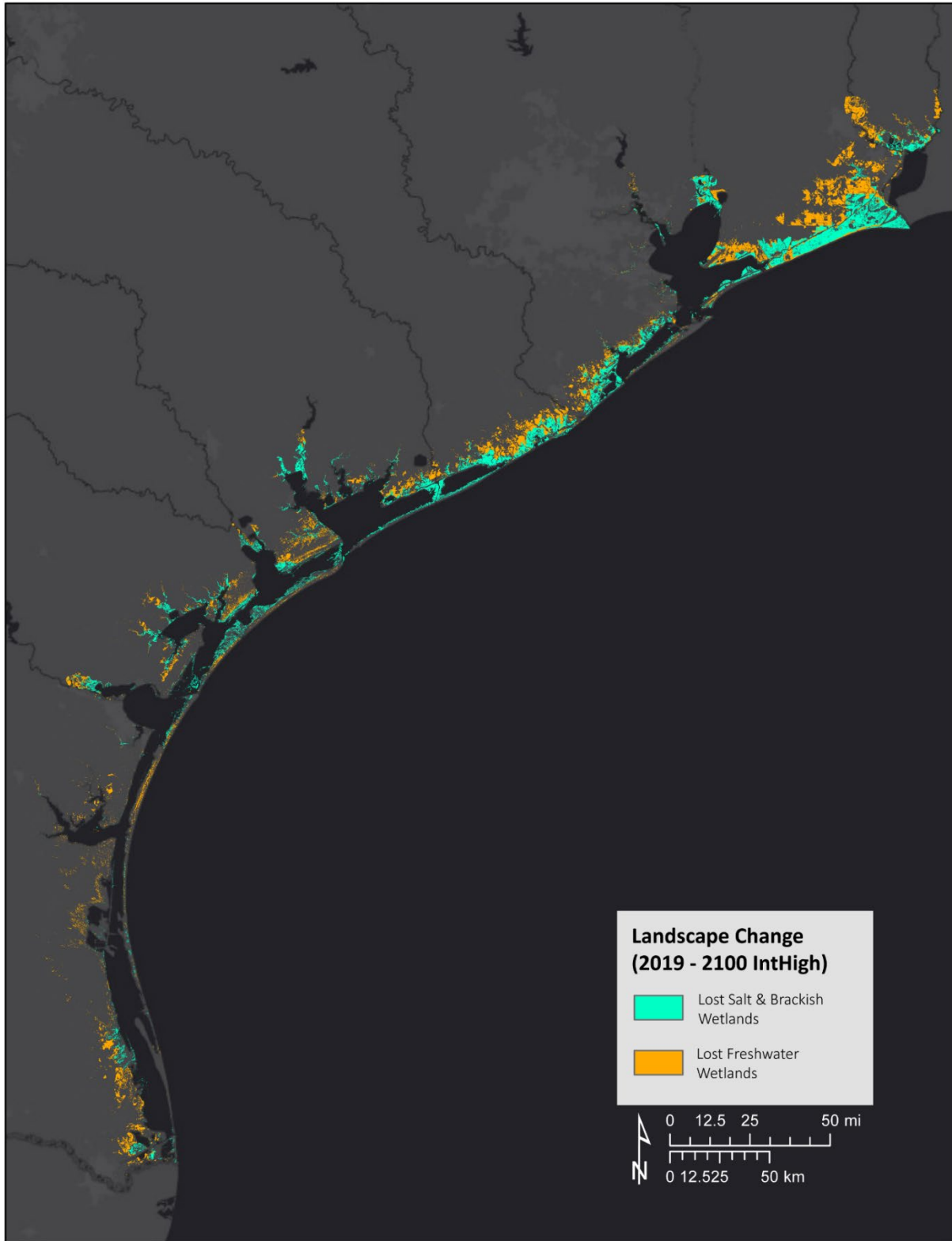
Figure 24. Map showing the extent of lost salt and brackish water wetlands and freshwater wetlands by the year 2100 in the intermediate-high SLR scenario.
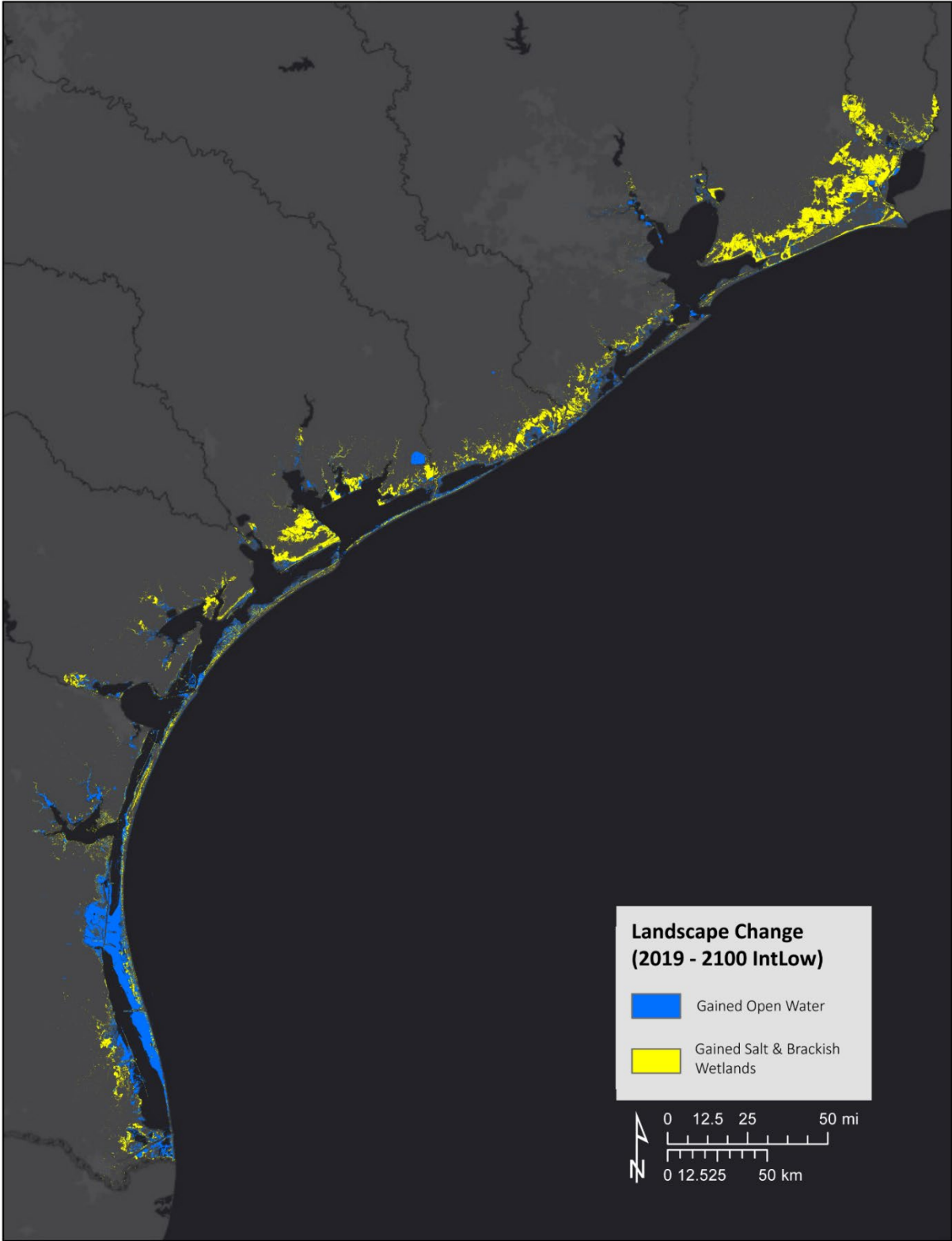
Figure 25. Map showing the extent of gained open water and salt and brackish wetlands by the year 2100 in the intermediate-low SLR scenario.
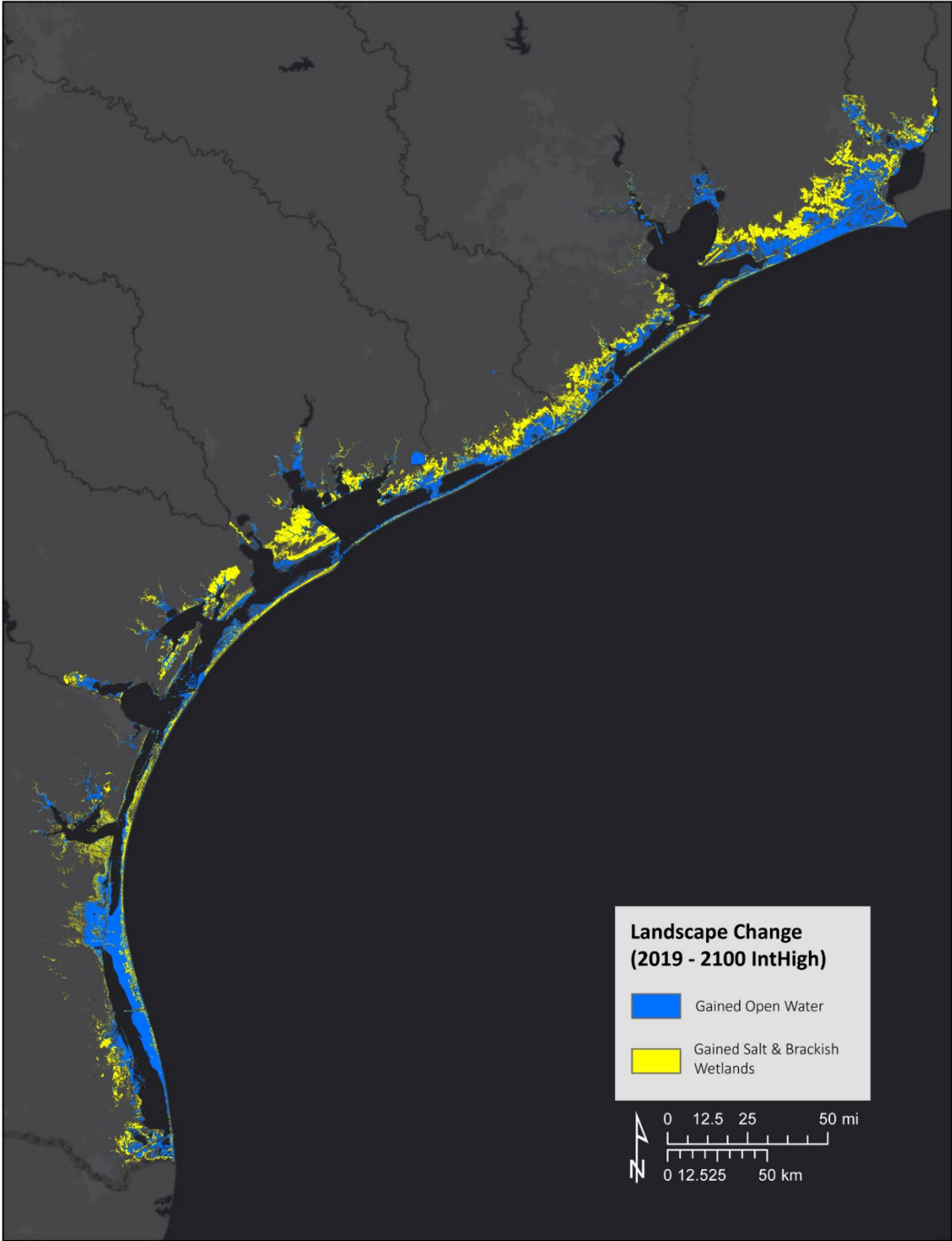
Figure 26. Map showing the extent of gained open water and salt and brackish wetlands by the year 2100 in the intermediate-high SLR scenario.

The area of open water is expected to increase by 18% and 40% by the year 2100 under the intermediate-low and intermediate-high SLR scenarios. This expansion of open water and loss of essential coastal habitats has the potential to increase the vulnerability of the coast to future hazards such as storm surge and nuisance flooding. Figure 27 and Figure 28 show relative vulnerability to land loss along the coast shown in a hexagonal grid, where land loss signifies any type of land (excluding intertidal flats) that has converted to open water by the year 2100 in the intermediate-low and intermediate-high SLR scenarios.

The hexagonal grid used in this analysis was developed by the Strategic Conservation Assessment of Gulf Coast Landscapes (SCA) project for the Gulf of Mexico Coastal Region (Shamaskin et al, 2019). Each hexagon in the grid has a side length of 0.61 km and an area of 1 km^2, or 240.1 acres. To find the amount of land lost by 2100 in each hexagon, the area of land in the initial input land cover dataset is compared against the modeled 2100 land cover outputs using GIS operations to quantify where and how much of present-day land has turned to open water over time. This is done by assessing the mean and standard deviation of the acres of land loss in each hexagon in the grid as in Figure 27 and Figure 28. On average, the Texas coast is predicted to lose an average of 55 acres of land to open water within each hexagon under the intermediate-low SLR scenario in Figure 27 and an average of 120 acres of land to open water within each hexagon under the intermediate-high SLR scenario in Figure 28. The map shows more vulnerable trends occurring on the backside of barrier islands and river deltas where low-lying coastal habitats reside. The most vulnerable habitats to become open water are tidal flats and low-lying salt and brackish marshes.
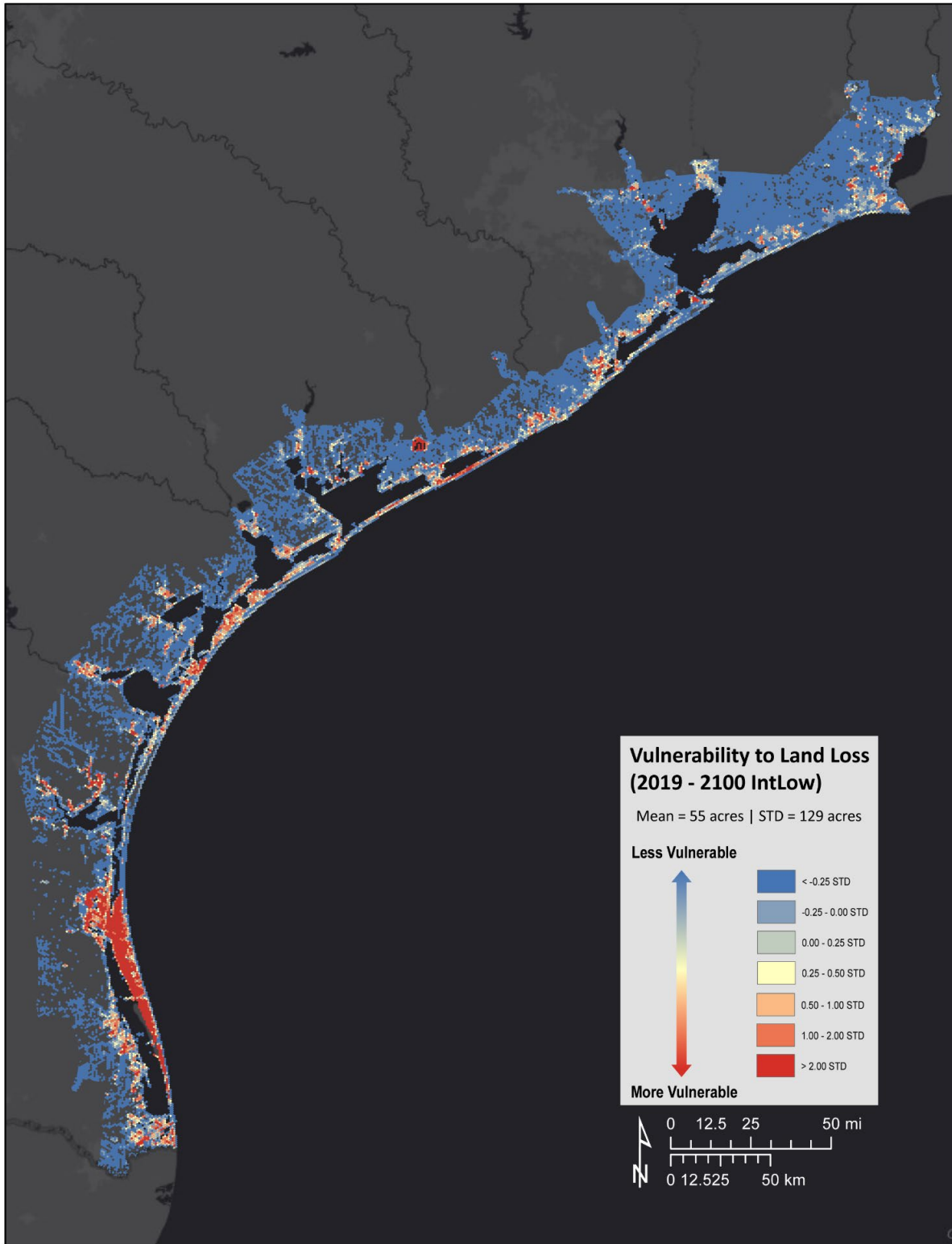
Figure 27. Map showing relative vulnerability to land loss, where land loss signifies any type of land (excluding intertidal flats) that has converted to open water by the year 2100 in the intermediate-low SLR scenario. The map is symbolized by standard deviations (STD) from the mean.
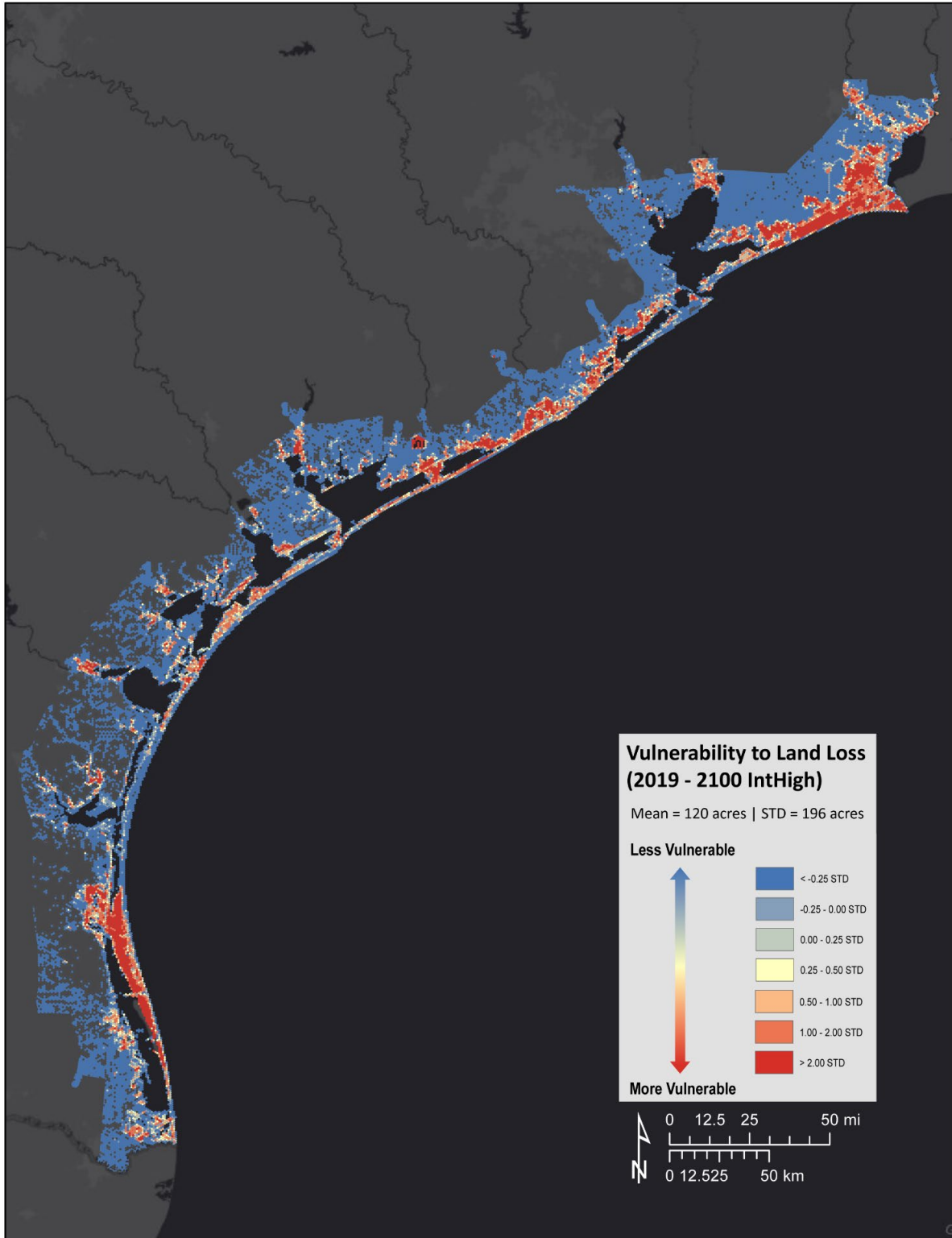
Figure 28. Map showing relative vulnerability to land loss, where land loss signifies any type of land (excluding intertidal flats) that has converted to open water by the year 2100 in intermediate-high SLR scenario. The map is symbolized by standard deviations (STD) from the mean.

Texas Coast vs. Regions

Each region along the Texas coast has unique characteristics that cause the landscape to change differently than the average trend of the coast. Figure 29 - Figure 30 and Table 12 compare the percent change of each land cover class between the Texas coast and each region in the intermediate-low and intermediate-high scenario. In both SLR scenarios, all regions are predicted to loss developed dry land, undeveloped dry land, and freshwater wetlands, while all regions are predicted to gain salt and brackish wetlands, given that there will be migration space for the wetlands in the future.

Region 1 has a greater percent loss of undeveloped dry land and Region 2 has a greater percent loss of developed dry land in both SLR scenarios. Region 1 also has a greater precent loss of freshwater wetlands in the intermediate-low scenario, but it is greater for Region 2 in intermediate-high scenario. Region 4 is predicted to withstand greater gain in salt and brackish wetlands than all other regions and the coastwide average. The lower rates of RSLR and erosion in Region 3 and Region 4, compared to the upper coast, allow the low marsh environments to keep pace with sea level rise as upland habitats become tidally influenced. The Texas coast is predicted to see an overall loss in beaches and tidal flats, except for the upper coast which sees a net gain in tidal flat habitats as saltwater marshes are eroded. Region 1 and Region 2 contain a large area of salt and brackish wetland habitats than the lower coast, and the lower coast contains a larger area of tidal flats than the upper coast. The large area of tidal flat habitats in Region 4 that exist today are predicted to drown by 2100 which contributes to the largest percent gain of open water for any of the regions in both SLR scenarios.
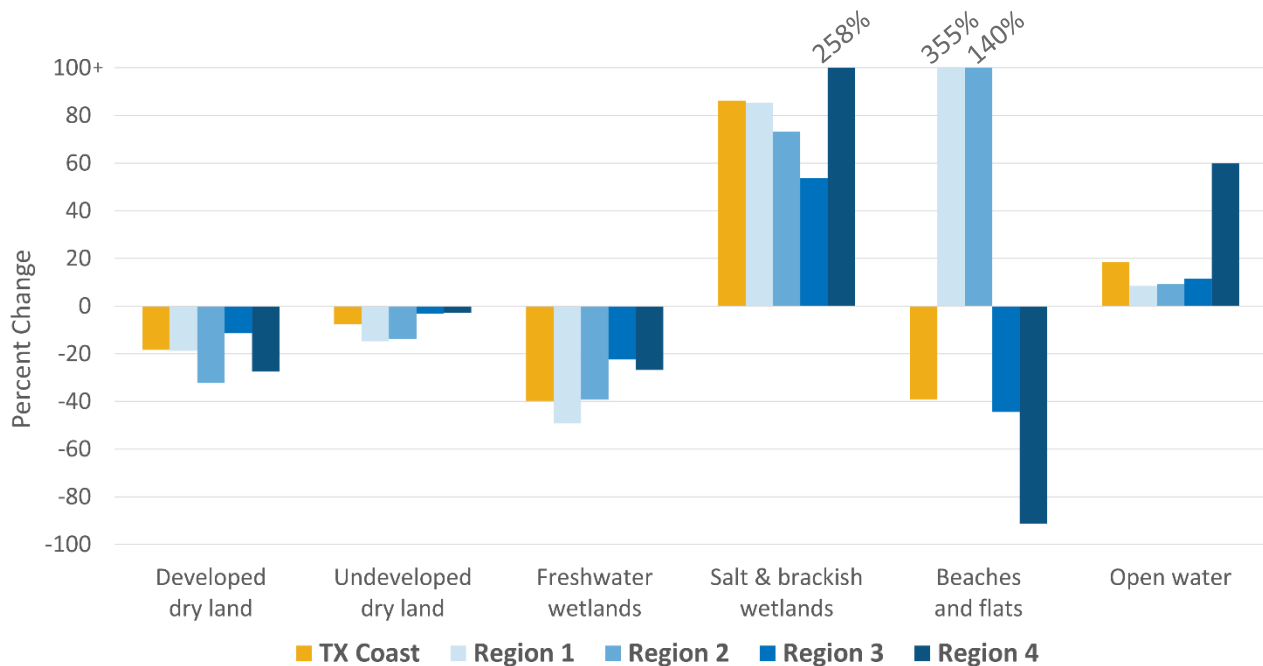
Figure 29. Graph showing the percent change of various land cover types from 2019 to 2100 in the intermediate-low SLR scenario for each region compared to the total change on the entire Texas coast.
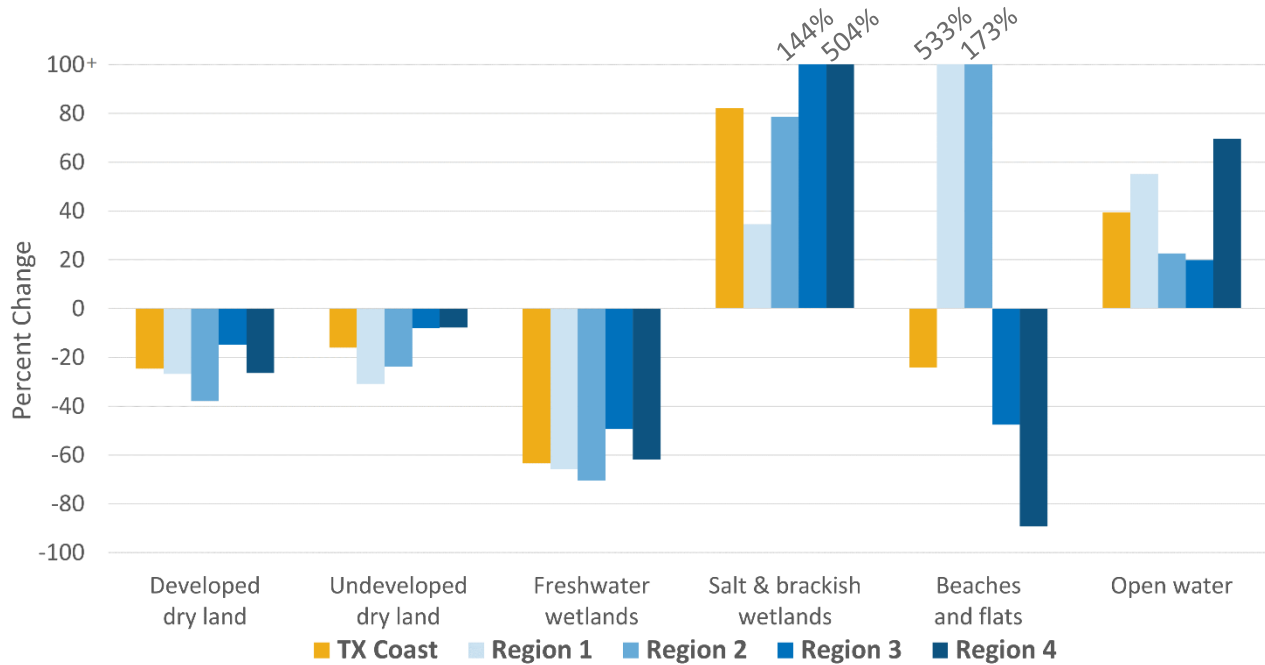
Figure 30. Graph showing the percent change of various land cover types from 2019 to 2100 in the intermediate-high SLR scenario for each region compared to the total change on the entire Texas coast.

Table 12. The percent change of various land cover types from 2019 to 2100 in both intermediate-low and intermediate-high SLR scenarios for each region compared to the total change on the entire Texas coast.

Land cover class	% Change									
	TX Coast		**Region 1**		**Region 2**		**Region 3**		**Region 4**	
	IntLow	IntHigh	IntLow	IntHigh	IntLow	IntHigh	IntLow	IntHigh	IntLow	IntHigh
Developed dry land	-18.37	-24.63	-18.76	-26.73	-32.31	-37.89	-11.36	-14.75	-27.44	-26.36
Undeveloped dry land	-7.57	-15.94	-14.71	-30.89	-13.67	-23.75	-3.04	-8.05	-2.86	-7.80
Freshwater wetlands, non-tidal	-39.71	-63.36	-49.24	-65.86	-39.28	-70.42	-22.41	-49.36	-26.83	-61.77
Salt & brackish emergent wetlands, tidal	86.18	82.20	85.31	34.60	73.31	78.69	53.71	144.18	257.70	503.75
Beaches and flats	-39.07	-24.14	355.23	533.21	140.00	172.71	-44.40	-47.58	-91.26	-89.26
Open water	18.44	39.51	8.49	55.11	9.23	22.64	11.57	19.84	59.91	69.73

Regions

Region 1

Anticipated consequences of SLR are expected to substantially alter the landscape of Region 1 by 2100. Figure 31 displays the current landscape of Region 1 and the projected future landscapes under the

intermediate-low and intermediate-high SLR scenarios for 2100. Table 13 and Figure 32 illustrate alterations in each land cover class. Figure 33 and Figure 34 map individual losses and gains of freshwater and saltwater marshes in Region 1. These figures demonstrate where freshwater wetlands and salt and brackish wetlands that are currently present are predicted to either remain unchanged, be transformed into a different land cover type or open water, or experience growth by 2100 in both SLR scenarios.

Considering 0.5 or 1.5 meters of SLR in addition to varying subsidence/uplift rates within Region 1 by 2100, substantial reductions in inland-fresh marshes and swamps are projected. In the 0.5m scenario, a little more than half of their original area is expected to persist by 2100, representing a combined loss of 49%, while in the 1.5m scenario, the combined loss is 66%. The model forecasts these habitats will transition into transitional scrub-shrub wetlands, regularly flooded marshes, or tidal flats. The majority of saltwater and brackish marshes in Region 1 are also predicted to be affected by SLR. Their initial area amounts to 308 square miles, but by 2100, only 166 square miles of their original area remains in the 0.5m SLR scenario, and even less in the 1.5m SLR scenario, at just 3 square miles. Alterations in salt and brackish marshes involve both expansion and contraction. On one hand, salt and brackish marshes will steadily migrate landward as the migration space becomes available, leading to an anticipated net gain of 85% in the 0.5m SLR scenario or 35% in the 1.5m SLR scenario by 2100. Conversely, Region 1 is also projected to experience a considerable increase in tidal flat habitats, from 29 square miles to 133 and 185 square miles in the 0.5m and 1.5m SLR scenarios by 2100, respectively. The gains of 355% and 533% result from the large areas of salt and brackish marshes being eroded into flats.

By 2100, the area of open water is projected to grow by 8% and 55% in the 0.5m and 1.5m SLR scenarios, respectively. The expansion of open water and the loss of crucial coastal habitats have the potential to heighten the region's susceptibility to future threats such as storm surges and nuisance flooding. Figure 35 and Figure 36 depict the relative vulnerability in both 0.5m and 1.5m SLR scenarios within this region. The maps display the areas that are converted into open water by 2100. On average, 125 acres of land are lost to open water within each hexagon in the 1.5m SLR scenario, while only an average of 23 acres become open water in the 0.5m SLR scenario. The areas most prone to land loss align with those experiencing the highest rates of subsidence. Marshes in these vulnerable areas are not vertically accreting quickly enough to match the rate of RSLR, leading to predictions of submersion by 2100.

Region 1
Land Cover Class

- Developed Dry Land
- Undeveloped Dry Land
- Freshwater Wetlands
- Salt & Brackish Wetlands
- Beaches and Flats
- Open Water

0 5 10   20 mi

N

0 5 10   20 km

A. Present Landscape

B. Future Landscape (2100) with 0.5 m SLR

C. Future Landscape (2100) with 1.5 m SLR
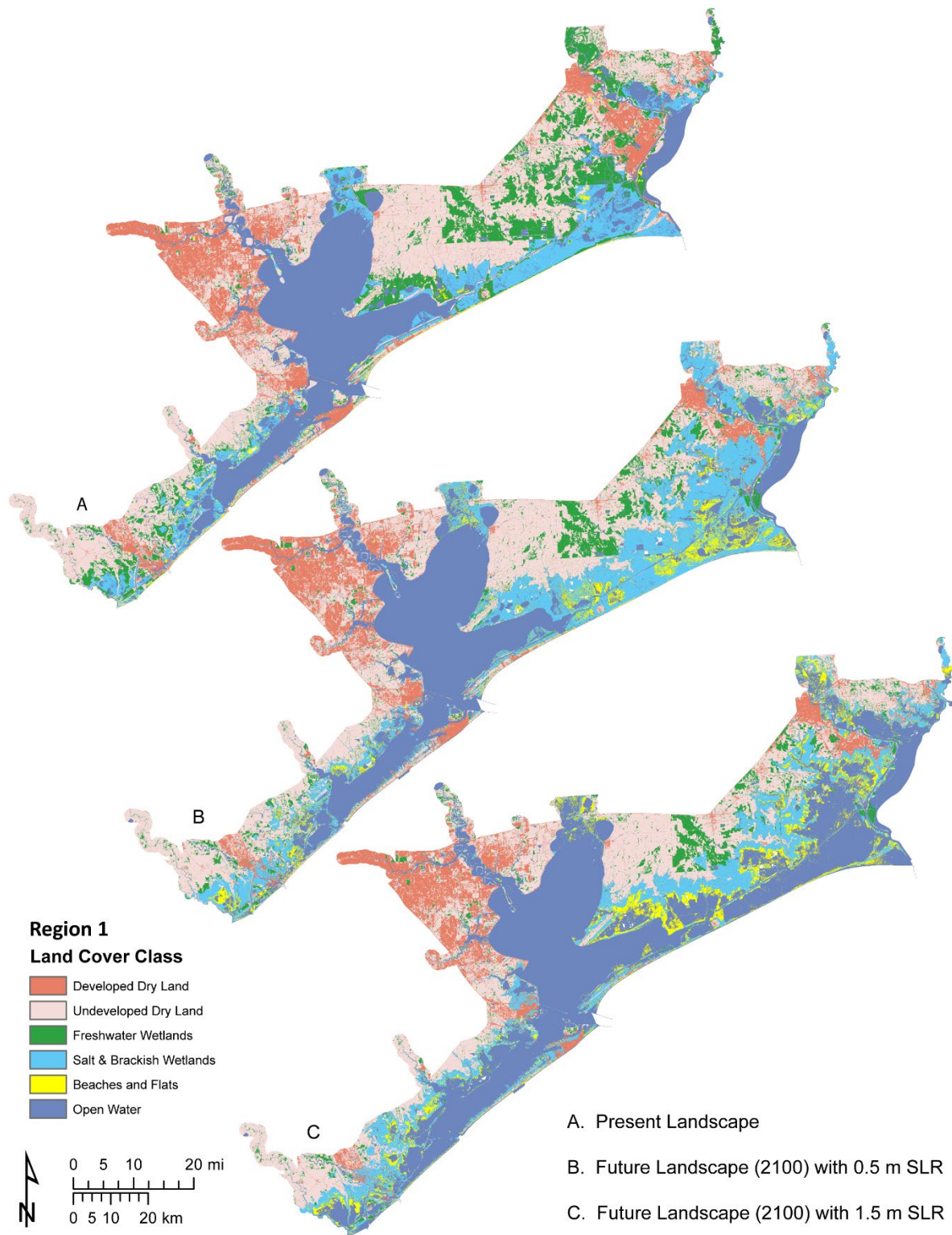
Figure 31. Comparison of Present Landscape and future landscapes in Region 1. (A) Present Condition (2019) land cover data used by SLAMM. (B) Future Condition with 0.5m SLR in 2100 land cover output from SLAMM. (C) Future Condition with 1.5m SLR in 2100 land cover output from SLAMM.
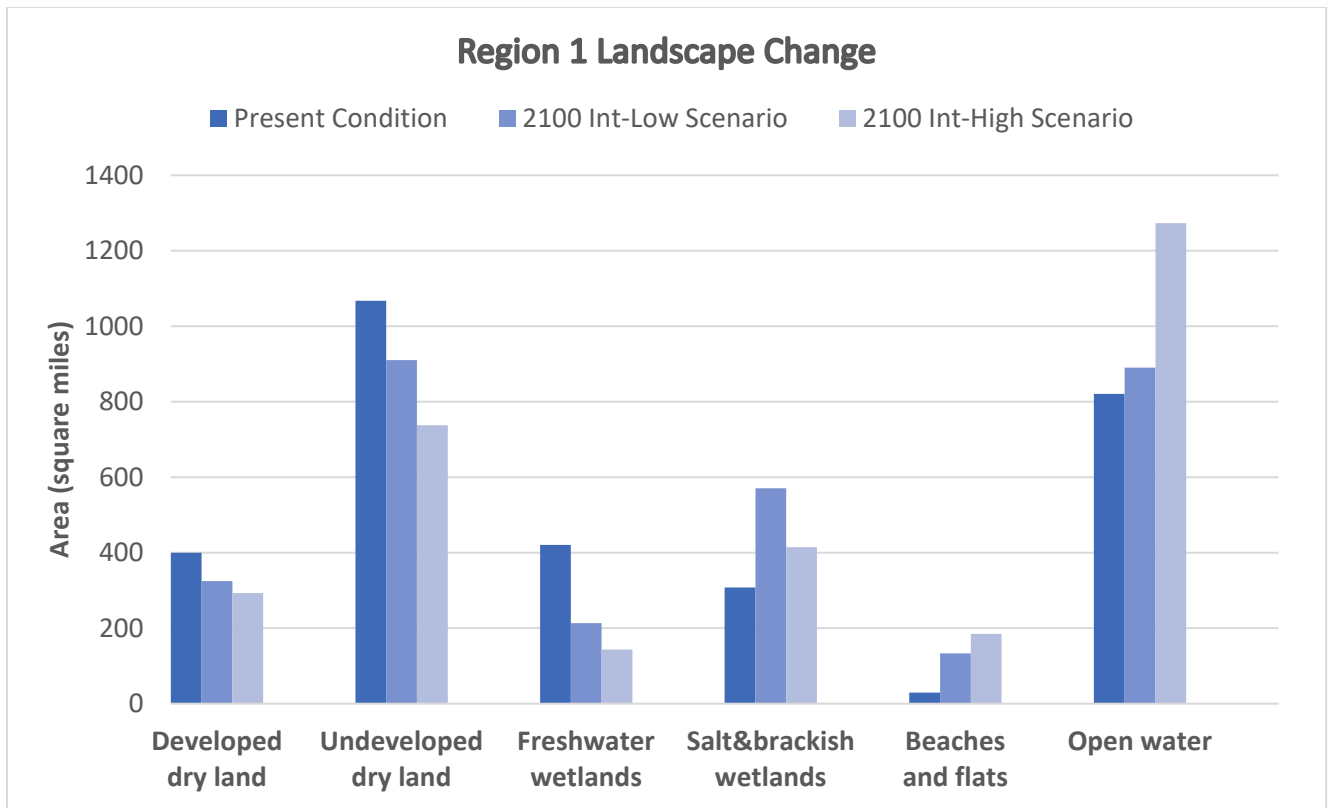
Figure 32. Areal changes (in square miles) of individual land cover types between Present Condition and two Future Conditions in Region 1.

Table 13. The percent difference between land cover types in Region 1 under the Present Condition and two 2100 Future Conditions.

Land cover class	Present Condition (Sq miles)	2100 Int-Low Scenario (Sq miles)	Percent Difference	2100 Int-High Scenario (Sq miles)	Percent Difference
Developed dry land	399.68	324.69	-18.76	292.85	-26.73
Undeveloped dry land	1067.38	910.36	-14.71	737.71	-30.89
Freshwater wetlands, non-tidal	420.48	213.42	-49.24	143.54	-65.86
Salt and brackish emergent wetlands, tidal	308.01	570.77	85.31	414.58	34.60
Beaches and flats	29.24	133.11	355.23	185.15	533.21
Open water	820.78	890.43	8.49	1273.09	55.11

Freshwater Wetlands Change in Region 1 (2019 - 2100)

Surviving
Lost
Gained
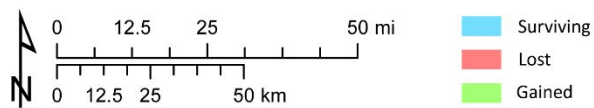
Figure 33. Map showing where freshwater wetlands that exist on the present landscape are modeled to either survive, be converted to another land cover type or open water or gain area by the year 2100 in both Intermediate-Low and Intermediate-High SLR scenarios.

Salt & Brackish Wetlands Change in Region 1 (2019 - 2100)

Surviving
Lost
Gained
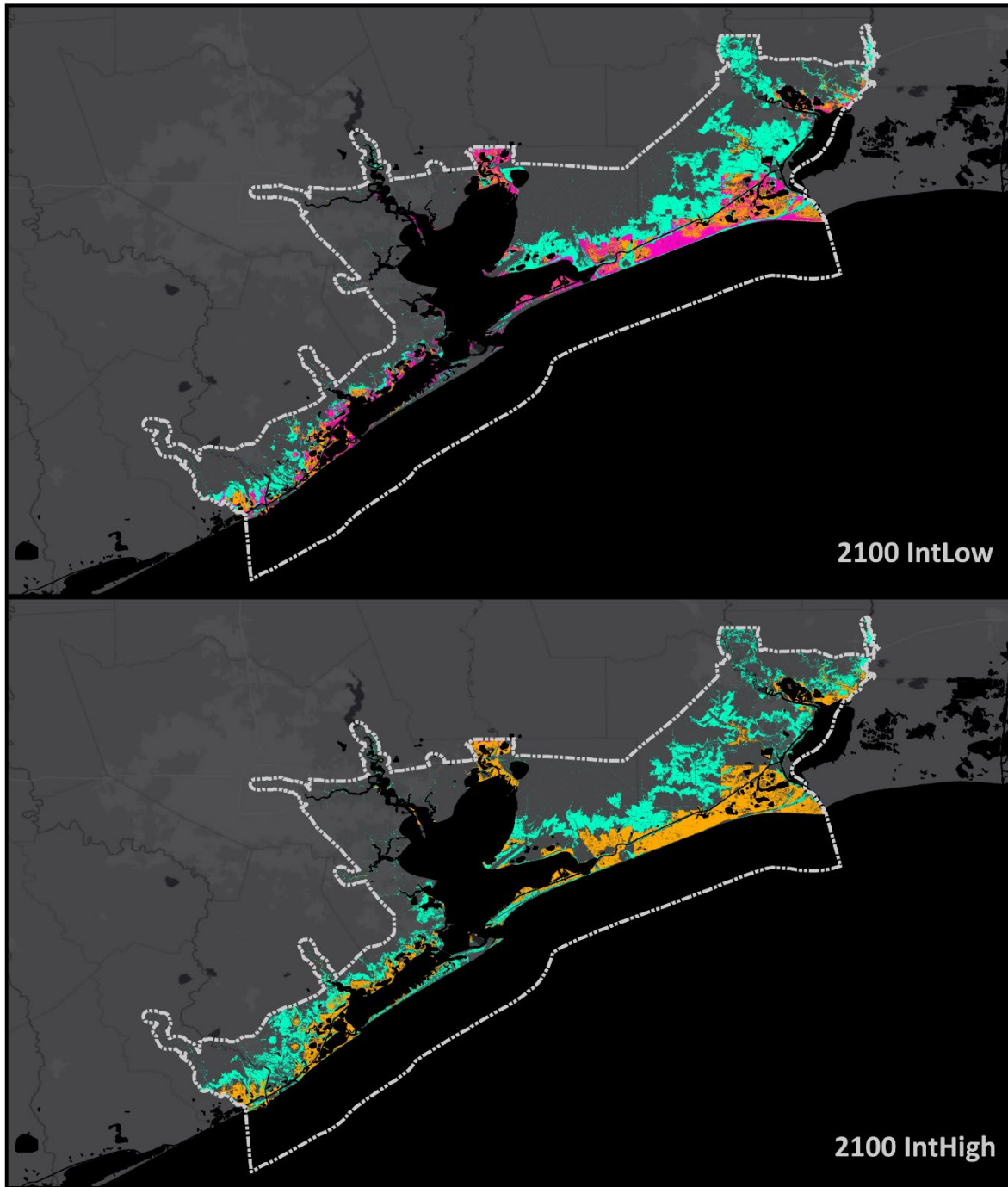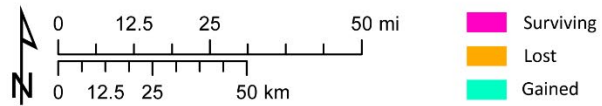
Figure 34. Map showing where brackish wetlands that exist on the present landscape are modeled to either survive, be converted to another land cover type or open water or gain area by the year 2100 in both Intermediate-Low and Intermediate-High SLR scenarios.
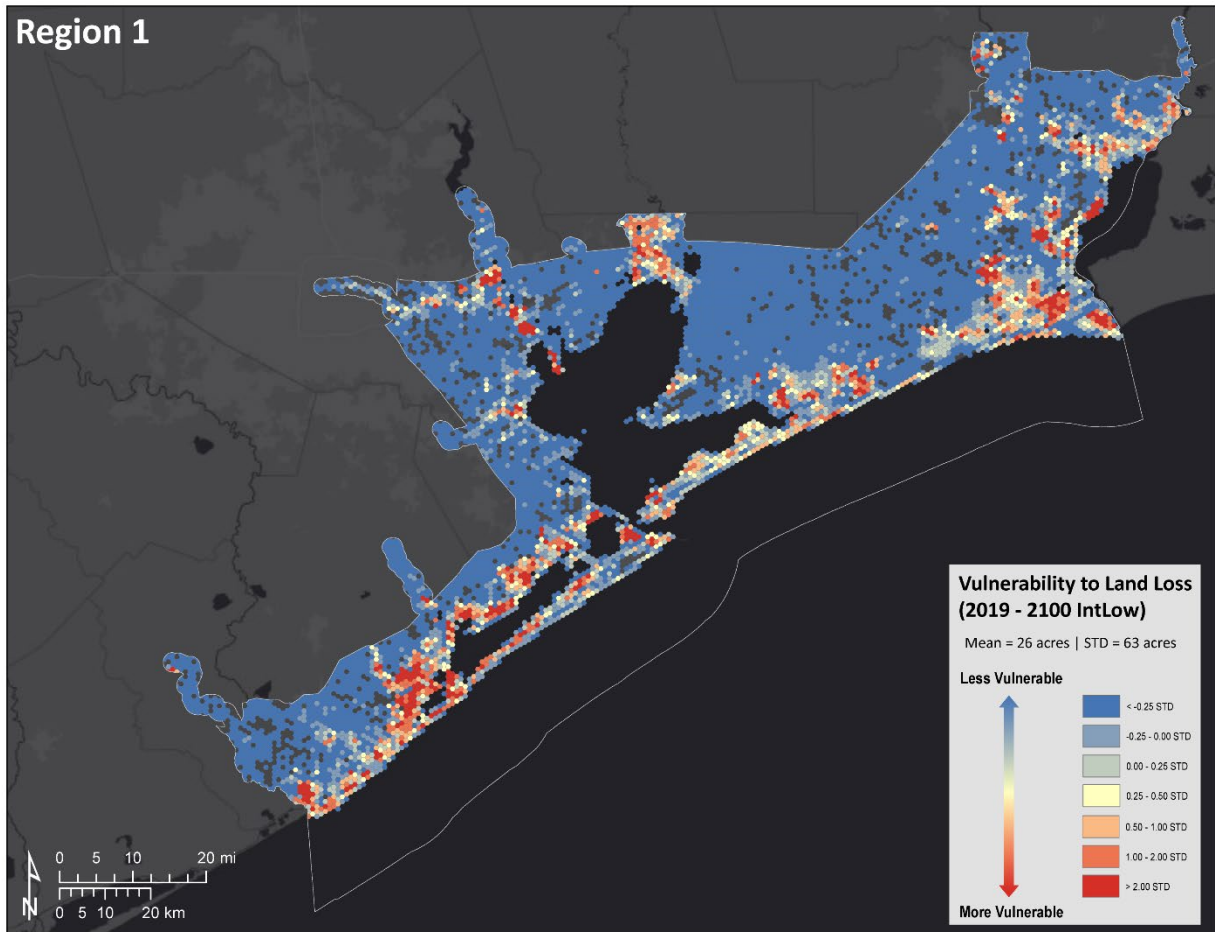
Figure 35. Map showing relative vulnerability to land loss in Region 1 where land loss means any type of land (excluding intertidal flats) that has converted to open water by the year 2100 in Intermediate-Low SLR scenario.
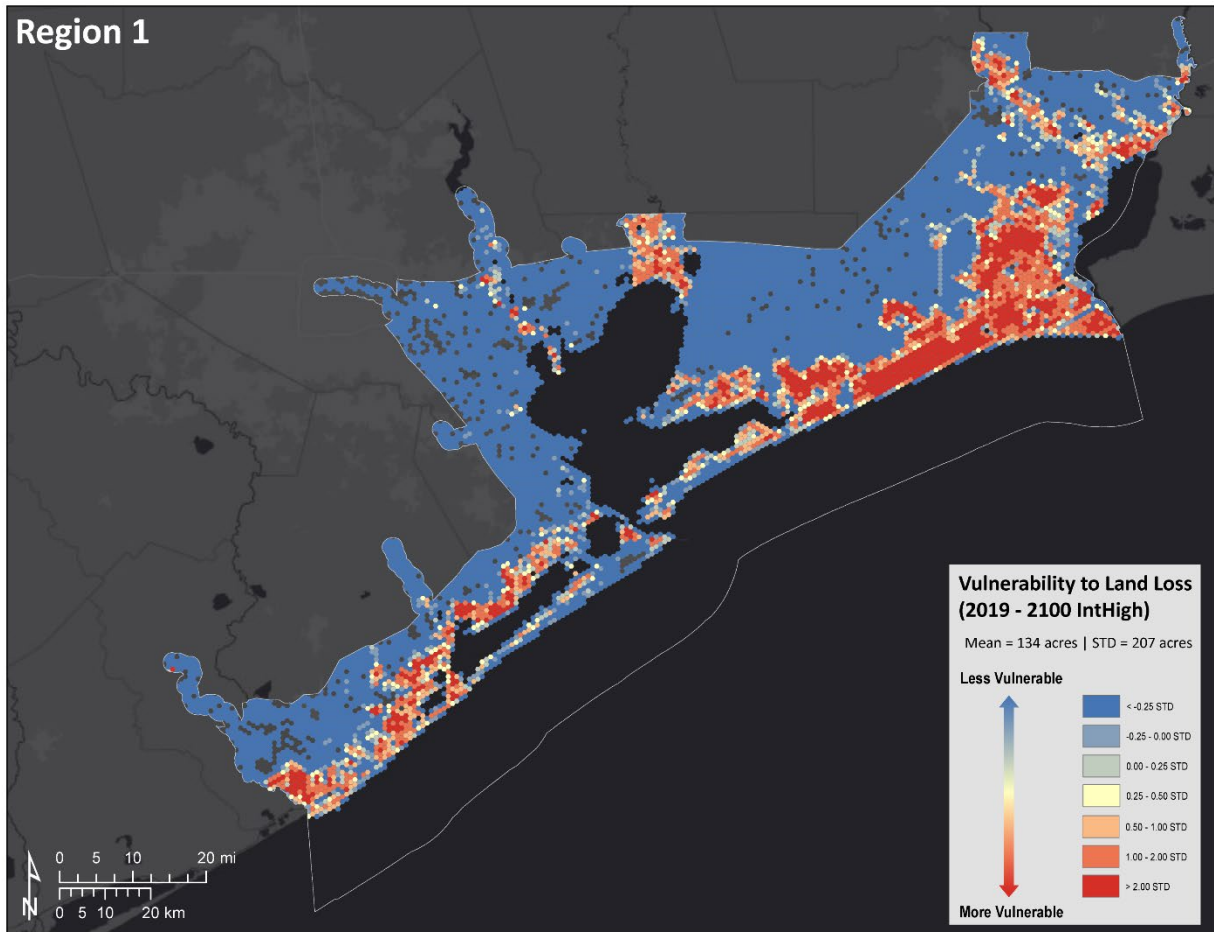
Figure 36. Map showing relative vulnerability to land loss in Region 1 where land loss means any type of land (excluding intertidal flats) that has converted to open water by the year 2100 in Intermediate-High SLR scenario.

Region 2

Substantial effects of SLR are anticipated to influence Region 2, significantly transforming the landscapes by 2100. Figure 37, Figure 38, and Table 14 present the current landscape of Region 2 and the projected future landscape in 2100. Figure 39 and Figure 40 display maps of individual losses and gains of freshwater and saltwater marshes in Region 2. These maps illustrate where freshwater wetlands and salt and brackish wetlands currently existing on the landscape are expected to either remain unchanged, be converted to a different land cover type or open water, or experience growth by 2100 in both 0.5m and 1.5m SLR scenarios.

Considering varying subsidence/uplift rates within this region by 2100, substantial reductions in inland-fresh marshes and swamps are projected. With the 0.5m scenario, a combined loss of 39% is anticipated, while the 1.5m scenario sees a dramatic shift to a 70% combined loss. The model forecasts these habitats will transition into transitional scrub-shrub wetlands, regularly flooded marshes, or tidal flats. The majority of saltwater and brackish marshes in Region 2 are also predicted to be affected by SLR. Their initial area amounts to 142 square miles, but by 2100, only 55 square miles of their original area remains in the 0.5m SLR scenario, and even less in the 1.5m SLR scenario, at just 3 square miles.

Alterations in salt and brackish marshes involve both expansion and contraction. On one hand, salt and brackish marshes will steadily migrate landward as the migration space becomes available, leading to an anticipated net gain of 73% in the 0.5m SLR scenario or 79% in the 1.5m SLR scenario by 2100. Conversely, Region 2 is also projected to experience a considerable increase in tidal flat habitats, from 28 square miles to 68 and 77 square miles in the 0.5m and 1.5m SLR scenarios by 2100, respectively. The gains of 140% and 173% result from the large areas of salt and brackish marshes being eroded into flats.

The open water area is projected to increase by 9% and 23% by the year 2100 in the 0.5m and 1.5m SLR scenarios, respectively. The expansion of open water and loss of vital coastal habitats can potentially heighten this region's vulnerability to future hazards such as storm surges and nuisance flooding. Figure 41 and Figure 42 display the relative vulnerability in both 0.5m and 1.5m SLR scenarios within this region. The maps illustrate where land is converted to open water by 2100. Within each hexagon, an average of 87 acres of land is lost to open water in the 1.5m SLR scenario, while only an average of 31 acres becomes open water in the 0.5m SLR scenario. The most vulnerable areas are the salt and brackish water wetlands bordering the bays, indicating that they are not accreting rapidly enough to keep up with RSLR.

Region 2
Land Cover Class

- Developed Dry Land
- Undeveloped Dry Land
- Freshwater Wetlands
- Salt & Brackish Wetlands
- Beaches and Flats
- Open Water

0 5 10 20 mi

0 5 10 20 km

A. Present Landscape

B. Future Landscape (2100) with 0.5 m SLR

C. Future Landscape (2100) with 1.5 m SLR
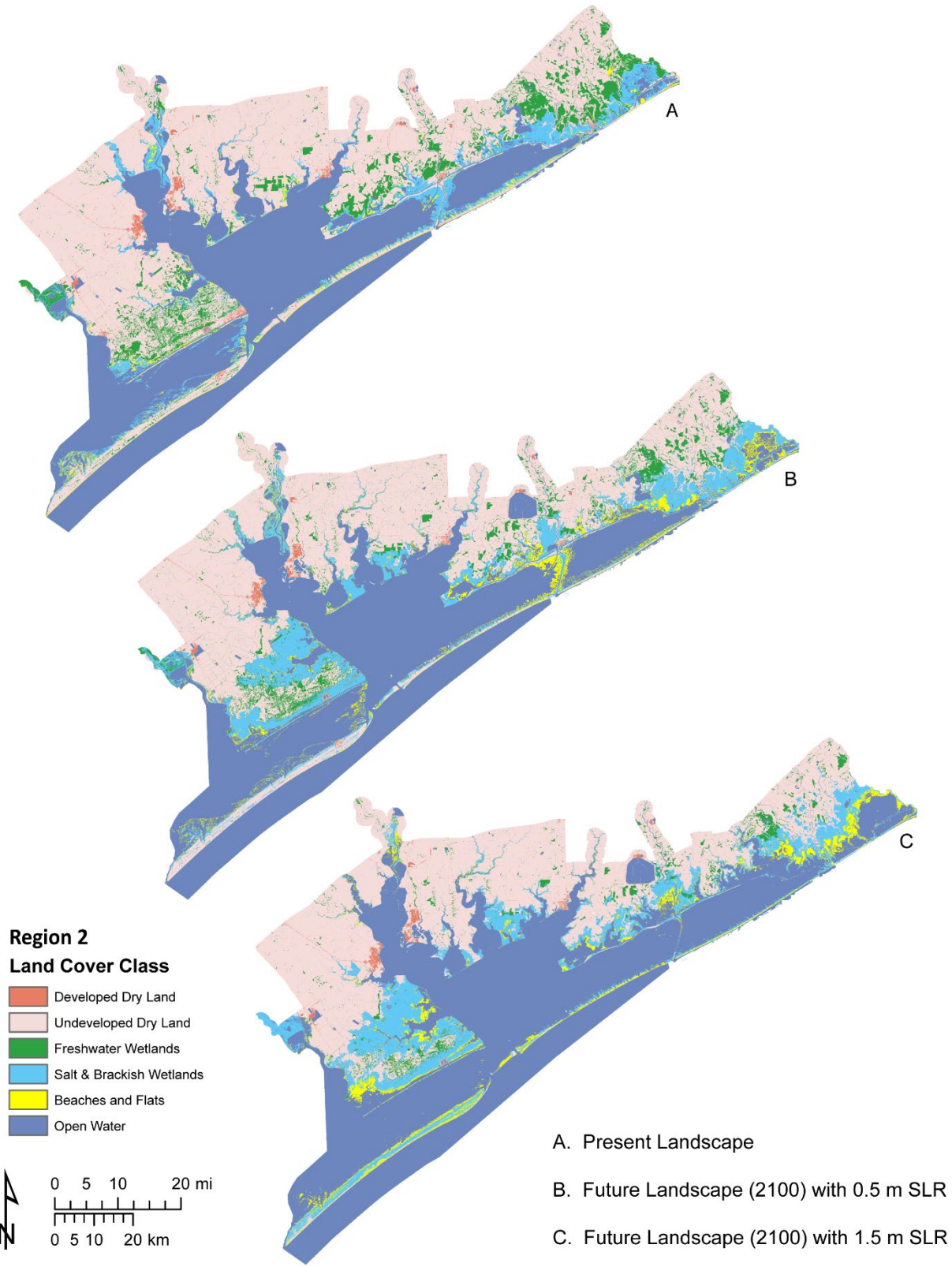
Figure 37. Map comparing the land cover distribution in Region 2 on the initial condition and 2100 conditions in both Intermediate-Low and Intermediate-High SLR scenarios.

57
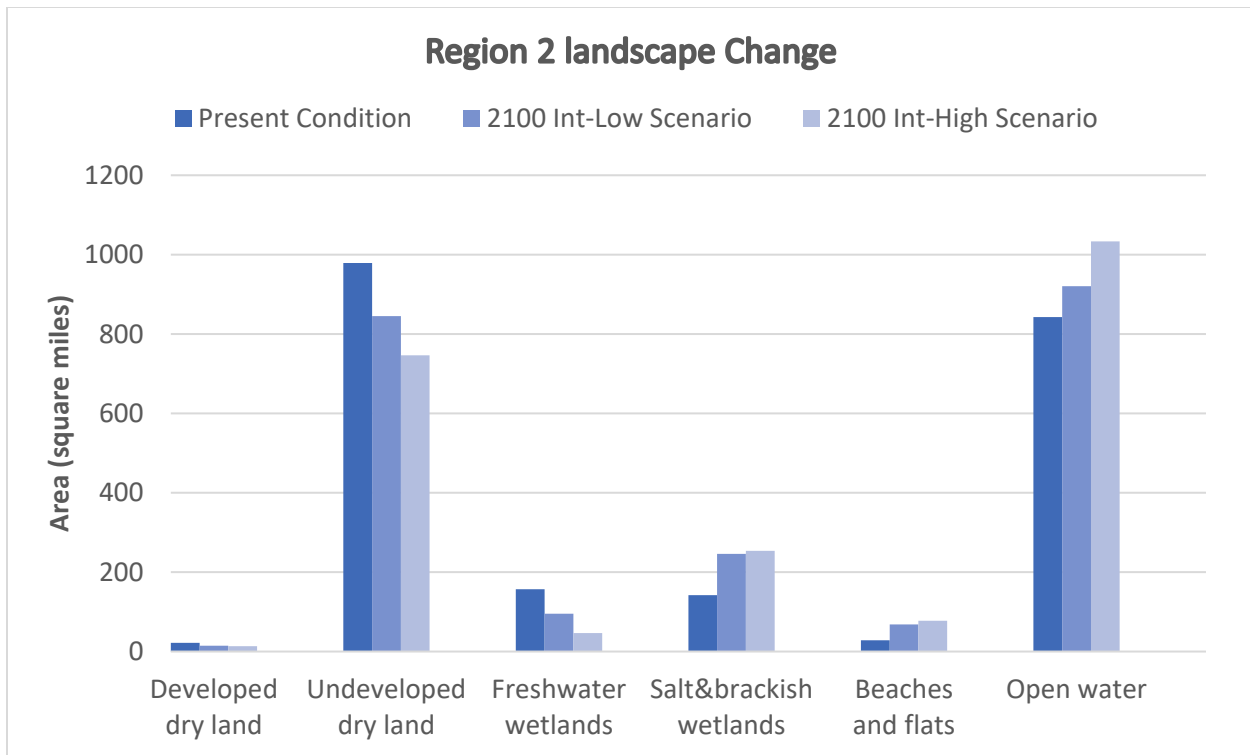
Figure 38. Areal changes (in square miles) of individual land cover types between Present Condition and two Future Conditions in Region 2.

Table 14. The percent difference between land cover types in Region 2 under the Present Condition and two 2100 Future Conditions

Land cover class	Present Condition (Sq miles)	2100 Int-Low scenario (Sq miles)	Percent Difference	2100 Int-High scenario (Sq miles)	Percent Difference
Developed dry land	21.85	14.79	-32.31	13.57	-37.89
Undeveloped dry land	978.77	844.94	-13.67	746.34	-23.75
Freshwater wetlands	157.09	95.39	-39.28	46.47	-70.42
Salt & brackish wetlands	141.94	246.00	73.31	253.63	78.69
Beaches and flats	28.40	68.16	140.00	77.45	172.71
Open water	842.56	920.32	9.23	1033.28	22.64

Freshwater Wetlands Change in Region 2 (2019 - 2100)

Surviving
Lost
Gained
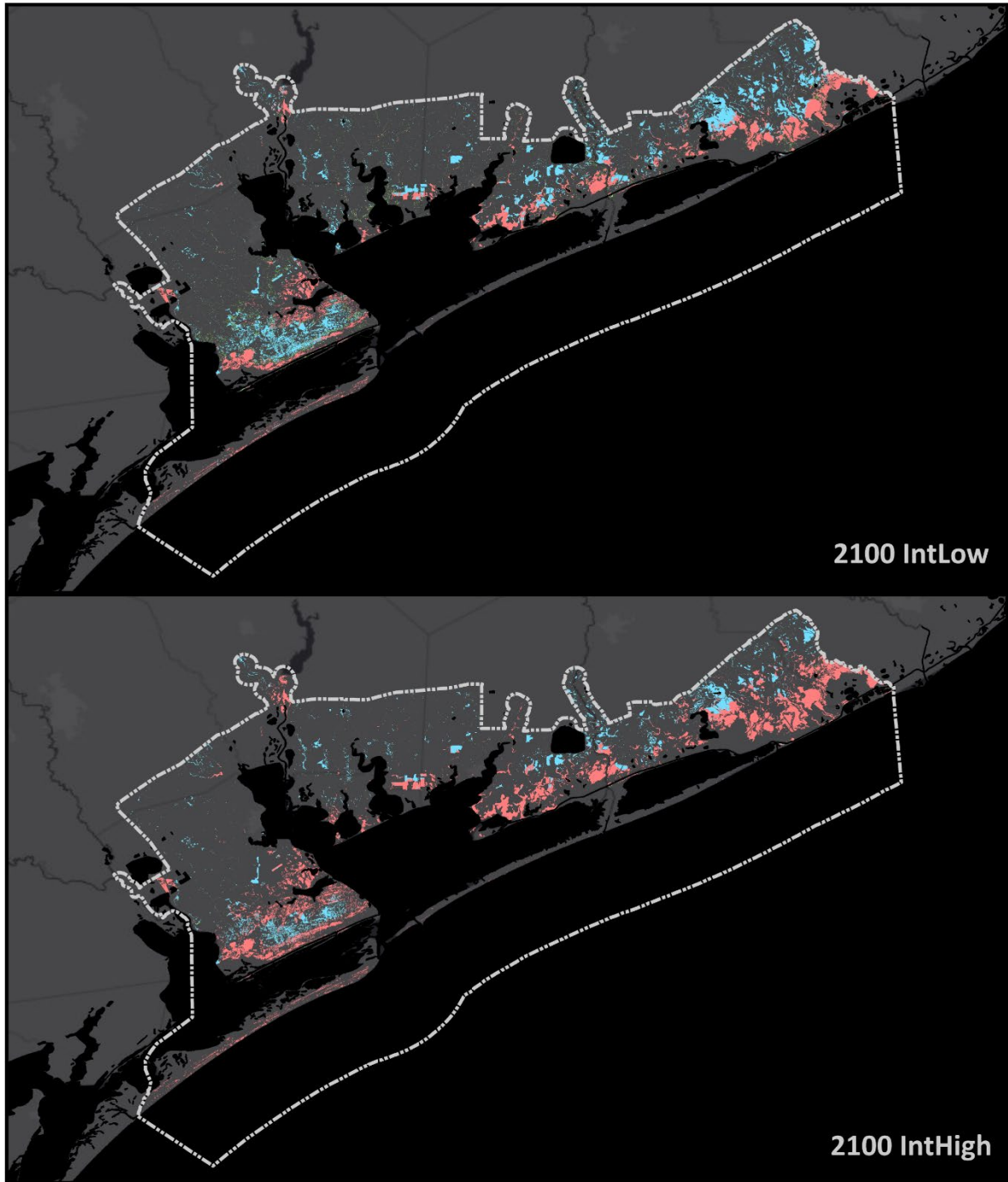
Figure 39. Map showing where freshwater wetlands that exist on the present landscape are modeled to either survive, be converted to another land cover type or open water or gain area by the year 2100 in both Intermediate-Low and Intermediate-Low SLR scenarios.

59

Salt & Brackish Wetlands Change in Region 2 (2019 - 2100)

0	12.5	25	50 mi
0	12.5	25	50 km

■ Surviving
■ Lost
■ Gained
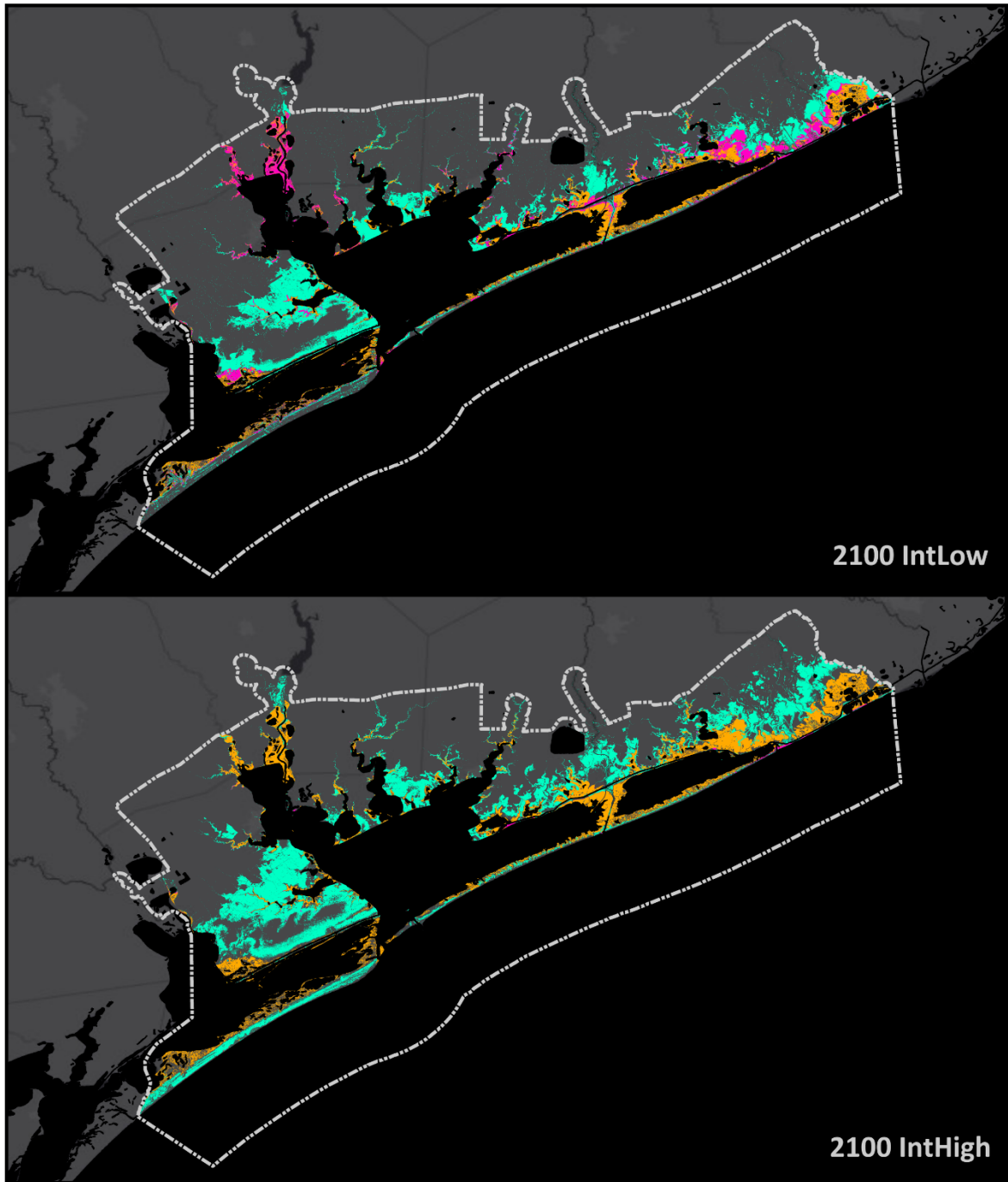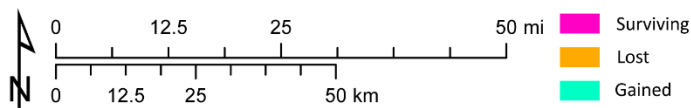
Figure 40. Map showing where brackish wetlands that exist on the present landscape are modeled to either survive, be converted to another land cover type or open water or gain area by the year 2100 in both Intermediate-Low and Intermediate-High SLR scenarios.
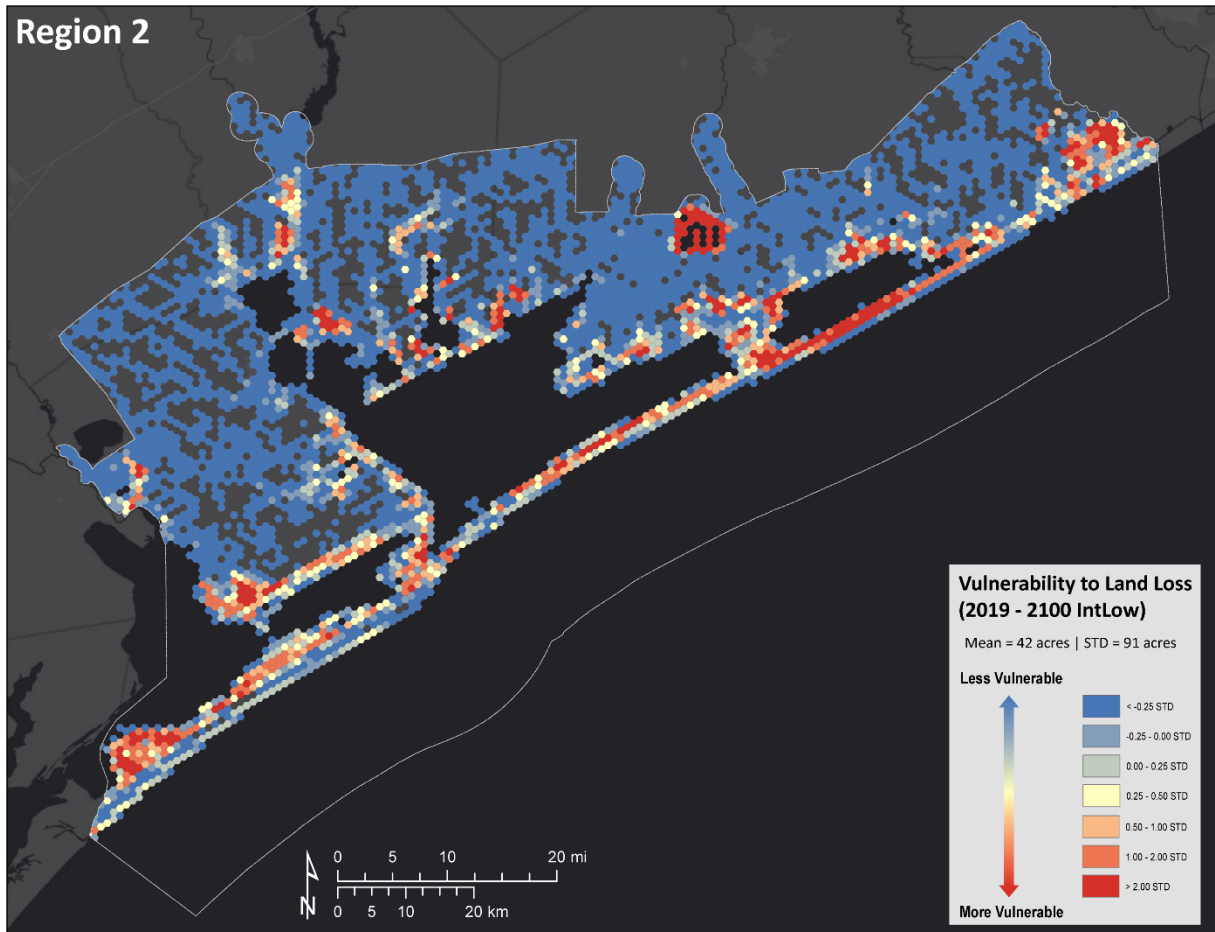
Figure 41. Map showing relative vulnerability to land loss in Region 2 where land loss means any type of land (excluding intertidal flats) that has converted to open water by the year 2100 in Intermediate-Low SLR scenario.
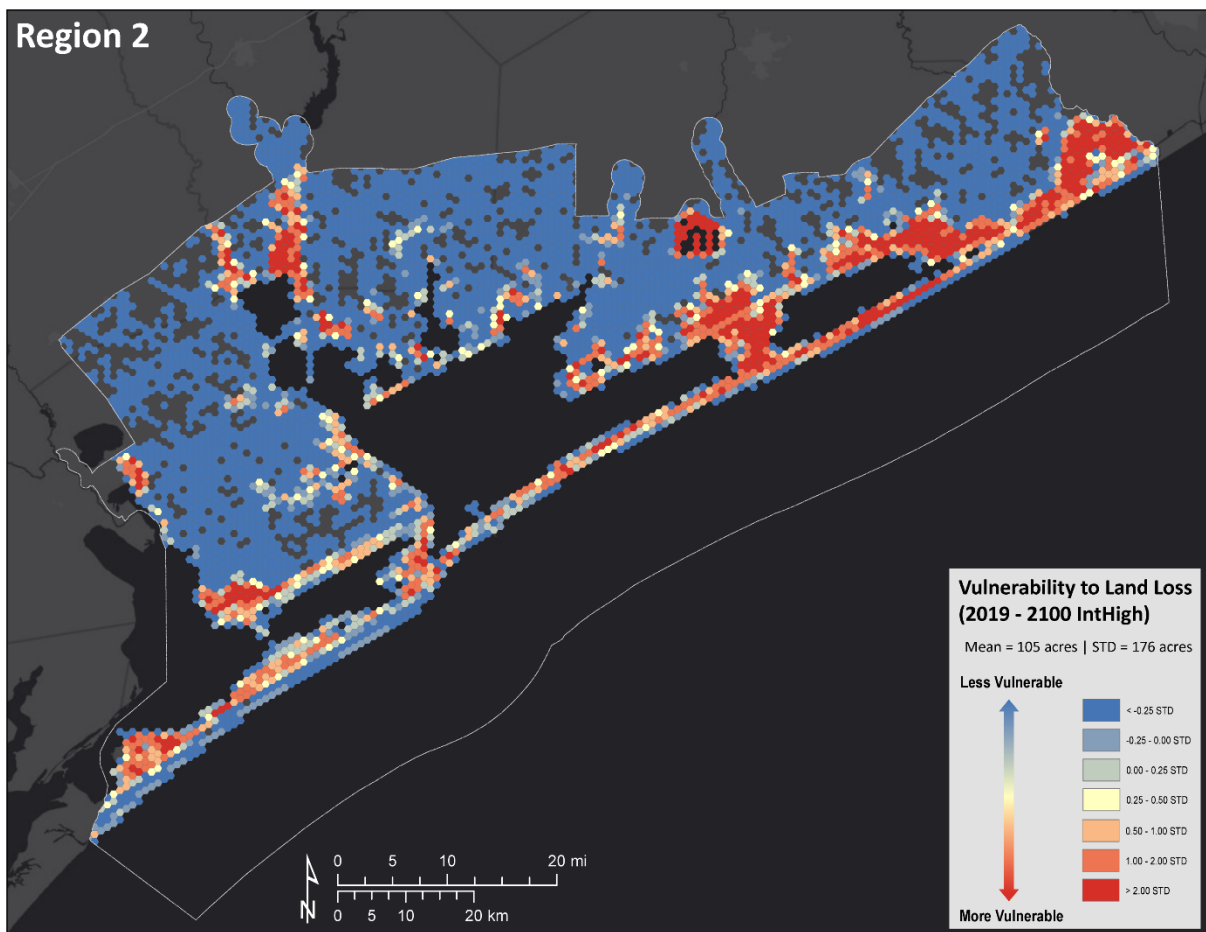
Figure 42. Map showing relative vulnerability to land loss in Region 2 where land loss means any type of land (excluding intertidal flats) that has converted to open water by the year 2100 in Intermediate-High SLR scenario.

Region 3

Considerable effects of SLR are forecasted to influence Region 3, drastically altering the landscapes by 2100. Figure 43, Figure 44, and Table 15 present the current landscape of Region 3 and the model projections of the future landscape in 2100. Figure 45 and Figure 46 display maps of individual losses and gains of freshwater and saltwater marshes in Region 3. These maps depict where freshwater wetlands and salt and brackish wetlands currently on the landscape are predicted to either remain unchanged, be converted to another land cover type or open water, or experience growth by 2100 in both 0.5m and 1.5m SLR scenarios.

Notable reductions in inland-fresh marshes and swamps are anticipated. With the 0.5m scenario, a combined loss of 22% is expected, while the 1.5m scenario sees a dramatic shift to a 49% combined loss. The model forecasts these habitats will transition into transitional scrub-shrub wetlands, regularly flooded marshes or tidal flats. The majority of saltwater and brackish marshes in Region 3 are also projected to be affected by SLR. Their initial area amounts to 71 square miles, but by 2100, only 26 square miles of their original area remains in the 0.5m SLR scenario, and even less in the 1.5m SLR scenario, at just 4 square miles. Changes in salt and brackish marshes involve both expansion and

contraction. On one hand, salt and brackish marshes will steadily migrate landward as the migration space becomes available, leading to an anticipated net gain of 54% in the 0.5m SLR scenario or 144% in the 1.5m SLR scenario by 2100. Conversely, the lost low marsh area is converted to either tidal flats or open water. Region 3 is expected to experience a significant decrease in tidal flat habitats, with losses of 44% and 48% in the 0.5m and 1.5m SLR scenarios by 2100, respectively. The loss is primarily observed in the arms of Baffin Bay and on the backside of the barrier islands.

The open water area is projected to increase by 12% and 20% by the year 2100 in the 0.5m and 1.5m SLR scenarios, respectively. The expansion of open water and loss of critical coastal habitats have the potential to heighten this region's vulnerability to future hazards, such as storm surges and nuisance flooding. Figure 47 and Figure 48 display the relative vulnerability in both 0.5m and 1.5m SLR scenarios within this region. The maps illustrate where land is converted to open water by 2100. Within each hexagon, an average of 43 acres of land is lost to open water in the 1.5m SLR scenario, while only an average of 25 acres becomes open water in the 0.5m SLR scenario. The areas most vulnerable to land loss correspond with the areas experiencing the highest rates of subsidence, particularly the marshes on the backside of the barrier islands, especially San Jose Island, and around the bayhead deltas. Similar to other regions, this suggests RSLR is outpacing the vertical accretion rate of the salt and brackish water wetlands.

Region 3
Land Cover Class

- Developed Dry Land
- Undeveloped Dry Land
- Freshwater Wetlands
- Salt & Brackish Wetlands
- Beaches and Flats
- Open Water

0 5 10   20 mi

0 5 10   20 km

A. Present Landscape

B. Future Landscape (2100) with 0.5 m SLR

C. Future Landscape (2100) with 1.5 m SLR
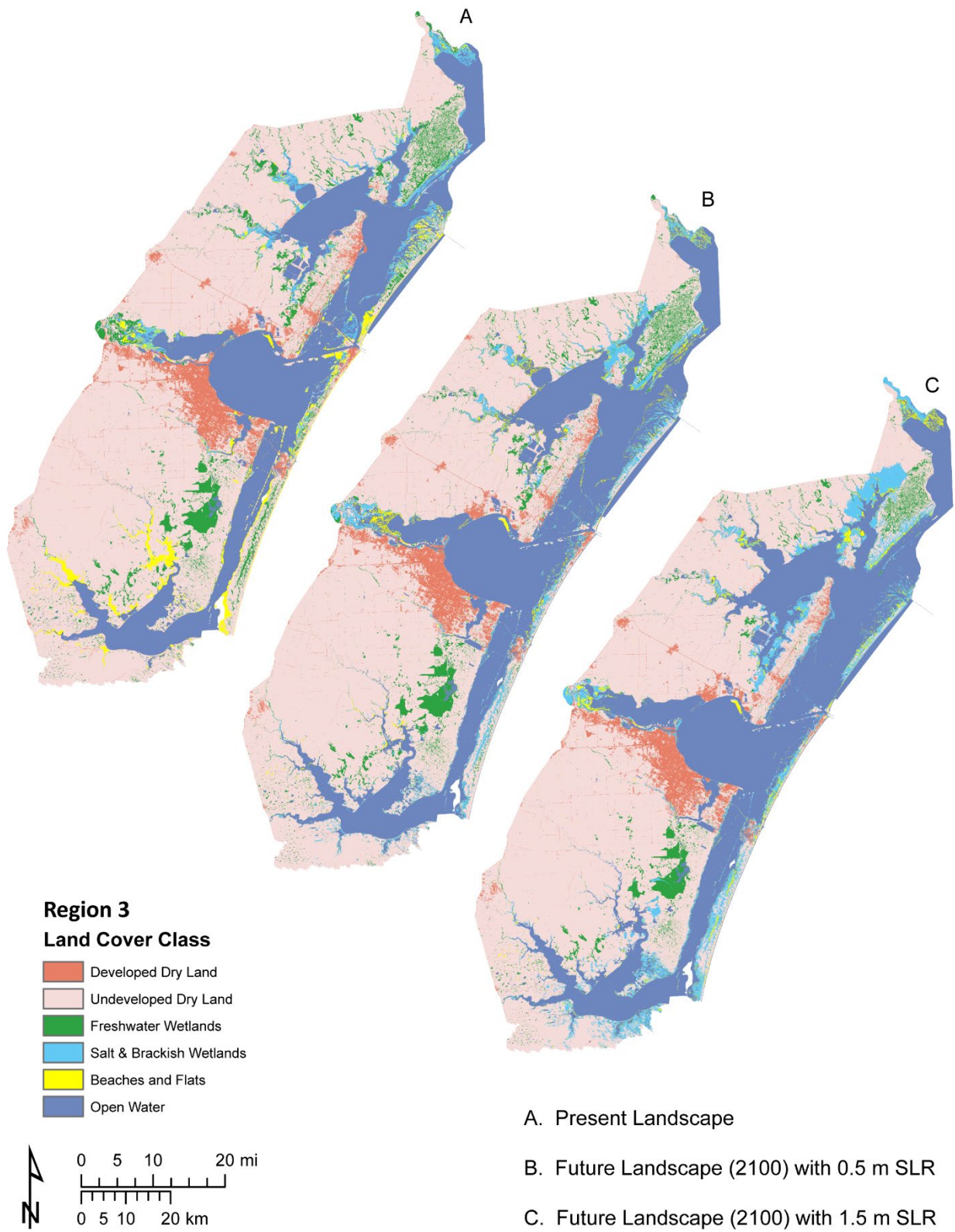
Figure 43. Map comparing the land cover distribution in Region 3 on the initial condition and 2100 conditions in both Intermediate-Low and Intermediate-High SLR scenarios.
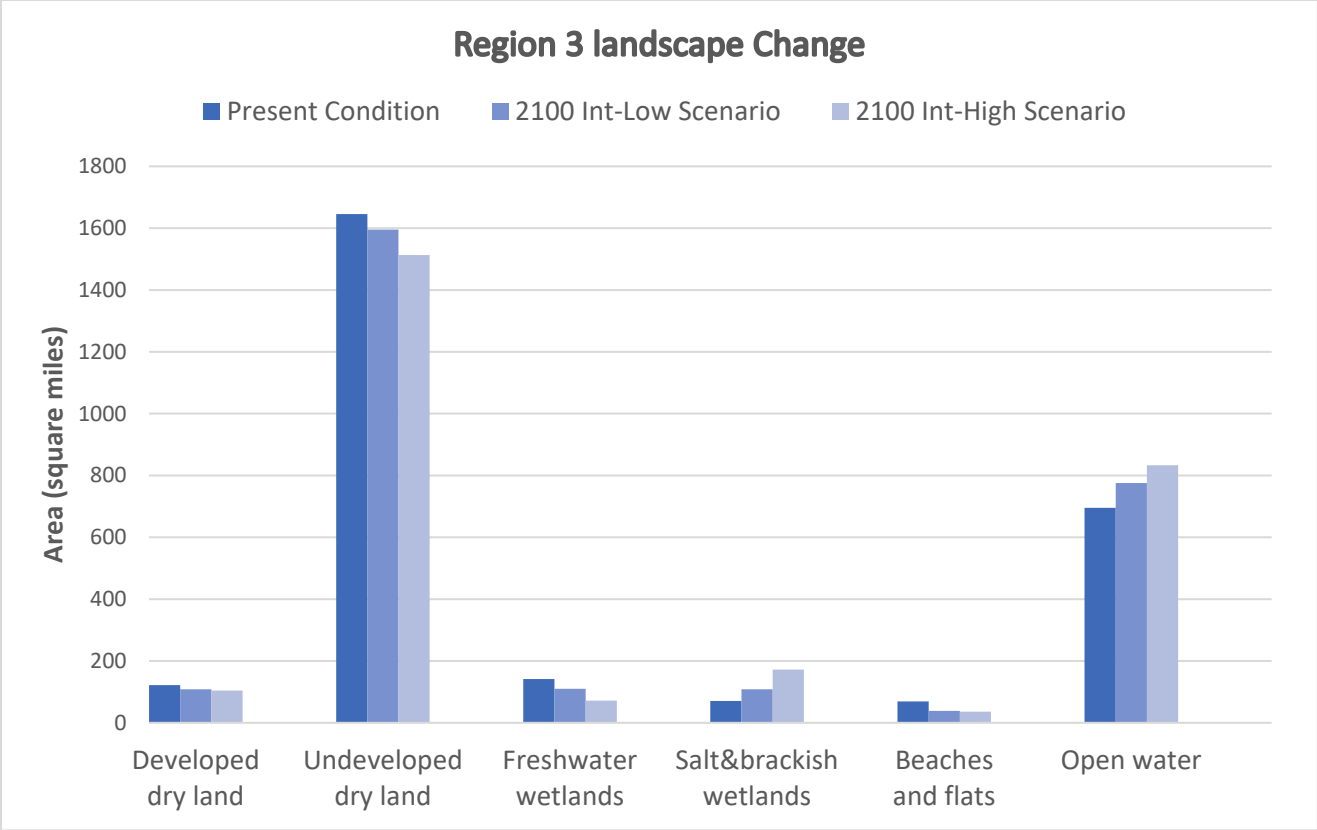
Figure 44. Areal changes (in square miles) of individual land cover types between Present Condition and two Future Conditions in Region 3.

Table 15. The percent difference between land cover types in Region 3 under the Present Condition and two 2100 Future Conditions

Land cover class	Present Condition (Sq miles)	2100 Int-Low scenario (Sq miles)	Percent Difference	2100 Int-High scenario (Sq miles)	Percent Difference
Developed dry land	122.10	108.23	-11.36	104.09	-14.75
Undeveloped dry land	1645.53	1595.49	-3.04	1513.14	-8.05
Freshwater wetlands, non-tidal	141.54	109.82	-22.41	71.67	-49.36
Salt and brackish emergent wetlands, tidal	70.58	108.49	53.71	172.34	144.18
Beaches and flats	69.10	38.42	-44.40	36.22	-47.58
Open water	695.24	775.66	11.57	833.20	19.84

Freshwater Wetlands Change in Region 3 (2019 - 2100)

Surviving
Lost
Gained
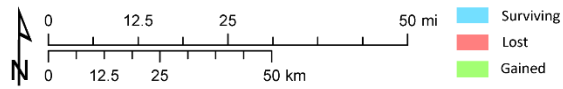
Figure 45. Map showing where freshwater wetlands that exist on the present landscape are modeled to either survive, be converted to another land cover type or open water or gain area by the year 2100 in both Intermediate-Low and Intermediate-Low SLR scenarios.
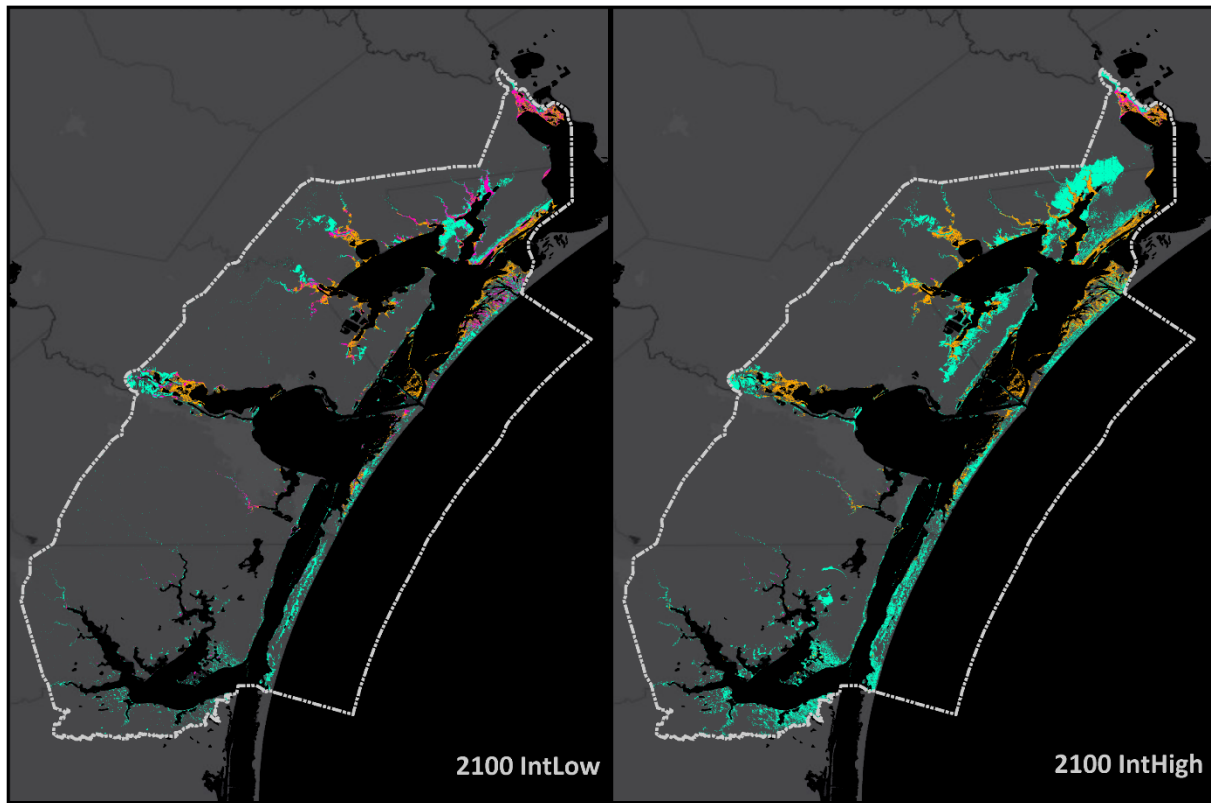
Salt & Brackish Wetlands Change in Region 3 (2019 - 2100)

Legend: Surviving, Lost, Gained

Figure 46. Map showing where brackish wetlands that exist on the present landscape are modeled to either survive, be converted to another land cover type or open water or gain area by the year 2100 in both Intermediate-Low and Intermediate-High SLR scenarios.

Figure 47. Map showing relative vulnerability to land loss in Region 3 where land loss means any type of land (excluding intertidal flats) that has converted to open water by the year 2100 in Intermediate-Low SLR scenario.
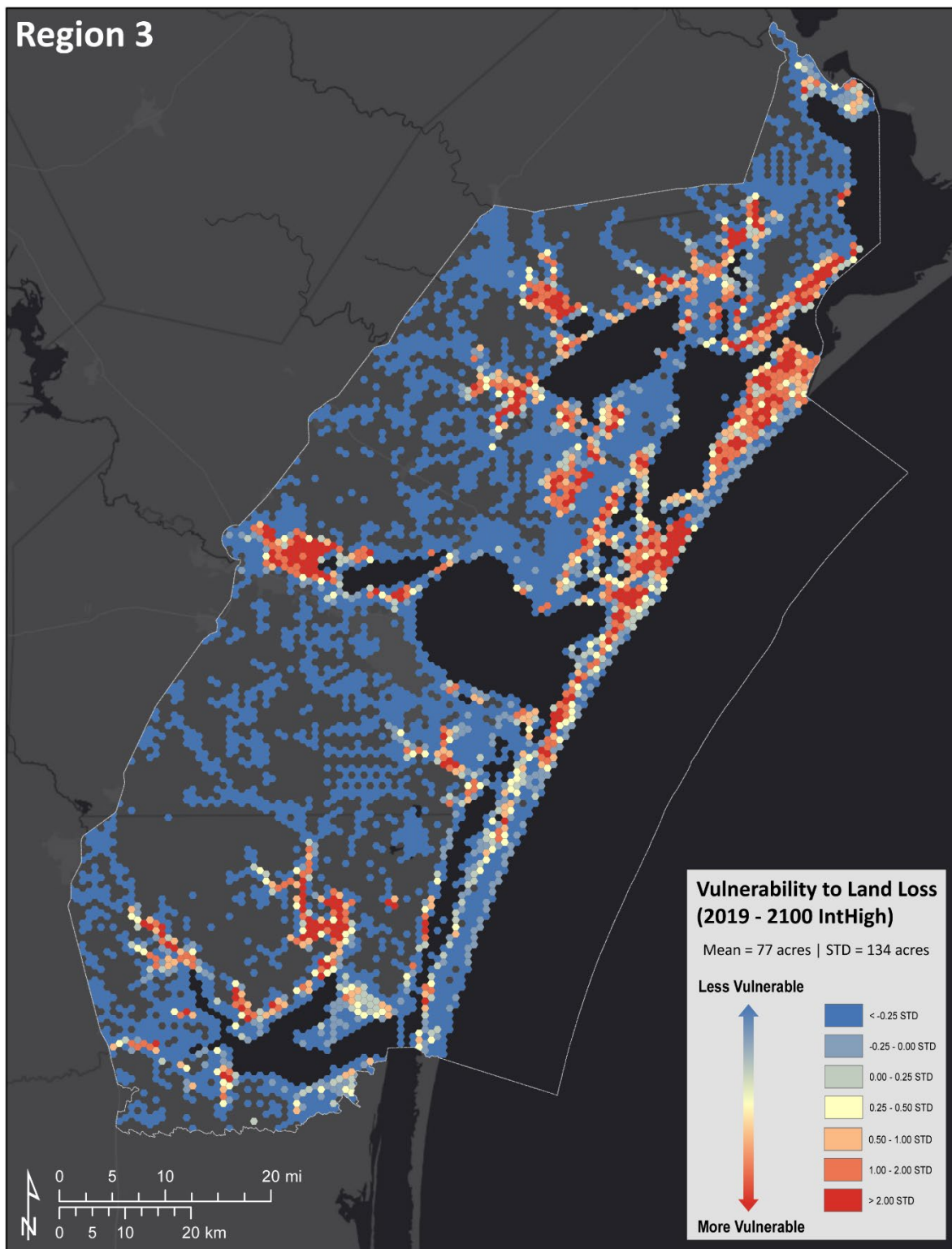
Figure 48. Map showing relative vulnerability to land loss in Region 3 where land loss means any type of land (excluding intertidal flats) that has converted to open water by the year 2100 in Intermediate-High SLR scenario.

Region 4

Substantial effects of SLR are anticipated to impact Region 4, greatly transforming the landscapes by 2100. Figure 49, Figure 50, and Table 16 present the current landscape of Region 4 and the model projections of the future landscape in 2100. Figure 51 and Figure 52 display maps of individual losses and gains of freshwater and saltwater marshes in Region 4. These maps show where freshwater wetlands and salt and brackish wetlands currently on the landscape are predicted to either remain unchanged, be converted to another land cover type or open water, or experience growth by 2100 in both 0.5m and 1.5m SLR scenarios.

Accounting for varying subsidence/uplift rates within this region by 2100, notable reductions in inland-fresh marshes and swamps are expected. With the 0.5m scenario, a combined loss of 27% is predicted, while the 1.5m scenario sees a dramatic shift to a 62% combined loss. The model forecasts these habitats will transition into transitional scrub-shrub wetlands, regularly flooded marshes or tidal flats. The saltwater and brackish marshes in Region 4 are also anticipated to be affected by SLR. Their initial area amounts to 26 square miles, but by 2100, only 19 square miles of their original area remains in the 0.5m SLR scenario, and even less in the 1.5m SLR scenario, at just 4 square miles. Changes in salt and brackish marshes involve both expansion and contraction. On one hand, salt and brackish marshes will steadily migrate landward as the migration space becomes available, resulting in a predicted net gain of 258% in the 0.5m SLR scenario and 504% in the 1.5m SLR scenario by 2100. Conversely, the lost low marsh area is converted to either tidal flats or open water. Region 3 is expected to experience a significant decrease in tidal flat habitats, with losses of 91% and 89% in the 0.5m and 1.5m SLR scenarios by 2100, respectively.

The open water area is projected to increase by 60% and 70% by the year 2100 in the 0.5m and 1.5m SLR scenarios, respectively. The expansion of open water and loss of critical coastal habitats have the potential to heighten this region's vulnerability to future hazards, such as storm surges and nuisance flooding. Figure 53 and Figure 54 display the relative vulnerability in both 0.5m and 1.5m SLR scenarios within this region. The maps illustrate where land is converted to open water by 2100. Within each hexagon, an average of 92 acres of land is lost to open water in the 1.5m SLR scenario, while only an average of 78 acres becomes open water in the 0.5m SLR scenario. The backside of South Padre Island and the Laguna Atascosa National Wildlife Refuge are both highly susceptible to land loss driven by RSLR. The loss of the barrier island and the habitats in the refuge could greatly impact the communities and wildlife in this region.

Region 4
Land Cover Class

- Developed Dry Land
- Undeveloped Dry Land
- Freshwater Wetlands
- Salt & Brackish Wetlands
- Beaches and Flats
- Open Water

0 5 10   20 mi
0 5 10   20 km

N

A. Present Landscape

B. Future Landscape (2100) with 0.5 m SLR
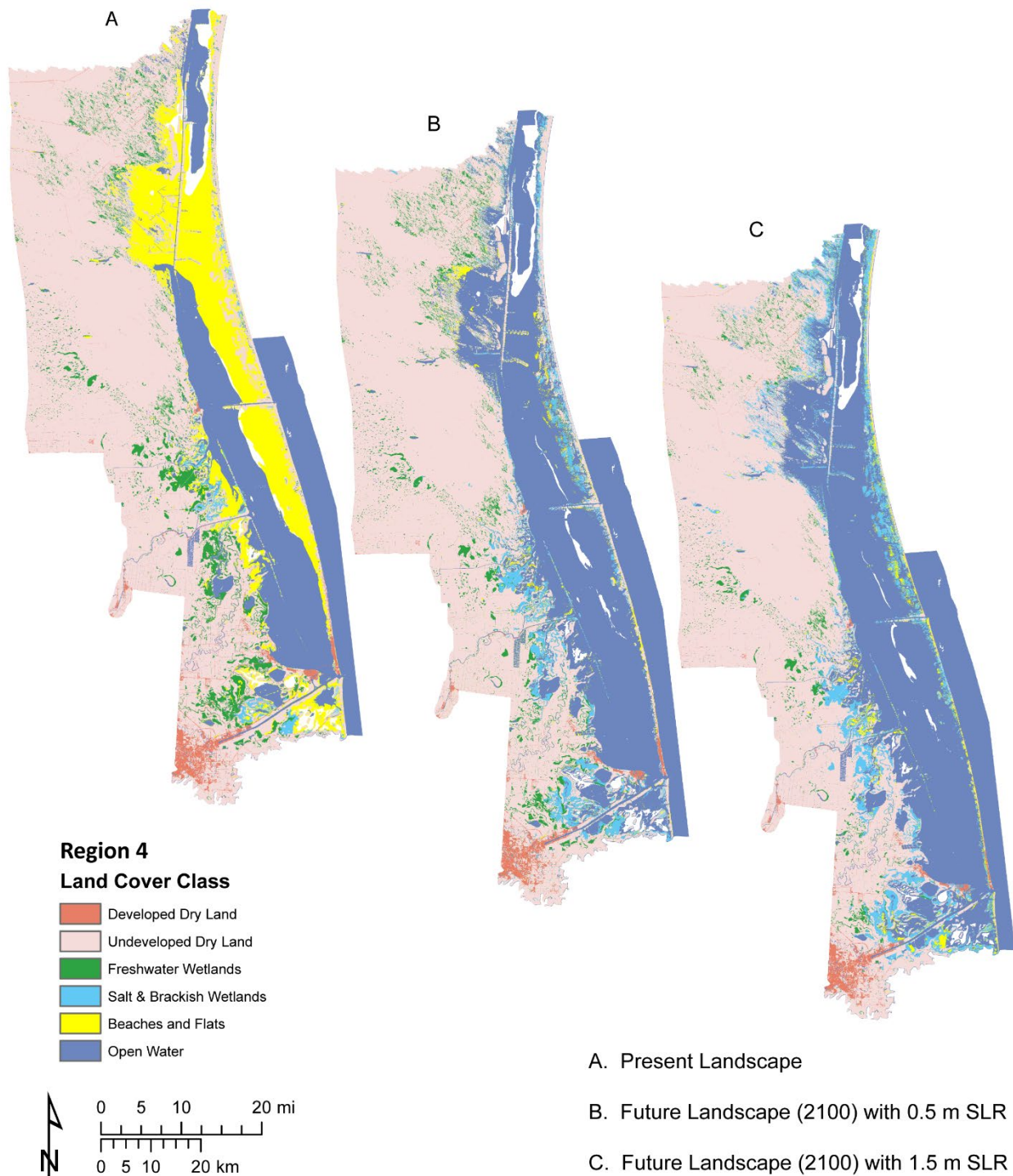
C. Future Landscape (2100) with 1.5 m SLR

Figure 49. Map comparing the land cover distribution in Region 4 on the initial condition and 2100 conditions in both Intermediate-Low and Intermediate-High SLR scenarios.
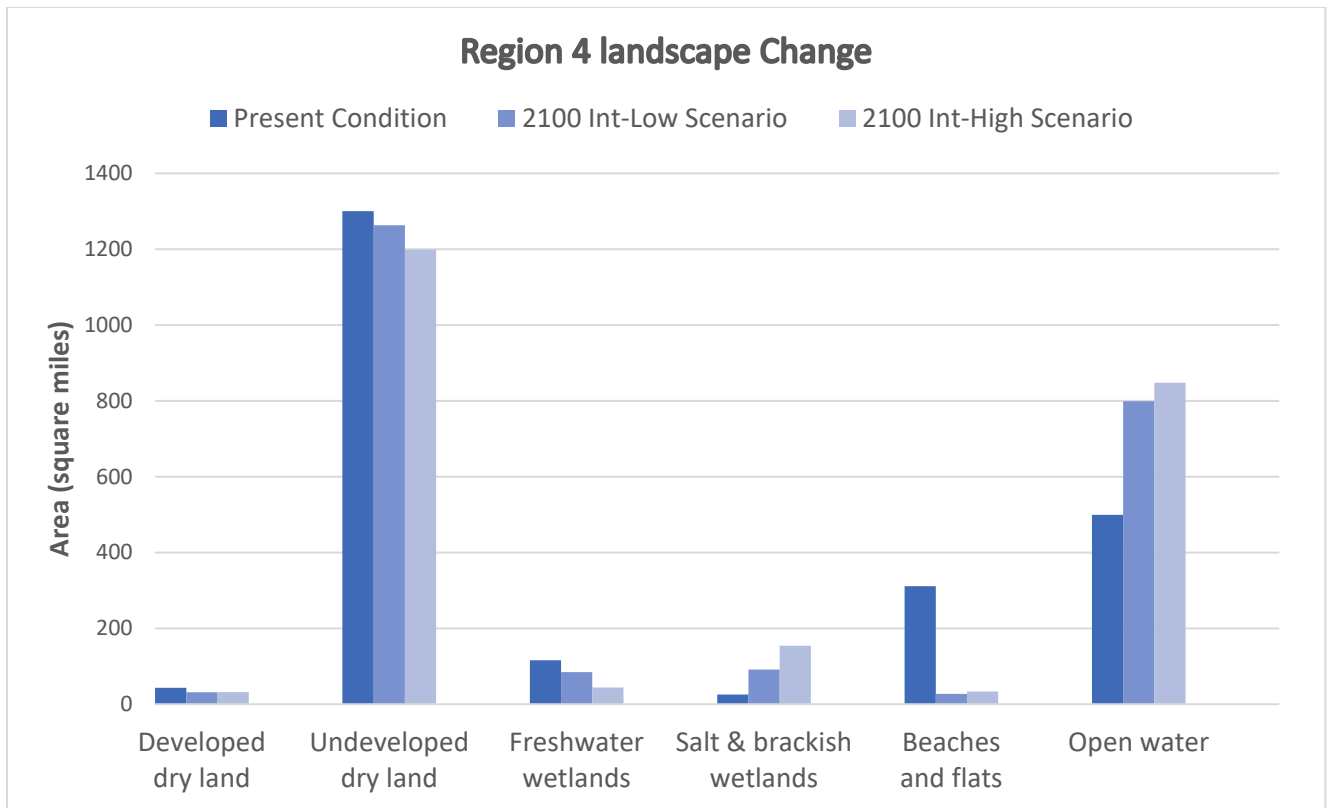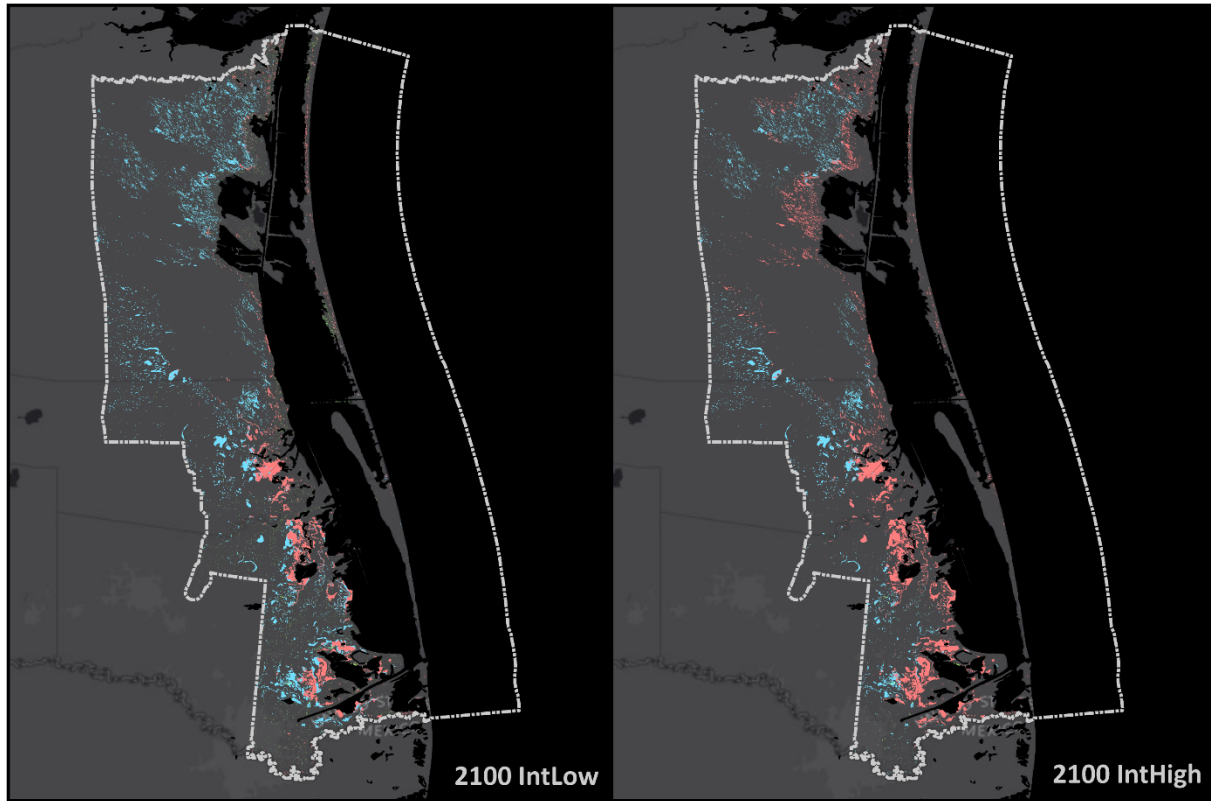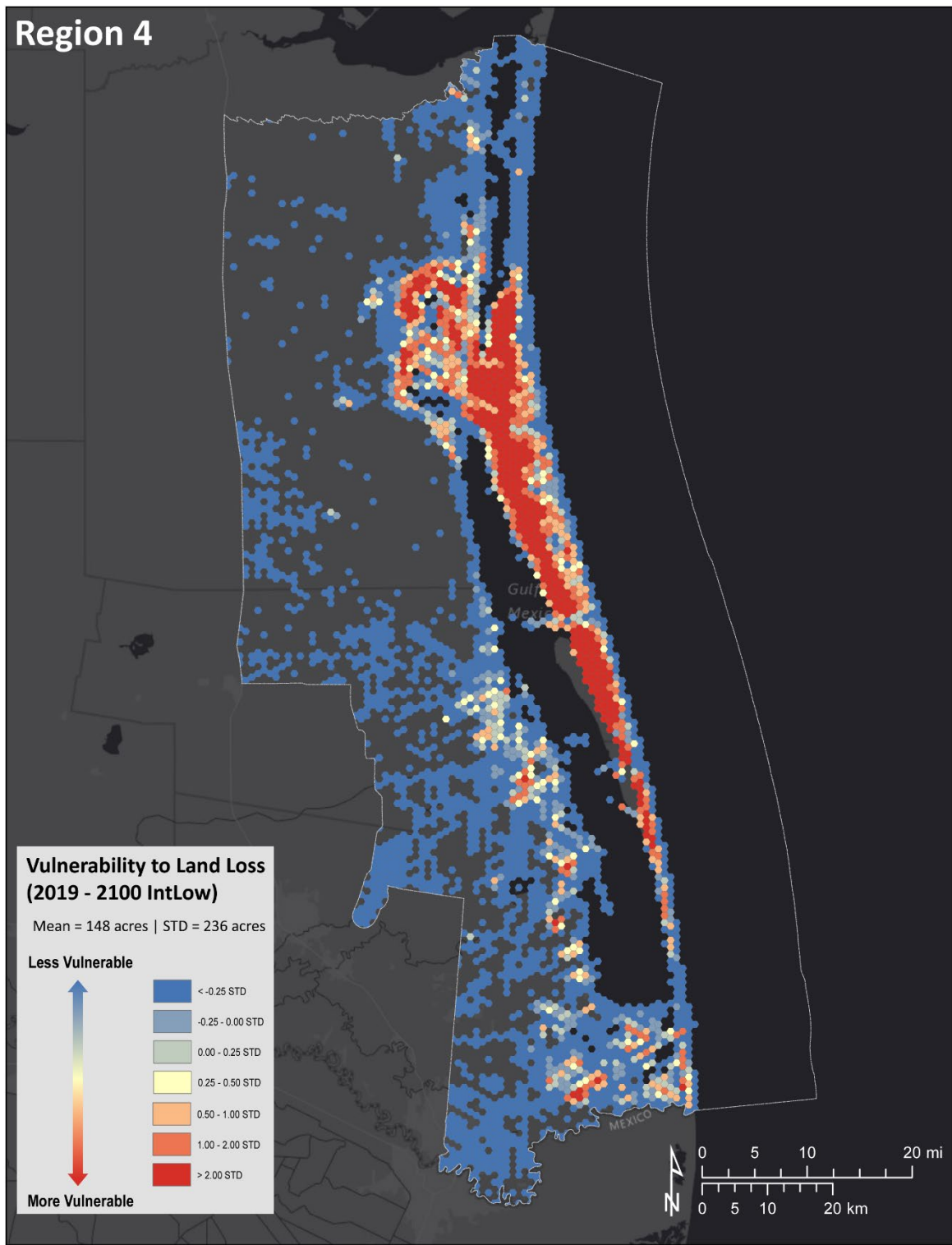
Figure 50. Areal changes (in square miles) of individual land cover types between Present Condition and two Future Conditions in Region 4.

Table 16. The percent difference between land cover types in Region 4 under the Present Condition and two 2100 Future Conditions

Land cover class	Present Condition (Sq miles)	2100 Int-Low scenario (Sq miles)	Percent Difference	2100 Int-High scenario (Sq miles)	Percent Difference
Developed dry land	43.36	31.46	-27.44	31.93	-26.36
Undeveloped dry land	1300.22	1262.99	-2.86	1198.83	-7.80
Freshwater wetlands, non-tidal	115.80	84.73	-26.83	44.27	-61.77
Salt and brackish emergent wetlands, tidal	25.58	91.50	257.70	154.44	503.75
Beaches and flats	311.27	27.19	-91.26	33.44	-89.26
Open water	499.62	798.93	59.91	848.02	69.73

Freshwater Wetlands Change in Region 4 (2019 - 2100)

Surviving
Lost
Gained
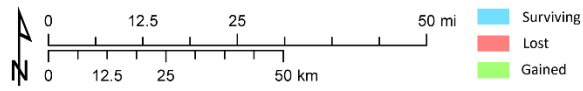
Figure 51. Map showing where freshwater wetlands that exist on the present landscape are modeled to either survive, be converted to another land cover type or open water or gain area by the year 2100 in both Intermediate-Low and Intermediate-Low SLR scenarios.
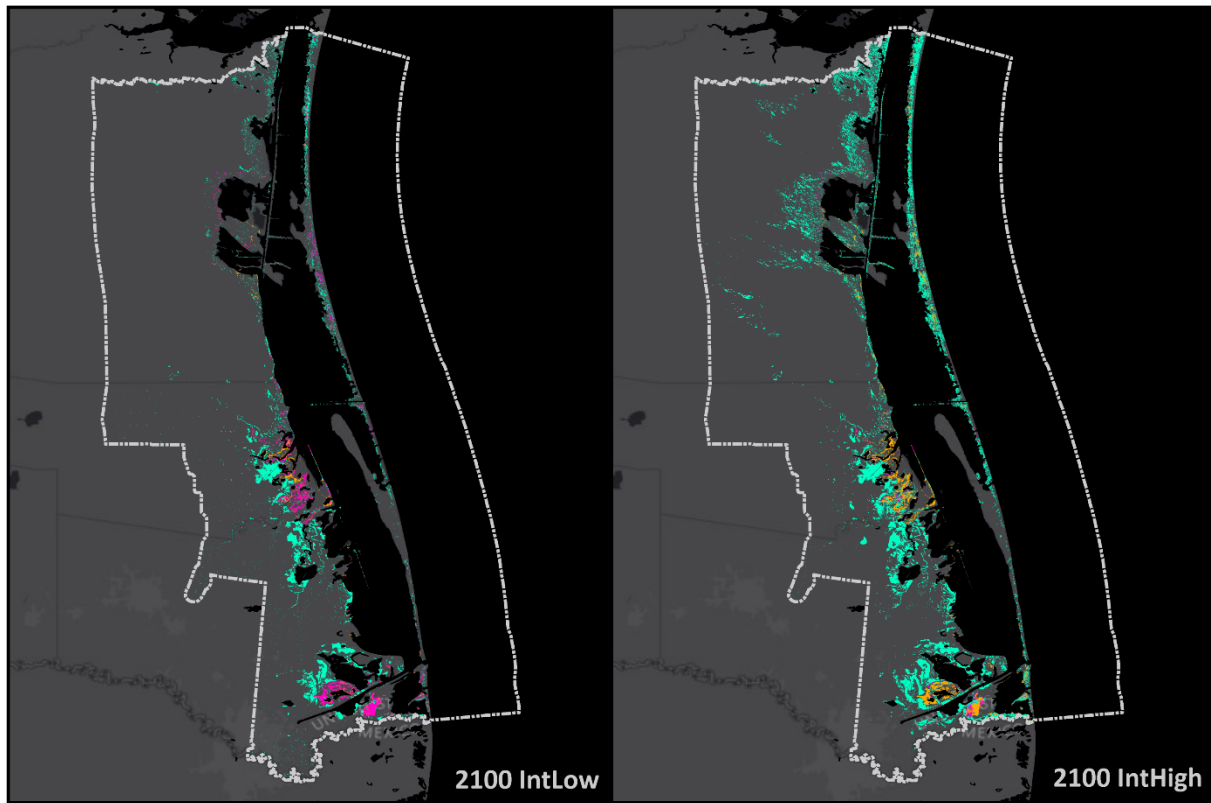
Salt & Brackish Wetlands Change in Region 4 (2019 - 2100)

Surviving
Lost
Gained

Figure 52. Map showing where brackish wetlands that exist on the present landscape are modeled to either survive, be converted to another land cover type or open water or gain area by the year 2100 in both Intermediate-Low and Intermediate-High SLR scenarios.

Figure 53. Map showing relative vulnerability to land loss in Region 4 where land loss means any type of land (excluding intertidal flats) that has converted to open water by the year 2100 in Intermediate-Low SLR scenario.
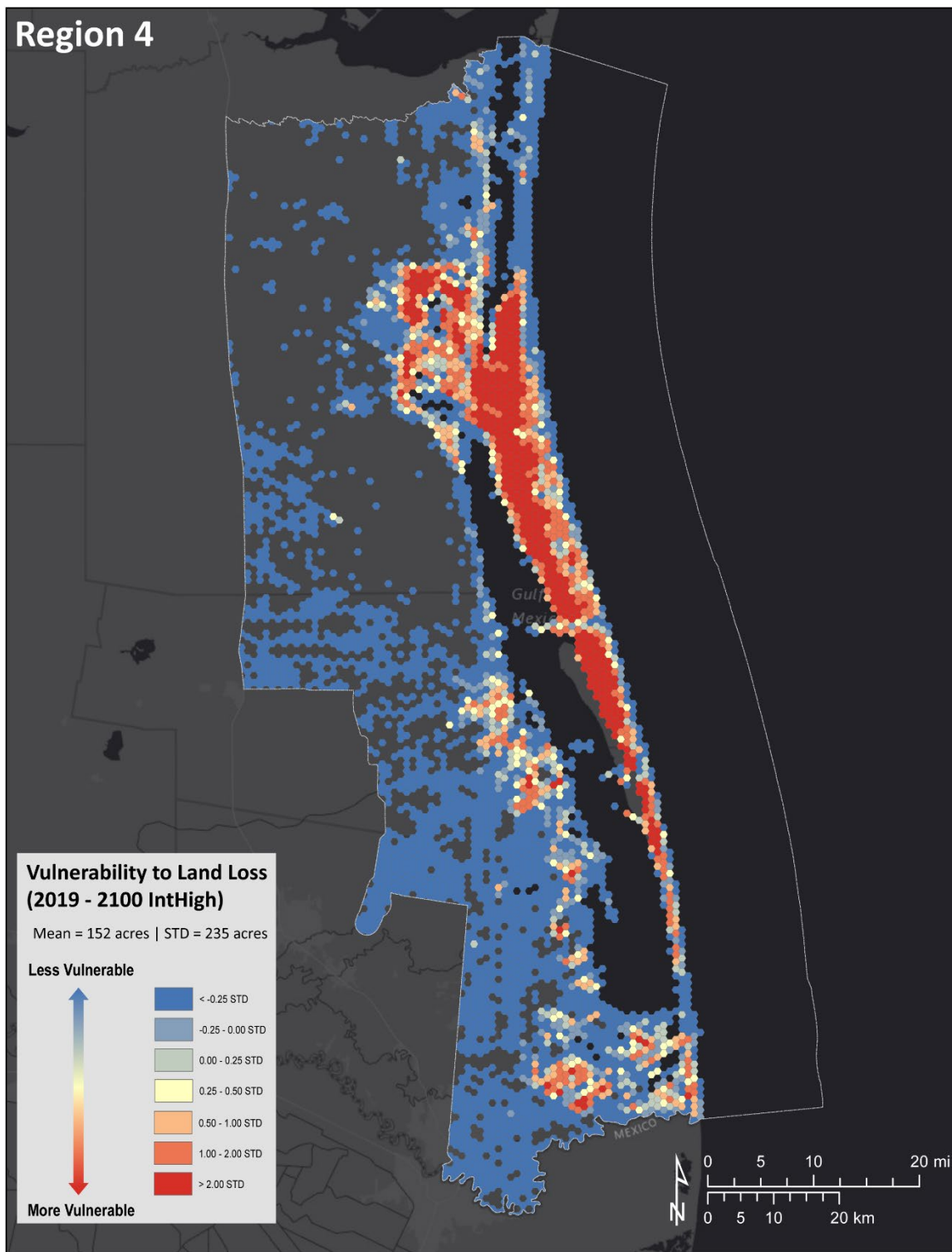
Figure 54. Map showing relative vulnerability to land loss in Region 4 where land loss means any type of land (excluding intertidal flats) that has converted to open water by the year 2100 in Intermediate-High SLR scenario.

Storm Surge Modeling

The following subsections present the maximum inundation extent for 19 synthetic storms in both the present and future landscapes with SLR. It also provides detail on the simulated maximum water surface elevation (MAXELE) analysis for a handful of storms. The MAXELE, also known as the maximum envelope of water (MEOW), is the maximum storm surge elevation computed at any point during the hurricane and provides information about the maximum inundation patterns. The maximum inundation extent maps illustrate the increased extent of maximum surge in the future landscape compared to the present landscape. To determine the amount of flooding caused by storm surge, the total inundated land area was calculated for each region where the storm made landfall.

In both the present and future landscapes, the right side (east) of the storm track experienced the highest storm surge impact due to the counterclockwise direction of the circulating winds during the hurricane, and the stronger winds passing on the right side (east) of the storm track. Most storms under the present landscape had a maximum storm surge elevation of 4-6 m, with a few storms having a MAXELE higher than 6 m, such as Storm 322, Storm 214, and Storm 216. In contrast, Storm 466, Storm 160, and Storm 240 had a MAXELE lower than 4 m under present conditions.

The future landscape simulations showed that the maximum storm surge elevation followed similar trends as observed in the present conditions. However, the water level was significantly higher under the future conditions than in the present condition, penetrating considerably farther inland. The intermediate-low scenario resulted in a 0.5 m increase in maximum storm surge offshore, which was equivalent to the sea level rise value used in the model. The intermediate-high scenario led to a 1.5 m increase in maximum storm surge offshore, which was the sea level rise value added to the model. It could be due to relatively deep water and low bottom friction offshore.

The increase in surge throughout the region ranged from 0.5-3 m in the future landscape simulations. However, it is important to note that storm surge flooding under SLR in the future landscape along the nearshore and complex coastlines was nonlinear. A significant variation in storm surge elevation between the present and future conditions was observed for all storm simulations. The increase in surge inland was higher by a factor of 1 m or more under the intermediate-low SLR scenario and 3 m or more under the intermediate-high scenario in many locations, which showed a nonlinear increase above the sea level rise value added to the model. Some locations showed an increment of less than the added SLR value, possibly due to the additional SLR allowing water to go farther inland and exposing new areas to inundation, which decreased water levels in the newly exposed flooded area.

The study also found that the higher sea level enabled an early arrival of the peak surge in the future condition compared to the present condition and significantly increased the time of inundation along the barrier islands and inland regions. The surge driven inland took longer to recede back to the Gulf of Mexico due to the increased sea level, significantly prolonging the timing of inundation in future condition.

Region 1

The study analyzed a total of 9 storms that made landfall in Region 1 under the present condition and two future conditions – Storm 466, Storm 160, Storm 363, Storm 262, Storm 358, Storm 154, Storm 587, Storm 449, and Storm 524. Among these storms, four were Category 1 storms, 4 were Category 2 and the remaining 1 storm was a Category 3 storm. Storm 466 and Storm 154 were also modeled for the

2019 Plan. Each storm possesses unique characteristics, such as forward speed, a radius of maximum wind (RMW), central pressure, orientation, and more (refer to Table 17). Therefore, their storm surge impacts differed from one another.

Table 17. Selected storms that made landfall in Region 1 and their characteristics

Storm	Wind Speed (kt)	RMW (Nmi)	Forward Speed (kt)	Central Pressure (mb)	Heading (deg)	Landfall Location
Storm 466	63.14	37.33	6.5	963.7	-20	High Island
Storm 160	86.99	7.29	8.6	927.3	-80	Bolivar Peninsula
Storm 363	76.84	20.17	6.2	927.3	-40	Anahuac Wildlife Refuge
Storm 262	84.21	22.86	5.9	921.3	-60	Galveston
Storm 358	86.91	10.08	9.5	955.4	-40	Galveston Island
Storm 154	87.77	34.71	10.3	940.4	-80	Follets Island
Storm 587	96.55	17.33	7.9	910.2	20	Galveston Island
Storm 449	74.67	34.9	19.5	947.7	-20	Freeport
Storm 524	81.35	23.58	13.1	940.4	0	Freeport (Brazos River)

In order to measure the extent of flooding caused by a more intense storm surge in the future landscape, the study computed the total area of inundated land within Region 1 for both present and future landscapes in the intermediate-low and intermediate-high scenarios. Based on the landscape change modeling, it was discovered that in the intermediate-low scenario, approximately 68 square miles of land in Region 1 were lost and converted to open water due to RSLR. This area significantly increased to 457 square miles in the intermediate-high scenario.

Storm 466

Figure 55 shows the MAXELE resulting from Storm 466 in four distinct landscape and sea-level scenarios. In addition to two future scenarios modeled, it includes the MAXELE resulting from the intermediate SLR scenario modeled for the 2019 Plan as a point of reference. An area with 1 – 2.5 m of inundation observed on the right side of the landfall along the McFaddin National Wildlife Refuge in the present landscape increased to more than 4 m in the future landscapes. Additionally, the water level was significantly higher in the future scenarios, causing a significant area to the west of the landfall to become flooded and extended considerably farther inland compared to the present landscape.

Within the Region 1 area, Storm 466 caused a total land inundated area of 626 square miles in the present landscape. In the future landscape, the total area of inundation resulting from Storm 466 in Region 1 was 1,036 square miles in the intermediate-low scenario, which represents a 65% increase. In the intermediate-high scenario, the total area of inundation resulting from Storm 466 in Region 1 was 1,376 square miles, representing a 120% increase. Figure 56 shows the extent of the inundation (inundation envelope) due to Storm 466 in the present landscape compared to two future landscapes.
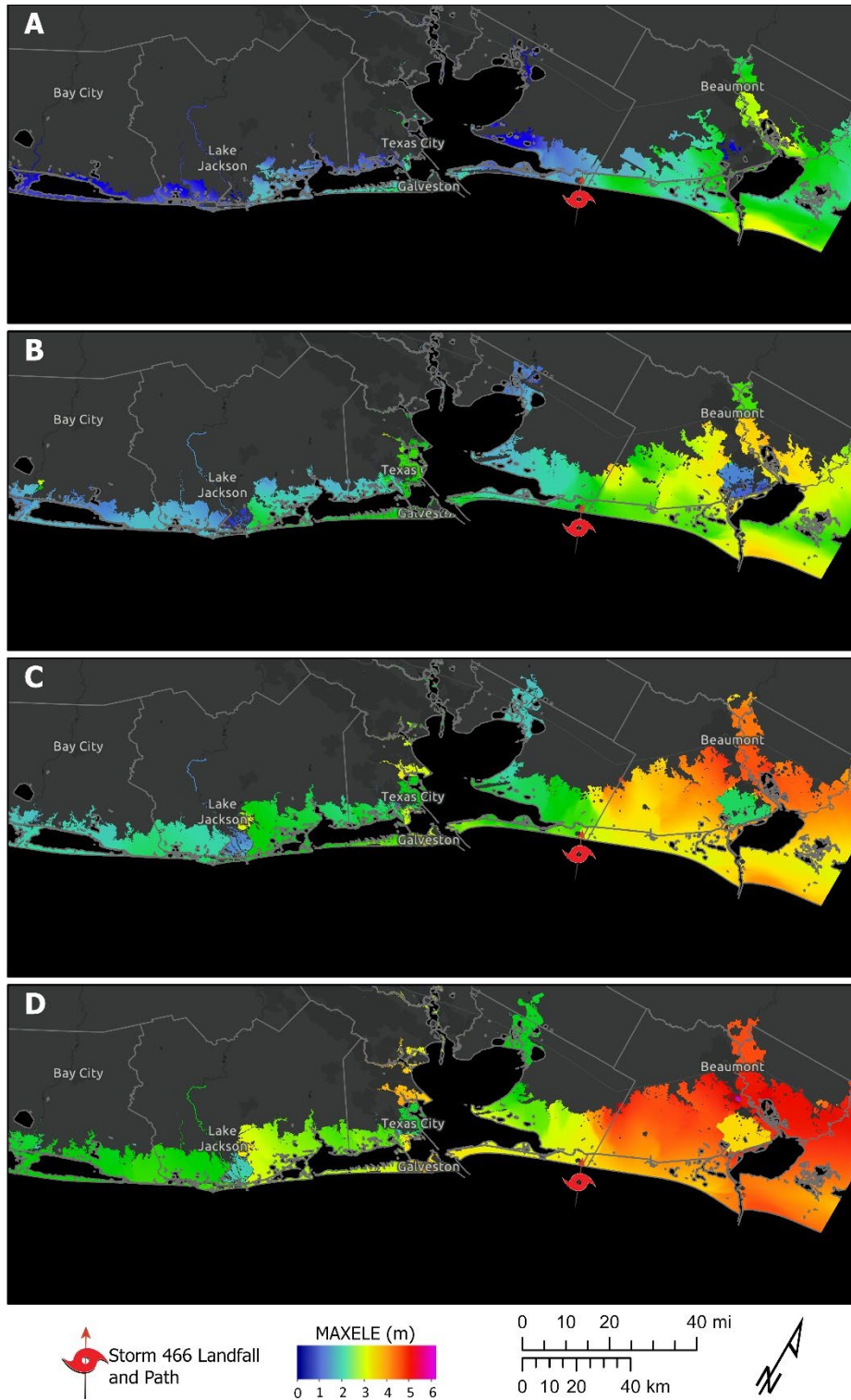
Figure 55. Maximum water surface elevation (MAXELE) due to Storm 466 on (A) Present landscape, (B) Future landscape - Intermediate-Low SLR scenario, (C) Future landscape - Intermediate SLR scenario (from 2019 Plan), and (D) Future landscape - Intermediate-high SLR scenario.
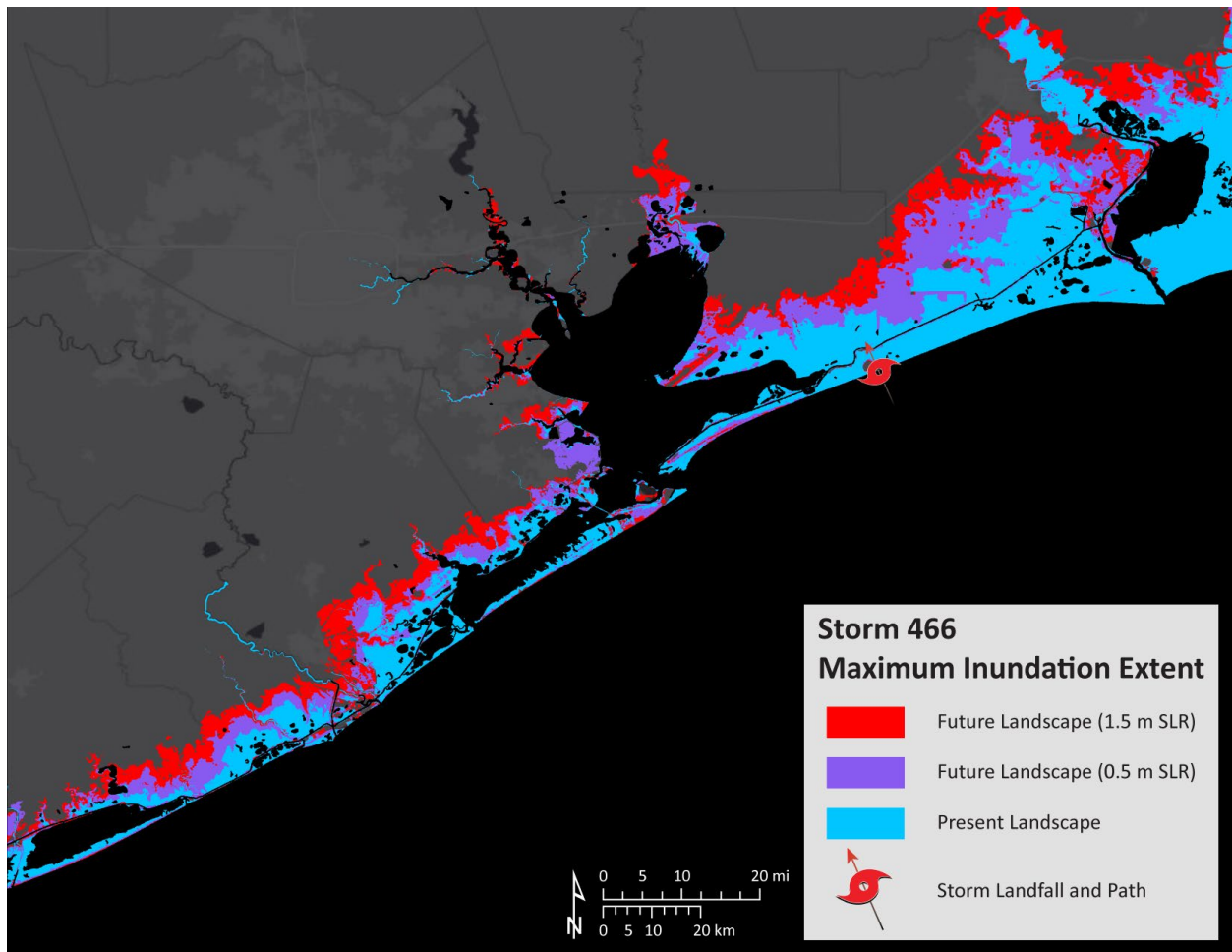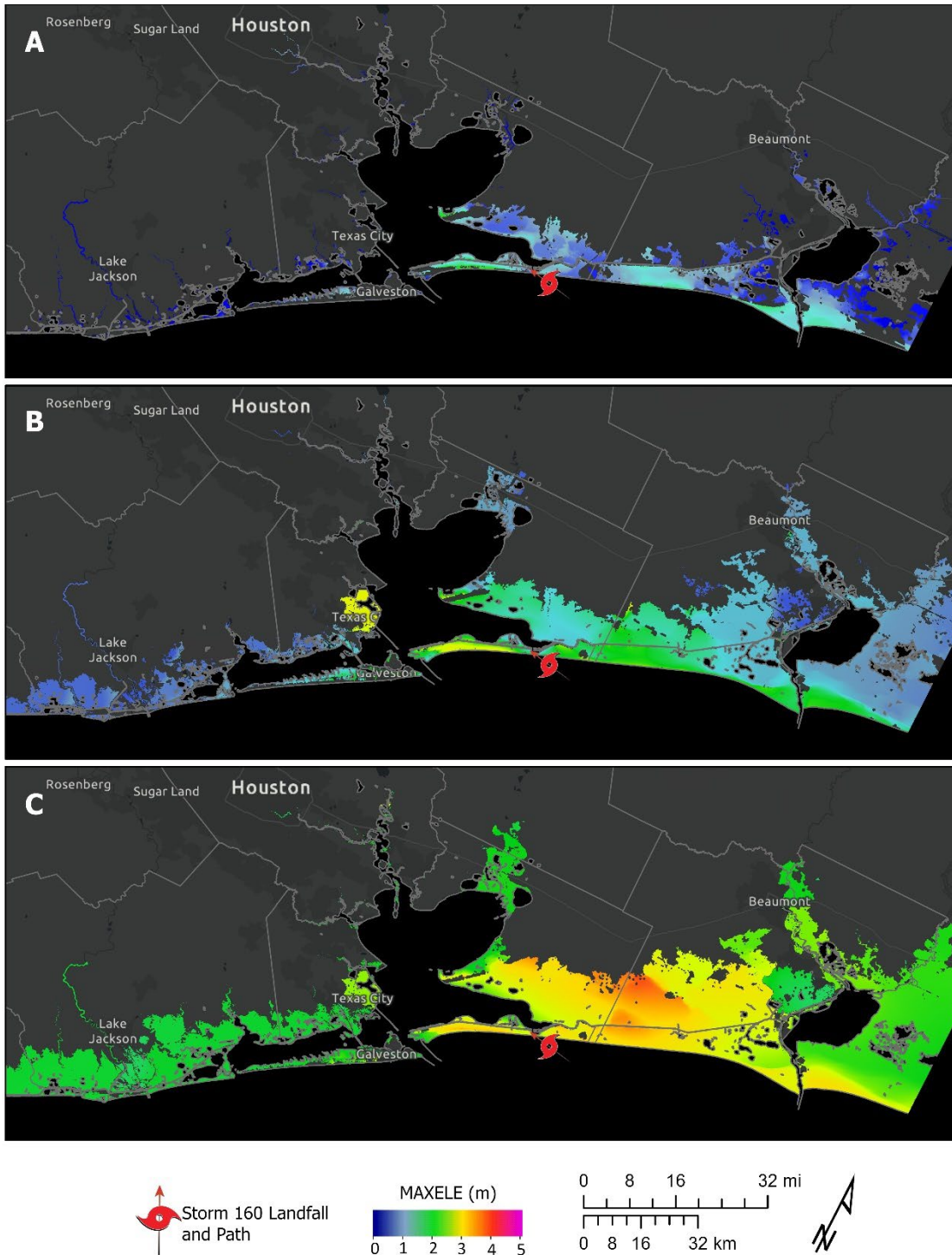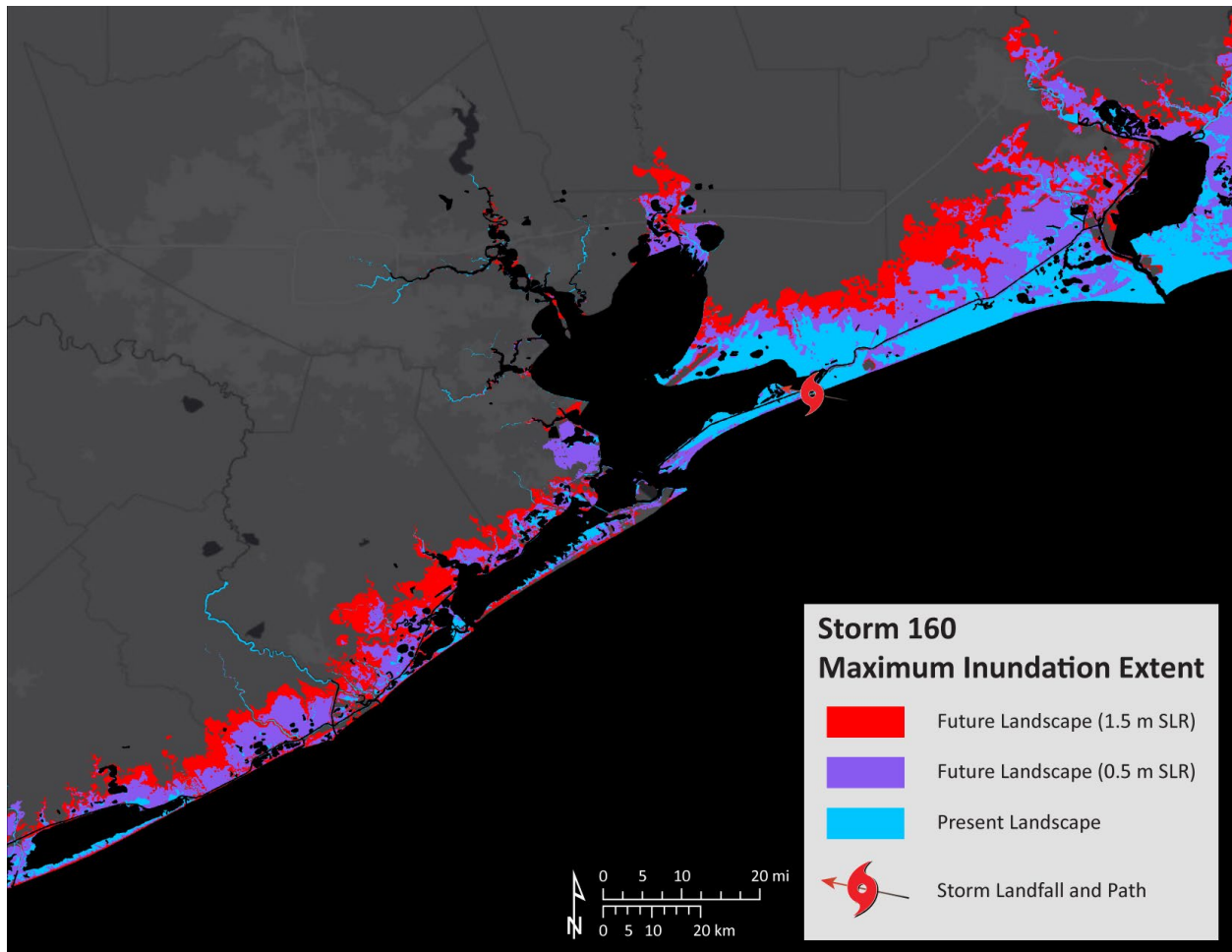
Figure 56. Maximum extent of inundation due to Storm 466

Storm 160

Figure 57 displays the maximum water surface elevation resulting from Storm 160 in the present landscape and two future landscapes modeled for the 2023 Plan. Despite being a Category 2 hurricane with a wind speed of 100 miles per hour at landfall, Storm 160 has the smallest radius of maximum wind (8.4 miles at landfall) among the modeled 19 storms. The surge height caused by the storm was the smallest among all modeled storms, with a general surge height of 1-2 meters on the east side of the landfall location. The increase in surge height nearshore was consistent with the added sea level rise value in the future landscape. However, the storm surge was able to penetrate much farther inland in the future landscape compared to the present landscape. A significant increase in storm surge inundation was observed on the west side of the landfall in the future landscape, resulting in a considerable increase in the inundation area in future scenarios.

Figure 58 shows the maximum extent of inundation resulting from Storm 160 in the present landscape and two future landscapes. The total inundated land area within Region 1 in the present landscape was 273 square miles. In future landscapes, the total area of inundation was 698 square miles in the intermediate-low scenario and 1,052 square miles in the intermediate-high scenario, which is a 156% and 285% increase from the present landscape, respectively.
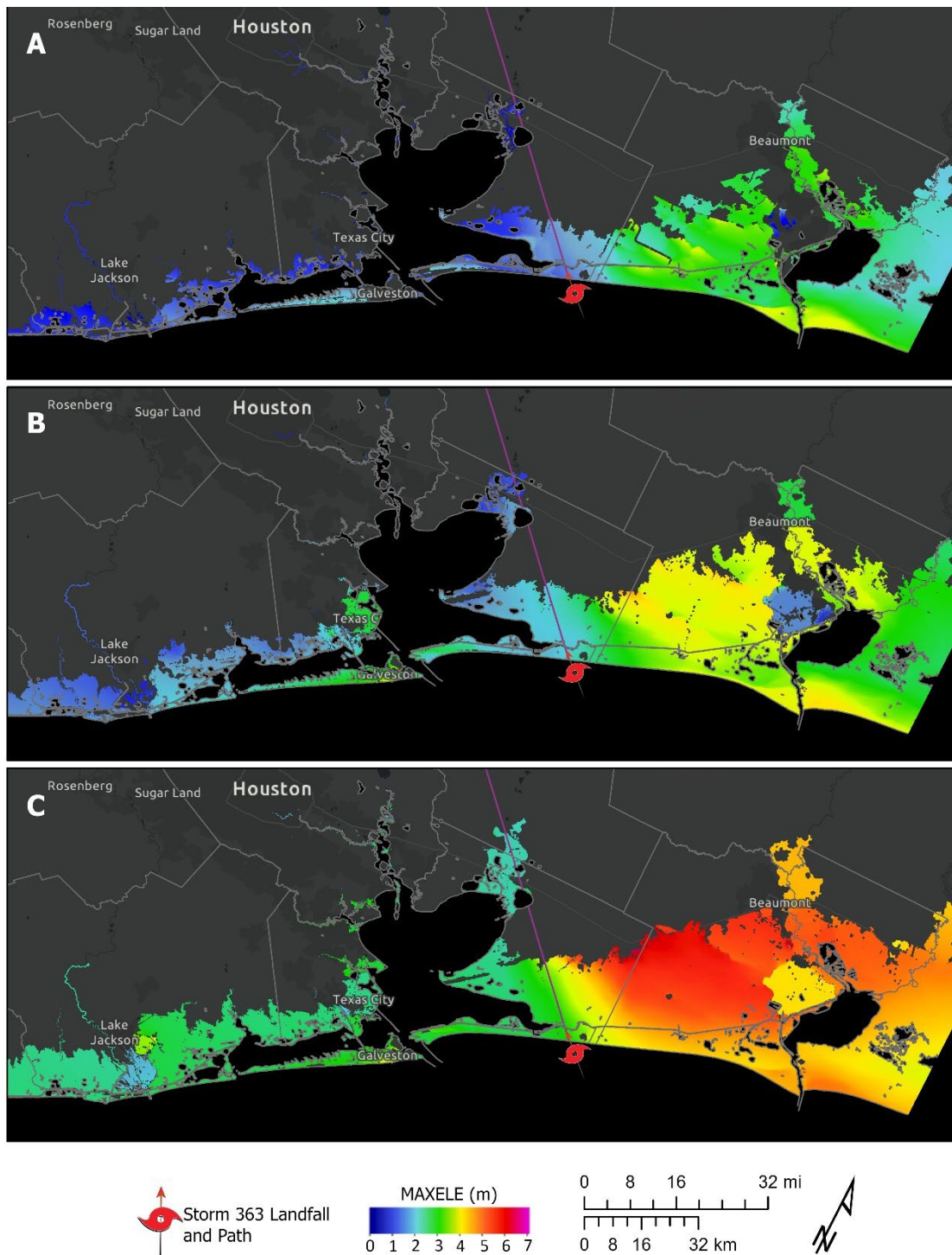
Figure 57. Maximum water surface elevation (MAXELE) due to Storm 160 on (A) Present landscape, (B) Future landscape - Intermediate-Low SLR scenario, and (C) Future landscape – Intermediate-High SLR scenario.
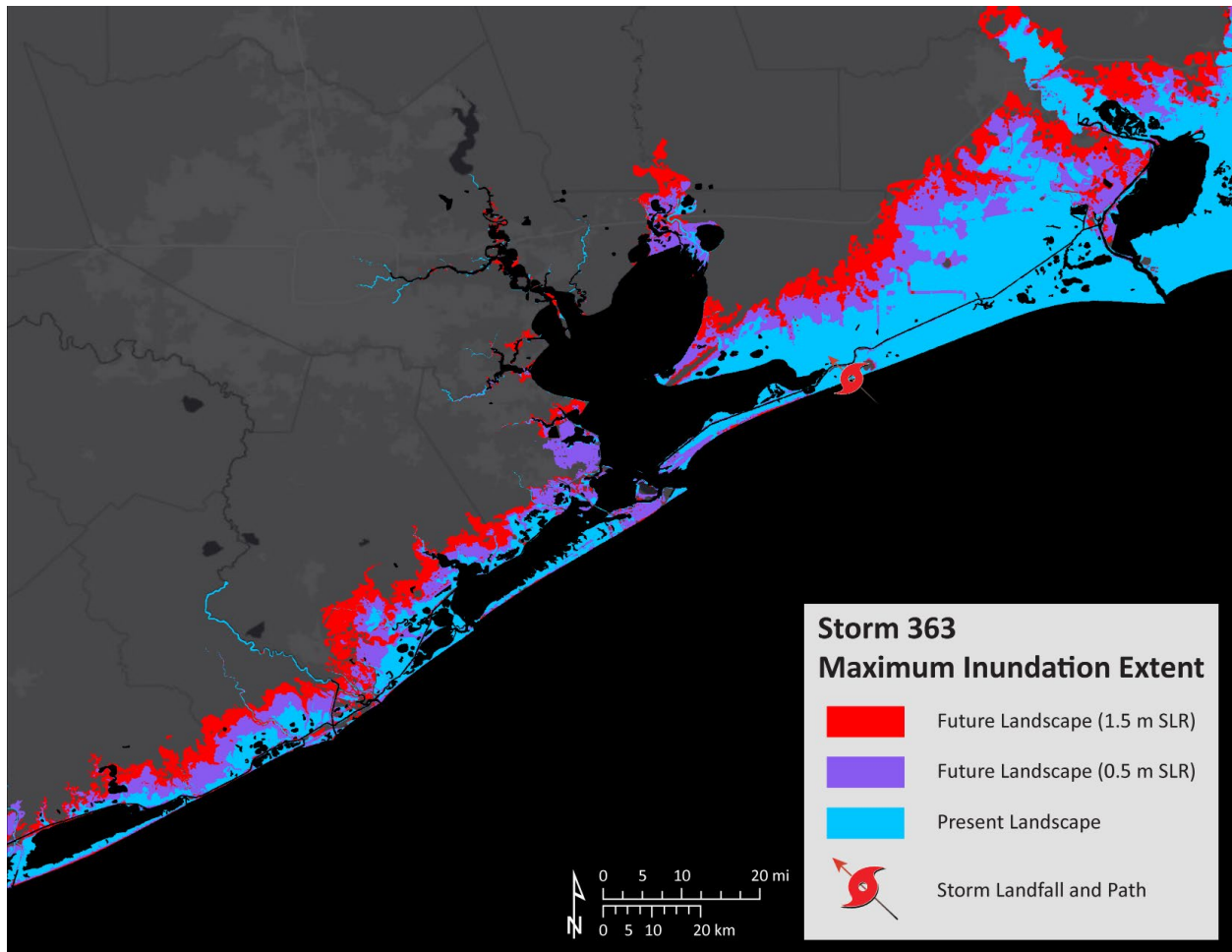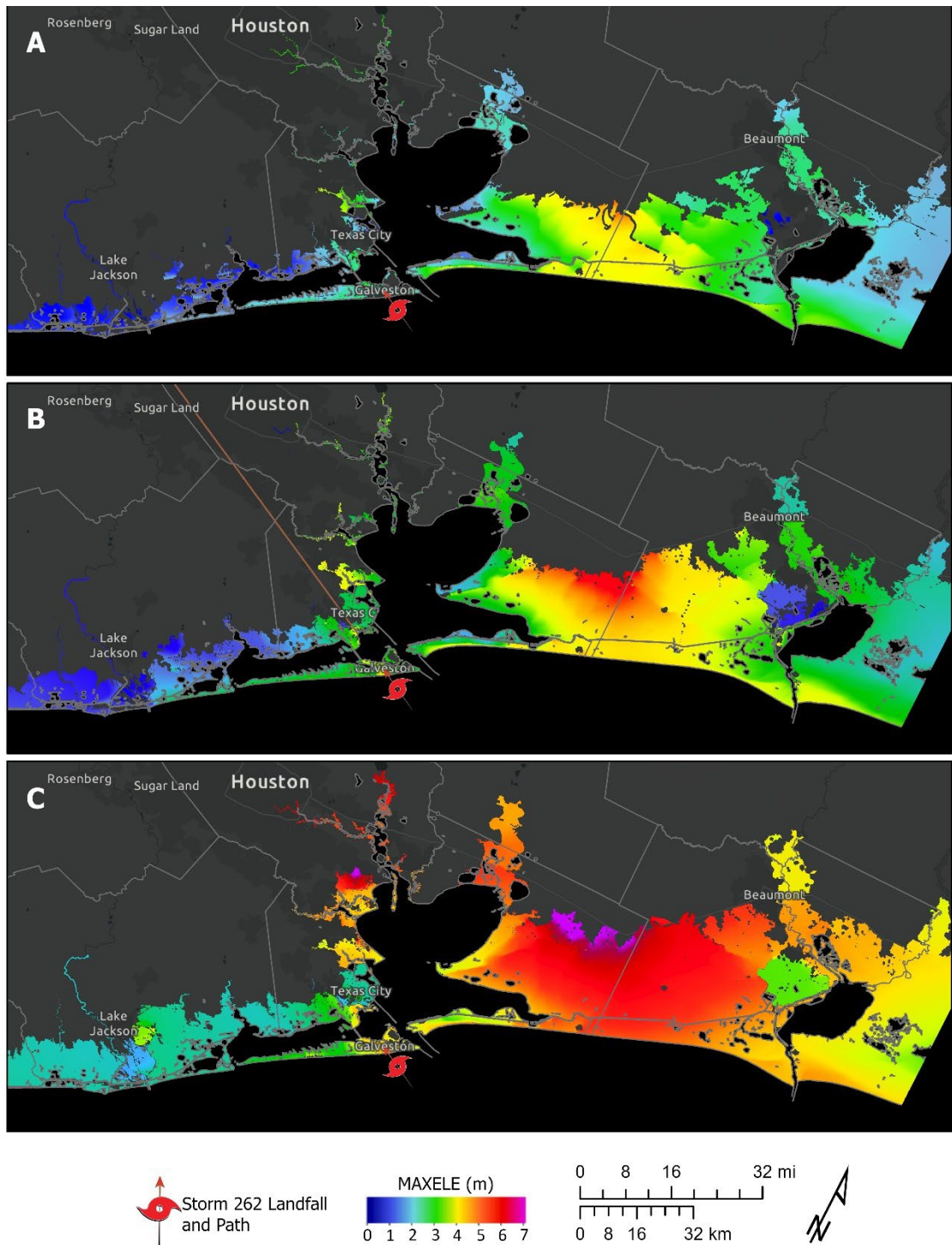
Figure 58. Maximum extent of inundation due to Storm 160.

Storm 363

Figure 59 shows the maximum water surface elevation resulting from Storm 363 in the present landscape and two future landscapes modeled for the 2023 Plan. In the present landscape, an area with 2.5 – 4 m of inundation is visible on the right side of the landfall along the McFaddin National Wildlife Refuge, which escalates to more than 5 m in the future landscapes. The storm surge impact was found to be similar to Storm 466 (Figure 55) which made landfall just 3 miles east of Storm 363. However, the water level was considerably higher in the future scenarios, causing a significant area to the west of the landfall to become flooded and extended considerably farther inland compared to the present landscape.

In the Region 1 area, Storm 363 caused a total land inundated area of 689 square miles in the present landscape which was very similar to the inundation area due to Storm 466. In the intermediate-low scenario of the future landscape, the total area of inundation resulting from Storm 363 in Region 1 was 1,063 square miles, representing a 54% increase. In the intermediate-high scenario, the total area of inundation resulting from Storm 363 in Region 1 was 1,395 square miles, representing a 102% increase. Figure 60 shows the extent of the inundation due to Storm 363 in the present landscape compared to two future landscapes.

Figure 59. Maximum water surface elevation (MAXELE) due to Storm 363 on (A) Present landscape, (B) Future landscape - Intermediate-Low SLR scenario, and (C) Future landscape – Intermediate-High SLR scenario.
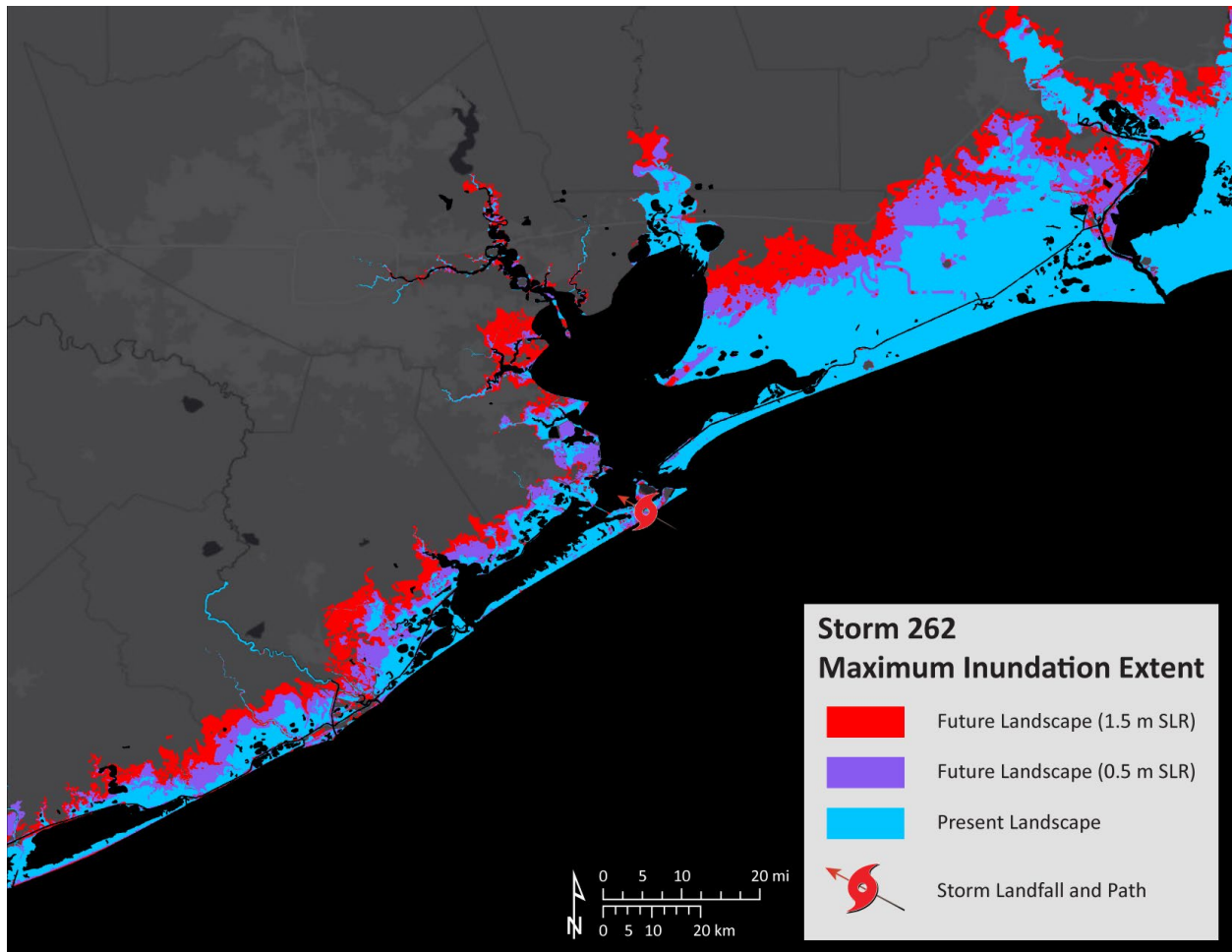
Figure 60. Maximum extent of inundation due to Storm 363.

Storm 262

Figure 61 shows the maximum water surface elevation resulting from Storm 262 in the present landscape and two future landscapes with SLR. This slow moving, relatively large Category 2 storm made landfall in Galveston, causing a storm surge of 2 – 3 m in the Galveston Island under the present landscape. In the future landscapes, the surge height increased to 4 -5 m in the island. The storm surge was able to penetrate much farther inland in the future landscapes causing a significant impact in the west side of Galveston Bay as well as in Houston.

In the present landscape, Storm 262 caused a total inundated land area of 851 square miles within Region 1. In the intermediate-low and intermediate-high scenarios of future landscapes, the total inundation areas resulting from Storm 262 were 1,174 and 1,526 square miles, respectively, representing a 38% and 79% increase from the present landscape. Figure 62 shows the maximum extent of inundation resulting from Storm 262 in the present landscape and two future landscapes.
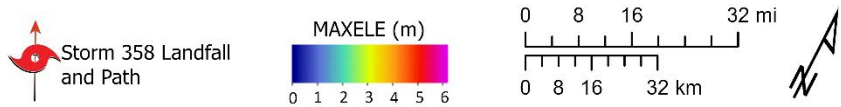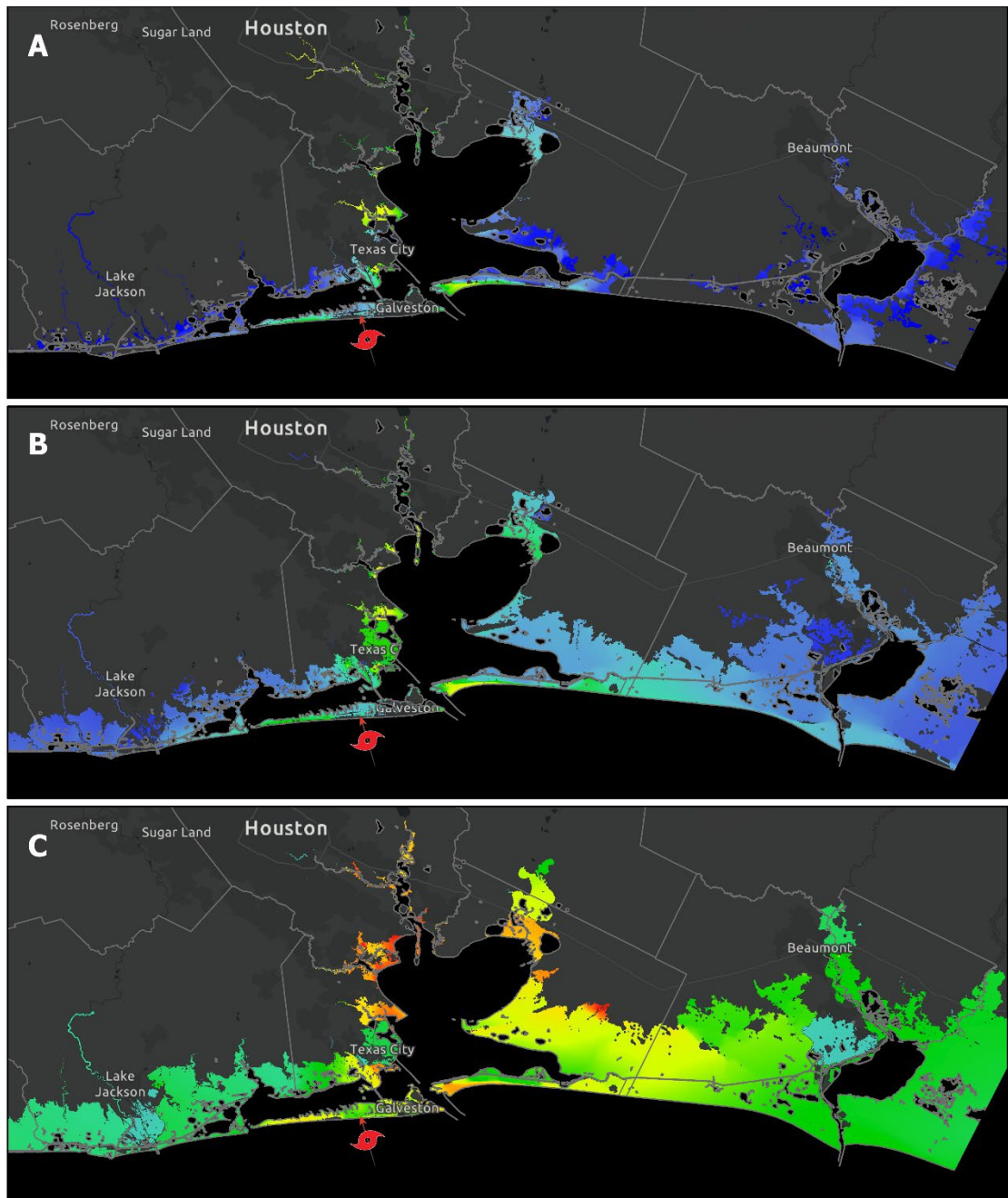
Figure 61. Maximum water surface elevation (MAXELE) due to Storm 262 on (A) Present landscape, (B) Future landscape - Intermediate-Low SLR scenario, and (C) Future landscape – Intermediate-High SLR scenario.
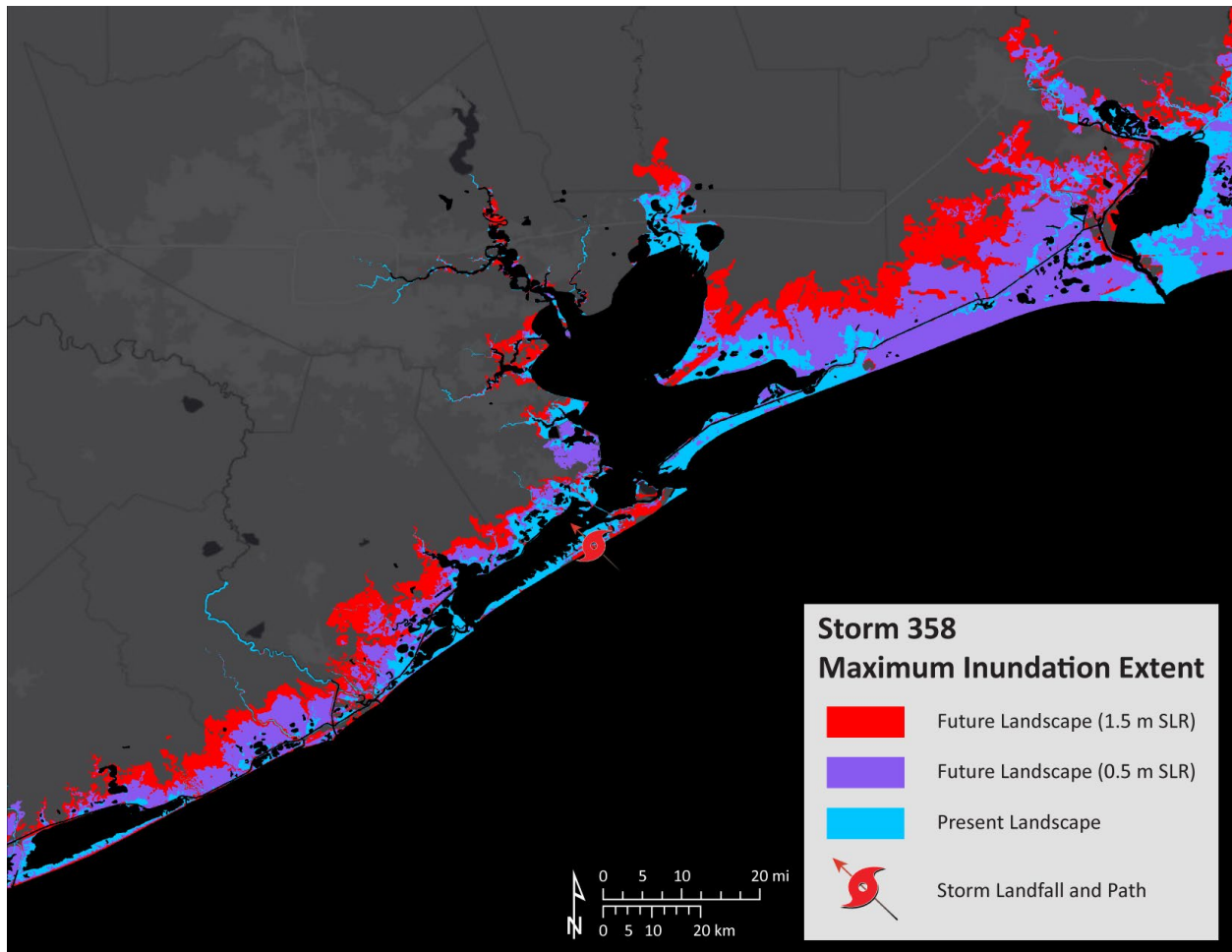
Figure 62. Maximum extent of inundation due to Storm 262.

Storm 358

Figure 63 shows the maximum water surface elevation resulting from Storm 358 in the present and two future landscapes modeled for the 2023 Plan. Storm 358 made landfall 7 miles west of Storm 262 in Galveston Island and was also a Category 2 hurricane with wind speeds similar to Storm 262. However, Storm 358 has a relatively small radius of maximum wind compared to Storm 262 but has higher central pressure. Despite these differences, the storm surge impact between the two storms was significantly different.

In the present landscape, Storm 358's storm surge penetration was considerably less than that of Storm 262, with a surge height of less than 1 meter in most areas except for Galveston Island, Bolivar Peninsula, and Texas City. The future landscape showed that the storm surge was able to penetrate further inland, but the surge height and inundation area were still significantly less than that of Storm 262.

In the Region 1 area, Storm 358 caused a total land inundation area of 246 square miles in the present landscape, which was 71% less than that caused by Storm 262. In the intermediate-low and intermediate-high scenarios of the future landscape, the total area of inundation resulting from Storm 358 in Region 1 was 744 and 1,157 square miles, representing a 202% and 370% increase from the present landscape,

respectively. Although the percentage increase from the present to future landscapes was higher than that of Storm 262, the total inundation area within Region 1 in the future landscapes was still 37% and 24% less than that due to Storm 262 in the intermediate-low and intermediate-high scenarios. Figure 64 shows the extent of the inundation due to Storm 363 in the present landscape compared to two future landscapes.
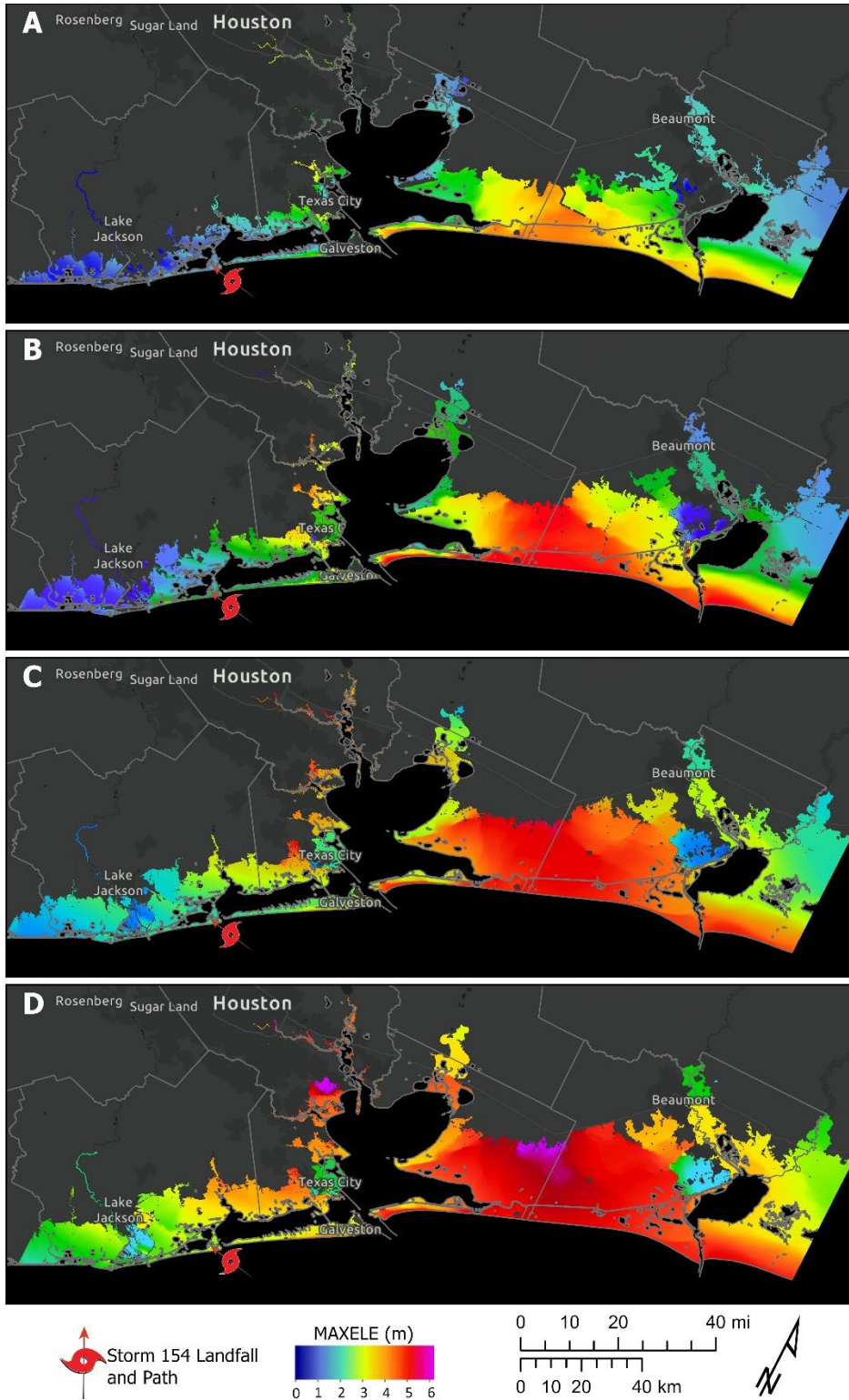
Figure 63. Maximum water surface elevation (MAXELE) due to Storm 358 on (A) Present landscape, (B) Future landscape - Intermediate-Low SLR scenario, and (C) Future landscape – Intermediate-High SLR scenario.

Figure 64. Maximum extent of inundation due to Storm 358.

Storm 154

Figure 65 shows the maximum water surface elevation resulting from Storm 154 in four distinct landscape and sea-level scenarios. In addition to two future scenarios modeled, it includes the MAXELE resulting from the intermediate SLR scenario modeled for the 2019 Plan as a point of reference. The storm surge impact due to Storm 154 in the present landscape looked similar to Storm 262 (Figure 61). An area with 2 - 4 m of inundation was observed in Galveston Island, Bolivar Peninsula, and McFaddin National Wildlife Refuge area in the present landscape, which increased to more than 4 m in the future landscapes. Additionally, the storm surge was significantly higher in all three future landscape scenarios, causing a significant area in Galveston, Chambers, and Jefferson County to become flooded, and extended considerably farther inland to Harris and Orange County compared to the present landscape.

In the present landscape, Storm 154 caused a total inundated land area of 805 square miles within Region 1, which is very similar to Storm 262. In the future landscape, the total area of inundation resulting from Storm 154 in Region 1 was 1,114 square miles in the intermediate-low scenario, which represents a 39% increase. In the intermediate-high scenario, the total area of inundation resulting from Storm 154 in Region 1 was 1,439 square miles, representing a 79% increase from the present landscape. Figure 66

shows the maximum extent of the inundation due to Storm 154 in the present landscape compared to two future landscapes.

Figure 65. Maximum water surface elevation (MAXELE) due to Storm 154 on (A) Present landscape, (B) Future landscape - Intermediate-Low SLR scenario, (C) Future landscape - Intermediate SLR scenario (from 2019 Plan), and (D) Future landscape - Intermediate-high SLR scenario
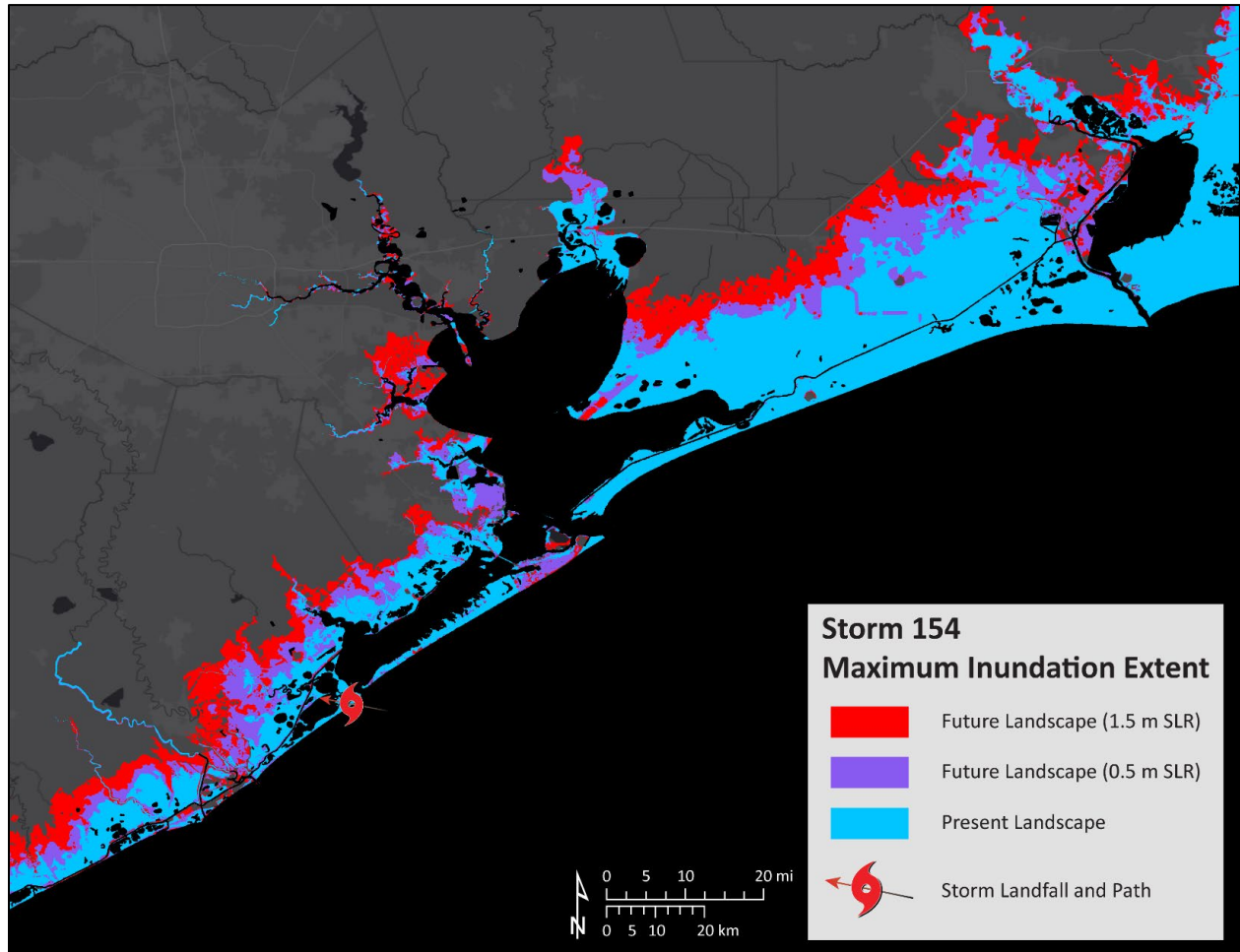

Figure 66. Maximum extent of inundation due to Storm 154

Storm 587

Figure 67 presents the maximum water surface elevation resulting from Storm 587 in the present landscape and two future landscapes with SLR. This slow-moving and relatively large storm has made landfall on the western end of Galveston Island and is the only Category 3 hurricane modeled in Region 1. The amount of storm surge impact seen in the Texas City and Seabrook area in the present landscape was not observed in any other storms modeled for Region 1. Additionally, the inland penetration observed due to this powerful storm was significantly higher than any other storms modeled in Region 1. The storm surge was able to reach much farther inland in the future landscapes, causing a massive increase in the flooding area. In the intermediate-high scenario, more than 5 m of surge height was observed throughout the region.

Figure 68 shows the maximum extent of inundation resulting from Storm 587 in the present landscape and two future landscape scenarios. The total inundated land area within Region 1 in the present landscape is 939 square miles. In future landscapes, the total area of inundation was 1,260 square miles

in the intermediate-low scenario and 1,654 square miles in the intermediate-high scenario, which is a 34% and 76% increase from the present landscape, respectively.
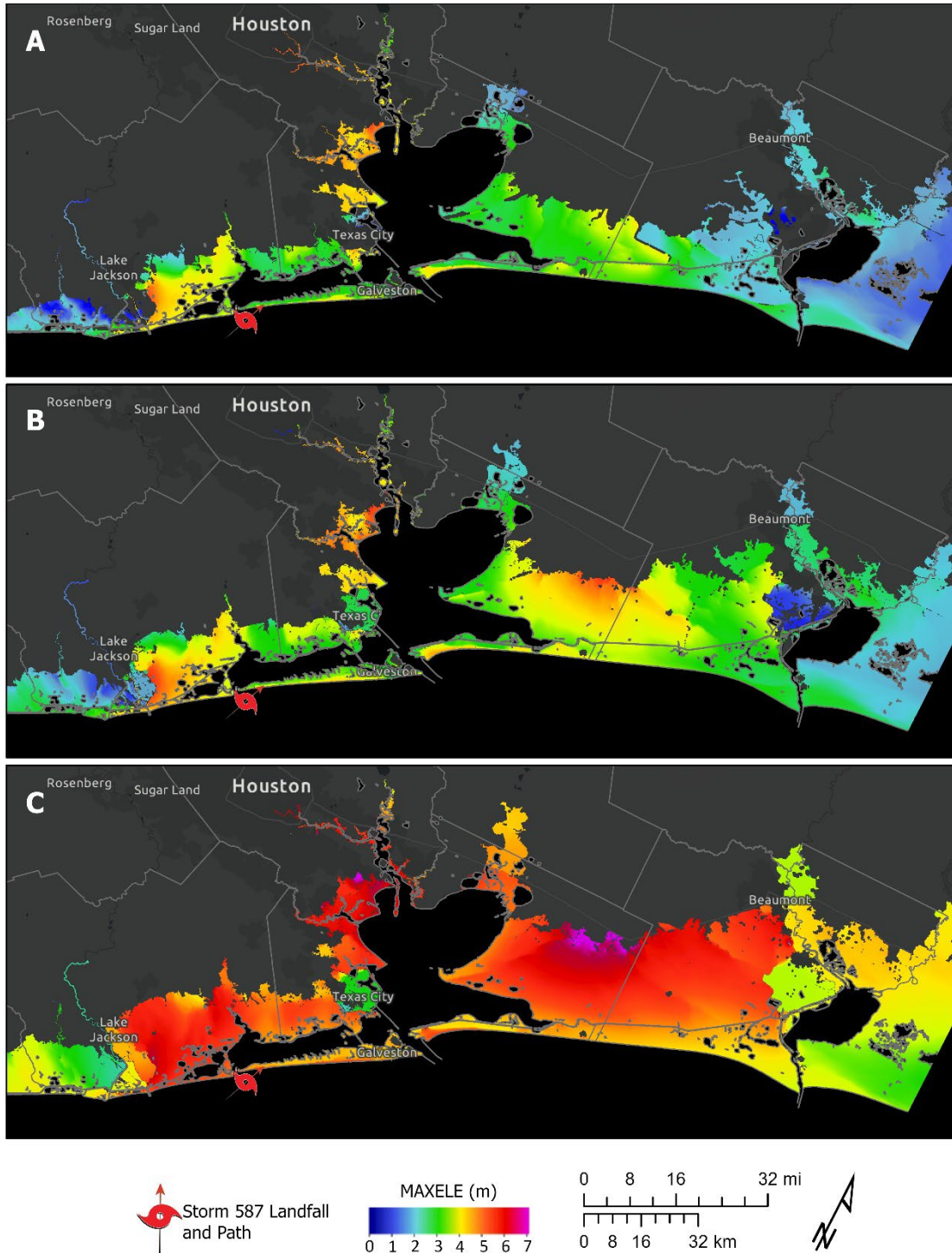

Figure 67. Maximum water surface elevation (MAXELE) due to Storm 587 on (A) Present landscape, (B) Future landscape - Intermediate-Low SLR scenario, and (C) Future landscape – Intermediate-High SLR scenario.
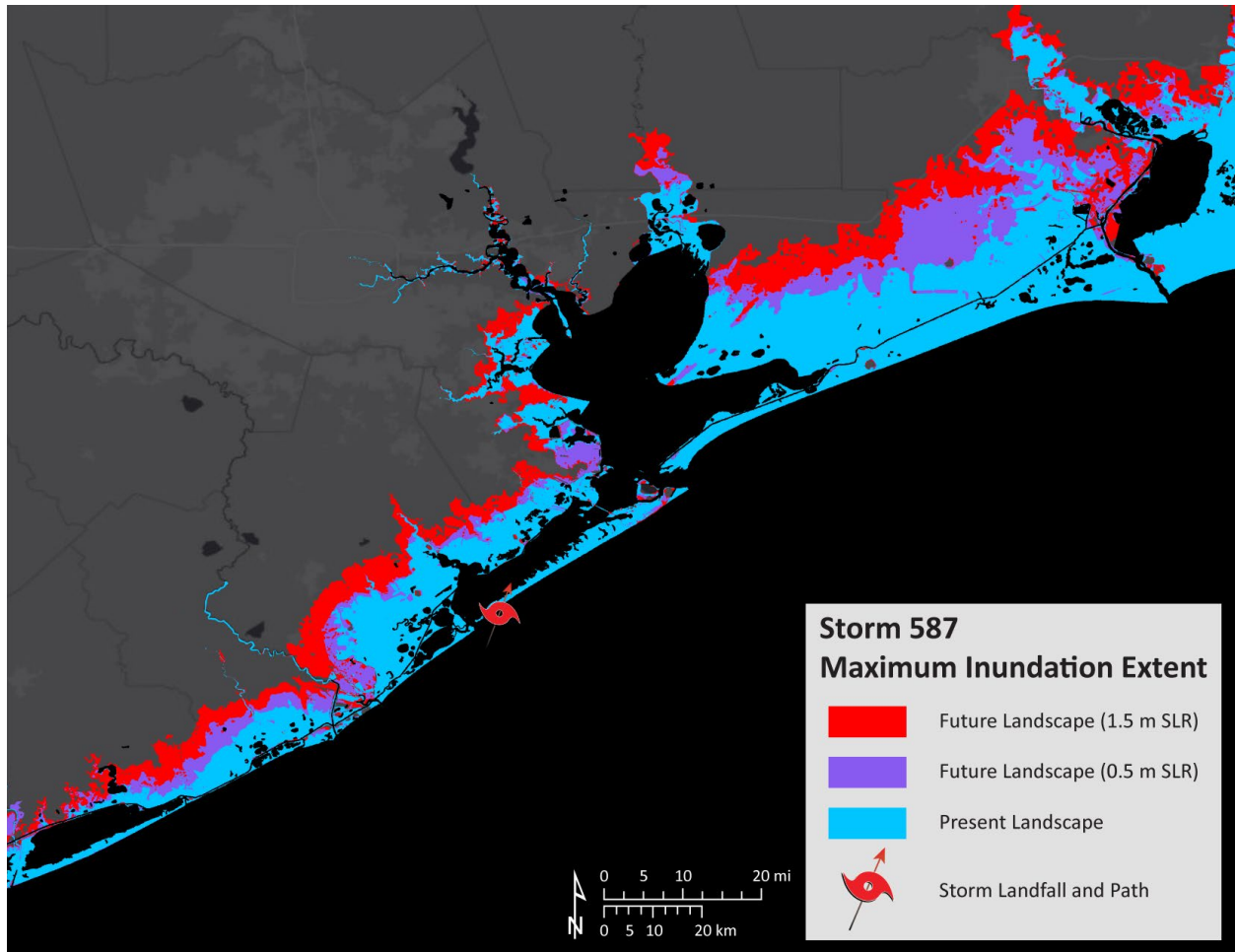
Figure 68. Maximum extent of inundation due to Storm 587.

Storm 449

Figure 69 shows the maximum water surface elevation resulting from Storm 449 in the present landscape and two future landscapes with SLR. This Category 1 hurricane has the highest forward speed among the 19 modeled storms for the 2023 Plan and is a relatively large radius of maximum wind (RMW). The large wind field of Storm 449 generated strong currents that caused a significant buildup of water, leading to widespread flooding in the region. The storm surge impact in the region was even greater than that of the Category 3 hurricane, Storm 587 (see Figure 67). Despite making landfall near Freeport, the present landscape experienced 3.5 – 4.5 m of inundation in the Bolivar Peninsula and the McFaddin National Wildlife Refuge area. In the future landscape, an additional 2-3 m of surge height was observed throughout the region. The storm surge reached considerably farther inland compared to the present landscape causing massive widespread flooding of 6 m and more.

In the present landscape, Storm 449 caused a total inundated land area of 980 square miles in Region 1, which is 4% more than that caused by Category 3 Storm 587. In the intermediate-low and intermediate-high scenarios of the future landscape, the total area of inundation resulting from Storm 449 in Region 1 was 1,249 and 1,655 square miles, representing a 27% and 69% increase from the present landscape, respectively. These inundation areas in the future landscapes were similar to those caused by Storm

587. Figure 70 shows the extent of the inundation due to Storm 449 in the present landscape compared to two future landscapes.
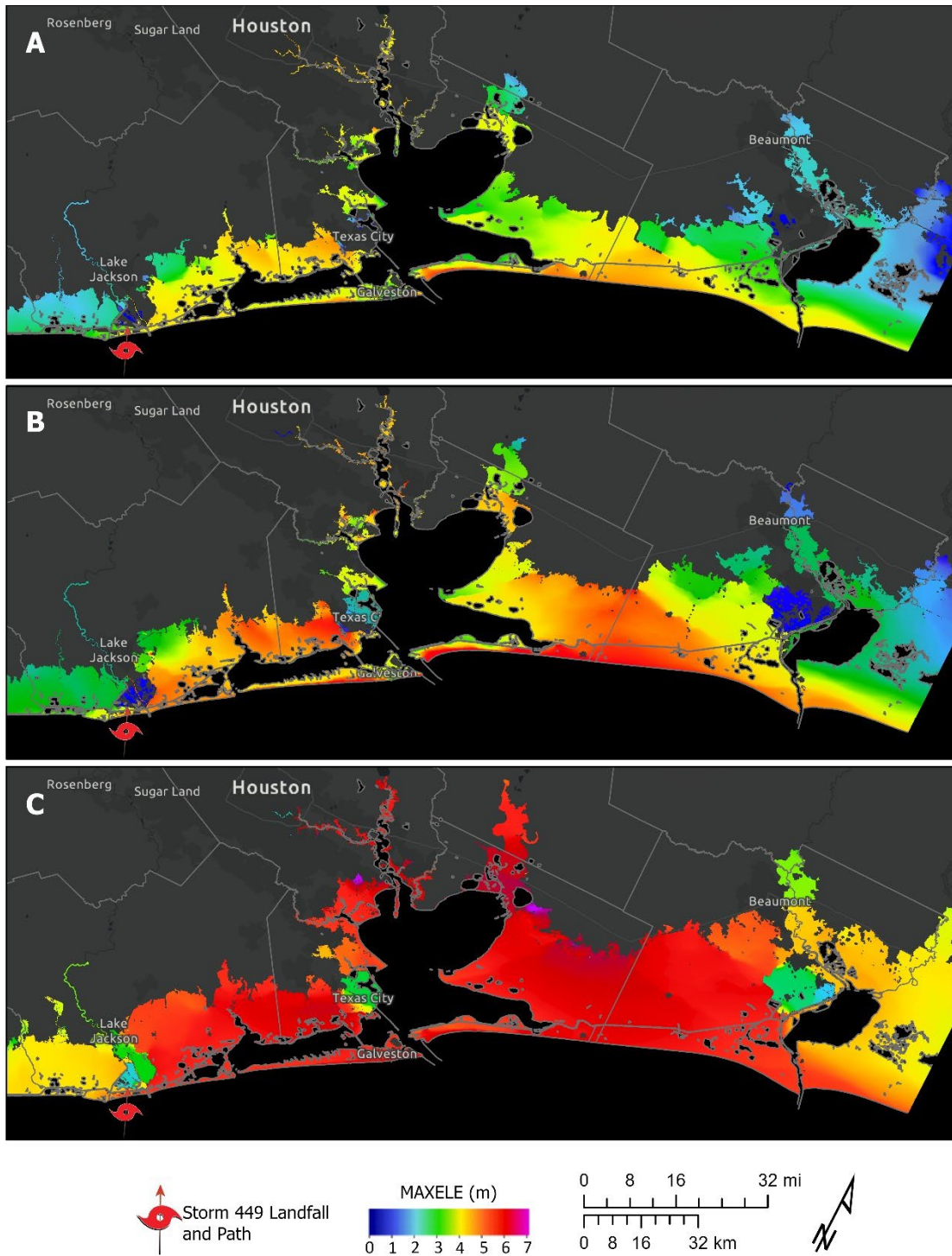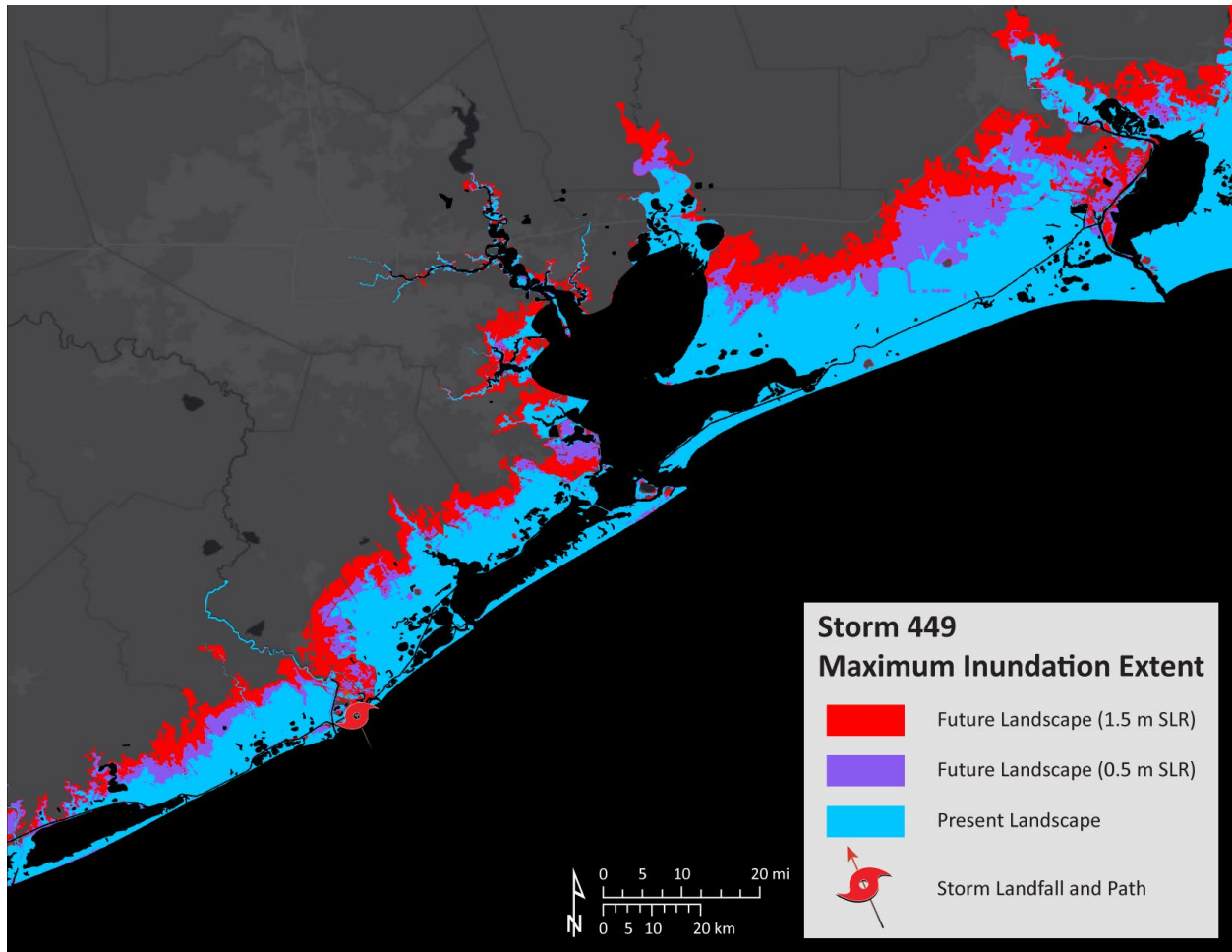

Figure 69. Maximum water surface elevation (MAXELE) due to Storm 449 on (A) Present landscape, (B) Future landscape - Intermediate-Low SLR scenario, and (C) Future landscape – Intermediate-High SLR scenario.

Figure 70. Maximum extent of inundation due to Storm 449.

Storm 524

Figure 71 presents the maximum water surface elevation caused by Storm 524 in the present landscape and two future landscapes with SLR. This Category 1 hurricane made landfall 7 miles west of Storm 449 near the mouth of the Brazos River, with higher wind speed and a smaller radius of maximum wind compared to Storm 449. While the storm surge impact due to Storm 524 was similar to Storm 449 along the west side of Galveston Bay, Storm 449 had a greater impact on the east side of the bay due to its larger wind field. Both future landscape scenarios exhibited significantly higher storm surge impacts, causing extensive flooding throughout the region and extending much farther inland to Harris County and Orange County compared to the present landscape.

In the present landscape, Storm 524 caused a total inundated land area of 894 square miles within Region 1 and also caused a significant impact in Region 2 as it made landfall near the border of these two regions. In the future landscape, the total area of inundation resulting from Storm 524 in Region 1 was 1,124 square miles in the intermediate-low scenario, which represents a 25% increase. In the intermediate-high scenario, the total area of inundation resulting from Storm 524 in Region 1 was 1,607 square miles, representing an 80% increase from the present landscape. Figure 72 shows the maximum extent of the inundation due to Storm 524 in the present landscape compared to two future landscapes.
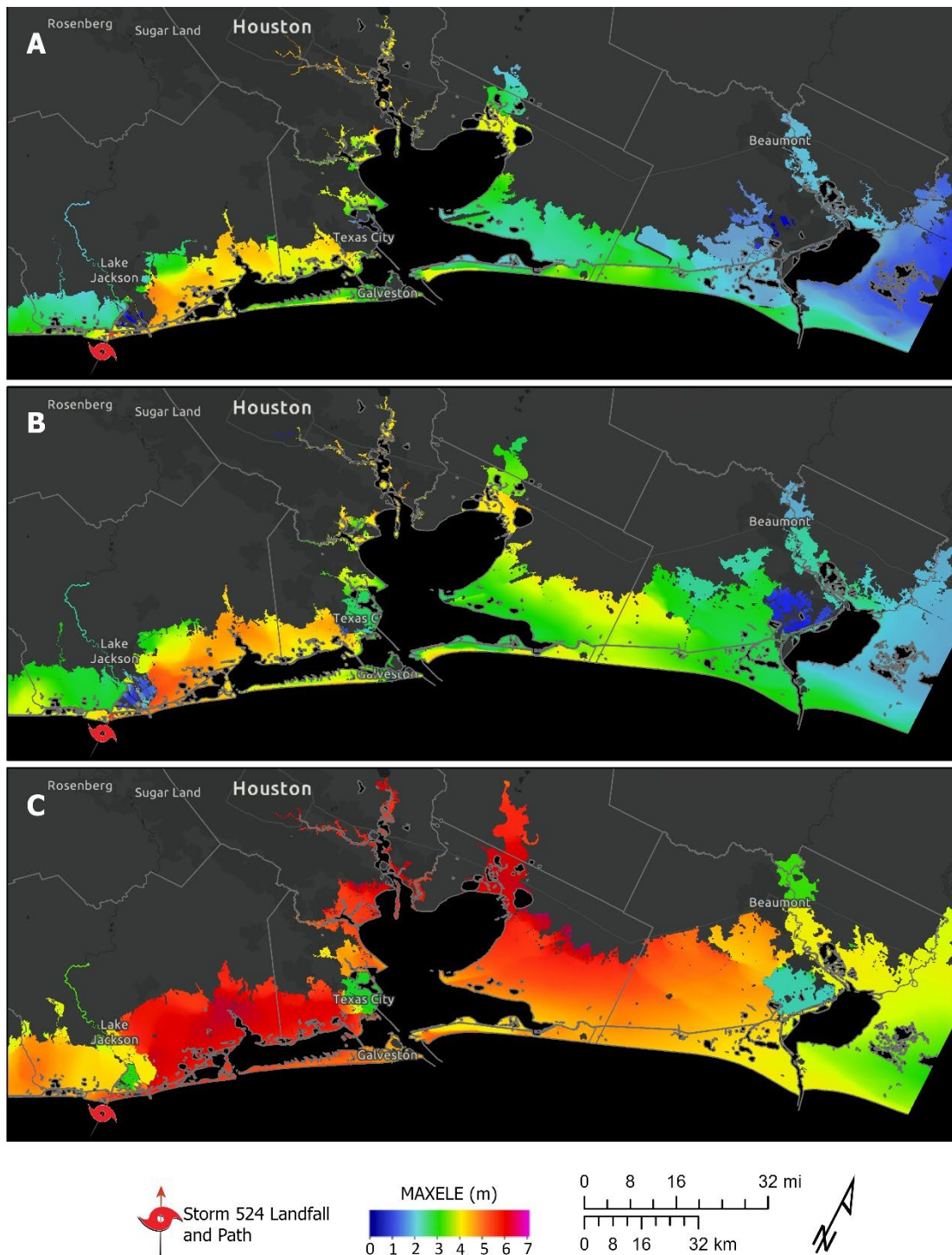
Figure 71. Maximum water surface elevation (MAXELE) due to Storm 524 on (A) Present landscape, (B) Future landscape - Intermediate-Low SLR scenario, and (C) Future landscape – Intermediate-High SLR scenario.
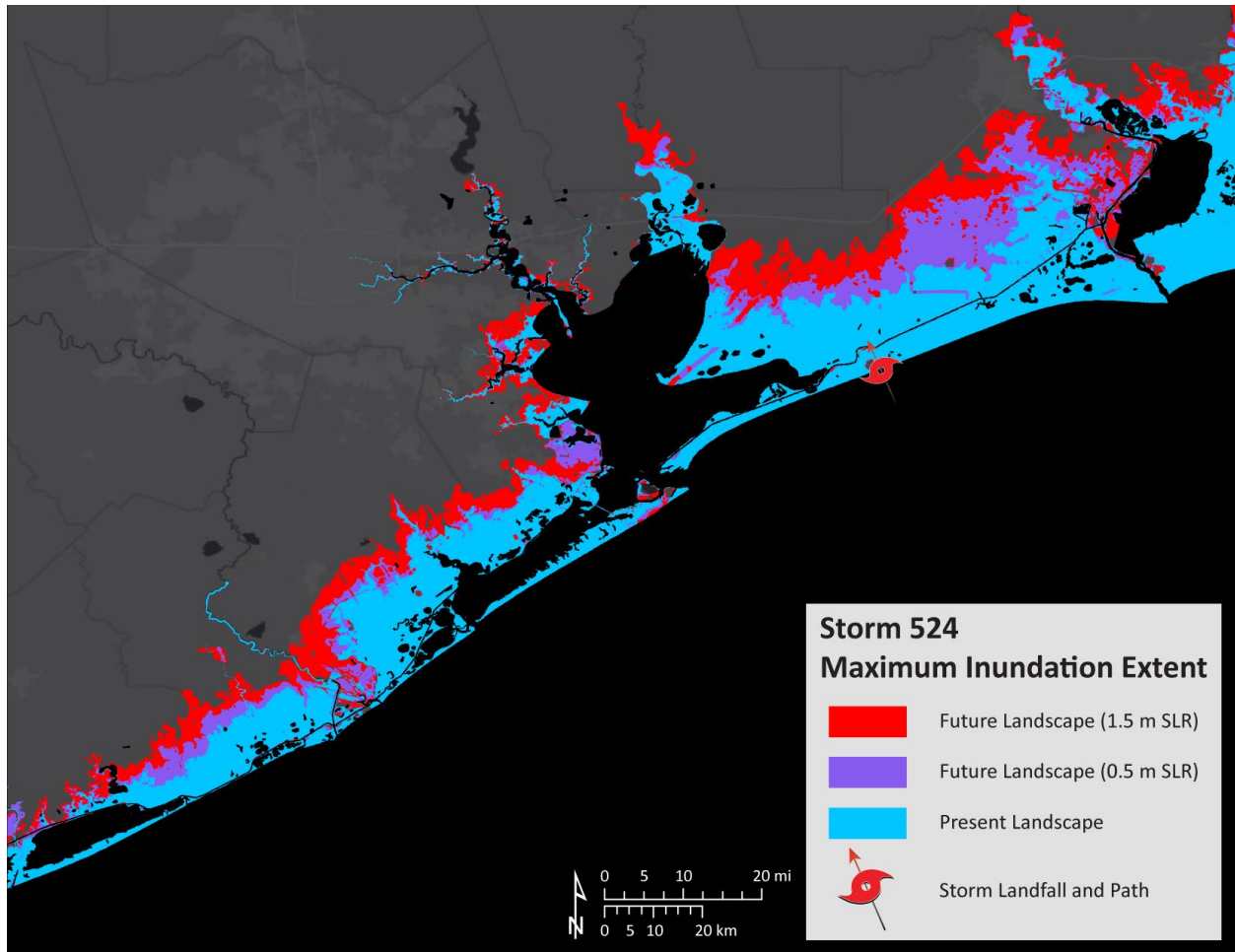
Figure 72. Maximum extent of inundation due to Storm 524.

Region 2

The study examined the impact of two Category 2 storms, Storm 146 and Storm 240, that made landfall in Region 2 under present and future conditions. These storms were also analyzed in the 2019 Plan, and their characteristics, including forward speed, the radius of maximum wind (RMW), central pressure, orientation, and landfall location, are presented in Table 18.

To estimate the extent of flooding caused by intensified storm surges in the future landscape, the study calculated the total inundated land area in Region 2 for both present and future landscapes under the intermediate-low and intermediate-high scenarios. The landscape change modeling showed that in the intermediate-low scenario, around 68 square miles of land in Region 2 were lost and converted to open water due to RSLR. This area increased to 191 square miles in the intermediate-high scenario.

Table 18. Selected storms that made landfall in Region 2 and their characteristics

Storm	Wind Speed (kt)	RMW (Nmi)	Forward Speed (kt)	Central Pressure (mb)	Heading (deg)	Landfall Location
Storm 146	83.83	34.89	18.3	927.3	-80	Matagorda Peninsula
Storm 240	84.61	23.26	17.7	947.7	-60	Matagorda Island

Figure 73 shows the MAXELE resulting from Storm 146 in four distinct landscape and sea-level scenarios, including the MAXELE resulting from the intermediate SLR scenario modeled for the 2019 Plan for reference. Storm 146, a Category 2 hurricane with a large wind field, was able to fill in the bays and inland lakes hours before making landfall in the present landscape. In the future landscapes, higher water levels and more inland penetration of surge completely inundated the barrier islands with 2-5 m of water well before the storm's landfall. During landfall, there was an extensive surge buildup that penetrated farther inland in both the present and future conditions as the bays and inland lakes were already filled with extra water from the forerunner surge.

The impact of Storm 146 was significantly higher in Region 1 all the way to Chambers County compared to Region 2. In the present landscape, an area with 2 – 4 m of inundation was observed on the right side of the landfall along the Freeport area to the West Bay region, which increased to more than 5 m in the future landscapes. Additionally, the water level was significantly higher in the future scenarios, causing a significant area to the west of the landfall along Matagorda Bay region to become flooded and extended considerably farther inland compared to the present landscape.

Within the Region 2 area, Storm 146 caused a total land inundated area of 245 square miles in the present landscape. In the future landscape, the total area of inundation resulting from Storm 146 in Region 2 was 375 square miles in the intermediate-low scenario, which represents a 53% increase. In the intermediate-high scenario, the total area of inundation resulting from Storm 146 in Region 2 was 588 square miles, representing a 140% increase. However, the storm surge impact within Region 1 was significantly greater than that of Region 2 as higher inundation was observed on the right side of the landfall. For example, the total area of inundation within Region 1 in the present landscape due to Storm 146 was 884 square miles and it increased by 65% in the intermediate-high scenario. Figure 74 shows the extent of the inundation (inundation envelope) due to Storm 146 in the present landscape compared to two future landscapes.
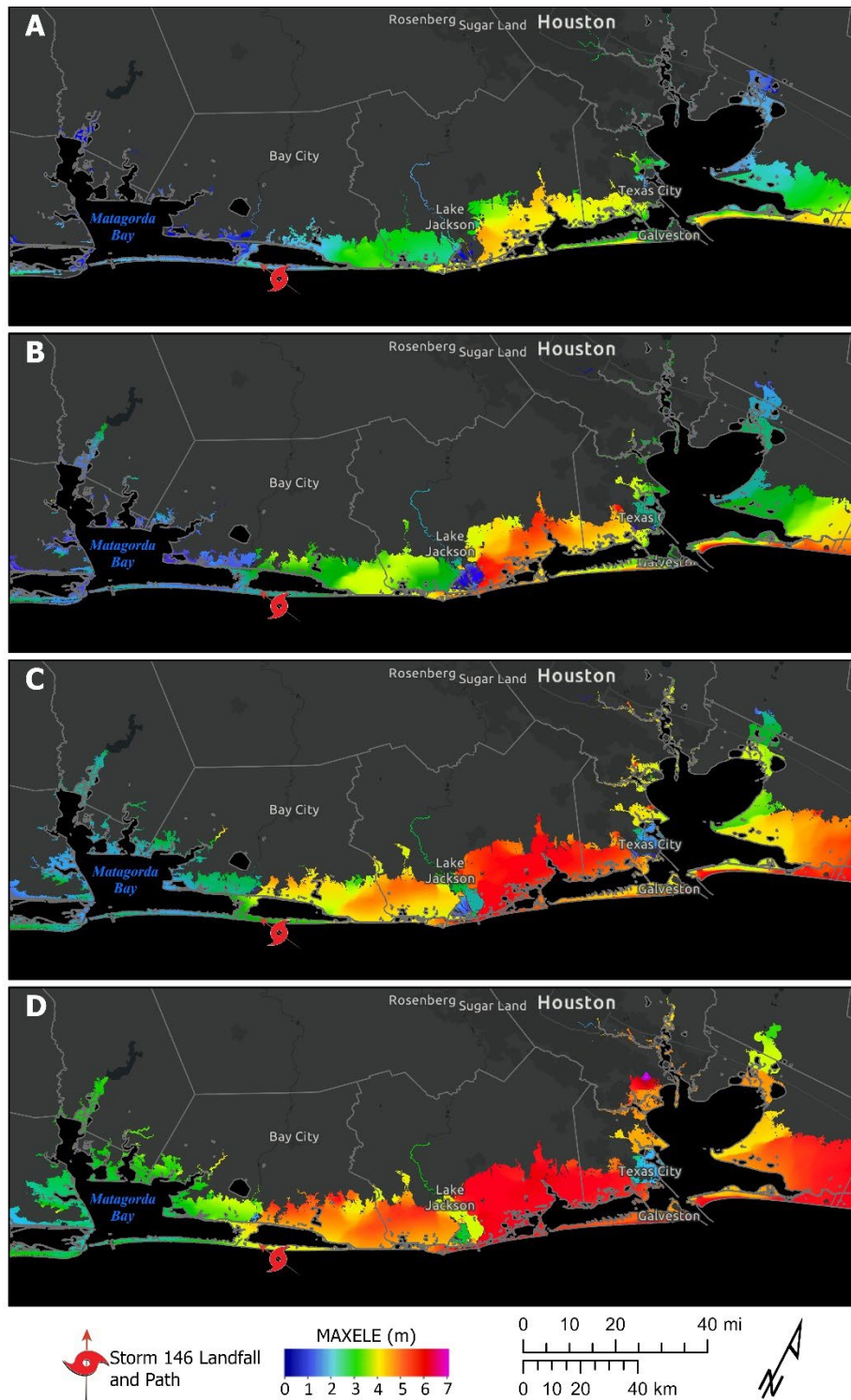
Figure 73. Maximum water surface elevation (MAXELE) due to Storm 146 on (A) Present landscape, (B) Future landscape - Intermediate-Low SLR scenario, (C) Future landscape - Intermediate SLR scenario (from 2019 Plan), and (D) Future landscape - Intermediate-high SLR scenario.
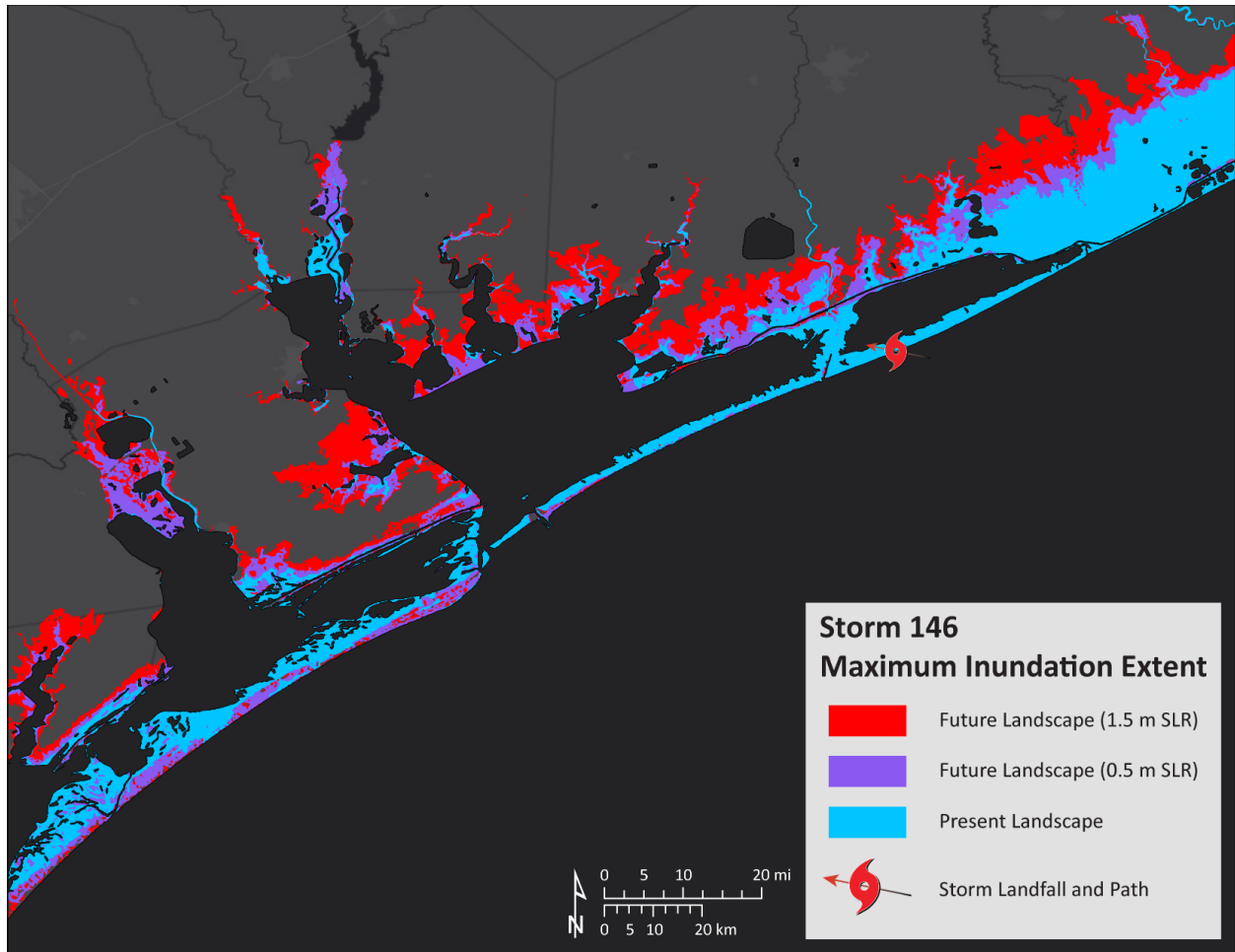
Figure 74. Maximum extent of inundation due to Storm 146.

Storm 240

Figure 75 shows the maximum water surface elevation resulting from Storm 240 in four distinct landscape and sea-level scenarios. In addition to two future scenarios modeled, it includes the MAXELE resulting from the intermediate SLR scenario modeled for the 2019 Plan for a reference. Despite Storm 146 and Storm 240 having very similar characteristics and making landfall 40 miles apart from each other at the two end of Matagorda Bay, they had different surge height and extent of water pushed inland. Storm 240, for instance, caused more inundation and higher surge height in Matagorda Peninsula than Storm 146, even though the latter made landfall on the peninsula. Similarly, Storm 240 had a more significant impact in and around the Matagorda Bay system in both the present and future landscape than Storm 146.

In the Region 2 area, Storm 240 caused a total land inundation area of 339 square miles in the present landscape, which is 38% higher than that caused by Storm 146. In the intermediate-low and intermediate-high scenarios of the future landscape, the total area of inundation resulting from Storm 240 in Region 2 was 504 and 731 square miles, representing a 49% and 116% increase from the present landscape, respectively. Although the percentage increase from the present to future landscapes was higher than that of Storm 146, the total inundation area within Region 2 in the future landscapes was still 37% and

24% higher than that due to Storm 146 in the intermediate-low and intermediate-high scenarios. Figure 76 shows the extent of the inundation due to Storm 240 in the present landscape compared to two future landscapes.
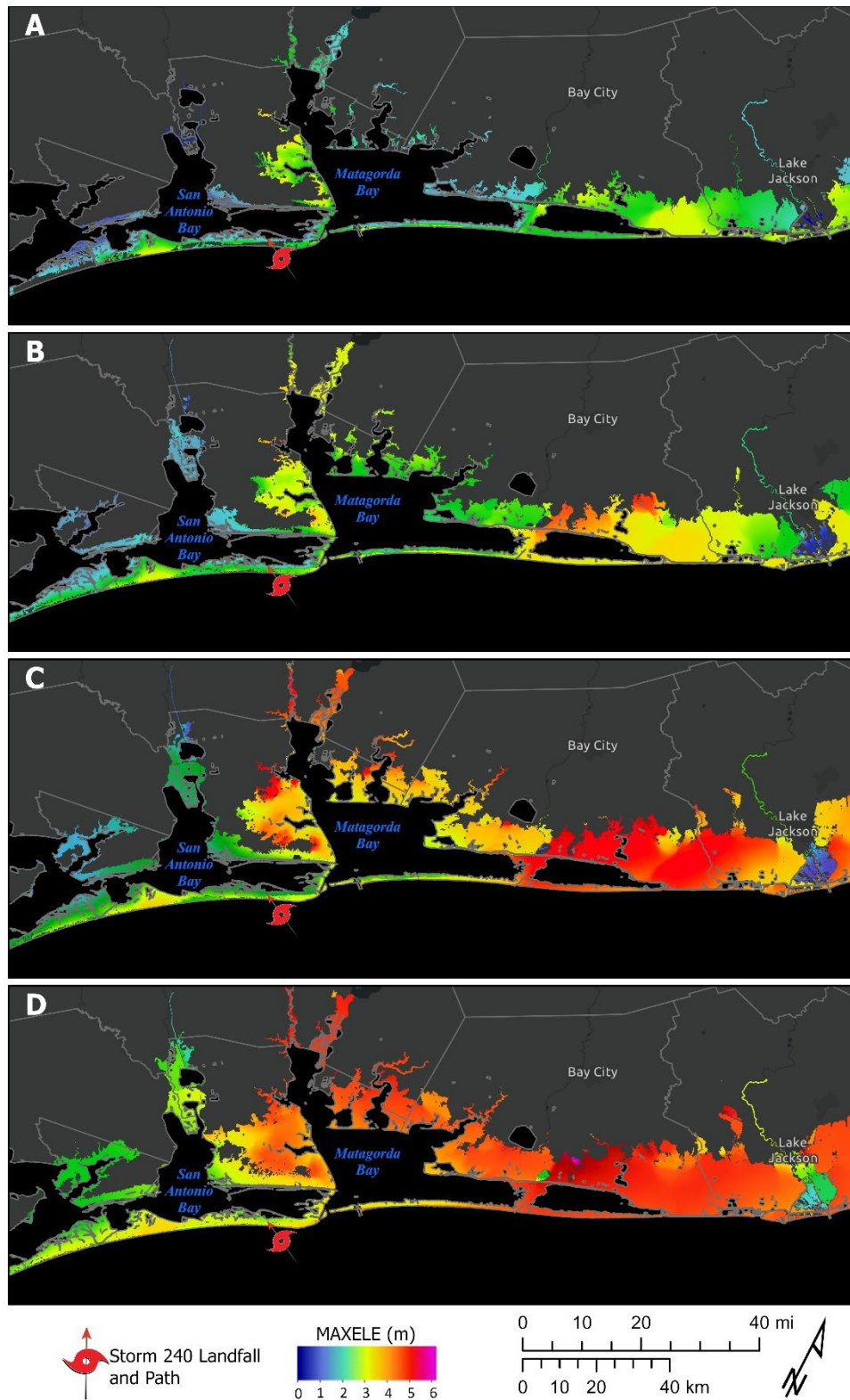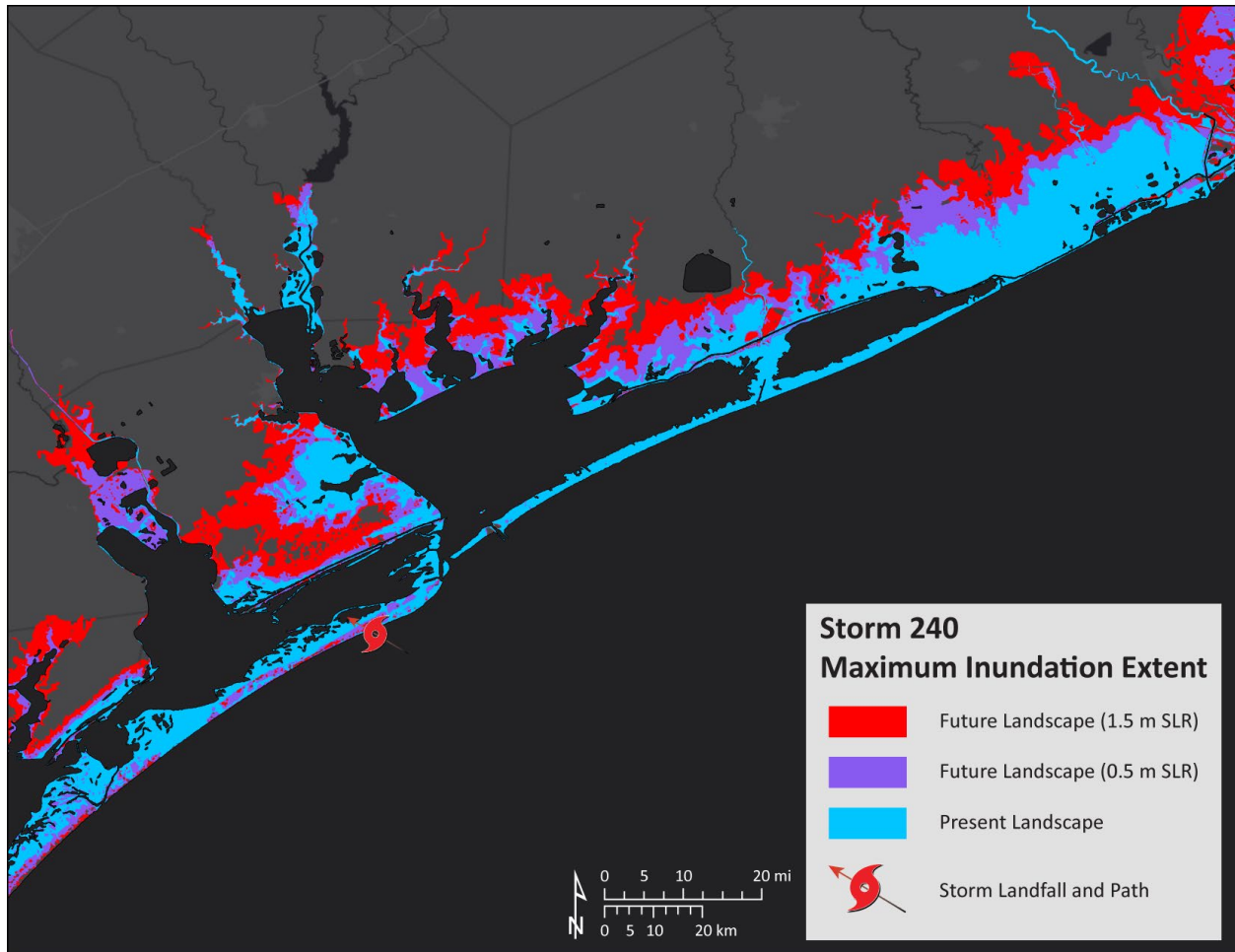
Figure 75. Maximum water surface elevation (MAXELE) due to Storm 240 on (A) Present landscape, (B) Future landscape - Intermediate-Low SLR scenario, (C) Future landscape - Intermediate SLR scenario (from 2019 Plan), and (D) Future landscape - Intermediate-high SLR scenario.

Figure 76. Maximum extent of inundation due to Storm 240.

Region 3

This study analyzed four storms that made landfall in Region 3 under the present condition and two future conditions – Storm 328, Storm 322, Storm 222, and Storm 416. Of these storms, three were Category 2, and the remaining Storm 222 was a Category 3 storm. Storm 416 was also modeled for the 2019 Plan. Each storm had unique characteristics, such as forward speed, a radius of maximum wind (RMW), central pressure, orientation, and more (see Table 19), which resulted in different storm surge impacts.

Table 19. Selected storms that made landfall in Region 3 and their characteristics

Storm	Wind Speed (kt)	RMW (Nmi)	Forward Speed (kt)	Central Pressure (mb)	Heading (deg)	Landfall Location
Storm 328	95	15.12	10.4	927.3	-40	San Jose Island
Storm 322	86.77	30.28	4.6	940.4	-40	Padre Balli Park
Storm 222	96.68	18.98	8.4	921.3	-60	North Padre Island
Storm 416	87	16.86	11	933.7	-20	Malaquite Beach

To quantify the extent of flooding caused by a more intense storm surge in the future landscape, the total area of inundated land within Region 3 was calculated for both present and future landscapes in the intermediate-low and intermediate-high scenarios. Based on the landscape change modeling, it was found that in the intermediate-low scenario, approximately 83 square miles of land in Region 3 were lost and converted to open water due to RSLR. This area increased significantly to 143 square miles in the intermediate-high scenario.

Storm 328

Figure 77 shows the maximum water surface elevation resulting from Storm 328 in the present landscape and two future landscapes with SLR. This strong Category 2 storm made landfall in San Jose Island, causing a storm surge of 2 – 3 m in the Matagorda Island and Mustang Island under the present landscape. In the future landscapes, the surge height increased to 4 -6 m in the islands. The storm surge penetrated much farther inland in the future landscapes around Matagorda and San Antonio Bay systems, causing a significant impact in the Port Lavaca area.

In the present landscape, Storm 328 caused a total inundated land area of 144 square miles within Region 1. However, the storm surge impact was higher in Region 2 than in Region 3, as higher inundation was observed on the right side of the landfall. Therefore, the total area of inundation within Region 2 in the present landscape due to Storm 328 was 266 square miles. In the intermediate-low and intermediate-high scenarios of future landscapes, the total inundation areas in Region 3 resulting from Storm 328 were 209 and 395 square miles, respectively, representing a 45% and 174% increase from the present landscape. Figure 78 shows the maximum extent of inundation resulting from Storm 328 in the present landscape and two future landscapes.
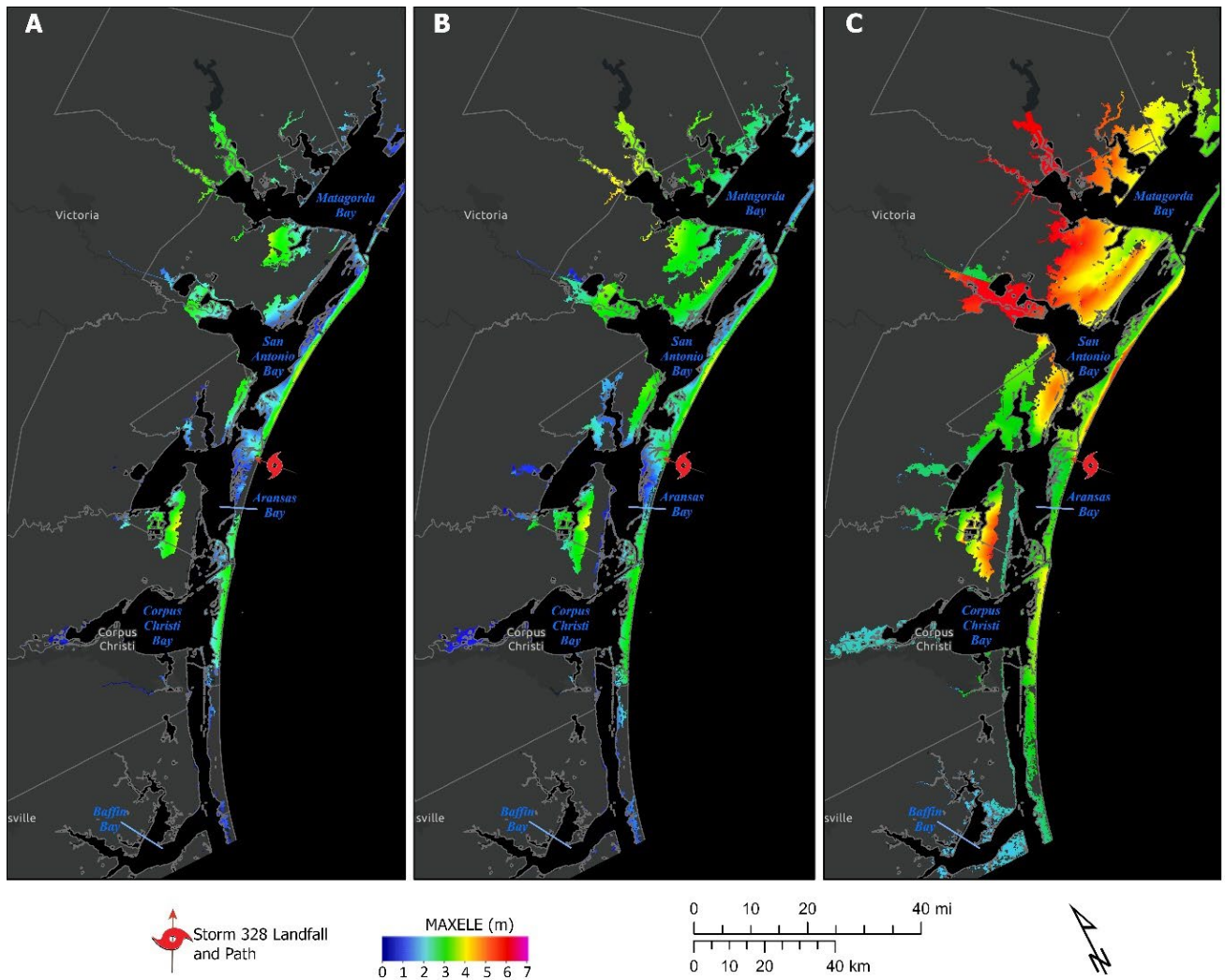
Figure 77. Maximum water surface elevation (MAXELE) due to Storm 328 on (A) Present landscape, (B) Future landscape - Intermediate-Low SLR scenario, and (C) Future landscape – Intermediate-High SLR scenario.
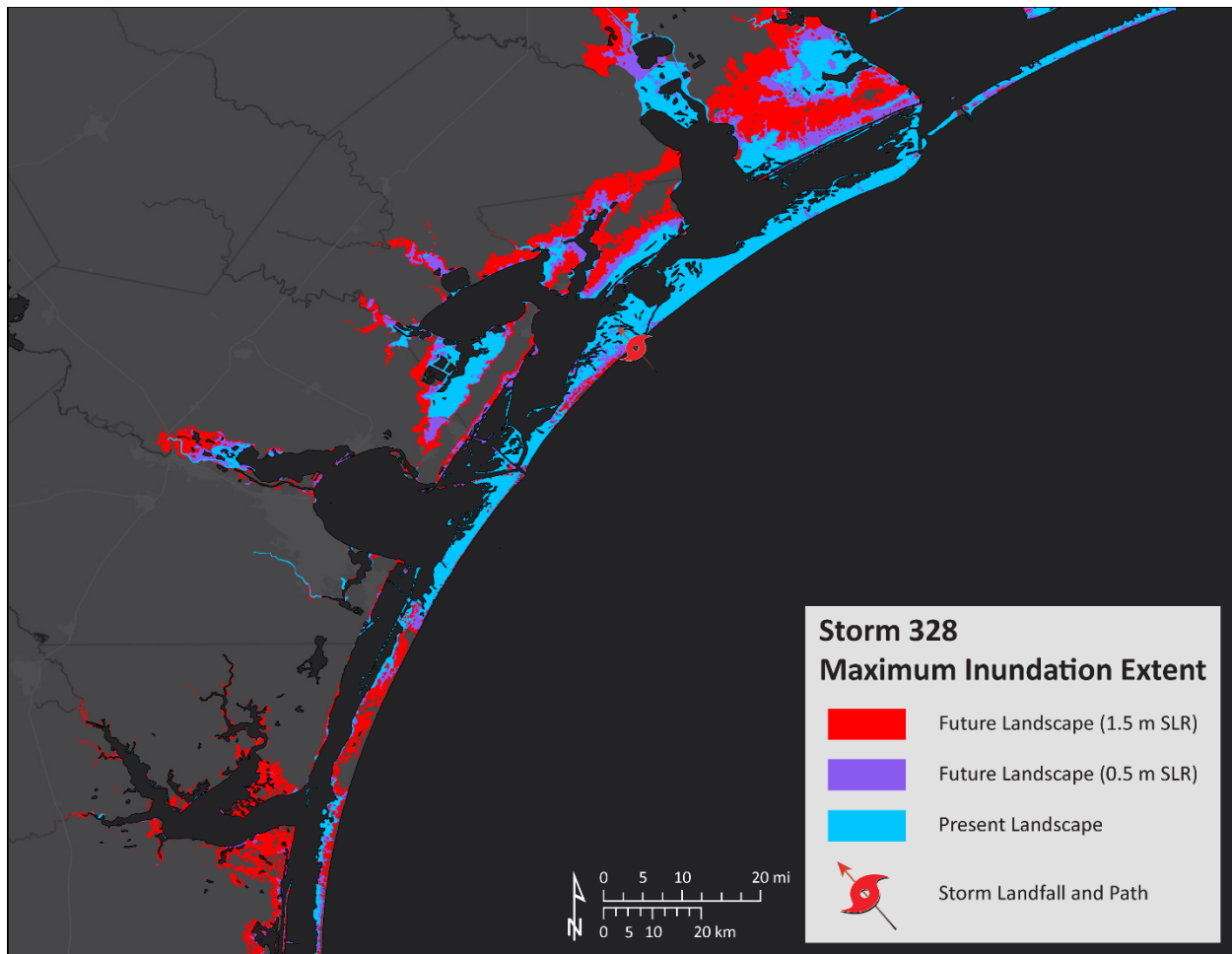
Figure 78. Maximum extent of inundation due to Storm 328.

Storm 322

Storm 322, the slowest storm among nineteen storms modeled with a forward speed of 5.3 miles per hour, made landfall in Padre Balli Park at the northern end of North Padre Island and. Figure 79 shows the maximum water surface elevation resulting from Storm 322 in the present landscape and two future landscapes with SLR. In the present landscape, the barrier islands throughout the region experienced 2 – 3.5 m of inundation, and a significant surge penetrated inland around the Aransas Bay and Nueces River Delta area. In future landscapes, the water level rose significantly higher in the barrier island systems, reaching up to 6 m. Additionally, widespread inundation was observed, extending considerably farther inland and reaching a wide area in the City of Corpus Christi.

Storm 322 caused a total land inundation area of 372 square miles within Region 3 in the present landscape. In the intermediate-low and intermediate-high scenarios of the future landscape, the total area of inundation resulting from Storm 322 in Region 3 was 519 and 794 square miles, representing a 40% and 113% increase from the present landscape, respectively. Figure 80 shows the maximum extent of inundation resulting from Storm 322 in the present landscape and two future landscapes.
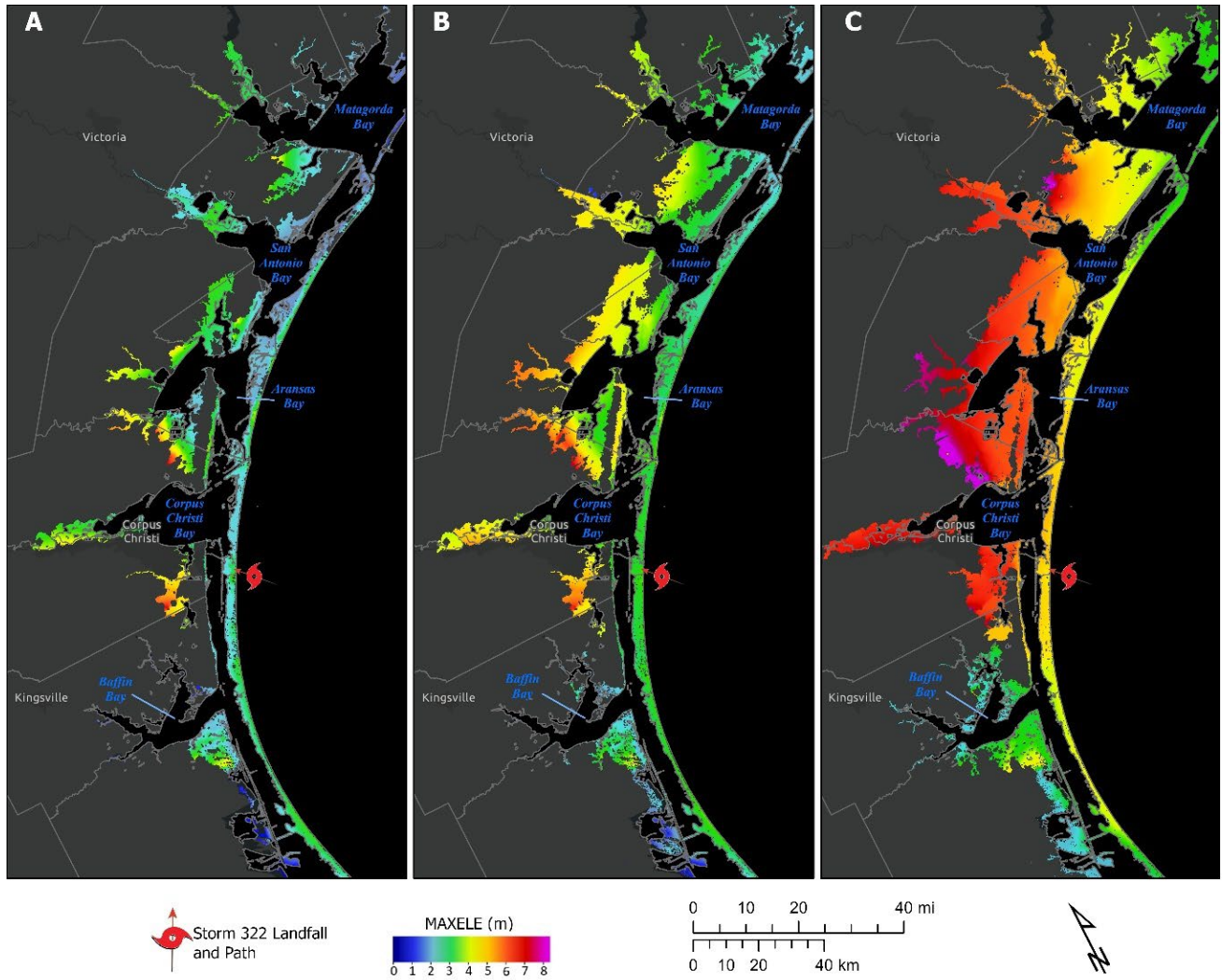
Figure 79. Maximum water surface elevation (MAXELE) due to Storm 322 on (A) Present landscape, (B) Future landscape - Intermediate-Low SLR scenario, and (C) Future landscape – Intermediate-High SLR scenario.
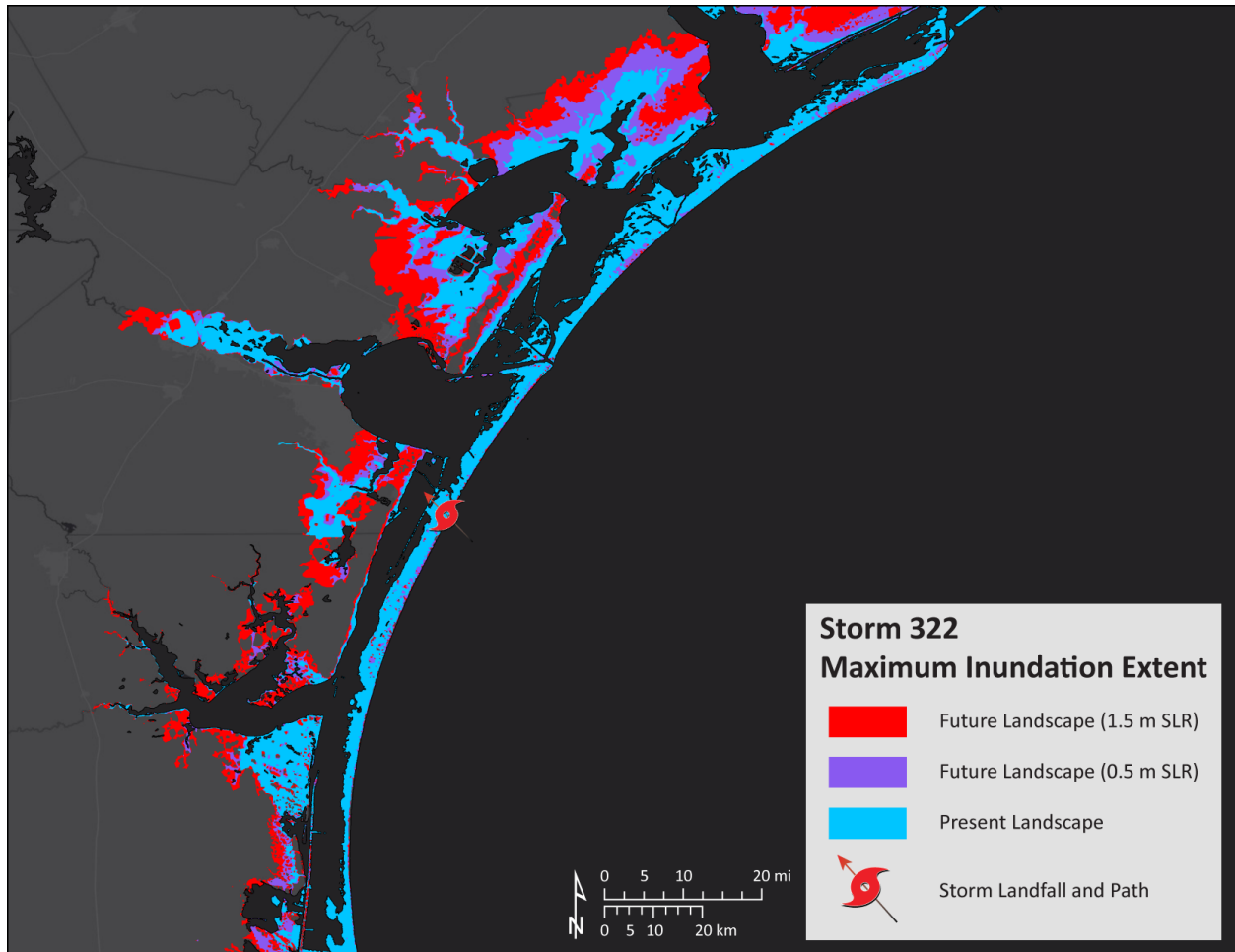
Figure 80. Maximum extent of inundation due to Storm 322.

Storm 222

Storm 222 is a slow-moving and relatively large storm that made landfall 9 miles south of Storm 322 at North Padre Island and is the only Category 3 hurricane modeled in Region 3. Figure 81 displays the maximum water surface elevation resulting from Storm 222 in the present landscape and two future landscapes with SLR. Despite being a Category 3 hurricane, Storm 222 did not cause widespread storm surge inundation as seen in Storm 322. However, the barrier islands throughout the region experienced 2 – 3 m of inundation, and up to 4 m of surge was seen along the Nueces River Delta area and south of Aransas Bay in the present landscape. The storm surge was able to reach much farther inland in the future landscapes, causing a significant increase in the flooding area. In the intermediate-high scenario, the region experienced more than 4.5 m of surge height.

Storm 222 caused a total land inundation area of 240 square miles in the present landscape within Region 3, which is 36% less than that caused by Storm 322, a Category 2 storm that made landfall near it. In the intermediate-low and intermediate-high scenarios of the future landscape, the total area of inundation resulting from Storm 222 in Region 3 was 346 and 579 square miles, representing a 44% and 141% increase from the present landscape, respectively. Figure 82 shows the extent of the inundation due to Storm 222 in the present landscape compared to two future landscapes.
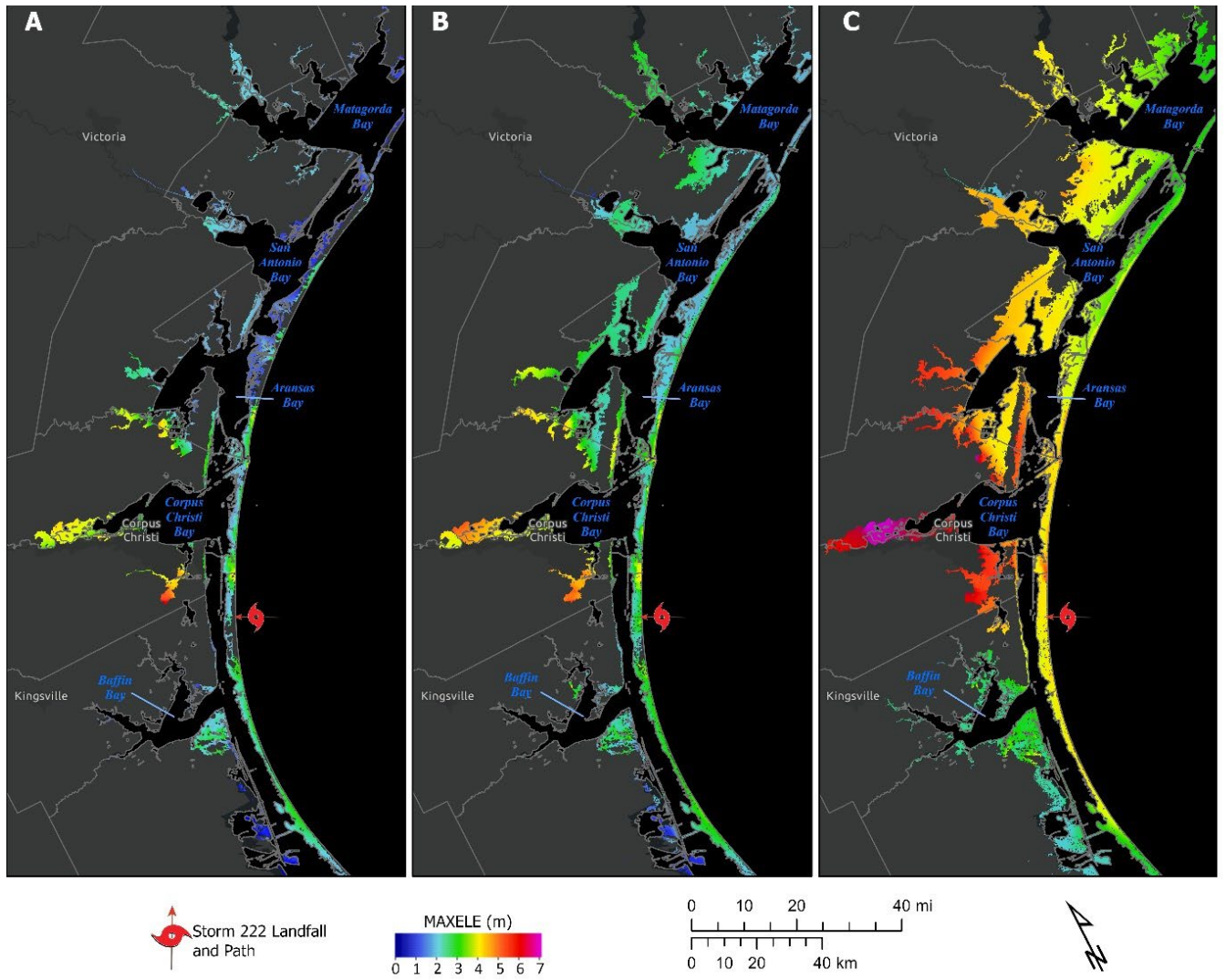
Figure 81. Maximum water surface elevation (MAXELE) due to Storm 222 on (A) Present landscape, (B) Future landscape - Intermediate-Low SLR scenario, and (C) Future landscape – Intermediate-High SLR scenario.
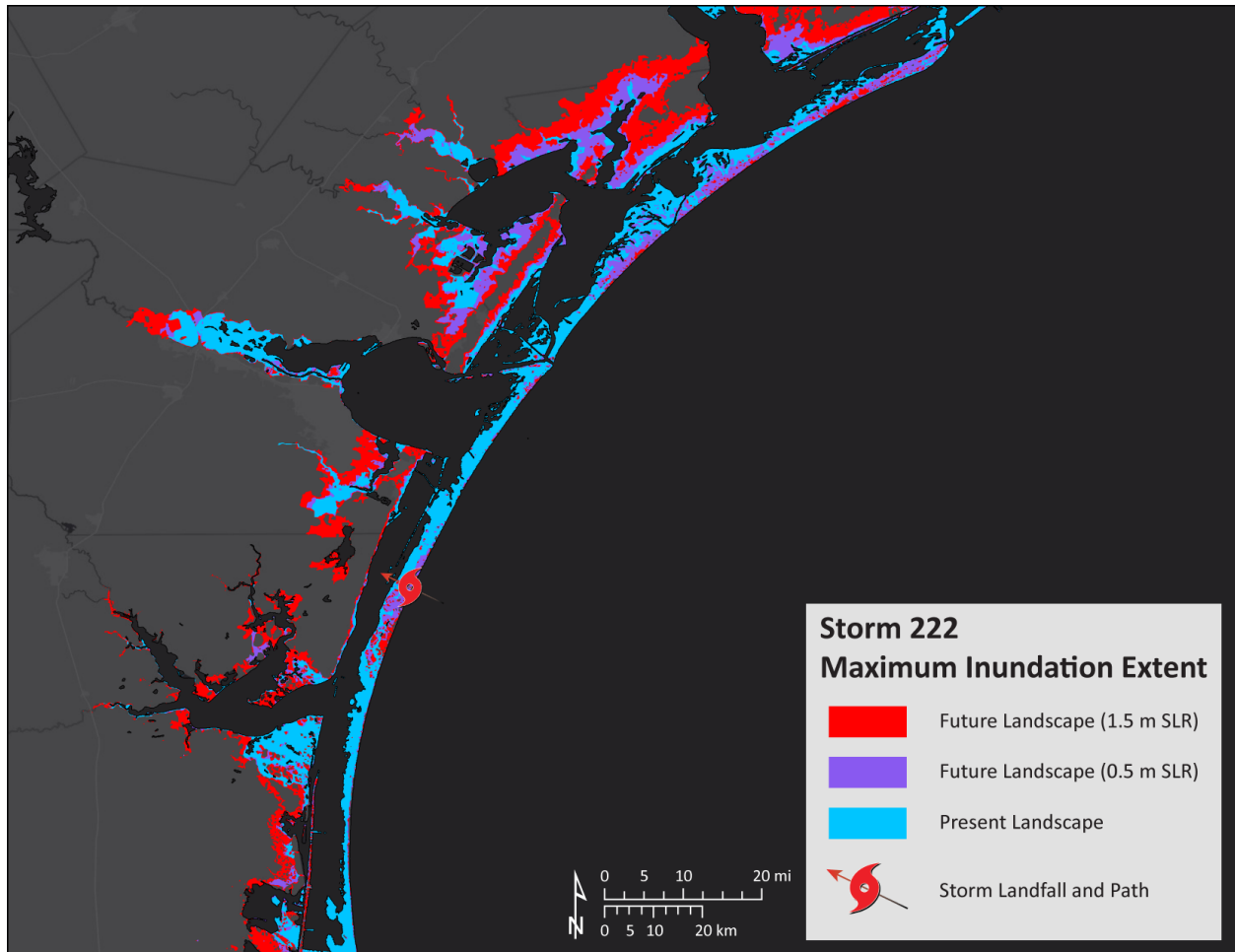
Figure 82. Maximum extent of inundation due to Storm 222.

Storm 416

Figure 83 shows the maximum water surface elevation resulting from Storm 416 in four distinct landscape and sea-level scenarios, including the MAXELE from the intermediate SLR scenario modeled for the 2019 Plan as a reference. This Category 2 storm made landfall near Malaquite Beach at North Padre Island, between the landfall of Storm 322 and Storm 222. Despite its strong wind speed similar to Storm 322, the storm surge impact due to Storm 416 was the least among these three storms. Under the present landscape, no widespread storm surge flooding was observed in the barrier islands, unlike the other two storms. However, a similar trend of storm surge inundation was observed in the Nueces River Delta area and around Aransas Bay and Baffin Bay. In all three future landscape scenarios, the storm surge inundation extended considerably farther inland in the east of Corpus Christi Bay along the Aransas Bay and San Antonio Bay areas.

In the Region 3 area, Storm 416 caused a total land inundation area of 177 square miles under the present landscape, which is less than that caused by Storm 322 and Storm 222. However, in the intermediate-low and intermediate-high scenarios of the future landscape, the total area of inundation resulting from Storm 416 in Region 3 was 288 and 498 square miles, representing a 63% and 181%

increase from the present landscape, respectively. Figure 84 shows the extent of the inundation due to Storm 416 in the present landscape compared to two future landscapes.
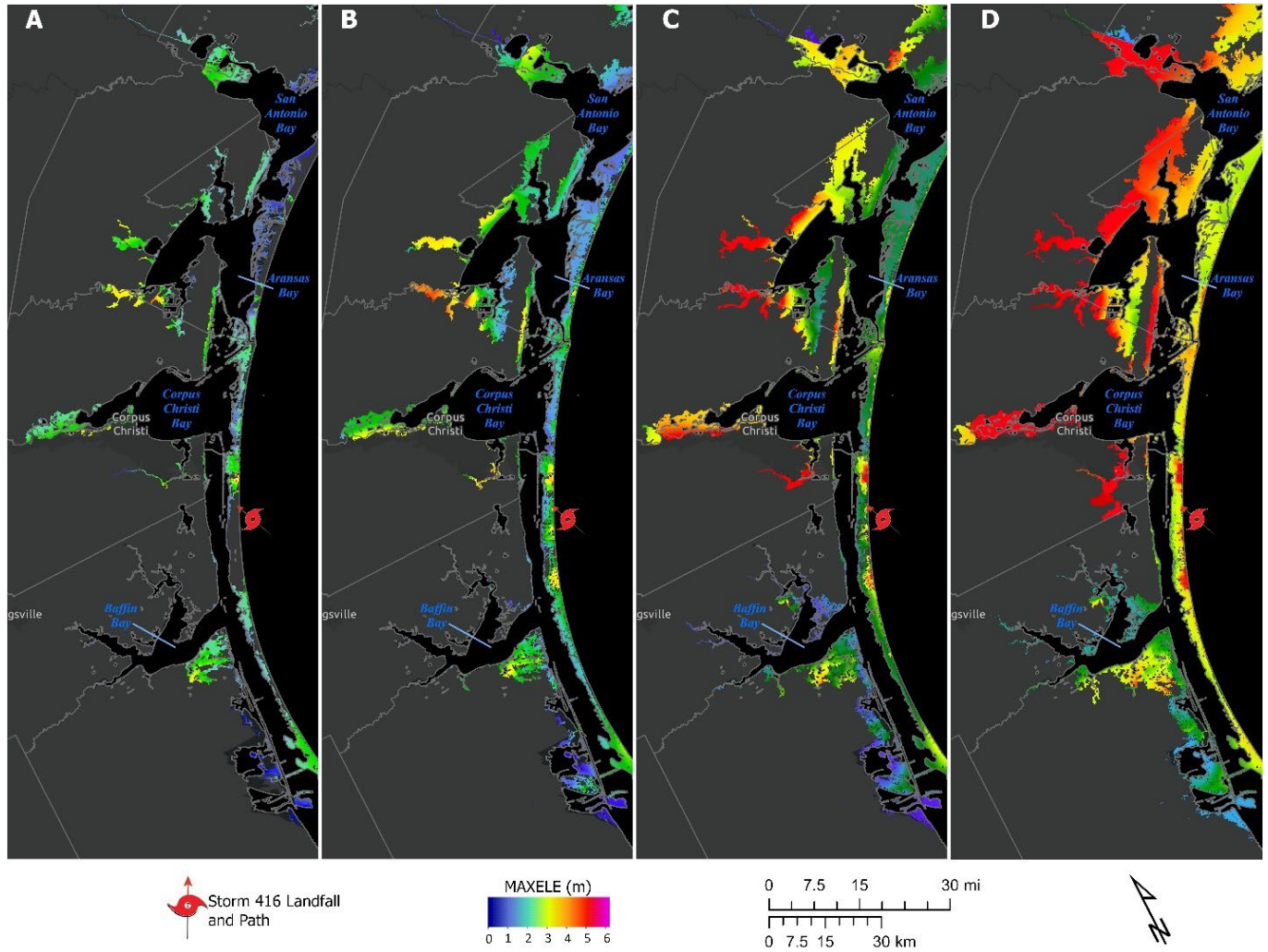

Figure 83. Maximum water surface elevation (MAXELE) due to Storm 416 on (A) Present landscape, (B) Future landscape - Intermediate-Low SLR scenario, (C) Future landscape - Intermediate SLR scenario (from 2019 Plan), and (D) Future landscape - Intermediate-high SLR scenario.
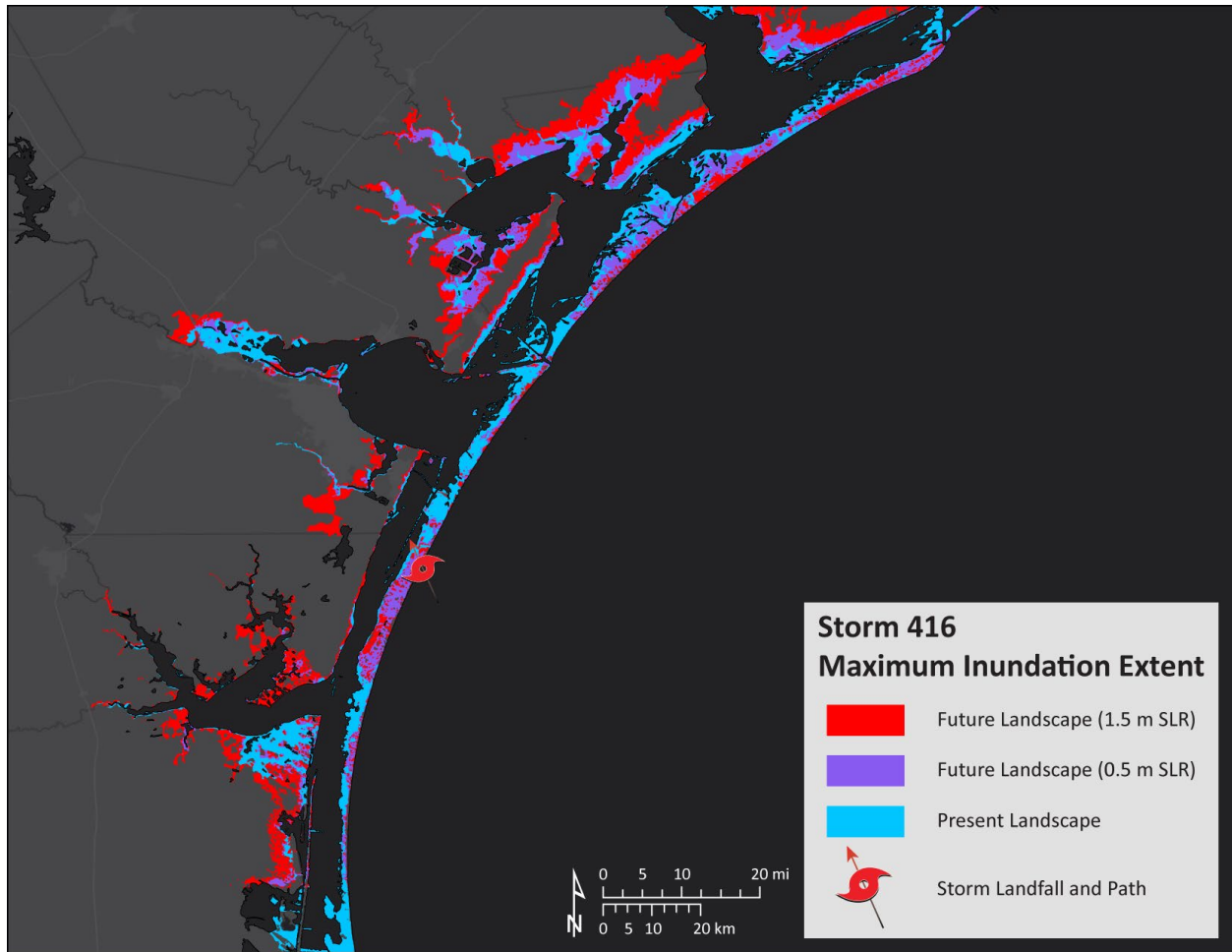
Figure 84. Maximum extent of inundation due to Storm 416.

Region 4

This study analyzed four storms that made landfall in Region 4 under the present condition and two future conditions – Storm 214, Storm 206, Storm 305, and Storm 400. Of these storms, two were Category 1, one was Category 2 and the remaining Storm 222 was a Category 3 storm. Storm 400 was also modeled for the 2019 Plan. Each storm had unique characteristics, such as forward speed, a radius of maximum wind (RMW), central pressure, orientation, and more (see Table 20), which resulted in different storm surge impacts as presented in the following subsections.

Table 20. Selected storms that made landfall in Region 4 and their characteristics.

Storm	Wind Speed (kt)	RMW (Nmi)	Forward Speed (kt)	Central Pressure (mb)	Heading (deg)	Landfall Location
Storm 214	76.44	35.06	4.6	921.3	-60	Northern Laguna Madre
Storm 206	83.4	31.19	13.4	921.3	-60	South Padre Island
Storm 305	101.3	9.89	6.8	905.2	-40	6 miles south of US-Mexico border
Storm 400	79.44	32.17	13.6	933.7	-20	65 miles south of US-Mexico border

To quantify the extent of flooding caused by a more intense storm surge in the future landscape, the total area of inundated land within Region 4 was calculated for both present and future landscapes in the intermediate-low and intermediate-high scenarios. Based on the landscape change modeling, it was found that in the intermediate-low scenario, approximately 302 square miles of land in Region 3 were lost and converted to open water due to RSLR. This area increased significantly to 351 square miles in the intermediate-high scenario.

Storm 214

Storm 214 was a slow-moving Category 1 storm with a large wind field that made landfall at the northern Laguna Madre. The strong currents generated by the large wind field drove storm surge not only in Region 4 but also inundated a significant area in Region 3. The Baffin Bay area experienced up to 5 m of storm surge where as the Nueces River Delta area experienced more than 5 m of surge in the present landscape. Region 4 is the most vulnerable region to land loss among the four regions and is predicted to lose significant land and convert to open water in the future landscape. As a result, storm surge was able to penetrate much farther inland in the future landscape compared to the present landscape. A significant increase in storm surge inundation was observed throughout the region in the future landscapes, resulting in a considerable increase in the inundation area. Figure 85 displays the maximum water surface elevation resulting from Storm 214 in the present landscape and two future landscapes with SLR.

Within the Region 4 area, Storm 214 caused a total land inundated area of 431 square miles in the present landscape. In the future landscape, the total area of inundation resulting from Storm 214 in Region 4 was 580 square miles in the intermediate-low scenario, which is a 35% increase. In the intermediate-high scenario, the total area of inundation resulting from Storm 214 in Region 4 was 914 square miles, representing a 112% increase. However, the storm surge impact within Region 3 was also similar to that of Region 4 as higher inundation was observed on the right side of the landfall. For example, the total area of inundation within Region 3 in the present landscape due to Storm 214 was 371 square miles and it increased by 130% to 855 square miles in the intermediate-high scenario. Figure 86 shows the extent of the inundation due to Storm 214 in the present landscape compared to two future landscapes.
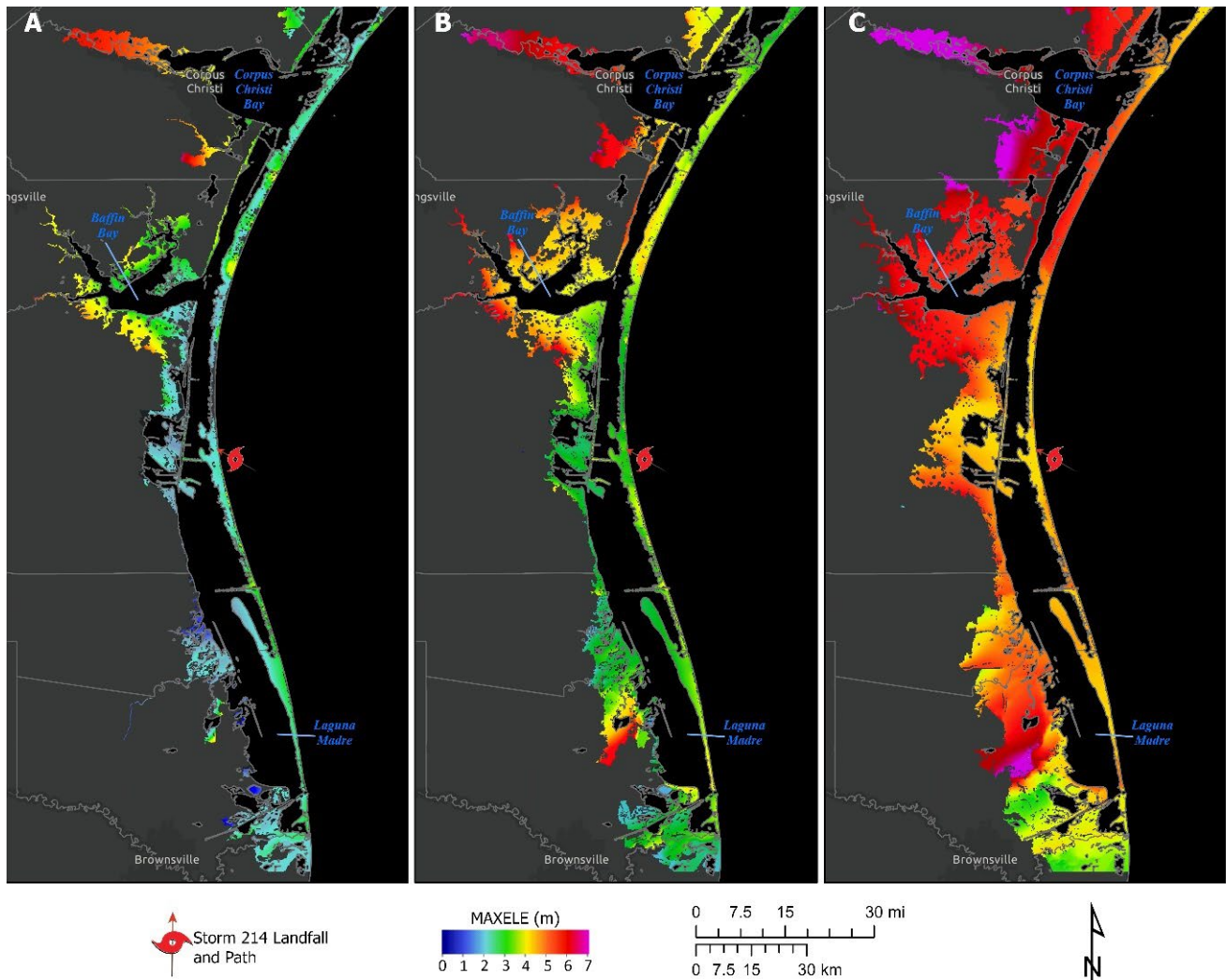
Figure 85. Maximum water surface elevation (MAXELE) due to Storm 214 on (A) Present landscape, (B) Future landscape - Intermediate-Low SLR scenario, and (C) Future landscape – Intermediate-High SLR scenario.
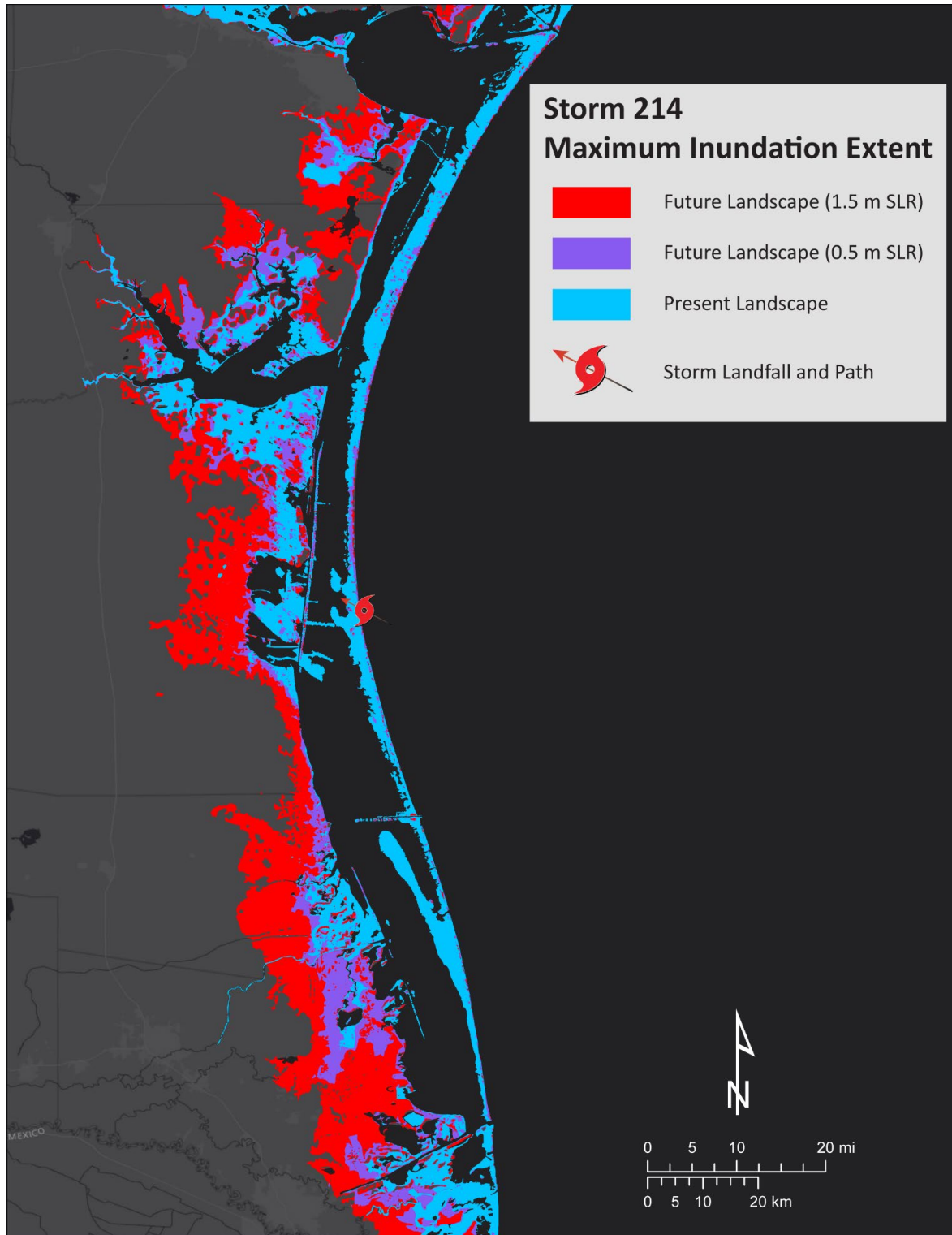
Figure 86. Maximum extent of inundation due to storm 214.

Storm 206

Figure 87 shows the maximum water surface elevation resulting from Storm 206 in the present landscape and two future landscapes with SLR. This strong Category 2 hurricane with a large wind field

made landfall in South Padre Island, causing a storm surge of 2 – 3.5 m in the island in the present landscape. In the intermediate-low scenario, the surge height increased to 3 – 5 m in the island that increased to more than 6 m in the intermediate-high scenario. The storm surge penetrated much farther inland in the future landscapes around Laguna Madre, Baffin Bay and Corpus Christi Bay systems, causing a widespread inundation throughout the region.

In the Region 4 area, Storm 206 caused a total land inundation of 489 square miles in the present landscape. In the intermediate-low and intermediate-high scenarios of the future landscape, the total area of inundation resulting from Storm 206 was 621 and 951 square miles, representing a 27% and 94% increase from the present landscape, respectively. Figure 88 shows the extent of the inundation due to storm 206 in the present landscape compared to two future landscapes.
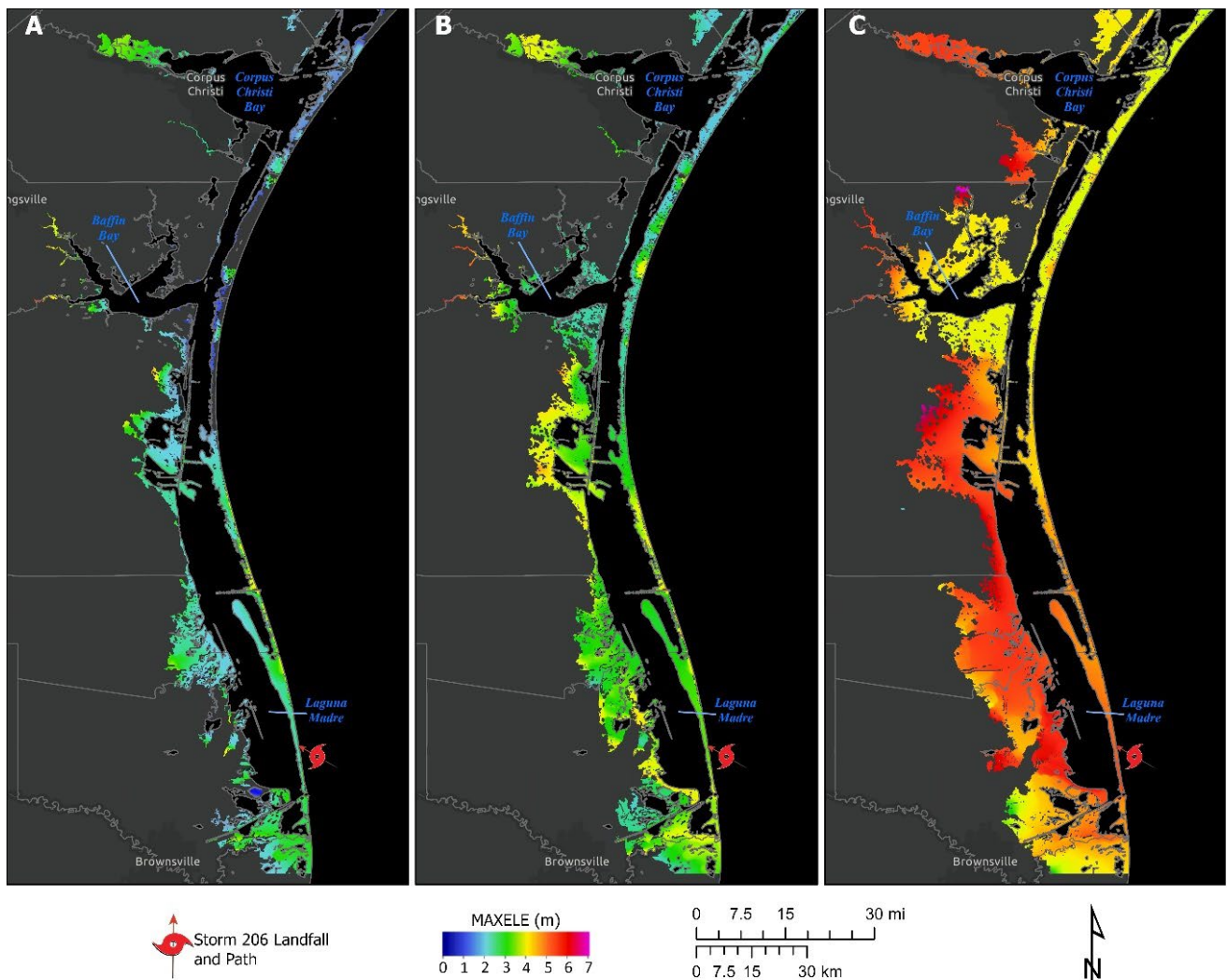

Figure 87. Maximum water surface elevation (MAXELE) due to Storm 206 on (A) Present landscape, (B) Future landscape - Intermediate-Low SLR scenario, and (C) Future landscape – Intermediate-High SLR scenario.
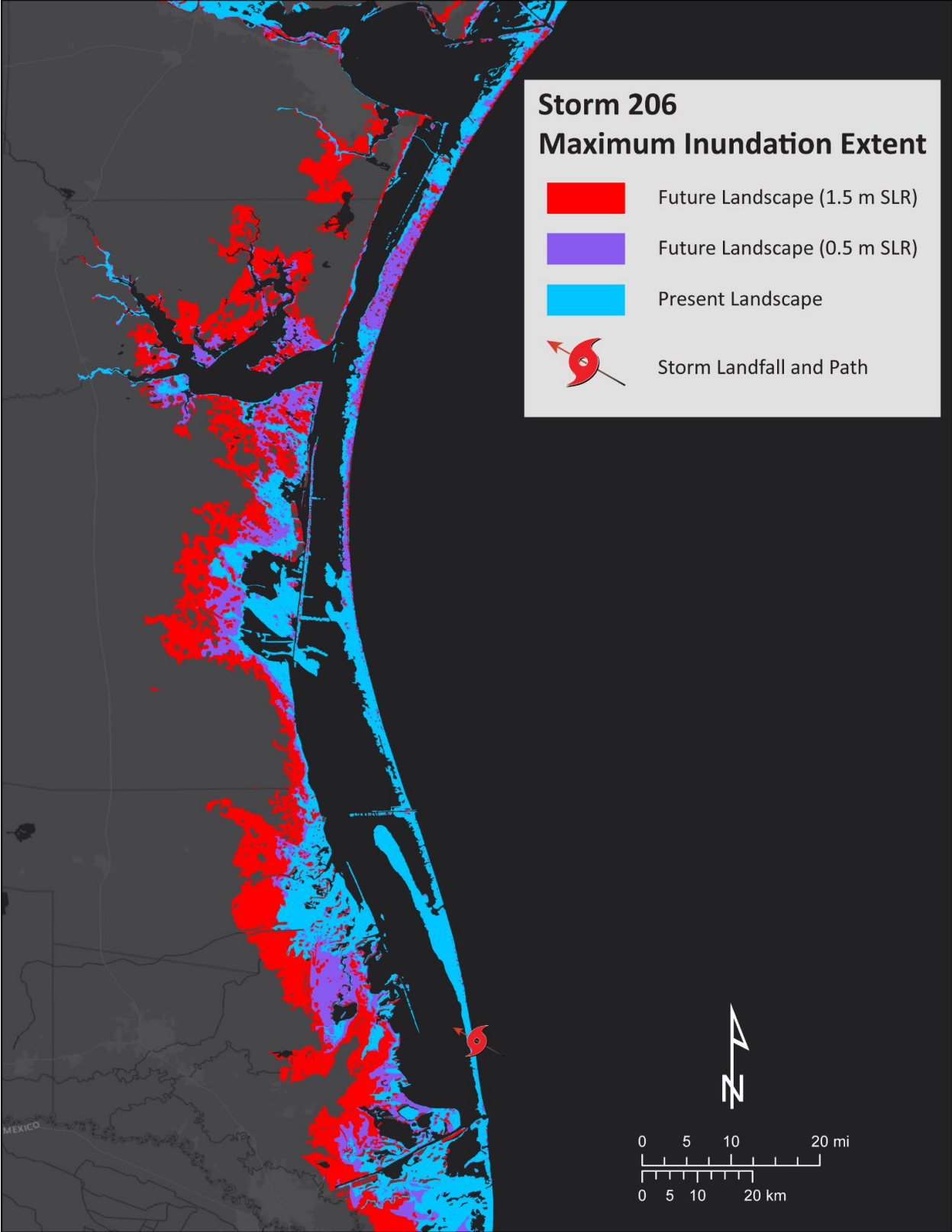
116

Figure 88. Maximum extent of inundation due to storm 206.

Storm 305

Storm 305 was a powerful Category 3 hurricane with a relatively small wind field that made landfall 6 miles south of the US-Mexico border. Figure 89 shows the maximum water surface elevation resulting from Storm 305 in the present landscape and two future landscapes with SLR. Despite its strength, Storm 305 did not cause widespread storm surge inundation as seen in other storms in Region 4, due to its small size. However, a surge height of 2 – 4 m was observed in the US-Mexico border area under the present landscape. It increased to 3 – 5 m in the intermediate-low scenario and to more than 5 m in the intermediate-high scenario. The storm surge penetrated much farther inland in the future landscapes around Laguna Madre, Baffin Bay, and the Nueces River Delta area, causing a widespread inundation throughout the region.

Storm 305 caused a total land inundation area of 399 square miles in the present landscape in the Region 4 area, which is 18% less than that caused by Storm 206. In the intermediate-low and intermediate-high scenarios of the future landscape, the total area of inundation resulting from Storm 305 in Region 4 was 507 and 745 square miles, representing a 27% and 87% increase from the present landscape, respectively. Figure 90 shows the extent of the inundation due to Storm 305 in the present landscape compared to two future landscapes.
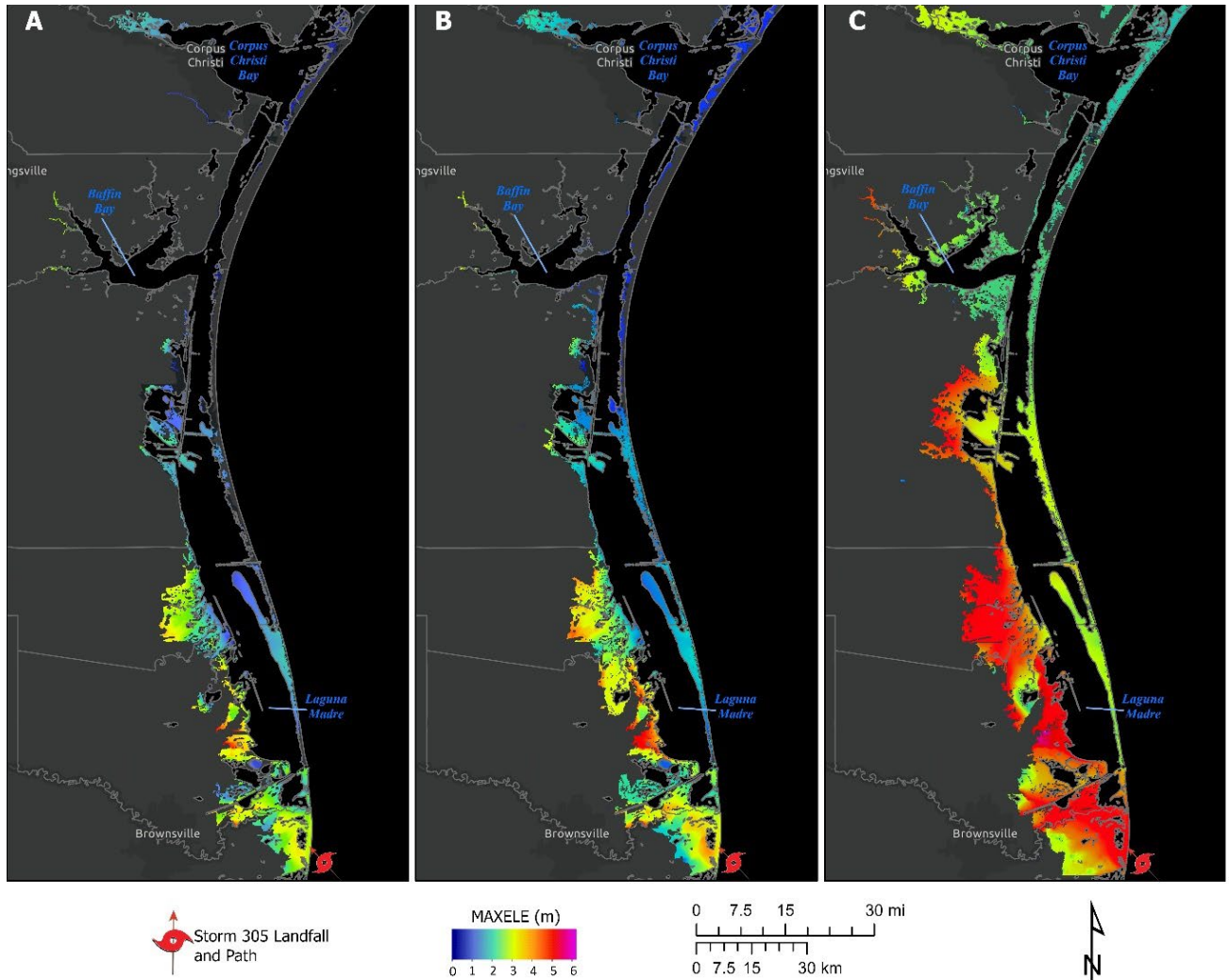
Figure 89. Maximum water surface elevation (MAXELE) due to Storm 305 on (A) Present landscape, (B) Future landscape - Intermediate-Low SLR scenario, and (C) Future landscape – Intermediate-High SLR scenario.
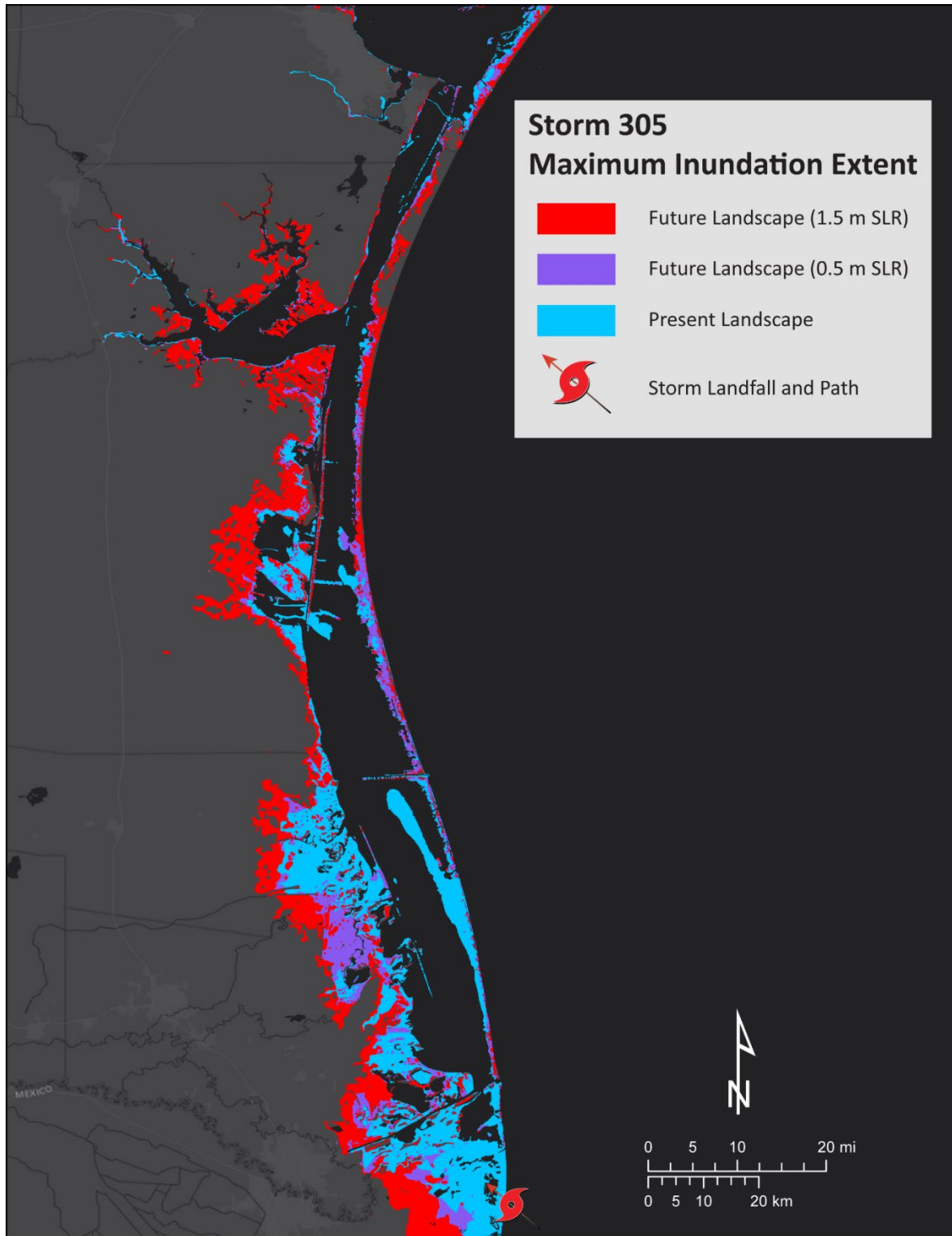
Figure 90. Maximum extent of inundation due to storm 305.

Storm 400

Figure 91 shows the maximum water surface elevation resulting from Storm 400 in four distinct landscape and sea-level scenarios, including the MAXELE resulting from the intermediate SLR scenario

modeled for the 2019 Plan for a reference. Storm 400 was a Category 1 hurricane with large wind field that made landfall 65 miles south of the US-Mexico border. Despite its wind speed, the strong currents generated by the large wind field drove storm surge into the Region 4, inundating barrier islands as well as inland area around Laguna Madre under the present landscape. The northern section of Region 4 in Kenedy County, which did not experience inundation in the present landscape, was inundated with a surge height of up to 6 m in the future landscapes.

In the Region 4 area, Storm 400 caused a total land inundation area of 412 square miles in the present landscape, which is 3% more than that caused by Storm 305. In the intermediate-low and intermediate-high scenarios of the future landscape, the total area of inundation resulting from Storm 400 in Region 4 is 535 and 855 square miles, respectively. This represents a 30% and 108% increase from the present landscape, respectively. While the percentage increase from the present to future landscapes is more than that of Storm 305, the total inundation area within Region 4 in the future landscapes is also 6% and 15% more than that due to Storm 305 in the intermediate-low and intermediate-high scenarios. Figure 92 shows the extent of the inundation due to Storm 400 in the present landscape compared to two future landscapes.
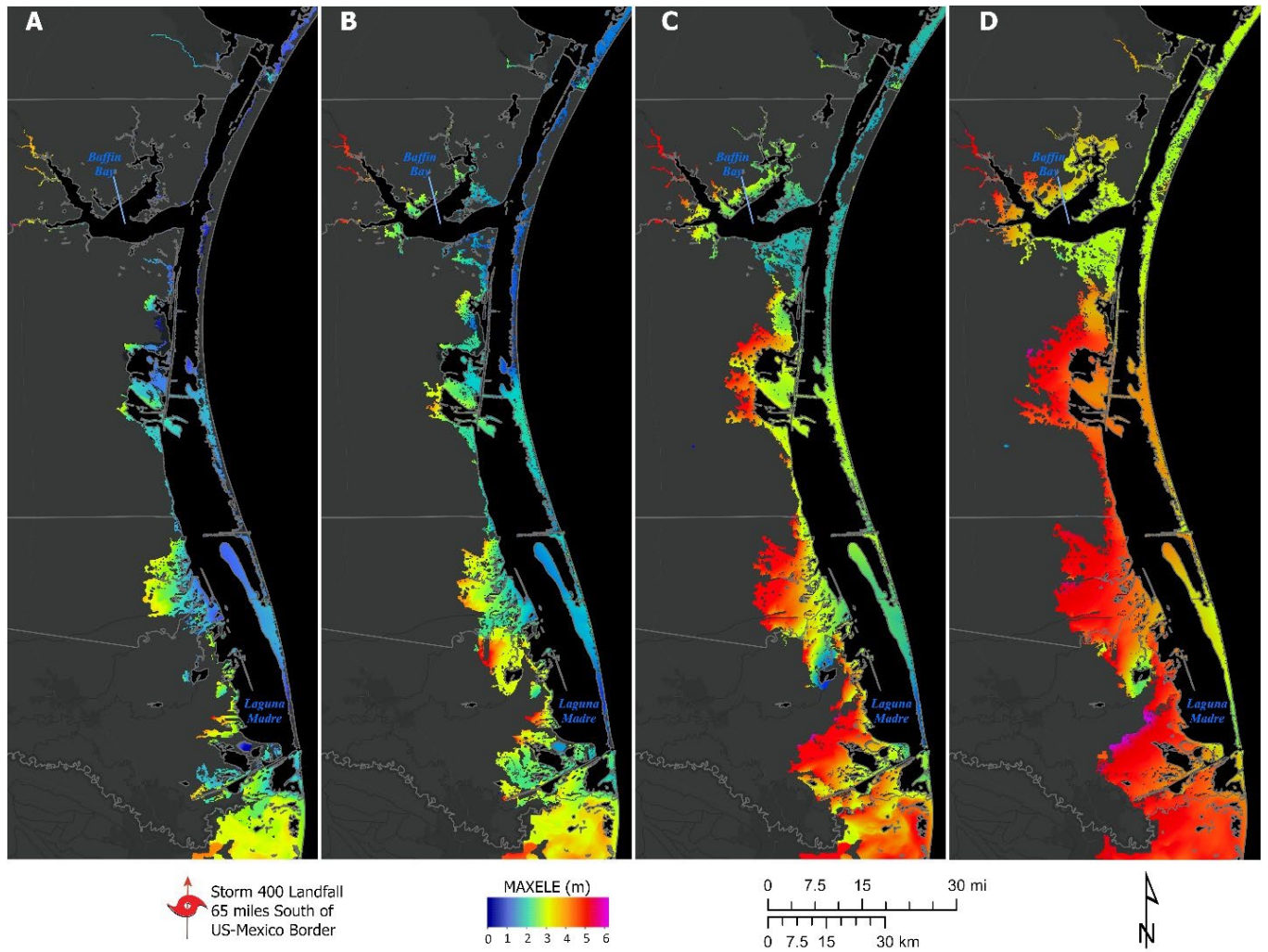
Figure 91. Maximum water surface elevation (MAXELE) due to Storm 400 on (A) Present landscape, (B) Future landscape - Intermediate-Low SLR scenario, (C) Future landscape - Intermediate SLR scenario (from 2019 Plan), and (D) Future landscape - Intermediate-high SLR scenario.
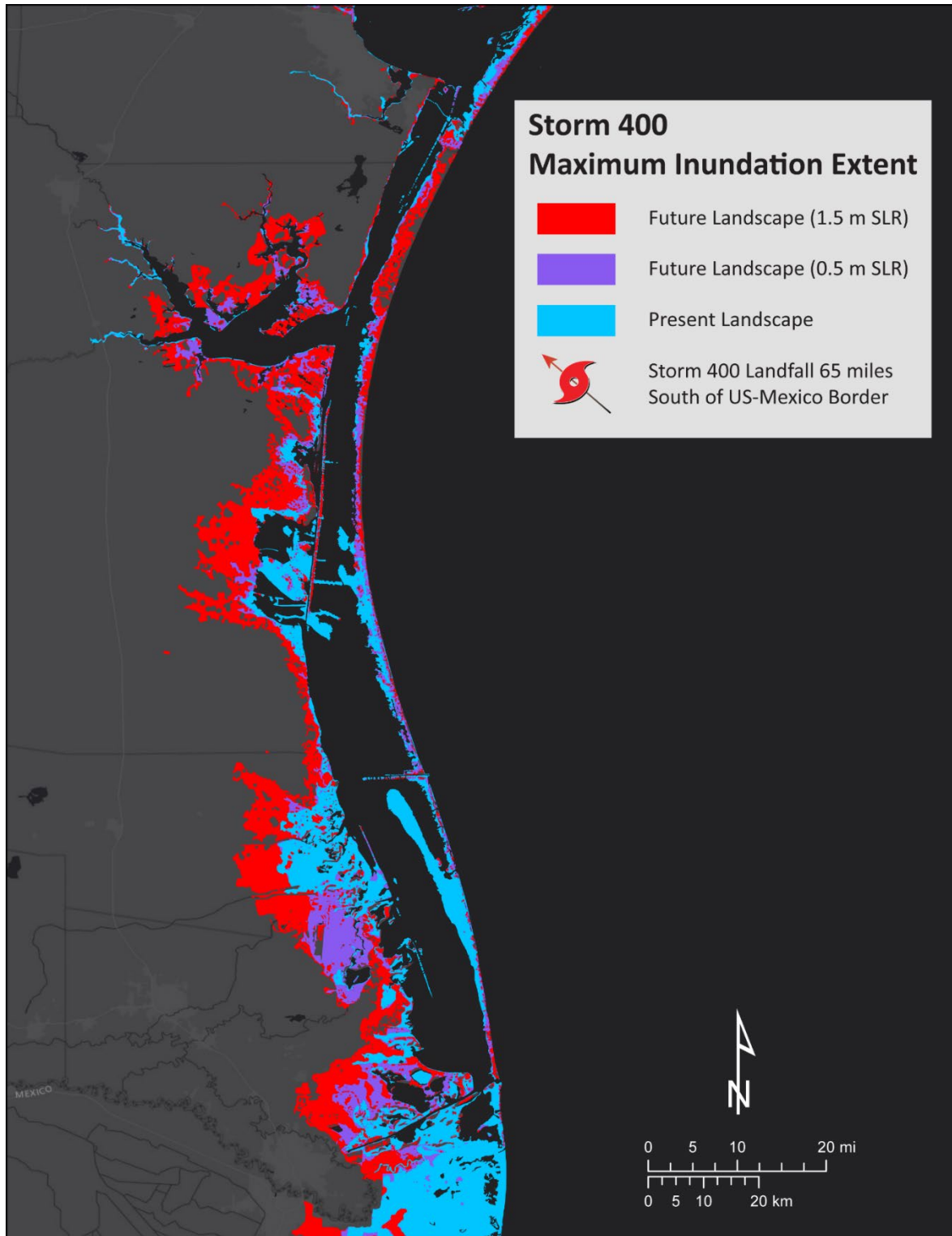
Figure 92. Maximum extent of inundation due to storm 400.

Storm Surge Vulnerability Mapping

A storm surge vulnerability map was developed by considering simulated storm surge inundation due to the modeled nineteen storms. These selected storms of varied characteristics pass throughout the Texas coast and provide thorough coverage along the coast. The same storms are simulated on the present landscape, and again on the two future 2100 landscapes with higher sea levels, thus a total of 57 storm surge model simulations are performed. The model simulations compute the maximum storm surge elevation at each node in the computational mesh which provides information about the maximum inundation pattern during a storm event.

The storm surge vulnerability index of the range 0 to 1 is calculated using the maximum storm surge elevation of all these 57 storm scenarios. Finally, a storm surge vulnerability index map is generated that has a value from 0 to 1 for each region. The value of 1 on the maps means an area is inundated in all 57 scenarios, and 0 means it is not inundated in any scenarios. The vulnerability index map shows spatial coverage of potential storm surge flooding vulnerability of the coast and provides baseline information to improve the resilient capacity of the community now and in the future. It is found that 72% of land along the coast has the vulnerability less than 0.5 and 28% of the land along the coast has the highest vulnerability. However, Region 1 has almost 50% of the land with the highest vulnerability to storm surge flooding. The following subsections present the results of storm surge vulnerability mapping effort of each regions.

Region 1

Figure 93 shows spatial coverage of potential storm surge flooding vulnerability in Region 1 by considering all modeled storms in the present and future landscape scenarios. The highest vulnerability (value 1) in this map shows an area inundated in all storm scenarios, and the lowest vulnerability (value 0) shows an area not being inundated due to the storm surge in any scenario. The map shows that 49% of the land in Region 1 has a high vulnerability (value greater than 0.5) and Jefferson county is the most vulnerable county in the region. Region 1 is the most vulnerable region to storm surge flooding among the four regions.
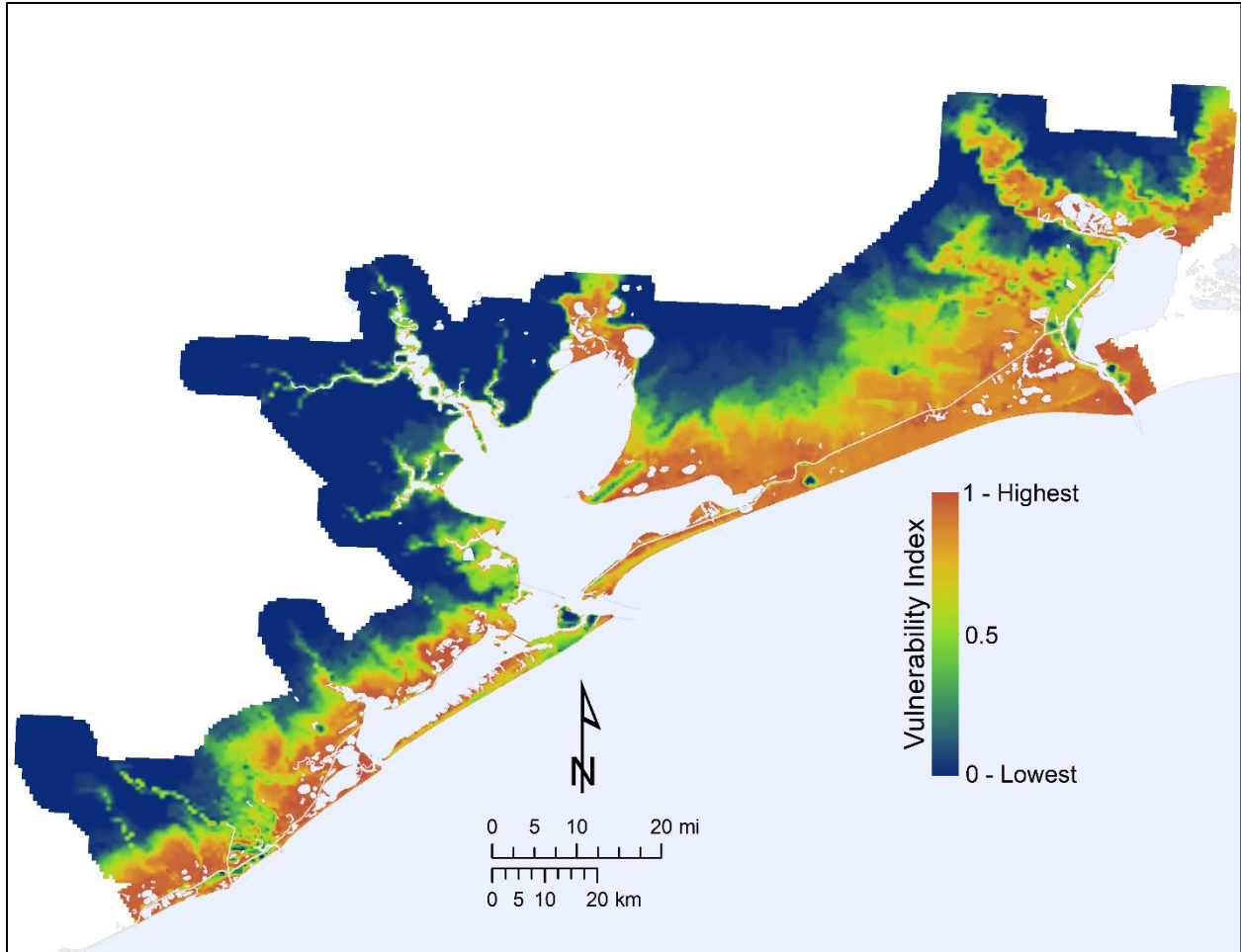
Figure 93. Map showing the vulnerability to storm surge in Region 1

Region 2

Figure 94 shows spatial coverage of potential storm surge flooding vulnerability in Region 2 by considering all modeled storms in the present and future landscape scenarios. The highest vulnerability in this map shows an area inundated in all storm scenarios and the lowest vulnerability shows an area not being inundated due to the storm surge in any scenario. The map shows that 30% of the land in Region 2 has a high vulnerability to storm surge (value greater than 0.5). Matagorda county is the most vulnerable county in Region 2.
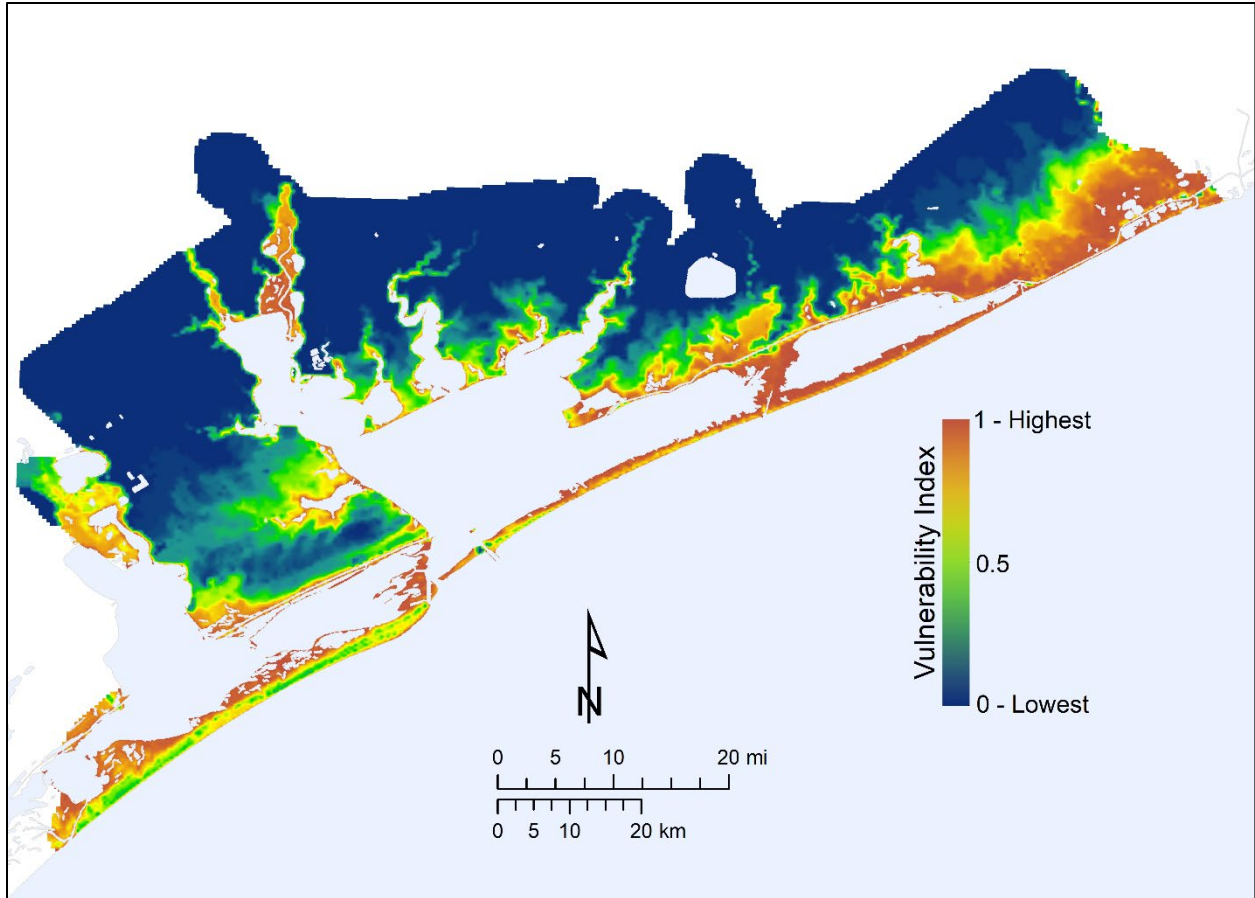
Figure 94. Map showing the vulnerability to storm surge in Region 2

Region 3

Figure 95 shows spatial coverage of potential storm surge flooding vulnerability in Region 3 by considering all modeled storms in the present and future landscape scenarios. The highest vulnerability (value 1) in this map shows an area inundated in all storm scenarios and the lowest vulnerability (value 0) shows an area not being inundated due to the storm surge in any scenario. The map shows that 13% of the land in Region 3 has a high vulnerability to storm surge. Aransas county is the most vulnerable county in the region with 40% of its land having the highest storm surge vulnerability.
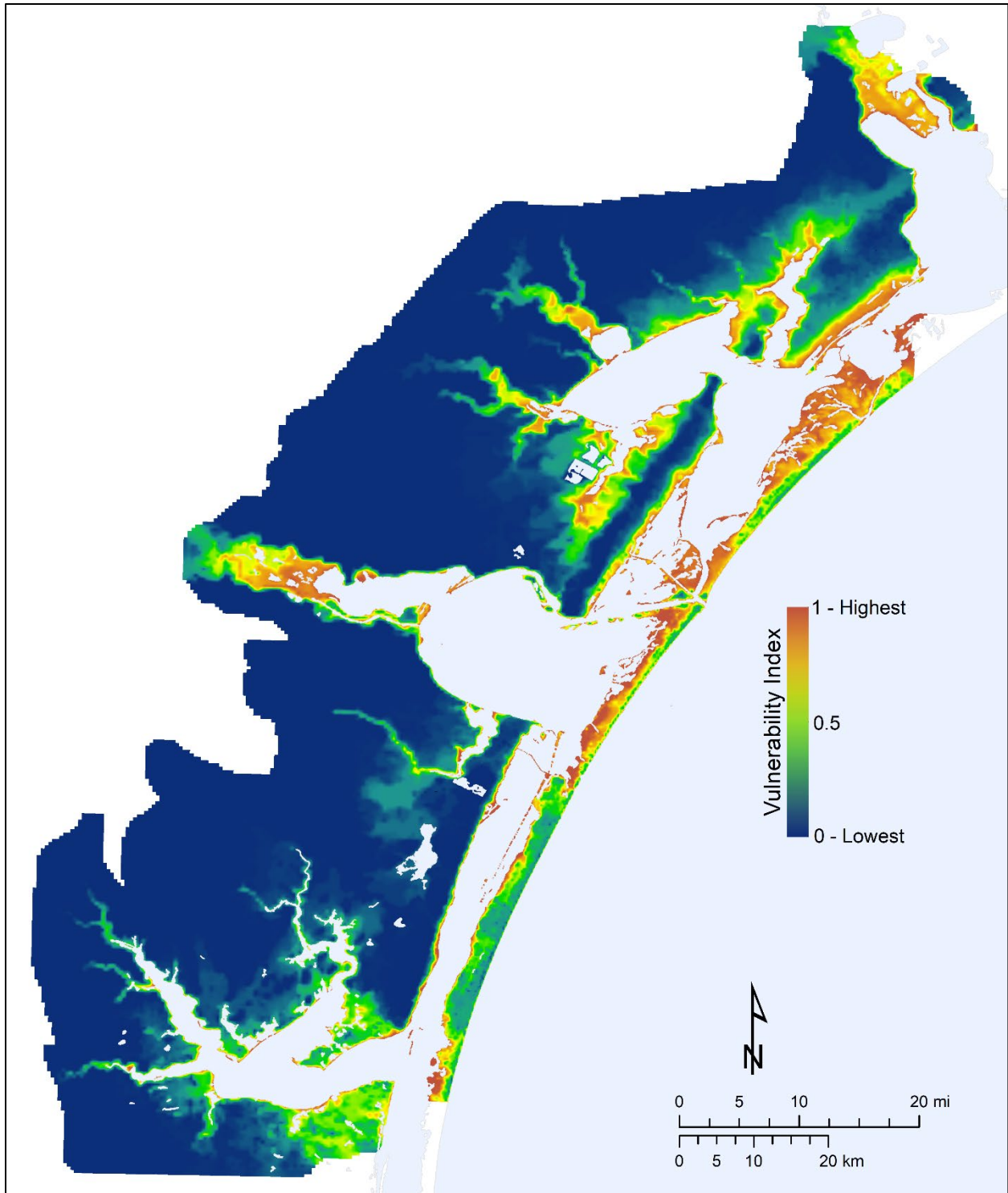
Figure 95. Map showing the vulnerability to storm surge in Region 3

Region 4

Figure 96 shows spatial coverage of potential storm surge flooding vulnerability in Region 4 by considering all modeled storms in the present and future landscape scenarios. The highest vulnerability

in this map shows an area inundated in all storm scenarios and the lowest vulnerability shows an area not being inundated due to the storm surge in any scenario. The map shows that 14% of the land in Region 4 has a high vulnerability to storm surge, especially along the backside of South Padre Island's shoreline and along the Lower Laguna Madre.
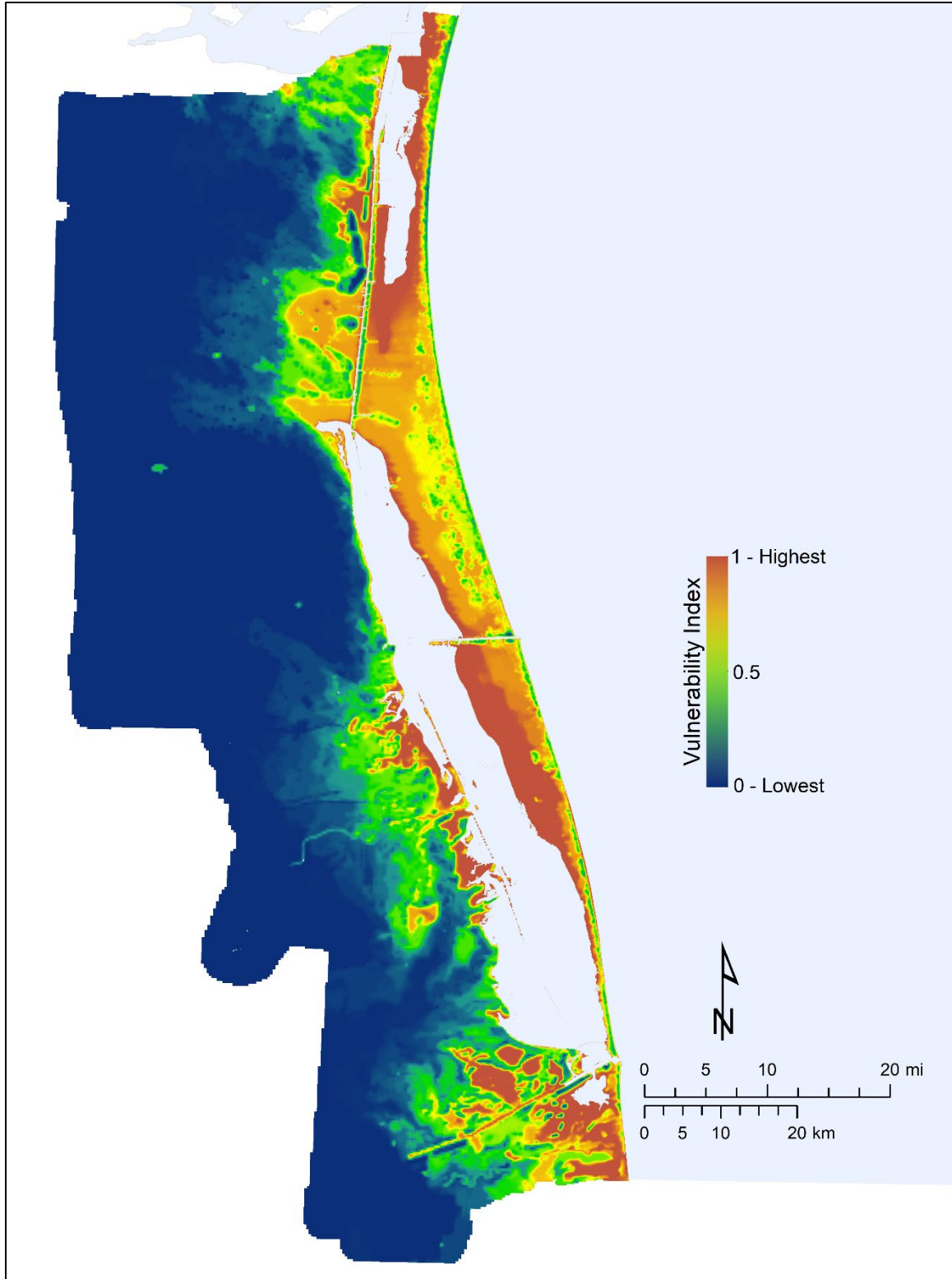
Figure 96. Map showing the vulnerability to storm surge in Region 4

Geohazards Mapping

The geohazards maps were developed using output from sea level rise and storm surge models. These maps are, therefore, a synthesis of all the modeling work done for the Plan as one product and provide detailed mapping of the present and future state of different geo-environments on the Texas coastal plain. Two sets of geohazards maps were developed for the two SLR scenarios. Each map is divided into six categories based on the level of hazard potential: Extreme, Imminent, Future Flooding, High, Moderate, and Low. These 6 hazard potentials are color-coded in the geohazards maps as following:

EXTREME
Historic storm washover channels and future open water

IMMINENT
Present day critical environments (wetlands, dunes, and beaches)

FUTURE FLOODING
Present day urban areas and roads expected to flood in 2100

HIGH
Area expected to become future critical environments in 2100

MODERATE
Upland areas not expected to become critical environments and storm surge vulnerability > 0.5

LOW
Upland areas not expected to become critical environments and storm surge vulnerability < 0.5

The following subsections describe the results of the geohazards mapping effort. First, the Texas coast as a whole is broadly examined, comparing each geohazard potential between two SLR scenarios modeled – intermediate-high and intermediate-low – in the form of maps and graphs. Subsequently, each of the four regions is discussed and analyzed in a more detailed approach.

Coastwide

Significant effects of SLR are predicted to impact the Texas coast which is vastly changing the landscape by 2100 in both SLR scenarios as shown in SLR modeling results (Figure 21). Similarly, more than a quarter of land along the coast has the highest storm surge vulnerability as shown in storm surge vulnerability mapping. Considering these results, an entire Texas coast was mapped based on the level of hazard potential as a geohazards map. Figure 97 shows the geohazards maps of the Texas coast for both intermediate-high and intermediate-low SLR scenarios. The total mapped area covers more than 7,500 square miles of Texas coastal plain.

In the intermediate-low SLR scenario, nearly 8% of the mapped area falls under the Extreme geohazard potential category, which doubles in the intermediate-high scenario. The Imminent geohazard potential category, covering about 19% of the mapped area in the intermediate-low scenario, decreases to 11% in the intermediate-high scenario. This category includes presently critical environments, such as freshwater wetlands, transitional wetlands, regularly flooded estuarine wetlands, tidal flats, and beach/foredune systems. These environments are under higher pressure in higher SLR scenario and have greater potential to convert to open water thus there is less area under Imminent category in the intermediate-high scenario. The High geohazard potential category, projected to become Imminent

geohazard areas in 2100, covers 5% of the mapped area in the intermediate-low SLR scenario, whereas the area doubles in the intermediate-high scenario.

The conversion of the current low marsh area to either tidal flat or open water by 2100 increases the area under Extreme and High geohazard potential categories. In addition to impacts on the natural environment, significant amounts of developed land and road networks are predicted to be inundated by 2100, which are mapped as Future Flooding geohazard potential category. In the intermediate-low scenario, about 1% of the mapped area is assigned the Future Flooding category, which doubles in the intermediate-high scenario.

The storm surge vulnerability index value help differentiate between the Moderate and Low geohazard potential areas. A cutoff value of 0.5 was used to distinguish between these two categories as both represent upland areas with higher elevation that are not expected to become critical environments in 2100. About 6% of the mapped area falls in the Moderate geohazard potential category in the intermediate-low scenario, which decreases to 2% of the mapped area in the intermediate-high scenario. The remaining 62% of the mapped area is categorized as having a Low geohazard potential in the intermediate-low SLR scenario, whereas 60% of the mapped area was categorized as Low geohazard potential in the intermediate-high scenario. However, in the higher SLR scenario, the Low and Moderate geohazard potential zones decrease as they transform to higher hazard potential categories, resulting in an increase in the area under the Extreme and High categories. Figure 98 shows the areal changes of each 6 geohazard potential categories in the intermediate-low and intermediate-high sea level rise scenarios.

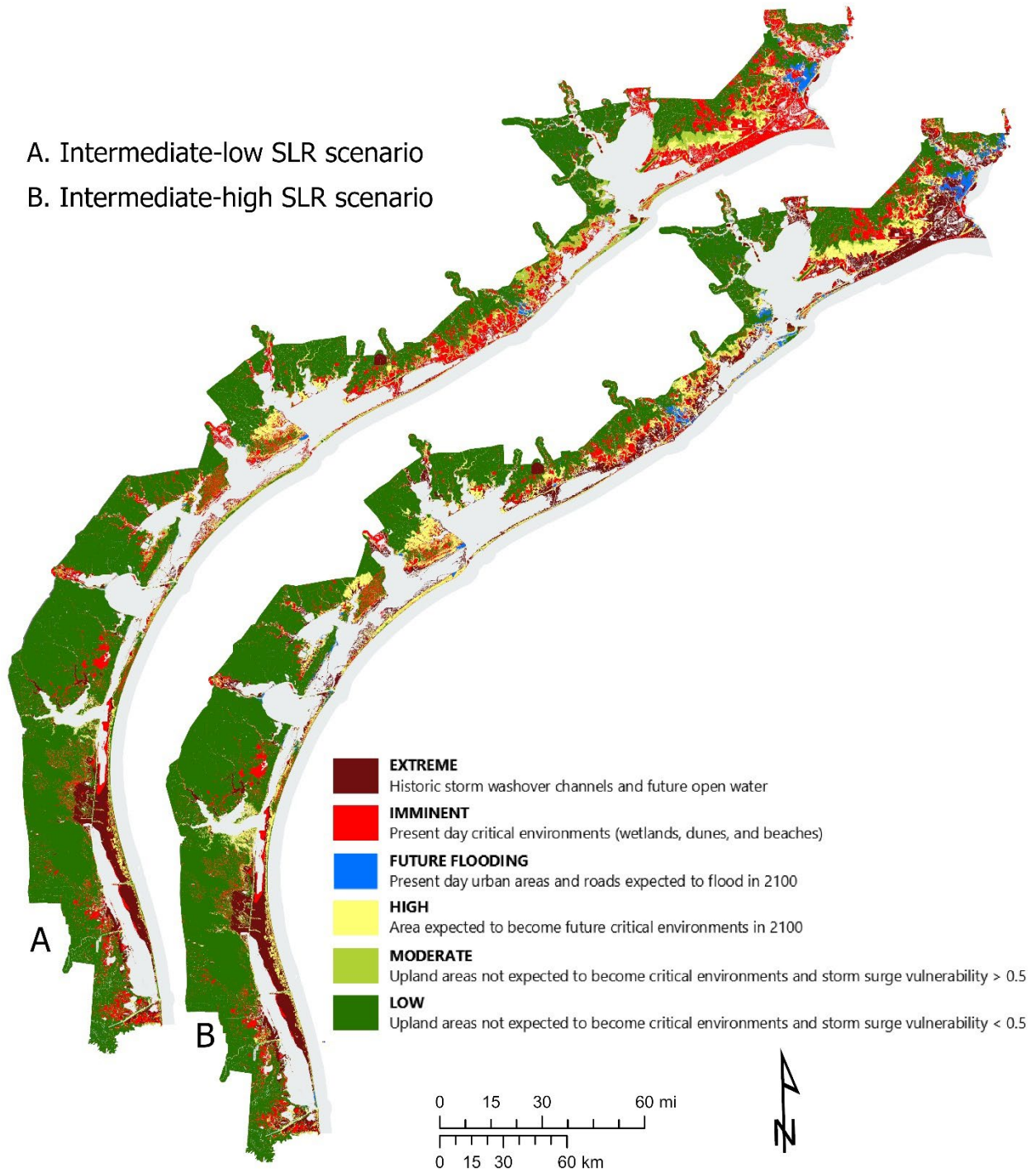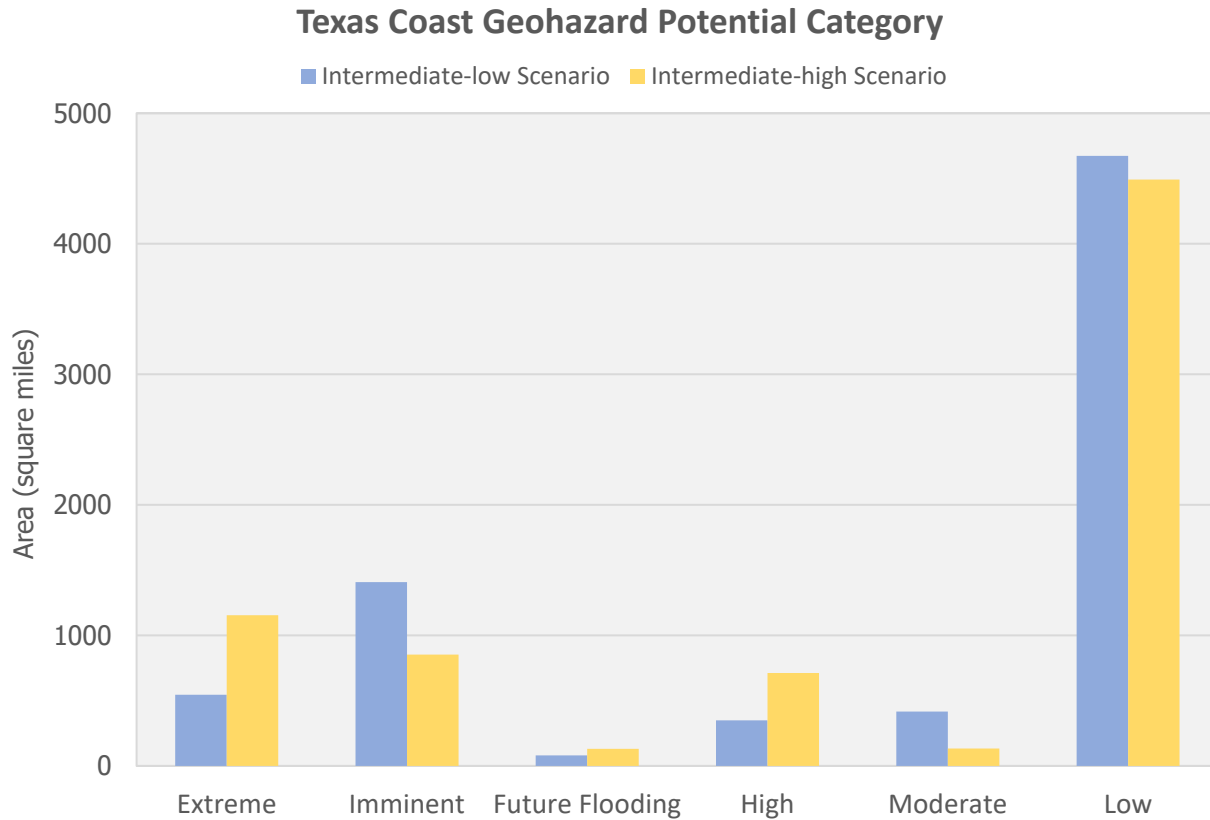A. Intermediate-low SLR scenario

B. Intermediate-high SLR scenario

EXTREME
Historic storm washover channels and future open water

IMMINENT
Present day critical environments (wetlands, dunes, and beaches)

FUTURE FLOODING
Present day urban areas and roads expected to flood in 2100

HIGH
Area expected to become future critical environments in 2100

MODERATE
Upland areas not expected to become critical environments and storm surge vulnerability > 0.5

LOW
Upland areas not expected to become critical environments and storm surge vulnerability < 0.5

0   15   30   60 mi

0   15 30   60 km

A

B

N

Figure 97. Geohazards map of the Texas coast. (A) Intermediate-high sea level rise scenario. (B)
Intermediate-low sea level rise scenario

Texas Coast Geohazard Potential Category

Figure 98. Areal difference (in square miles) of individual geohazard potential category between intermediate-low and intermediate-high sea level rise scenario along the Texas coast

Region 1

By 2100, Region 1 is expected to experience significant effects of sea level rise (SLR), leading to a drastic transformation of its landscape. In addition, this region is the most susceptible to storm surge flooding among the four regions, with nearly half of its land having the highest vulnerability. These findings have been confirmed by the geohazards map of Region 1, which was developed through landscape change and storm surge modeling. Figure 99 shows the geohazards maps of Region 1 on the intermediate-low and intermediate-high SLR scenarios and Figure 100 shows the geohazard potential category distribution under these two scenarios. These maps reveal a substantial increase in the Extreme geohazard category with the intermediate-high SLR scenario – it increases from 4% of the total mapped area within Region 1 in the intermediate-low scenario to 21% in the intermediate-high scenario.

There is a dramatic decrease in the amount of present-day critical environments between these two SLR scenarios which can be seen by the decrease in the Imminent category in Figure 100. This decrease in the Imminent zone in the intermediate-high scenario is due to the conversion of present-day environments to open water. Figure 100 shows that there is less area in the Low and Moderate categories in the intermediate-high scenario as these categories are converting to a higher hazard potential, increasing the area of the Extreme and High categories. The intermediate-high SLR scenario shows that 50% of the total mapped area falls in the Extreme, Imminent, and High geohazard potential categories, up from 42% in the intermediate-low scenario. In addition to impacts on the natural

environment, results show a significant amount of developed land in Region 1 is subject to inundation by 2100. A total of 63 square miles of an urban area and road in Region 1 is projected to be flooded in the intermediate-low SLR scenario which increases to 100 square miles in the intermediate-high scenario. Most of these inundated urban areas consist of low-lying coastal communities and critical infrastructure. Table 21 shows the percentage coverage of different geohazard potential categories in Region 1 for both SLR scenarios.
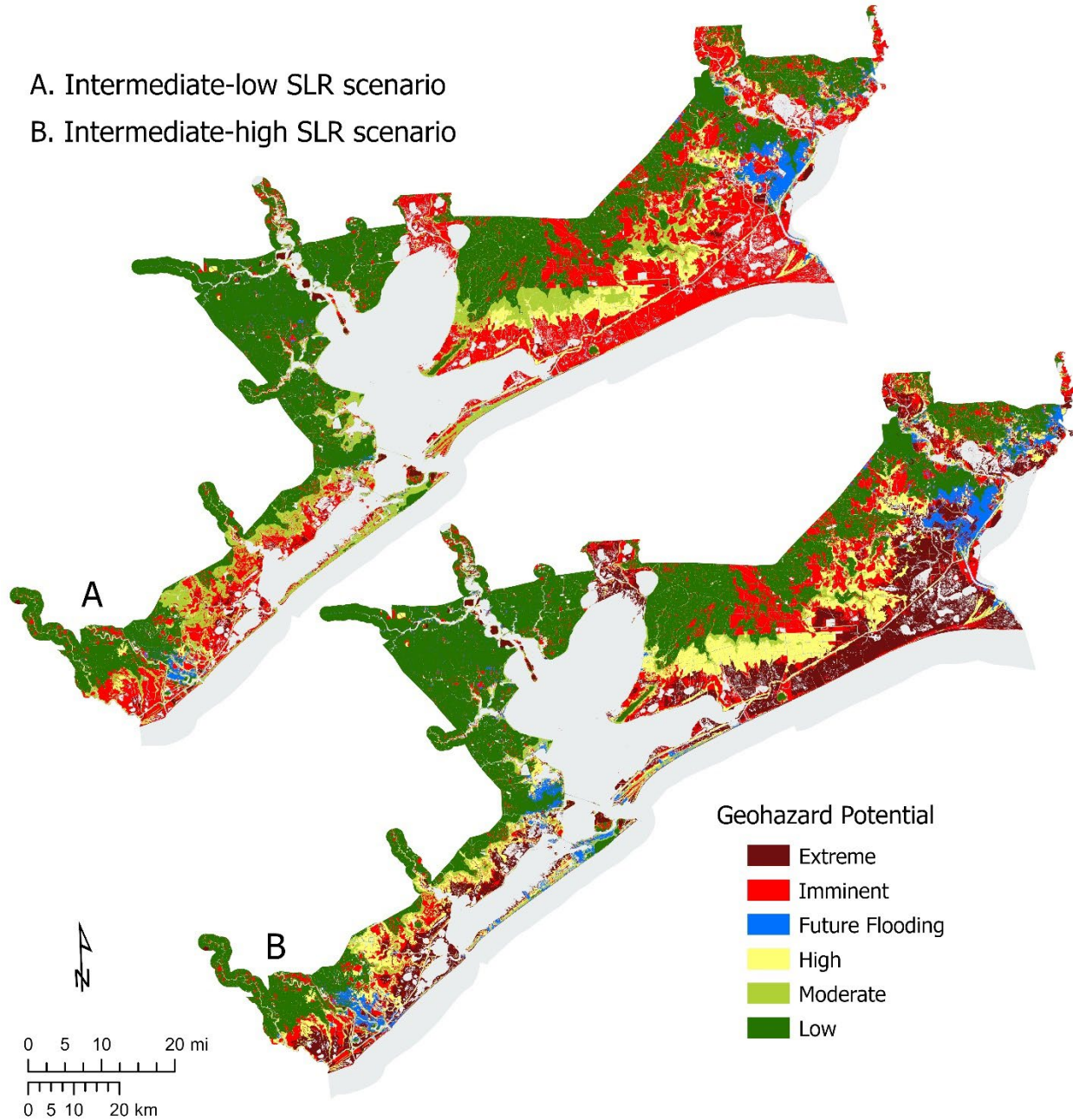

Figure 99. Map comparing geohazard potential category distribution in Regin 1 on (A) intermediate-low SLR scenario and (B) intermediate-high SLR scenario
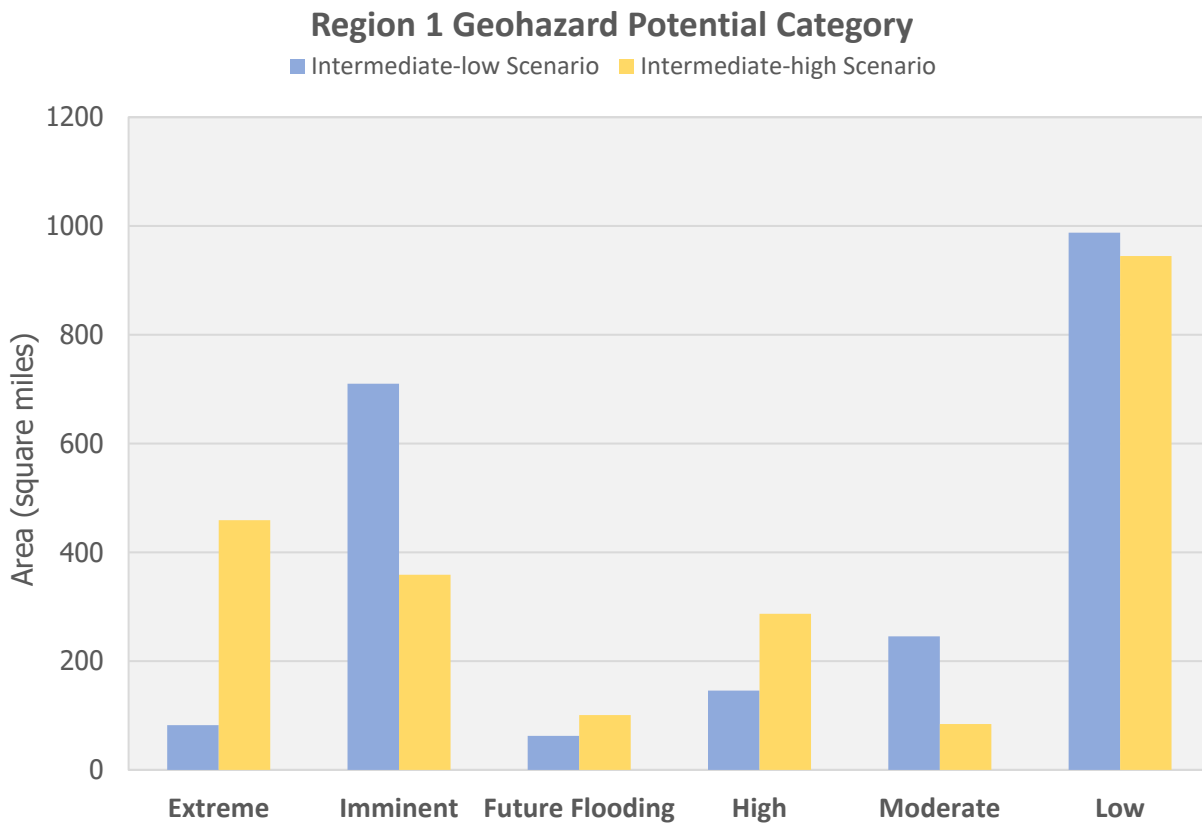
Region 1 Geohazard Potential Category

Figure 100. Graph comparing the geohazard potential category distribution in Region 1 on (A) the intermediate-low SLR scenario and (B) the intermediate-high SLR scenario

Table 21. Summary of geohazard potential category coverage in Region 1

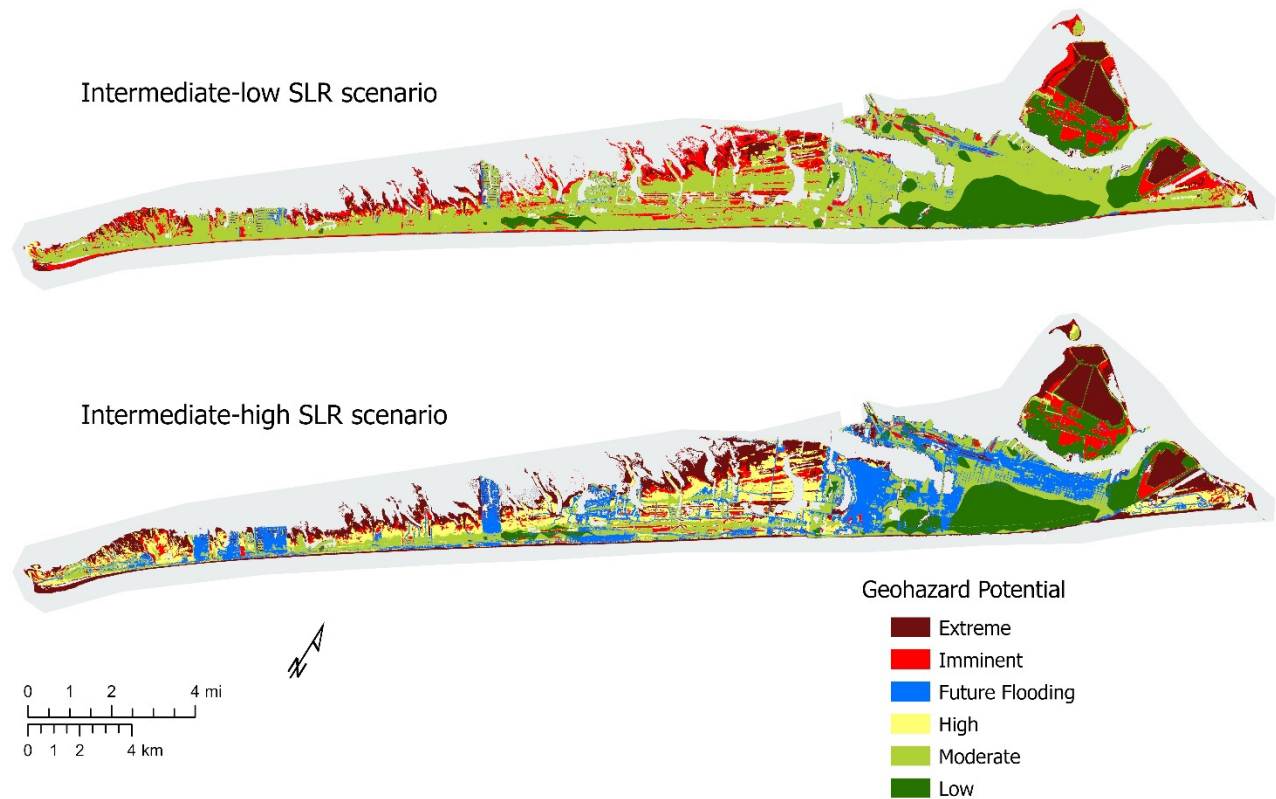| Geohazard Potential	Intermediate-Low Scenario	Intermediate High Scenario
Extreme	4%	21%
Imminent	32%	16%
Future Flooding	3%	5%
High	7%	13%
Moderate	11%	4%
Low	44%	42%

Figure 101. Map comparing geohazard potential category distribution in Galveston Island on intermediate-low SLR scenario and intermediate-high SLR scenario

Figure 101 provides a detailed view of Galveston Island showing the distribution of geohazard potential categories under intermediate-low and intermediate-high SLR scenarios. The maps reveal a substantial area of the island with a higher hazard potential in both SLR scenarios and cover a total of 42.8 square miles.

In the intermediate-low scenario, almost 13% of the mapped area falls under the Extreme geohazard potential category, which increases to nearly a quarter of the island in the intermediate-high scenario. The Imminent geohazard potential category covers about 17% of the mapped area in the intermediate-low scenario, mainly along the bay shoreline where the largest wetland extent is located, and the strip of beaches and foredunes on the Gulf side. However, this area decreases to 8% in the intermediate-high scenario.

The Future Flooding category, which represents areas at risk of flooding along the present-day urban areas and roads in the future, covers 2% of the mapped area in the intermediate-low scenario and increases to 21% in the intermediate-high scenario. The High geohazard potential category, which are areas projected to become imminent geohazard areas in 2100, covers 3% of the mapped area in the intermediate-low scenario and increases to 15% in the intermediate-high scenario.

Almost half of the mapped area falls under the Moderate geohazard potential category in the intermediate-low scenario, primarily located in the central area of Galveston Island. However, the Moderate category decreases significantly in the intermediate-high scenario, with a corresponding

increase in the Extreme, Future Flooding, and High categories. The remaining 16% of the mapped area falls under the Low geohazard potential category in the intermediate-low scenario, covering developed areas on the northern end of Galveston Island and undeveloped areas with higher ground elevation. This area decreases slightly in the intermediate-high scenario but remains relatively stable. To summarize, Figure 102 shows the distribution of geohazard potential categories in Galveston Island under both intermediate-low and intermediate-high SLR scenarios. The graph demonstrates that the island faces various types of geohazard potential, with some areas facing a significantly higher risk in the future.

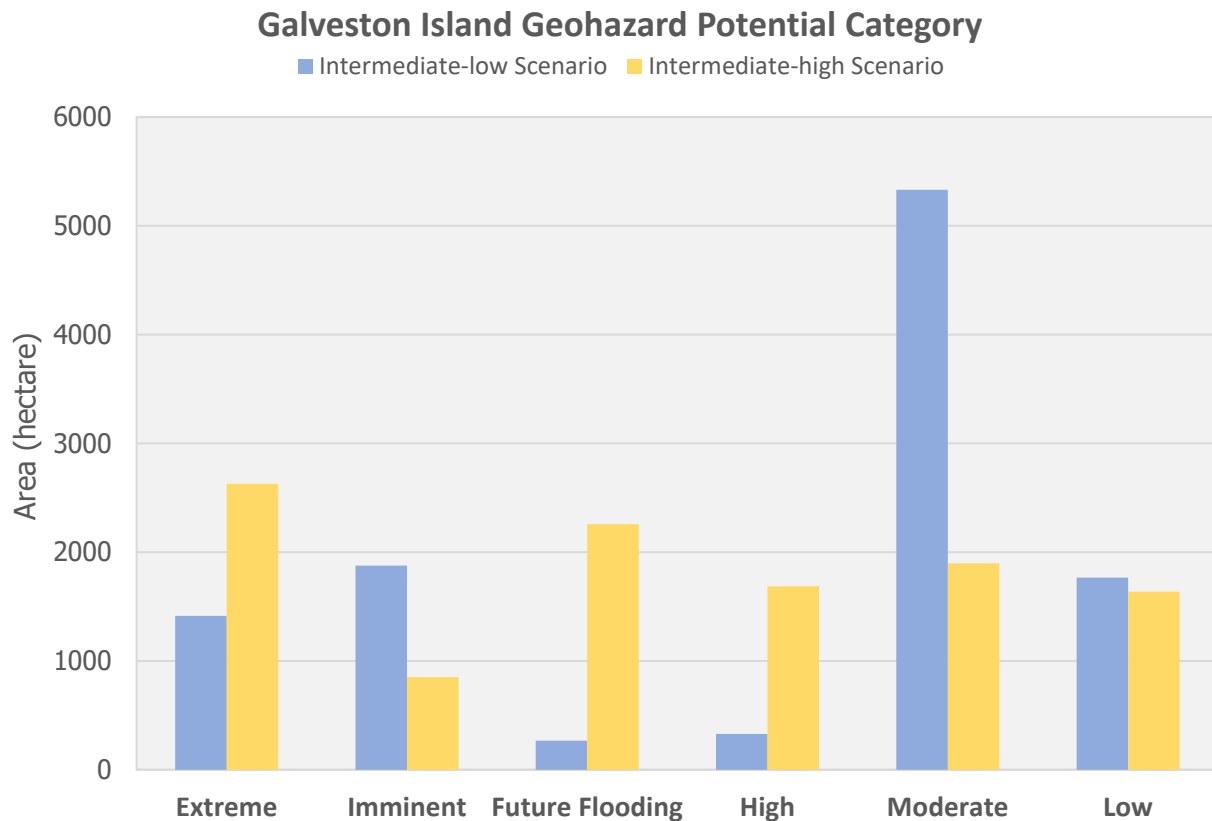## Galveston Island Geohazard Potential Category

Figure 102. Graph comparing the geohazard potential category distribution in Galveston Island shown in the map above on (A) the intermediate-low SLR scenario and (B) the intermediate-high SLR scenario.

Region 2

According to landscape change modeling, Region 2 is expected to experience significant effects from sea level rise (SLR), which will vastly alter the landscape by 2100. In addition, storm surge modeling reveals that 30% of the land in Region 2 is highly vulnerable to storm surge. These findings are depicted on the geohazards map of Region 2, as seen in Figure 103 for intermediate-low and intermediate-high SLR scenarios, and Figure 104 for geohazard potential category distribution under these scenarios.

Region 2's geohazard potential category distribution follows a similar trend as in Region 1, with the extreme geohazard category showing more than a two-fold increase from intermediate-low to intermediate-high scenario. Meanwhile, the imminent area decreases in the intermediate-high scenario compared to intermediate-low scenario, suggesting that critical environments today will convert to open water with higher SLR. The projected future flooding in Region 2 for the intermediate-low SLR

scenario is 9.5 square miles, which increases to 14 square miles in the intermediate-high scenario, affecting an urban area and road.

In the intermediate-low scenario, about 8.5% of the mapped area in Region 2 falls in the High geohazard potential category, increasing to 15% in the intermediate-high scenario. These areas are expected to become imminent geohazard areas in 2100 and are concentrated along the west side of the Matagorda Bay and barrier islands. Meanwhile, the Moderate geohazard potential category decreases from 5% in the intermediate-low scenario to 1% in the intermediate-high scenario, as these areas are exposed as High geohazard potential with higher SLR. The remaining 59% of the mapped area in the intermediate-low scenario falls under the Low geohazard potential category, mostly in inland undeveloped areas and higher ground elevations along the barrier island. However, this percentage decreases to 55% in the intermediate-high scenario, and no Low zone is found along the barrier island under higher SLR scenarios. Table 22 shows the percentage coverage of different geohazard potential categories in Region 2 for both SLR scenarios.

A. Intermediate-low SLR scenario

B. Intermediate-high SLR scenario

Geohazard Potential

- Extreme
- Imminent
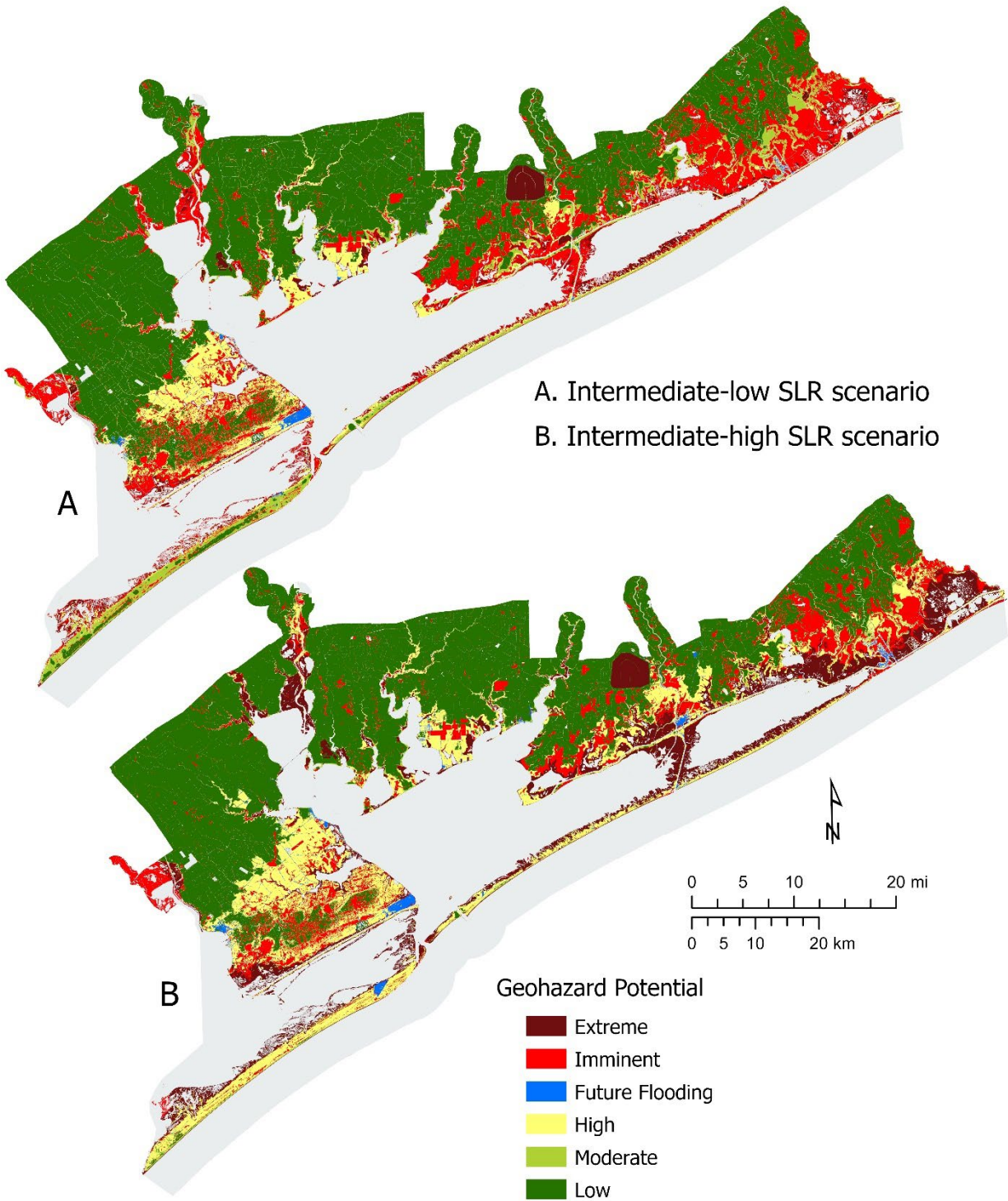- Future Flooding
- High
- Moderate
- Low

Figure 103. Map comparing geohazard potential category distribution in Regin 2 on (A) intermediate-low SLR scenario and (B) intermediate-high SLR scenario

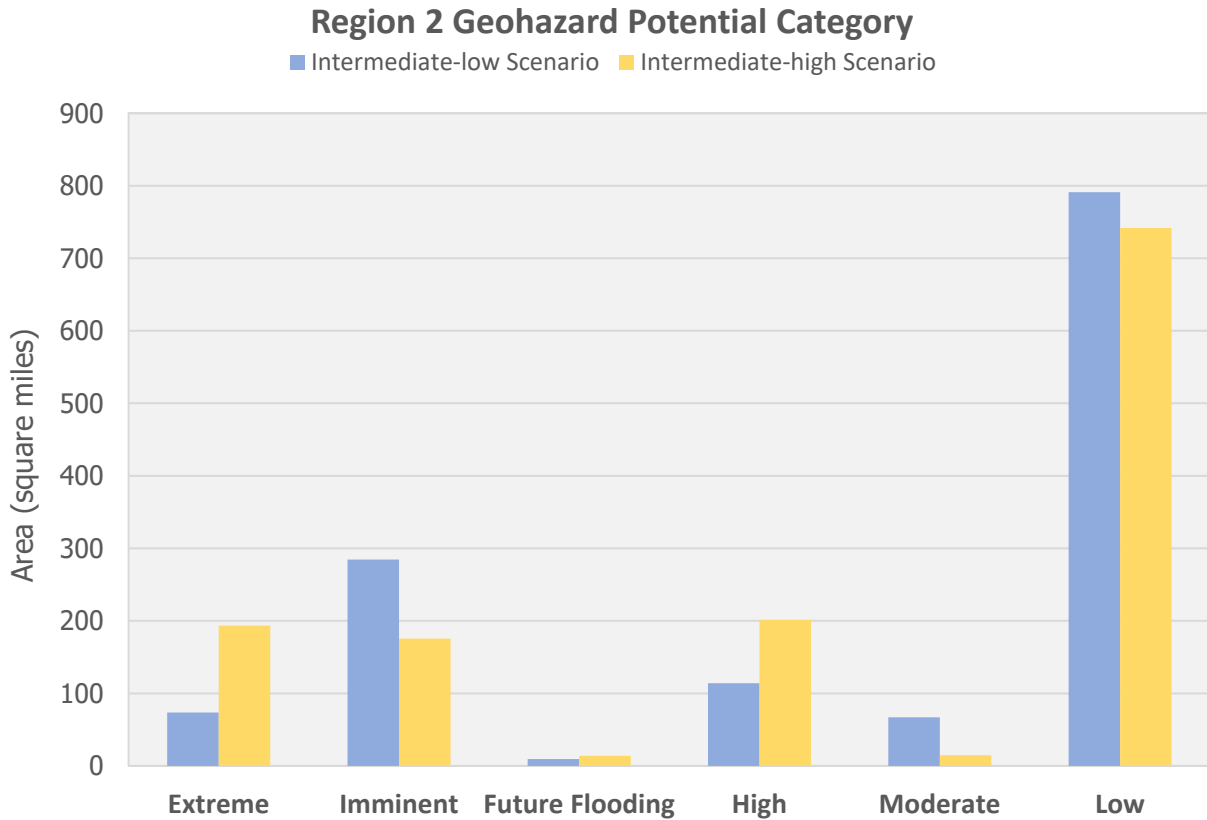## Region 2 Geohazard Potential Category

Figure 104. Graph comparing the geohazard potential category distribution in Region 2 on (A) the intermediate-low SLR scenario and (B) the intermediate-high SLR scenario

Table 22. Summary of geohazard potential category coverage in Region 2

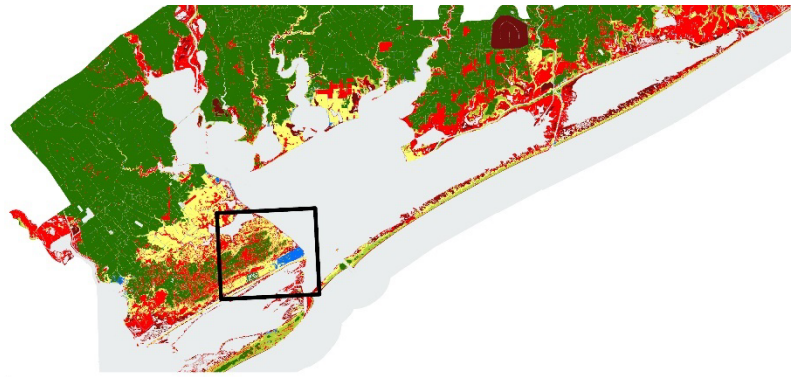|	Intermediate-Low Scenario	Intermediate High Scenario
Extreme	5.5%	14.4%
Imminent	21.2%	13.1%
Future Flooding	0.7%	1%
High	8.5%	15%
Moderate	5%	1.1%
Low	59.1%	55.3%

Figure 105 shows a close-up of the Port O'Connor area, where significant landscape changes are expected to occur by 2100, based on landscape change modeling. The map shows a substantial area east of Matagorda Bay with a higher hazard potential in both SLR scenarios. The total mapped area in these maps covers 48.4 sq. mile.

In the intermediate-low scenario, almost 79% of the mapped area falls under the High to Extreme geohazard potential category. This area increases to 90% in the intermediate-high scenario. The transition trend between the two scenarios follows a similar pattern observed in Galveston Island. For instance, the Extreme and High categories increase from 8% and 30% of the mapped area in intermediate-low scenario to 17% and 39%, respectively, in the intermediate-high scenario. Conversely, the Imminent category decreases from 35% to 27% between these two scenarios. The Future Flooding category remains relatively stable between the two SLR scenarios, as the area is largely undeveloped.

The remaining 21% of the mapped area falls under the Low geohazard potential in the intermediate-low scenario and includes undeveloped areas where the ground elevation is generally higher. The area decreases to 10% in the intermediate-high scenario and changes to higher geohazard potential category. Figure 106 displays the detail distribution of geohazard potential categories of the area under both intermediate-low and intermediate-high SLR scenarios. The maps highlight a significant area with a higher hazard potential in both scenarios, indicating the need for appropriate measures to mitigate the associated risks.

Geohazard Potential

- ■ Extreme
- ■ Imminent
- ■ Future Flooding
- ■ High
- ■ Moderate
- ■ Low

A. Intermediate-low SLR scenario
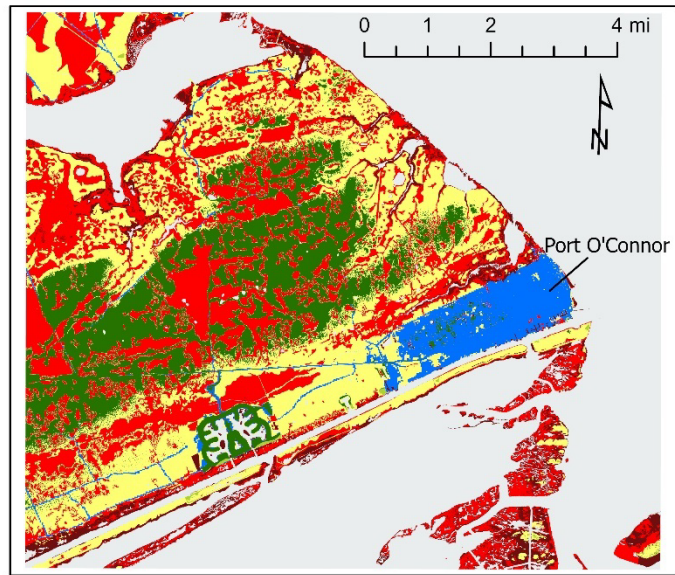
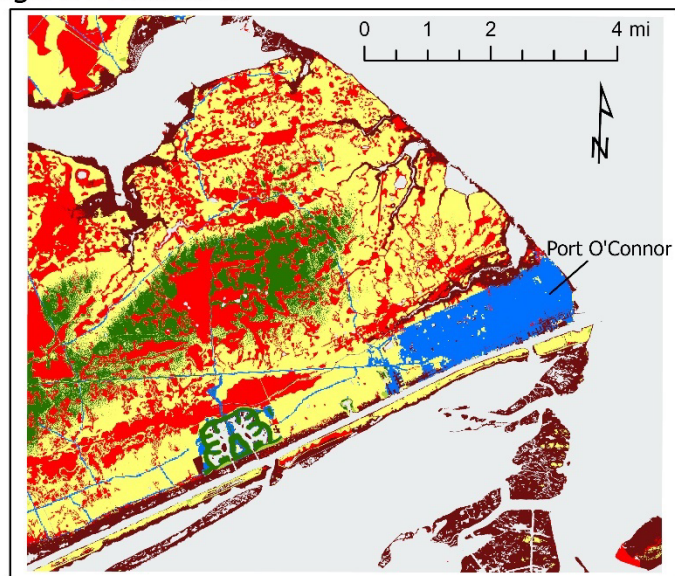### B. Intermediate-high SLR scenario

Figure 105. Map comparing geohazard potential category distribution around Port O'Connor area on intermediate-low SLR scenario and intermediate-high SLR scenario

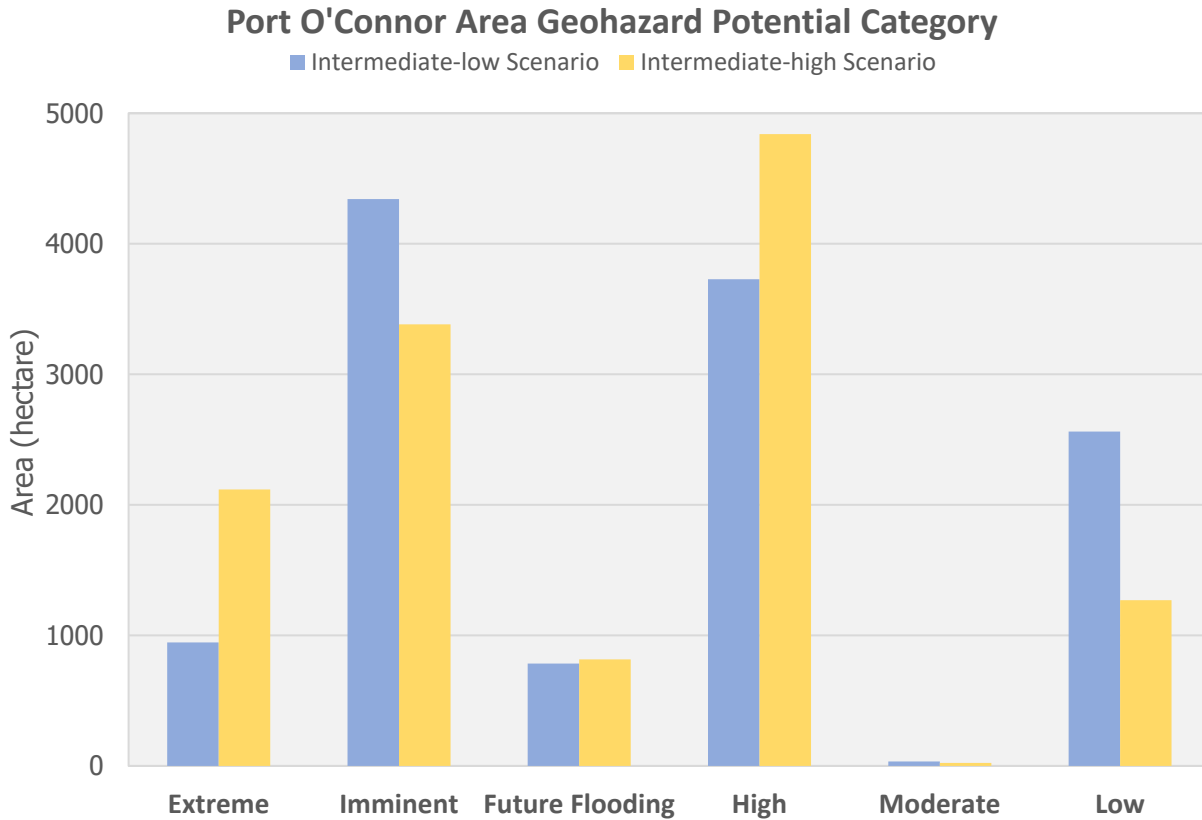## Port O'Connor Area Geohazard Potential Category

Figure 106. Graph comparing the geohazard potential category distribution in Port O'Connor area shown in the map above on (A) the intermediate-low SLR scenario and (B) the intermediate-high SLR scenario

Region 3

Region 3 is expected to undergo significant effects of SLR based on the landscape change modeling, resulting in a drastic transformation of its landscape by 2100. Although Region 3 is less vulnerable to storm surge compared to other regions, storm surge modeling shows that 13% of its land is highly vulnerable to this hazard. The geohazards map of Region 3, as seen in Figure 107 for intermediate-low and intermediate-high SLR scenarios, displays these findings. Figure 108 shows the geohazard potential category distribution under these two scenarios, which shows similar trend in the changes in distribution as the previous two regions.

These maps show about 4.2% of the total 2,050 sq. miles mapped area was assigned to the Extreme geohazard potential category in the intermediate-low scenario. This figure increases to about 7.3% of the mapped area in the intermediate-high scenario, mainly along the backside of barrier islands, Nueces River Delta, Baffin Bay, and Aransas Bay area. About 10.1% of the mapped area falls in the Imminent geohazard potential category in the intermediate-low scenario, which decreases to 7.4% in the intermediate-high scenario. The transition to the Extreme category due to the conversion to open water causes this decrease in the Imminent zone in the intermediate-high scenario. In the intermediate-low scenario, a total of 6.4 square miles of an urban area and road in Region 3 are projected to be flooded, which doubles in the intermediate-high scenario.

The high geohazard potential category, which includes areas projected to become imminent geohazard areas in 2100, covers 2.3% of the mapped area in the intermediate-low scenario. It is highly concentrated on the low-lying areas along the east side of Copano Bay and around Baffin Bay, as well as along the back side of barrier islands. In the intermediate-high scenario, it increases to 6.1% of the mapped area with a significant increase in the east side of Copano Bay. Meanwhile, the Moderate geohazard potential category decreases from 2.7% in the intermediate-low scenario to 1% in the intermediate-high scenario, as these areas are exposed to a higher geohazard potential with higher SLR. The remaining 80.4% of the mapped area is categorized as having a Low geohazard potential in the intermediate-low SLR scenario and mainly includes undeveloped areas where the ground elevation is generally higher. It decreases slightly to 77.6% in the intermediate-high scenario. In the intermediate-high scenario, there is a less area in the Low and Moderate geohazard potential zones as they are converting to a higher hazard potential, increasing the area of the Extreme and High classification. Table 23 shows the percentage coverage of different geohazard potential categories in Region 3 for both SLR scenarios.
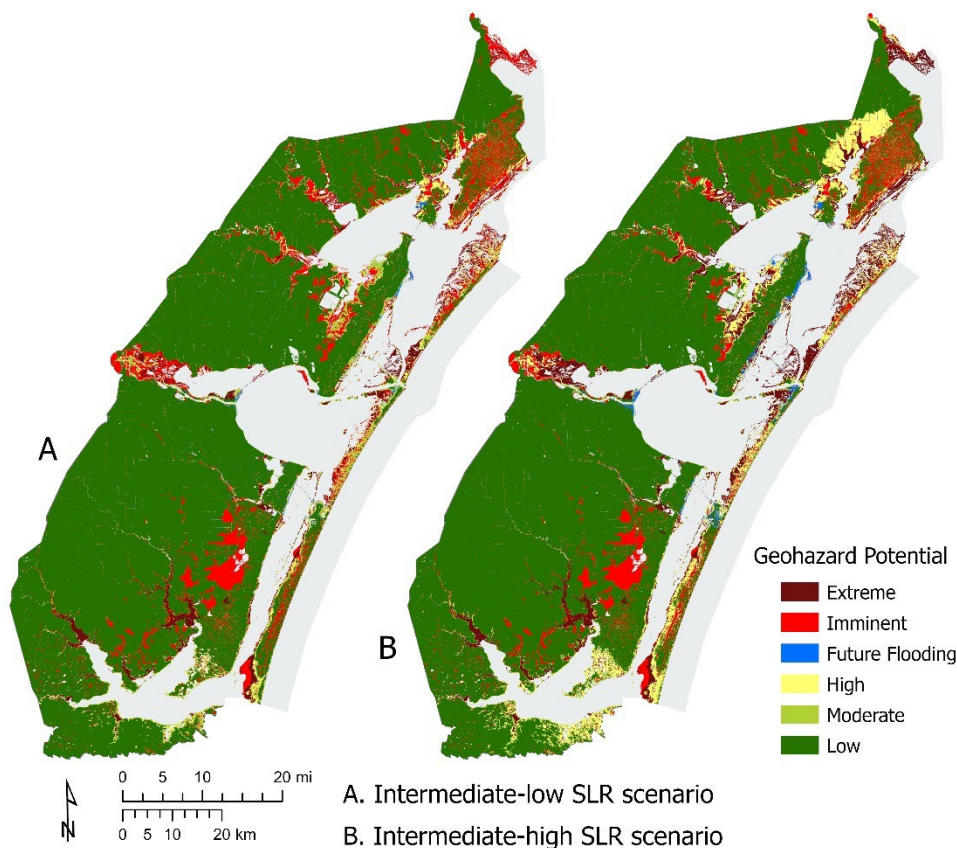

Figure 107. Map comparing geohazard potential category distribution in Regin 3 on (A) intermediate-low SLR scenario and (B) intermediate-high SLR scenario
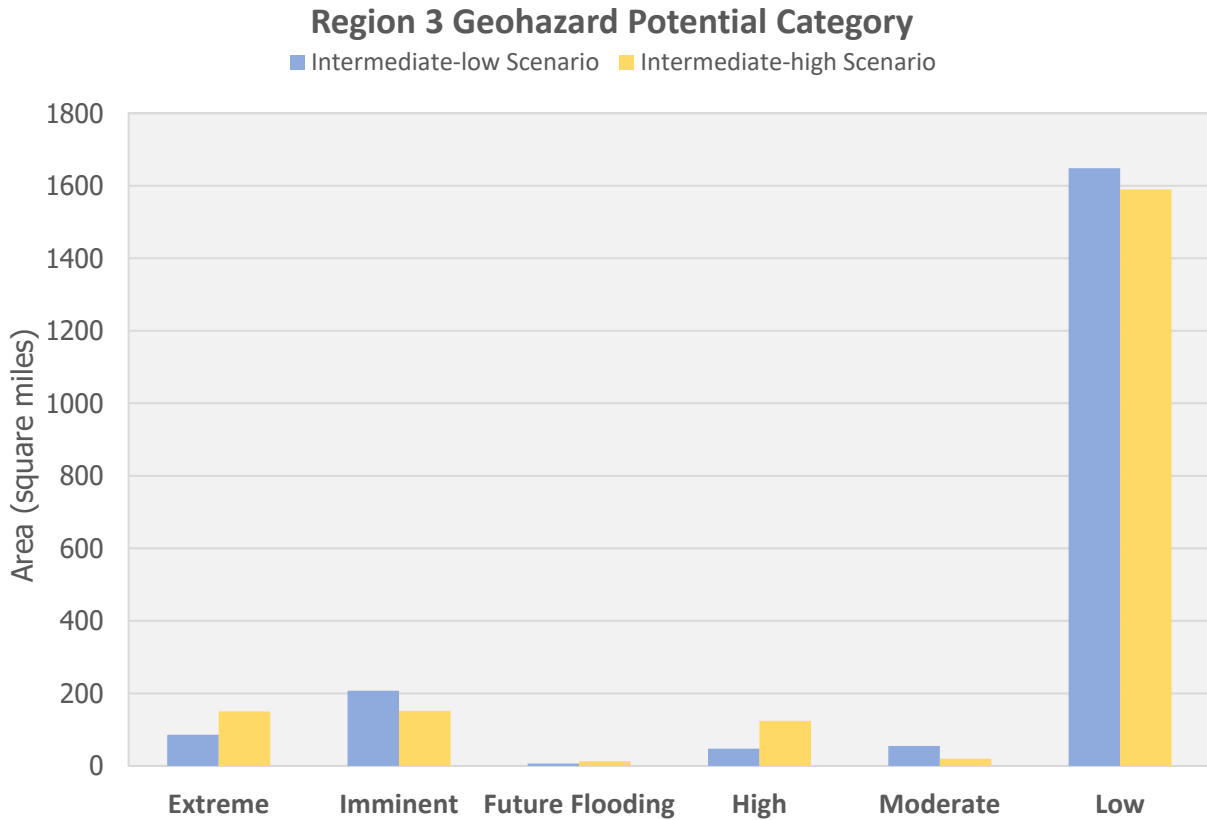
Region 3 Geohazard Potential Category

Figure 108. Graph comparing the geohazard potential category distribution in Region 3 on (A) the intermediate-low SLR scenario and (B) the intermediate-high SLR scenario

Table 23. Summary of geohazard potential category coverage in Region 3

	Intermediate-Low Scenario	Intermediate High Scenario
Extreme	4.2%	7.3%
Imminent	10.1%	7.4%
Future Flooding	0.3%	0.6%
High	2.3%	6.1%
Moderate	2.7%	1%
Low	80.4%	77.6%

Figure 109 shows a detailed view of Port Aransas/Redfish Bay area, displaying the distribution of geohazard potential categories in intermediate-low and intermediate-high SLR scenarios. This region is of significant economic importance as it serves as the mouth of the Corpus Christi Ship Channel, which connects to the Port of Corpus Christi - the largest port in the United States in terms of total revenue

tonnage. The map depicts a substantial area with a higher geohazard potential in both SLR scenarios, covering a total of 70 sq. miles.

Under the intermediate-low scenario, nearly 17% of the mapped area falls under the Extreme geohazard potential category, which increases to 30% in the intermediate-high scenario. Notably, almost all the Harbor Island falls under the Extreme zone in both scenarios. The Imminent geohazard potential category covers roughly 14% of the mapped area in the intermediate-low scenario, primarily to the north of Aransas Pass, and the strip of beaches and foredunes on both the Gulf and bay side. However, this area decreases to 7% in the intermediate-high scenario, indicating that critical environments today will convert to open water with higher SLR. The Future Flooding zone increases from 207 hectares to 616 hectares between the intermediate-low and intermediate-high scenarios, with an increase visible in both Aransas Pass and Port Aransas.
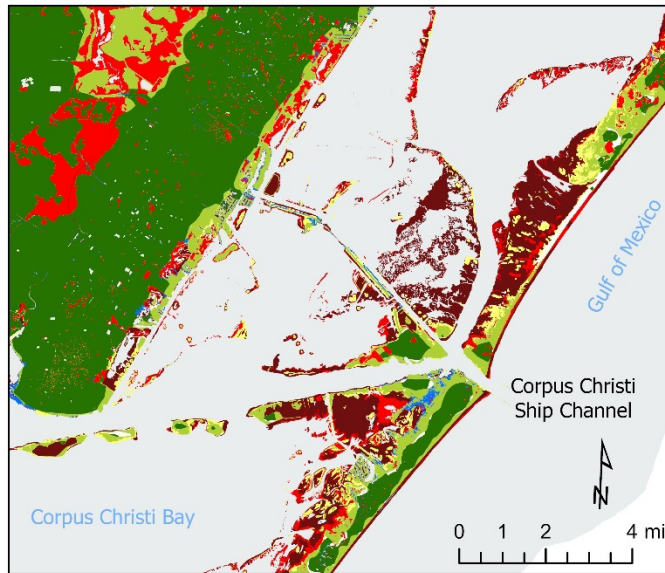
The High geohazard potential category, which shows areas that will become imminent geohazard areas in 2100, covers 5% of the mapped area in the intermediate-low scenario and increases to 8% in the intermediate-high scenario. The Moderate geohazard category, which is concentrated in the back of the barrier island and along the bay shoreline of the Redfish Bay in the intermediate-low scenario, converts to higher geohazard potential in the intermediate-high scenario, thereby decreasing the area from 12% to 4% of the mapped area between these two scenarios. The remaining 50% of the mapped area falls under the Low geohazard potential in the intermediate-low scenario and includes upland areas where the ground elevation is generally higher. This area decreases slightly to 47% in the intermediate-high scenario and remains relatively stable. Figure 110 shows the distribution of geohazard potential categories in Port Aransas/Redfish Bay area under both intermediate-low and intermediate-high SLR scenarios.

Geohazard Potential

- ■ Extreme
- ■ Imminent
- ■ Future Flooding
- ■ High
- ■ Moderate
- ■ Low
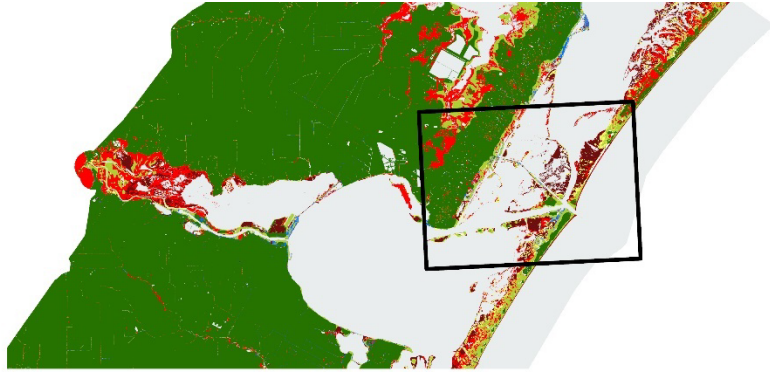
A. Intermediate-low SLR scenario
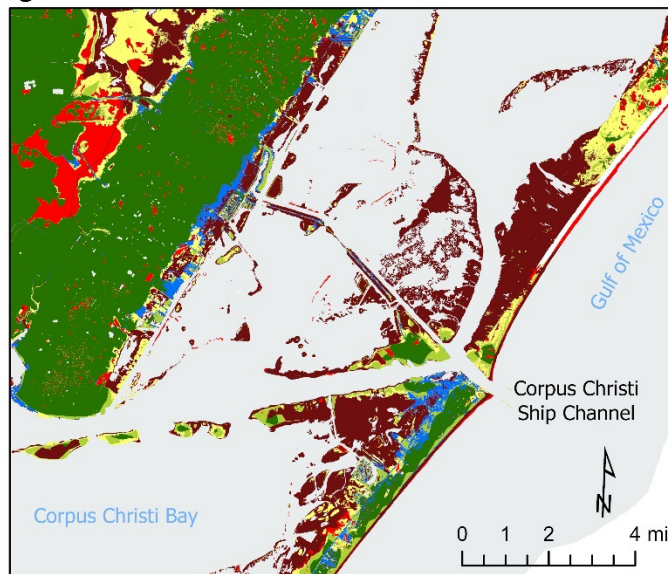
B. Intermediate-high SLR scenario

Figure 109. Map comparing geohazard potential category distribution around Port Aransas/Aransas Pass area on intermediate-low SLR scenario and intermediate-high SLR scenario

Port Aransas Area Geohazard Potential Category

■ Intermediate-low Scenario ■ Intermediate-high Scenario
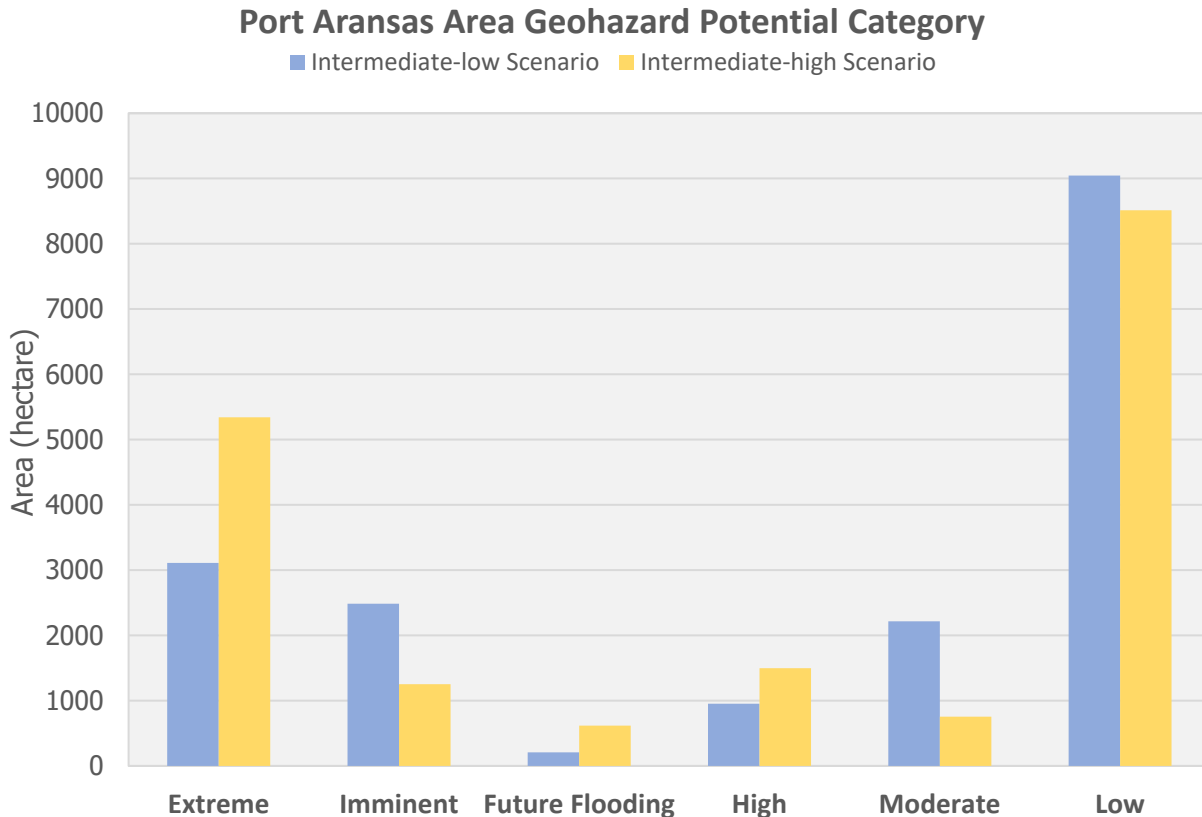

Figure 110. Graph comparing the geohazard potential category distribution in Port Aransas/Aransas Pass area shown in the map above on (A) the intermediate-low SLR scenario and (B) the intermediate-high SLR scenario

Region 4

The predicted effects of sea-level rise (SLR) are significant and expected to impact Region 4, leading to substantial changes in the landscape by 2100 based on landscape change modeling. The storm surge modeling shows that 14% of the land in Region 4 is highly vulnerable to storm surges, particularly along the backside of South Padre Island's shoreline and along the Lower Laguna Madre.. These findings are shown on the geohazards map of Region 4, as seen in Figure 111 for intermediate-low and intermediate-high SLR scenarios, and Figure 112 for geohazard potential category distribution under these scenarios. These maps show a similar trend in the changes in distribution as other regions in the upper coast.

Region 4 has the highest percentage of mapped area falling under the Extreme geohazard category among the four regions. Almost all of the tidal flats in the Laguna Madre lie in the Extreme zone. In the intermediate-low scenario, around 16.4% of the mapped area within Region 4 is categorized as Extreme, which increases to almost 19% in the intermediate-high scenario. Approximately 11.2% of the mapped area falls under the Imminent geohazard category in the intermediate-low scenario, primarily in the marshes and low-lying areas of the Lower Laguna, as well as along the bay shoreline of Laguna Madre. This percentage decreases to 9% in the intermediate-high scenario, mainly due to the transformation of present-day environments into open water.

In the intermediate-low scenario, a total of 1.7 square miles of an urban area and road, mainly in the South Padre Island and Port Isabel areas of Region 4, falls in the Future Flooding category, which increases to 2.9 square miles in the intermediate-high scenario. A significant portion of South Padre Island falls under the Future Flooding zone in the intermediate-high scenario. Additionally, about 2.3% of the mapped area in Region 4 is categorized as High geohazard potential category in the intermediate-low scenario, which increases to 5.3% in the intermediate-high scenario. These areas are expected to become imminent geohazard areas in 2100 and mainly located on the back side of the barrier island. As in other regions, the Moderate geohazard potential category decreases from 2.6% in the intermediate-low scenario to 0.8% in the intermediate-high scenario, as these areas are exposed to a higher geohazard potential with higher SLR. The remaining 67.4% of the mapped area fall under the Low geohazard potential category in the intermediate-low SLR scenario and it decreases slightly to 65.7% in the intermediate-high scenario. Table 24 shows the percentage coverage of different geohazard potential categories in Region 4 for both SLR scenarios.
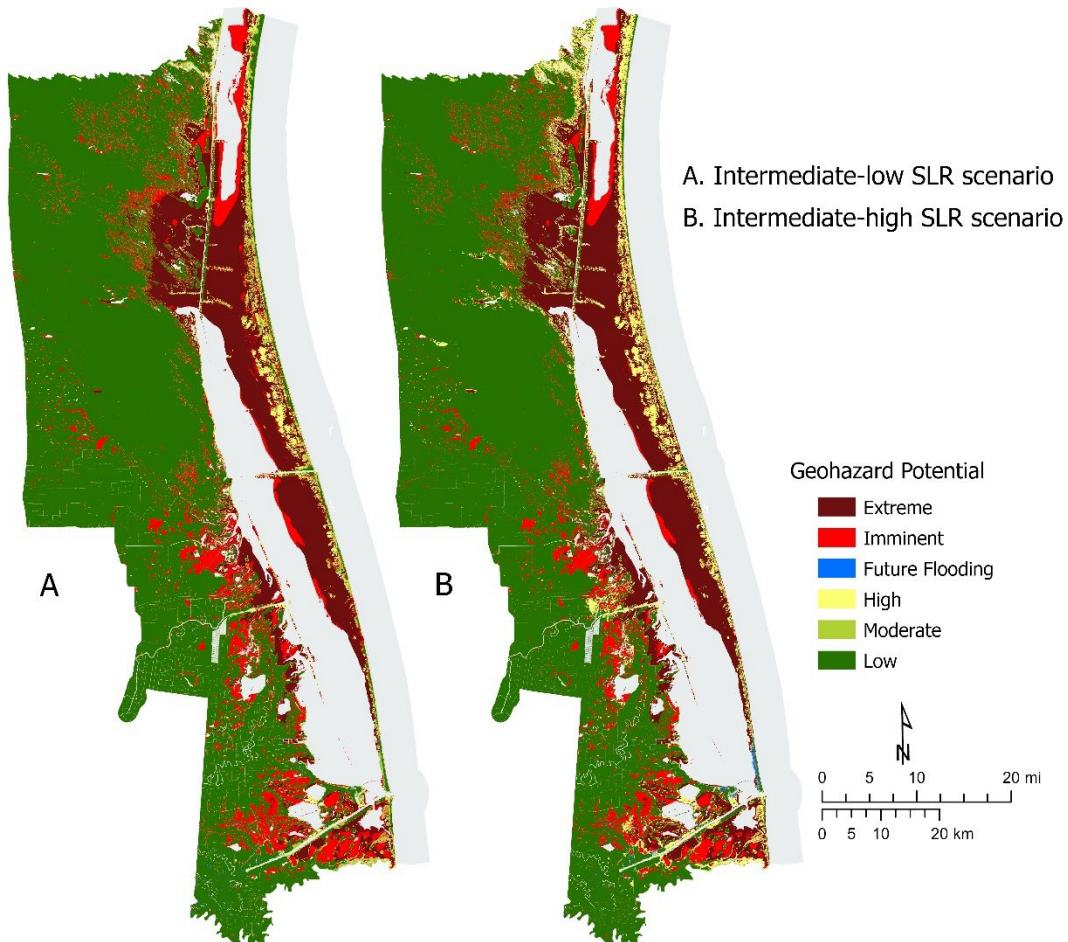

Figure 111. Map comparing geohazard potential category distribution in Regin 4 on (A) intermediate-low SLR scenario and (B) intermediate-high SLR scenario
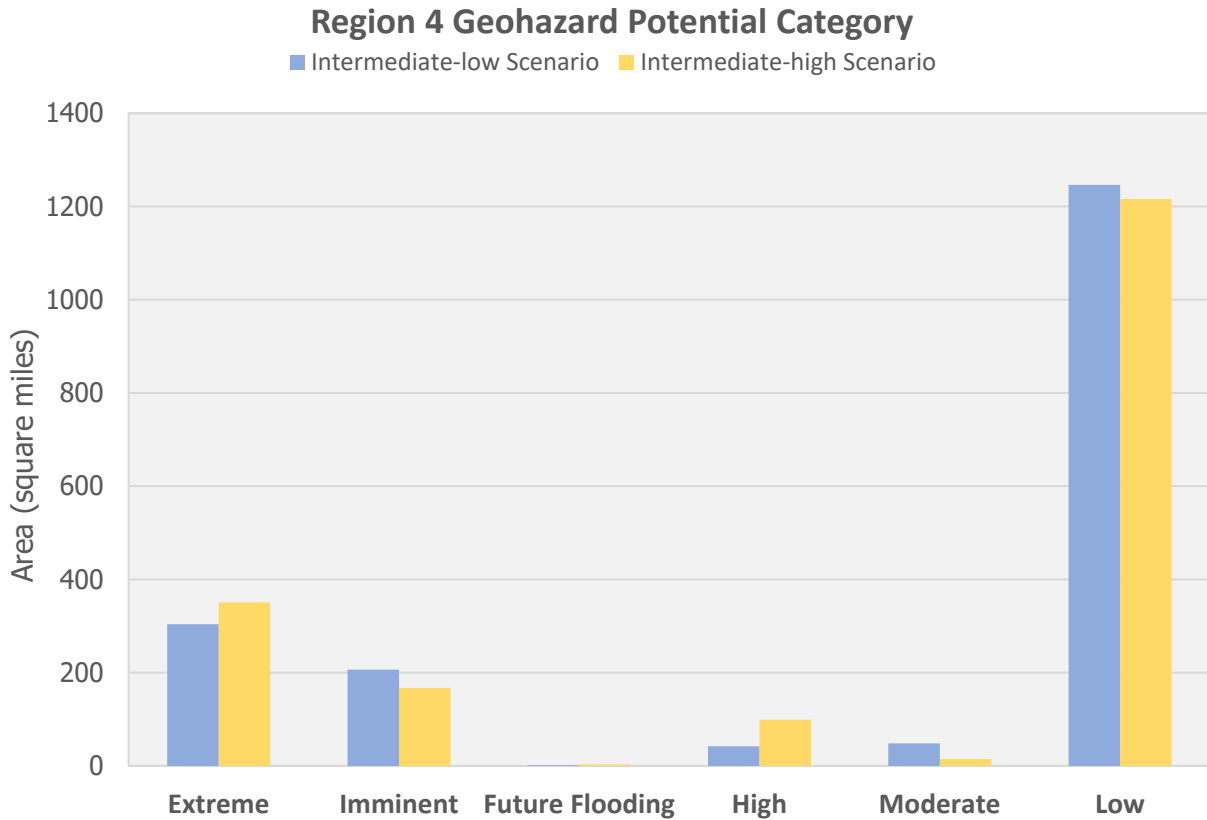
Figure 112. Graph comparing the geohazard potential category distribution in Region 4 on (A) the intermediate-low SLR scenario and (B) the intermediate-high SLR scenario

Table 24. Summary of geohazard potential category coverage in Region 4

	Intermediate-Low Scenario	Intermediate High Scenario
Extreme	16.4%	18.9%
Imminent	11.2%	9%
Future Flooding	0.1%	0.2%
High	2.3%	5.3%
Moderate	2.6%	0.8%
Low	67.4%	65.7%

Figure 113 provides a detailed view of South Padre Island showing the distribution of geohazard potential categories under intermediate-low and intermediate-high SLR scenarios. The maps reveal a substantial area of the island with a higher hazard potential in both SLR scenarios. The total area mapped covers 7.5 square miles.

In the intermediate-low scenario, nearly one-third of the mapped area falls under the Extreme geohazard potential category, increasing to almost half of the island in the intermediate-high scenario. Almost all the backside of the island in the north falls under the Extreme zone. The Imminent geohazard potential category covers about 7% of the mapped area in the intermediate-low scenario, mainly along the bay shoreline in the south of the island. However, this area decreases to 1% in the intermediate-high scenario.

The Future Flooding category, which represents areas at risk of flooding along the present-day urban areas and roads in the future, covers 2% of the mapped area in the intermediate-low scenario which increases to 13% in the intermediate-high scenario, flooding most of the South Padre Island. The High geohazard potential category, which are areas projected to become imminent geohazard areas in 2100, covers 5% of the mapped area in the intermediate-low scenario and increases to 15% in the intermediate-high scenario.

More than 31% of the mapped area falls under the Moderate geohazard potential category in the intermediate-low scenario. However, the Moderate category decreases significantly in the intermediate-high scenario, with a corresponding increase in the Extreme, Future Flooding, and High categories. The remaining 22% of the mapped area falls under the Low geohazard potential category in the intermediate-low scenario, covering developed areas on the south end of the Island and undeveloped areas with higher ground elevation. This area decreases to 15% in the intermediate-high scenario, changing to higher geohazard potential category. Figure 114 displays the detail distribution of geohazard potential categories of the area under both intermediate-low and intermediate-high SLR scenarios. The maps highlight that a significant area of the island is exposed to a higher hazard potential in both scenarios, indicating the need for appropriate measures to mitigate the associated risks.
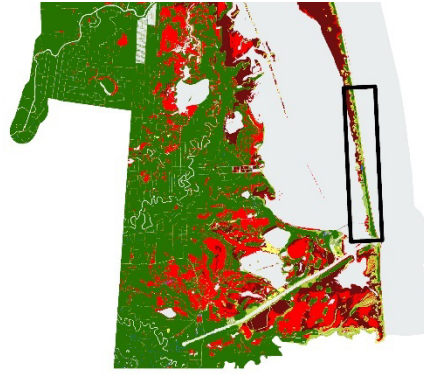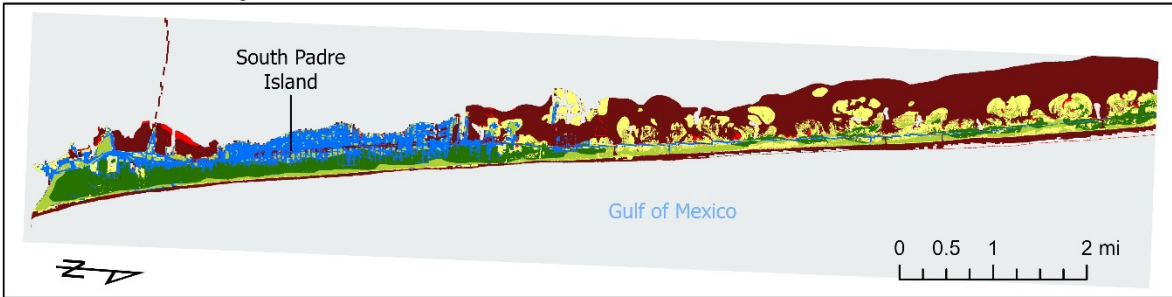
Figure 113. Map comparing geohazard potential category distribution in South Padre Island area on intermediate-low SLR scenario and intermediate-high SLR scenario

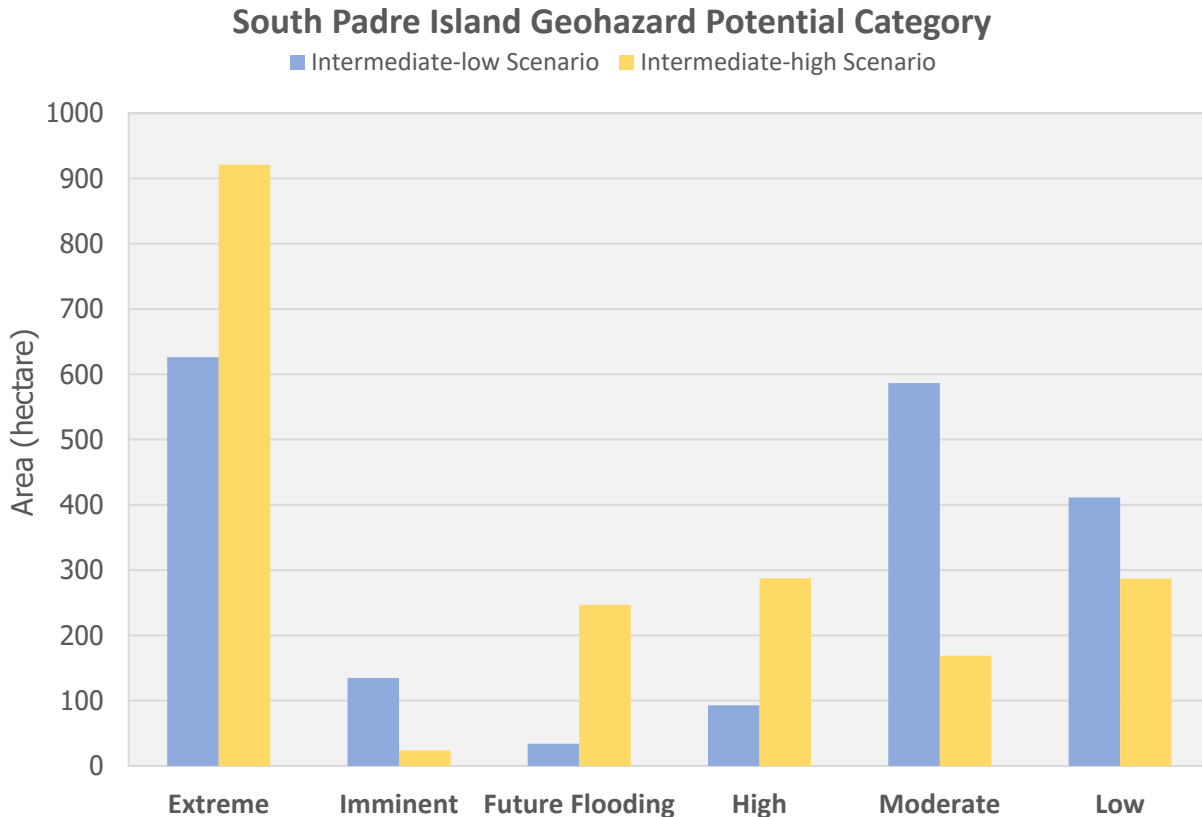## South Padre Island Geohazard Potential Category

Figure 114. Graph comparing the geohazard potential category distribution in South Padre Island area shown in the map above on (A) the intermediate-low SLR scenario and (B) the intermediate-high SLR scenario

Conceptual Resiliency Projects Modeling

The conceptual resiliency project modeling results have shown that the beneficial use of dredged material (BUDM) can be an effective solution to mitigate the impacts of SLR on habitats. Furthermore, the implementation of living shorelines and island restoration can reduce the detrimental effects of storm surge and wave damage in the immediate vicinity. The outcomes of these modeling show that large-scale resiliency projects can decrease water depth and inundation caused by storm surge by acting as buffers, suppressing wave energy, and mitigating storm surge impact beyond the project area. The analysis suggests that combining multiple resiliency projects can effectively reduce wave energy and minimize storm surge impact in the area. Nevertheless, there are challenges associated with coordinating funding, dredge cycles, and interagency participation, which need to be addressed to implement such large-scale projects effectively.

Region 1

Landscape Change Modeling

The BUDM restoration projects were built out mainly in Lower Neches WMA where all salt and brackish marshes are located to simulate raising the elevation of project site every 25 years to offset the rate of RSLR. Similarly, a few islands were created on Old River Cove and Pleasure Island and the land cover type was altered to align with the surrounding islands. The landscape change analysis shows a

considerable conservation of the low marshes in the Lower Neches WMA and the surrounding area, showing the efficacy of periodic elevation boosting in the SLAMM model (Figure 115).
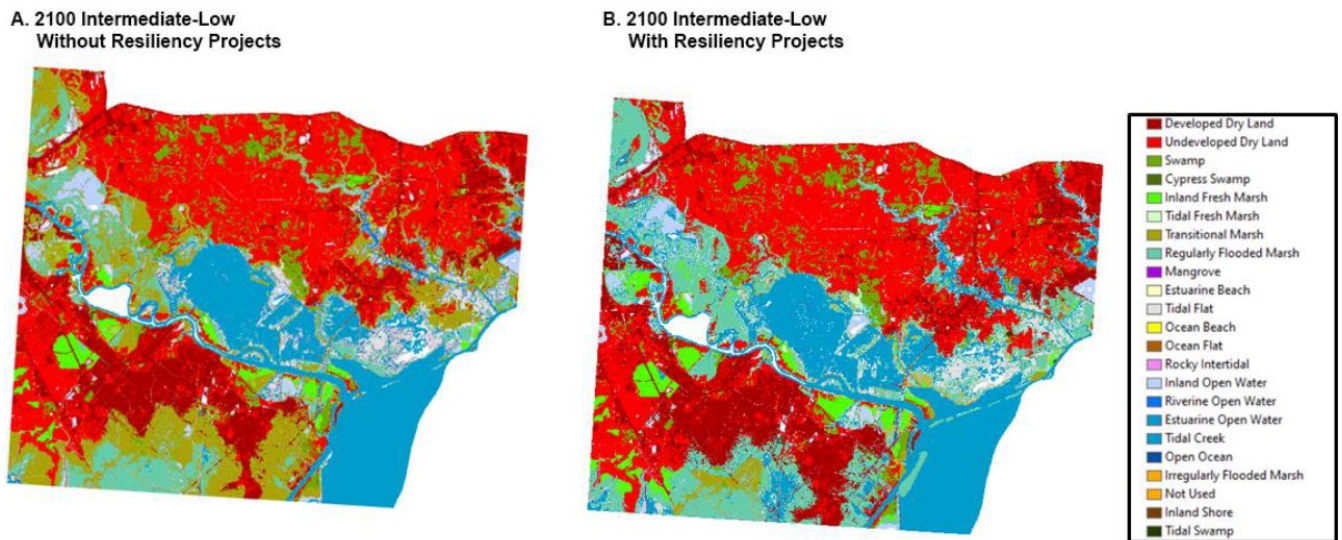

Figure 115. Comparison of land cover in 2100 on the future landscape with intermediate-low SLR scenario (A) without resiliency projects, and (B) with resiliency projects.

Storm Surge and Wave Modeling

Storm 160 was selected to investigate the impact of storm surge and wave with and without resiliency projects (marsh conservation and island restoration projects) in the future landscape under the intermediate-low SLR scenario. This storm made landfall on the eastward end of the Bolivar Peninsula near Rollover Pass as a Category 2 hurricane with a forward speed of 10 miles per hour and a maximum wind speed of 100 miles per hour (Table 7 and Figure 14).

Figure 116 shows the maximum water surface elevation due to Storm 160 with and without resiliency projects implemented in the future landscape with intermediate-low SLR scenario. Comparing the effect of resiliency projects on storm surge, the results showed that the large-scale marsh conservation projects in Lower Neches Wildlife Management Area act like buffers suppressing wave energy in turn reducing storm surge impact not only within the project area but also outside the project area. These projects also helped reduce the extent of storm surge inundation inland.

Figure 117 presents two maps showing the difference in extent of inundation and maximum water surface elevation due to Storm 160 with and without resiliency projects in place (top) and the difference in significant wave height with and without projects in place (bottom). The cool colors in the maps show an area with reduced water levels and wave height due to the presence of resiliency projects. Similarly, the purple color in the top map shows the area that is prevented from becoming inundation with the projects in place. It was found that more than 39 square miles of land in Orange and Jefferson counties did not get inundated with these resiliency projects in place.
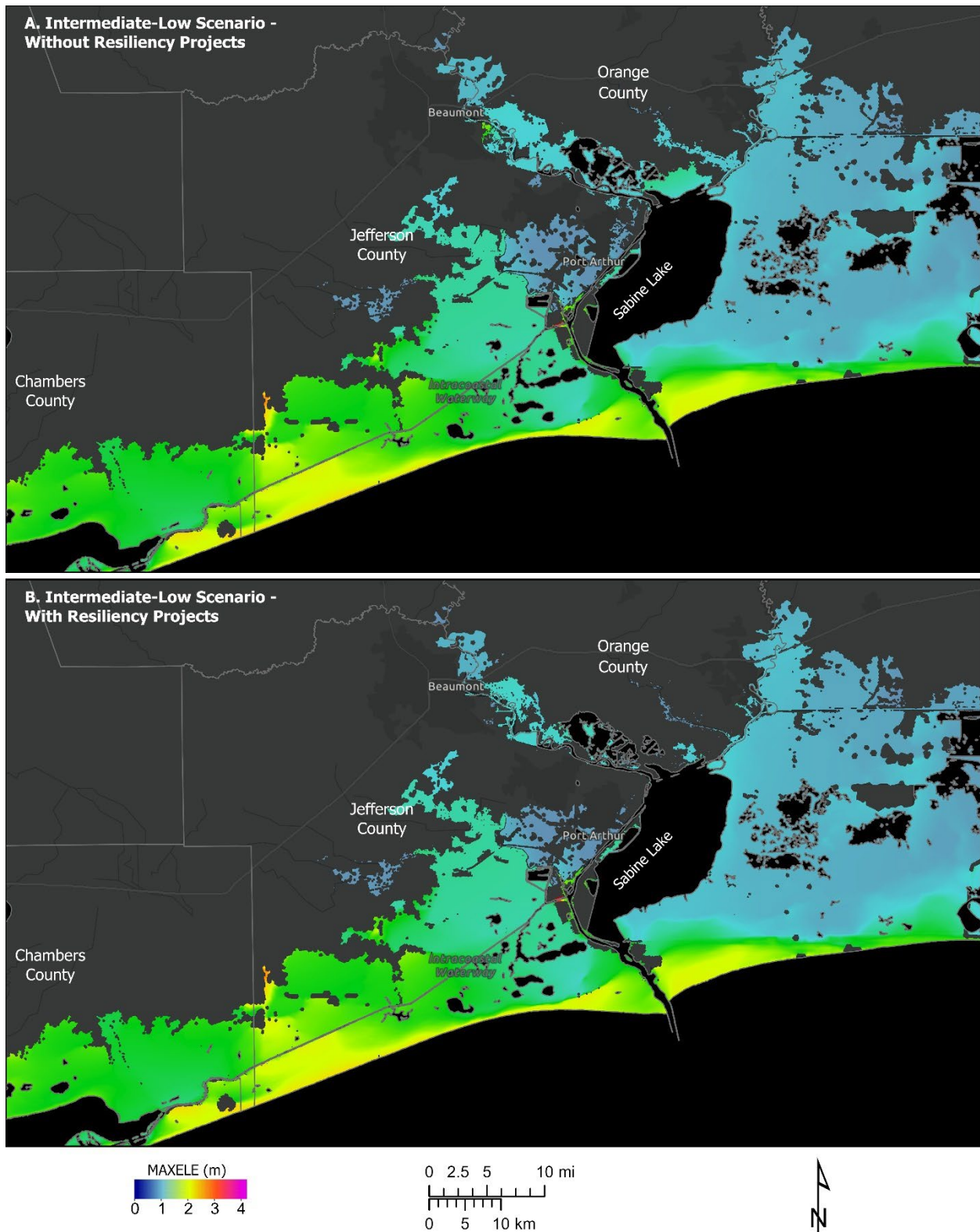
Figure 116. Comparison of maximum water surface elevation (MAXELE) due to Storm 160 in the future landscape with intermediate-low SLR scenario (A) without resiliency projects, and (B) with resiliency projects.
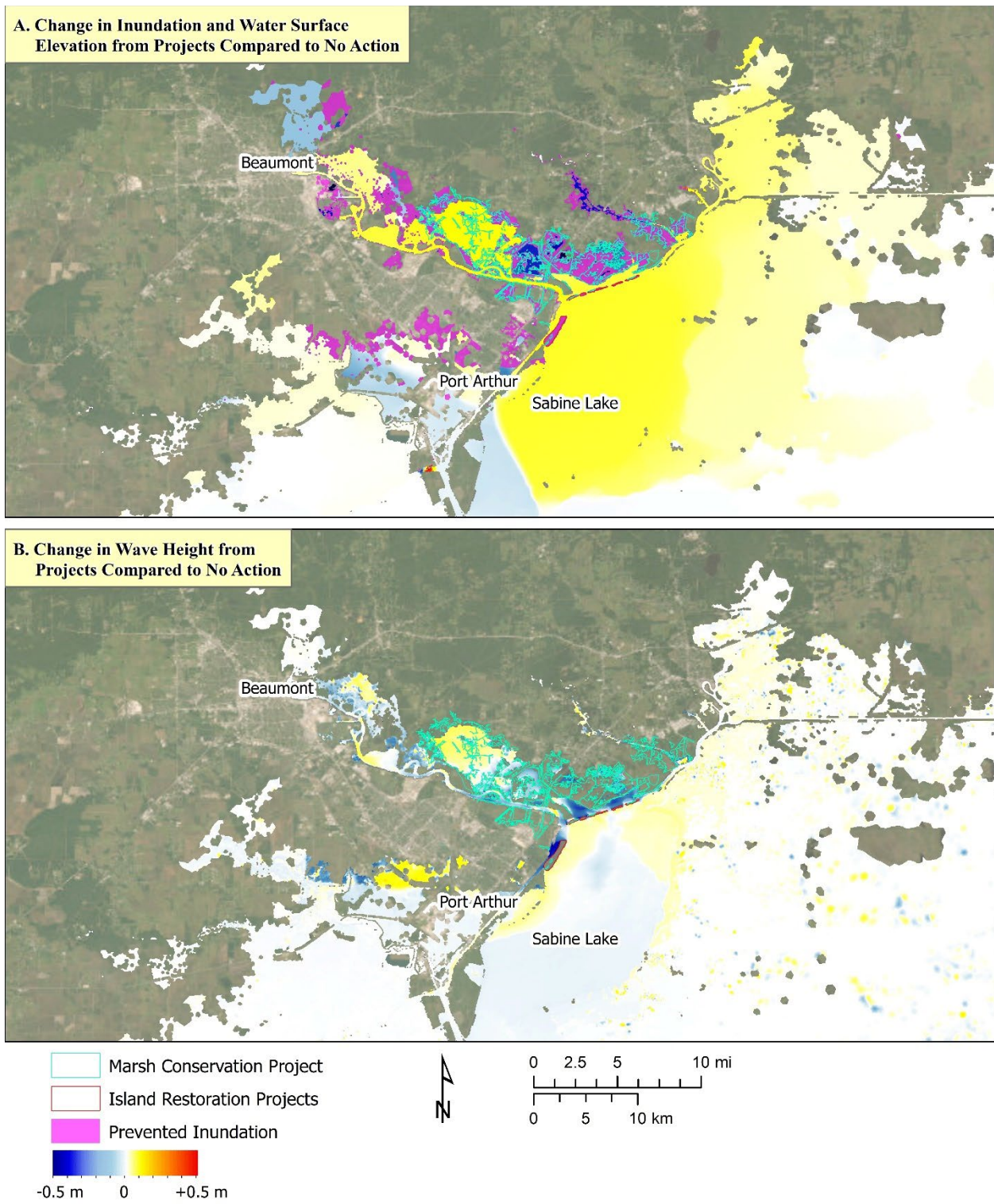
Figure 117. Difference maps showing (A) change in water surface elevation due to resiliency projects in place in the future landscape with intermediate-low SLR scenario, and (B) change in significant wave height due to the resiliency projects in place in the intermediate-low SLR scenario

156

Region 3

Landscape Change Modeling

A comprehensive approach to resiliency was represented in Region 3 "with-project" SLAMM modeling by building out four large-scale BUDM restoration projects in the Corpus Christi Bay area to simulate raising the elevation of the project site every 25 years to offset the rate of RSLR. Similarly, two shoreline armoring projects and two living shoreline projects were also built by altering the DEM to account for elevation change due to the installation of breakwaters, sills, and other structures. The landscape change analysis in SLAMM shows the conservation of estuarine and freshwater wetlands around the Nueces River delta and the preservation of estuarine marshes, including mangroves, on the backsides of Mustang and North Padre Islands (Figure 118). Similar to Region 1's model results, simulating BUDM is shown to be efficacious in the SLAMM model by periodically boosting elevation. Output from the 2100 SLAMM model run was processed and prepared to be used in the ADCIRC+SWAN models.

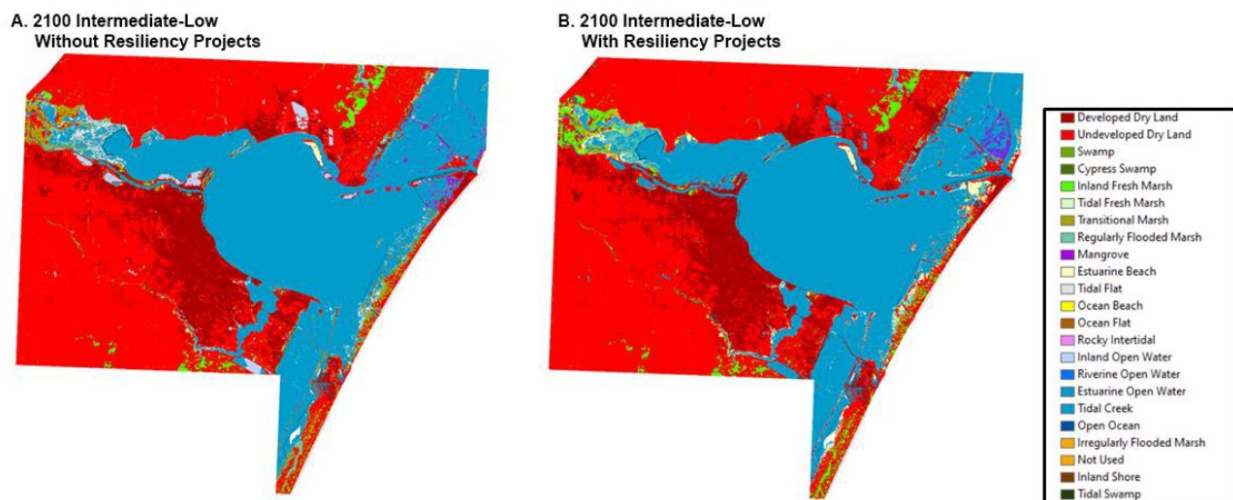*Figure 118. Comparison of land cover in 2100 on the future landscape with intermediate-low SLR scenario (A) without resiliency projects, and (B) with resiliency projects.*

Storm Surge and Wave Modeling

Storm 416 was selected to investigate the impact of storm surge and wave with and without resiliency projects (beneficial use of dredge material (BUDM), living shoreline and shoreline armoring projects) in the future landscape under the intermediate-low SLR scenario. This storm made landfall on the northern end of the North Padre Island near Malaquite Beach as a Category 2 hurricane with a forward speed of 13 miles per hour and a maximum wind speed of 113 miles per hour (Table 7 and Figure 14).

Figure 119 shows the maximum water surface elevation due to Storm 416 with and without resiliency projects implemented in the future landscape with intermediate-low SLR scenario. Comparing the effect of resiliency projects on storm surge in Region 3, the results show not as much change in water surface elevation and extent of inundation as seen in Region 1 with Storm 160. However, the large-scale BUDM projects did succeed in reducing surge depth within the project site as well as the extent of inundation in Oso Bay and several areas around Corpus Christi Bay, e.g. North Beach and Nueces River Delta area.

Figure 120 has two maps showing the difference in maximum water surface elevation and extent of inundation due to Storm 416 with and without resiliency projects in place (top) and the difference in

157

significant wave height with and without projects in place (bottom). The cool colors in the maps show an area with reduced water levels and wave height due to the presence of resiliency projects. Similarly, the purple color in the top map shows the area that is prevented from becoming inundation with the projects in place. The resiliency projects were able to reduce the wave the effects of storm surge and wave damage in the immediate area. E.g., The shoreline armoring project in Nueces River Delta was able to significantly reduce the wave height (bottom map in Figure 120).
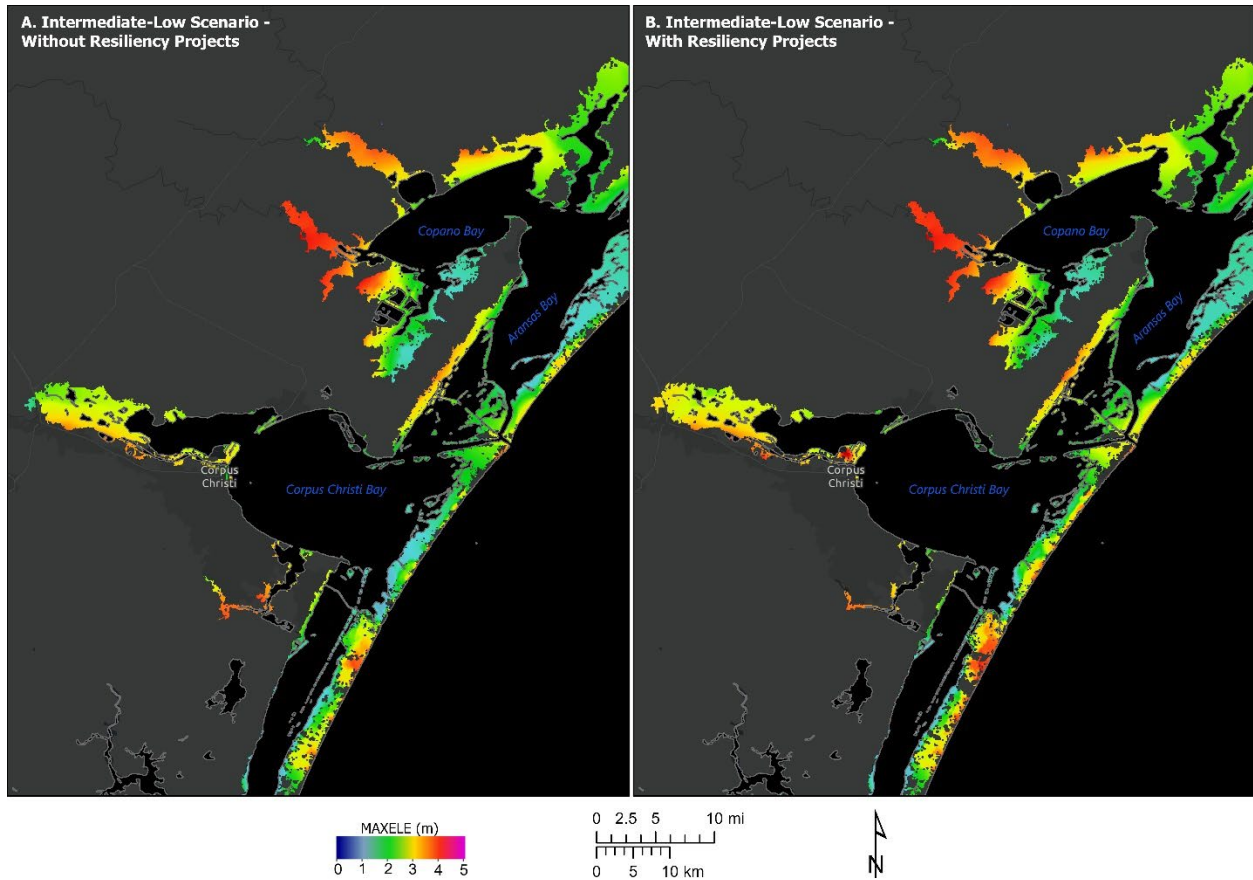
Figure 119. Comparison of maximum water surface elevation (MAXELE) due to Storm 416 in the future landscape with intermediate-low SLR scenario (A) without resiliency projects, and (B) with resiliency projects.

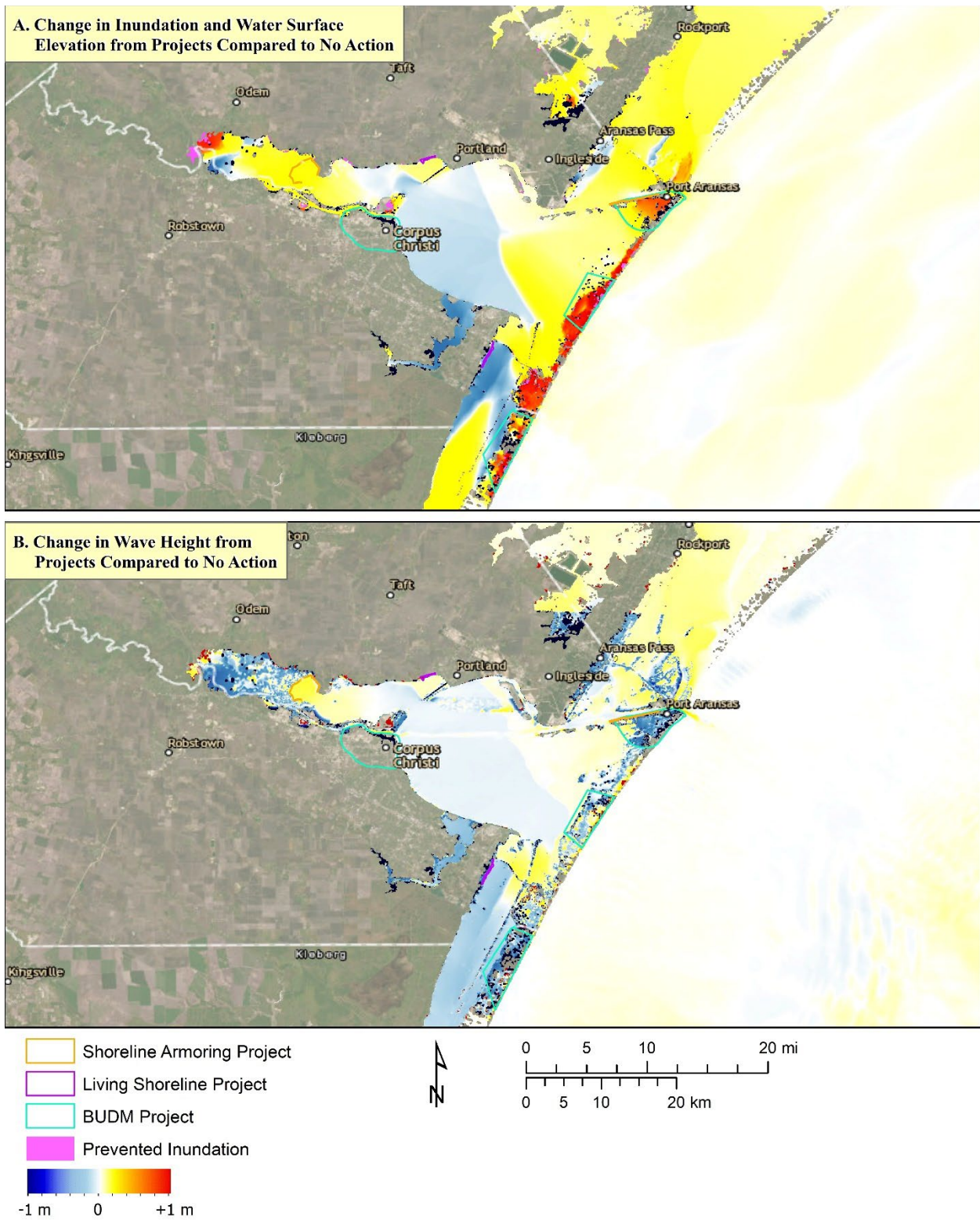*Figure 120. Difference maps showing (A) change in water surface elevation due to resiliency projects in place in the future landscape with intermediate-low SLR scenario, and (B) change in significant wave height due to the resiliency projects in place in the intermediate-low SLR scenario.*

Conclusion

This study provides crucial information for the development of the 2023 Texas Coastal Resiliency Master Plan and serves as a valuable resource for state, local, and federal decision-makers. This research enables them to prioritization of coastal resiliency projects and enhances the protection of the critical coastal environment by addressing the challenges posed by sea level rise and storm surge.

The modeling results highlight that critical habitats will migrate landwards or be lost to open water as the sea level rises, thus increasing the vulnerability of the natural and built environments to coastal storms by allowing farther inland penetration of storm surge. The results indicate that a significant portion of the Texas coast will be at risk of land loss in this century without mitigating action taken.

The results of the coastal wetland landscape change modeling illustrate the anticipated changes in critical environments under two SLR scenarios by 2100. The model results indicate areas where critical environments will be lost or gained, including currently undeveloped dry land that may transform into new critical environments. It is evident that nearly all saltwater and brackish marshes along the Texas coast will be impacted by SLR, with a combination of losses due to inundation and gains through upward migration.

The low marsh area that is lost is expected to transition into tidal flat or open water, while salt and brackish marshes have the potential to migrate landwards if adequate migration space is available. The availability of the migration space, therefore, contributes to a net gain of salt and brackish marshes to 86% by 2100 in the intermediate-low scenario and 82% in the intermediate-high scenario. The presence of undeveloped upland migration space plays a vital role in the long-term survival of coastal wetlands, providing necessary room for the future migration of wetlands as the sea levels continue to rise. However, a significant decrease in the area of inland-fresh marshes and swamps is observed. Slightly over 60% of their initial area is predicted to remain by 2100 in the intermediate-low scenario, while less than 27% of their initial area to remain by 2100 in the intermediate-high scenario. These findings highlight the vulnerability of inland-fresh marshes and swamps to SLR and emphasize the urgent need for their preservation and protection.

The vulnerability of land loss maps developed in this study show that a significant portion of the coast faces the risk of land loss, as current habitats and low-lying areas around communities are converted into open water. The modeling projection indicates that the area of open water will increase by 18% and 40% by 2100 under the intermediate-low and intermediate-high SLR scenarios. However, each region along the Texas coast has unique characteristics that result in varying landscape changes compared to the average trend of the coast. For instance, there is an 8% increase in open water in Region 1 under the intermediate-low SLR scenario, while Region 3 shows a 60% increase. These regional disparities highlight the diverse impacts of SLR on different coastal areas and emphasize the need for tailored approaches to address the specific vulnerabilities of each region.

The storm surge modeling results demonstrate the effects of higher sea levels and landscape changes on the timing and extent of surge inundation in future conditions compared to present conditions. The modeling outcomes reveal that the peak surge arrives earlier in the future scenario, and there is a significant increase in the duration of inundation along the barrier islands and inland regions. Furthermore, the surge that moves inland takes a longer time to recede back to the Gulf of Mexico due to the elevated sea level, resulting in a substantial prolongation of the inundation duration. A storm

surge vulnerability map developed based on the storm surge modeling provides a spatial coverage of the potential areas susceptible to storm surge flooding along the coast. Among the four regions analyzed, Region 1 exhibits the highest vulnerability to storm surge flooding. The map offers valuable insights into the areas that are most at risk and can guide decision-making and planning efforts to enhance resilience and mitigate the impacts of future storm surge events.

The geohazards maps synthesize the comprehensive modeling efforts conducted for the Texas Coastal Resiliency Master Plan in one product and offer a detailed depiction of both the present and future state of the coastal plain. These maps serve to identify areas that are particularly vulnerable to hazards and highlight critical coastal environments that should be prioritized for preservation or avoided. In the intermediate-high SLR scenario, the geohazards maps reveal a significant increase in the extent of land falling within the higher geohazards potential zones exposing critical environments and communities to greater risks. Furthermore, the maps illustrate a distinct pattern whereby the upper coast exhibits a higher susceptibility to the effects of coastal geohazards compared to the lower coast.

The findings from the conceptual resiliency project modeling demonstrate the effectiveness of implementing the BUDM, living shorelines, and restoration projects as viable solutions to mitigate the impacts of SLR on habitats. The outcomes illustrate that large-scale resiliency projects can reduce water depth and inundation caused by storm surge by acting as buffers, suppressing wave energy, and mitigating storm surge impact beyond the project area. This comprehensive approach showcases the potential of these projects to provide a wider range of benefits and contribute to the overall resilience of the coastal environment in the face of SLR challenges.

The findings of this study play a pivotal role in informing the 2023 Plan and providing valuable insights for decision-making at state, local, and federal levels. This study enables the prioritization of coastal resiliency projects along the coast, fostering a deeper understanding of the coastal environment and facilitating its long-term protection. The results underscore the importance of adopting a multi-faceted approach to enhance coastal resiliency, emphasizing the need for multiple lines of defense along the coast. Combining various resiliency projects emerges as a promising strategy to effectively reduce wave energy and mitigate the impact of storm surges within the region. However, there are challenges associated with coordinating funding, dredge cycles, and interagency participation to ensure the successful implementation of these large-scale projects. The strategies and types of projects may vary among different communities based on their unique circumstances. Nevertheless, this study highlights the criticality of timely intervention, as significant areas of the coast face increased risks without proactive measures. By addressing these challenges and implementing appropriate resiliency projects, it is possible to strengthen the coastal defenses, enhance overall resiliency, and safeguard the well-being of coastal communities and ecosystems for the long term.

References

Church, J.A., P.U. Clark, A Cazenave, J.M. Gregory, S. Jevrejeva, A. Levermann, M.A. Merrifield, et al. 2013. "Sea Level Change." In *Climate Change 2013: The Physical Science Basis. Contribution of Working Group I to the Fifth Assessment Report of the Intergovernmental Panel on Climate Change*, edited by T.F. Stocker, D. Qin, G.-K. Plattner, M. Tignor, S.K. Allen, J. Boschung, A. Nauels, Y. Xia, V. Bex, and P.M. Midgley. Cambridge, UK/ New York, USA: Cambridge University Press.

Church, J.A., and N.J. White. 2011. "Sea-Level Rise from the Late 19th to the Early 21st Century." *Surveys in Geophysics* 32 (4–5): 585–602. https://doi.org/10.1007/s10712-011-9119-1.

Clough, J.S., R.A. Park, and R. Fuller. 2010. "SLAMM 6 Beta Technical Documentation." Warren Pinnacle Consulting, Inc.

Cowardin, L.M., V. Carter, F.C. Golet, and E.T. LaRoe. 1979. "Classification of Wetlands and Deepwater Habitats of the United States." Washington, D.C., U.S.A.: U.S. Department of Interior, Fish and Wildlife Service.

Eggleston, Simon, Leandro Buendia, Kyoko Miwa, Todd Ngara, and Kiyoto Tanabe. 2006. "IPCC Guidelines for National Greenhouse Gas Inventories."

Kasmarek, Mark C., Michaela R. Johnson, and Jason K. Ramage. 2014. "Water-Level Altitudes 2014 and Water-Level Changes in the Chicot, Evangeline, and Jasper Aquifers and Compaction 1973–2013 in the Chicot and Evangeline Aquifers, Houston-Galveston Region, Texas." Scientific Investigations Map. United States Geological Survey. http://pubs.usgs.gov/sim/3308/.

Kopp, Robert E., Radley M. Horton, Christopher M. Little, Jerry X. Mitrovica, Michael Oppenheimer, D. J. Rasmussen, Benjamin H. Strauss, and Claudia Tebaldi. 2014. "Probabilistic 21st and 22nd Century Sea-Level Projections at a Global Network of Tide-Gauge Sites." *Earth's Future* 2 (8): 383–406. https://doi.org/10.1002/2014EF000239.

Liu, J., T. Dietz, S. R. Carpenter, M. Alberti, C. Folke, E. Moran, A. N. Pell, P. Deadman, T. Kratz, J. Lubchenco, E. Ostrom, Z. Ouyang, W. Provencher, C. L. Redman, S. H. Schneider, W. W. Taylor. 2007. Complexity of coupled human and natural systems. *Science* **317**, 1513–1516.

Mimura, Nobuo. 2013. "Sea-Level Rise Caused by Climate Change and Its Implications for Society." *Proceedings of the Japan Academy. Series B, Physical and Biological Sciences* 89 (7): 281–301. https://doi.org/10.2183/pjab.89.281.

Parris, Adam, Peter Bromirski, Virginia Burkett, Dan Cayan, Mary Culver, John Hall, Radley Horton, et al. 2012. "Global Sea Level Rise Scenarios for the US National Climate Assessment." NOAA Tech Memo OAR CPO-1.

Pekel, J., Cottam, A., Gorelick, N., and Belward, A. S.. 2016. High-resolution mapping of global surface water and its long-term changes. Nature, v. 540, doi:10.1038/nature20584.

Shamaskin, A., Samiappan, S., Liu, J., Roberts, J., Linhoss, A. and Evans, K., 2019. Multi-attribute ecological and socioeconomic geodatabase for the Gulf of Mexico coastal region of the United States. Data, 5(1), p.3.

Sohl, T.L., K.L. Sayler, M.A. Bouchard, R.R. Reker, A.M. Friesz, S.L. Bennett, B.M. Sleeter, et al. 2014. "Spatially Explicit Modeling of 1992–2100 Land Cover and Forest Stand Age for the Conterminous United States." *Ecological Applications* 24 (5): 1015–36. https://doi.org/10.1890/13-1245.1.

Subedee, Mukesh, Claire R. Pollard, Marissa Dotson, Brach Lupher, Lihong Su, and James C. Gibeaut. 2019. "Sea Level Rise and Storm Surge Modeling in Support of the 2019 Texas Coastal Resiliency Master Plan (TCRMP). Final Technical Report to the Texas General Land Office." Technical Report. Harte Research Institute for Gulf of Mexico Studies. Texas A&M University-Corpus Christi. https://www.researchgate.net/publication/354934745_Sea_Level_Rise_and_Storm_Surge_Modeling_in_support_of_the_2019_Texas_Coastal_Resiliency_Master_Plan_TCRMP.

Sweet, William V., Robert E. Kopp, Jayantha Obeysekera, Radley M. Horton, E. Robert Thieler, and Chris Zervas. 2017. "Global and Regional Sea Level Rise Scenarios for the United States." Technical Report NOS CO-OPS 083. National Oceanic and Atmospheric Administration. https://pubs.er.usgs.gov/publication/70190256.

U.S. Department of the Interior, Fish and Wildlife Service. 2019. "National Wetlands Inventory (NWI)."
2019. http://www.fws.gov/wetlands/.

Vuuren, Detlef P. van, Jae Edmonds, Mikiko Kainuma, Keywan Riahi, Allison Thomson, Kathy Hibbard,
George C. Hurtt, et al. 2011. "The Representative Concentration Pathways: An Overview."
Climatic Change 109 (1): 5. https://doi.org/10.1007/s10584-011-0148-z.

Yu, Jiangbo, Guoquan Wang, Timothy J. Kearns, and Linqiang Yang. 2014. "Is There Deep-Seated
Subsidence in the Houston-Galveston Area?" *International Journal of Geophysics* 2014 (July):
e942834. https://doi.org/10.1155/2014/942834.